Continental Margin Atmospheric Climatology and Sea Level 1974-75

By L. J. Pietrafesa, R. D'Amato, C. Gabriel and R. J. Sawyer, Jr.

UNC Sea Grant Publication UNC-SG-78-09

North Carolina State University
Department of Marine Sciences and Engineering

Report No. 78-2

Copies are available from: UNC Sea Grant
105 1911 Building
North Carolina State University
Raleigh, N.C. 27650

Continental Margin

Atmospheric Climatology and Sea Level

1974-1975

by

L. J. Pietrafesa, R. D'Amato,

C. Gabriel and R. J. Sawyer, Jr.

This work was partially supported by the Department of Energy under Contract No. E(38-1)-902, the Office of Sea Grant, NOAA, U.S. Department of Commerce, under Grant No. 04-6-158-44054, and the North Carolina Department of Administration. The U.S. Government is authorized to produce and distribute reprints for governmental purposes notwithstanding any copyright that may appear hereon.

Department of Energy
Contract No. E(38-1)-902

University of North Carolina Sea Grant College Publication
UNC-SG-78-09

North Carolina State University

Department of Marine Sciences and Engineering
Report No. 78-2

November, 1978

ACKNOWLEDGEMENTS

The authors would like to thank all those who have participated in this project to date. The list includes:

Jack Blanton
Marcus Bowen
Toni Clay
Jack Hickman
Jerry Janowitz
John Klinck
Tom Lee
Ken McDonald
Bob Weisberg

Table of Contents

List of Tables

List of Figures

List of Figures (Cont'd)

List of Figures (Cont'd)

List of Figures (Cont'd)

List of Figures (Cont'd)

List of Figures (Cont'd)

List of Figures (Cont'd)

List of Figures (Cont'd)

List of Figures (Cont'd)

List of Figures (Cont'd)

List of Figures (Cont'd)

CONTINENTAL MARGIN ATMOSPHERIC CLIMATOLOGY AND COASTAL SEA LEVEL

From the many continental shelf dynamics studies which have been made in the past decade, it has become increasingly apparent that a detailed analysis of continental margin waters can only be accomplished with an appreciation of the coastal meteorology. Fortunately, coastal meteorological and, in addition, coastal sea level data have been archived and thus provide coastal oceanographers with inexpensive, priceless and complimentary data sets. Past coastal sea level studies have demonstrated that these data contain not only tidal data but also sub-inertial frequency information which measurably details shelf response to atmospheric forcing. Additionally, a particular region, such as the South Atlantic Bight, can be characterized by the statistics of the temporal spectra of both data sets as well by the alongshore coherences which may exist between stations. In this study, atmospheric wind and pressure have been examined and correlated with coastal sea level changes at various coastal stations along the South Atlantic Bight (Tables 1 and 2).

The atmospheric climate overlying the South Atlantic Bight is determined by both polar and tropical marine air masses, resulting in a "temperate rainy" climate with mild winters, long hot summers, and adequate moisture in all seasons, according to Koppen (see Pettersen, 1969). The north-south surface temperature gradient over the eastern U. S. reaches a seasonal maximum in late winter of approximately 1.5°C per degree latitude, which is about four times the summer gradient. The polar front, the actual zone of maximum temperature contrast which separates the colder continental air from the warmer, more moist tropical air, both intensifies and shifts southward in the winter to near Cape Hatteras, resulting in a region of intense cyclogenesis stretching along the eastern U. S. seaboard from Florida towards northern Europe. Most of the intense extratropical lows develop over the southeast U. S. but show their greatest growth as the storms move offshore over the warmer ocean, especially in the neighborhood of the Gulf Stream. The mean speed of these synoptic-scale cyclones is 5-7 m/sec (10-15 kts), with less than 20% of the storms moving at speeds greater than 12.5 m/sec (25 kts) (NOAA, 1970).

These wintertime extratropical cyclones (and to a lesser extend the accompanying anticyclones) can affect the coastal oceanic circulation in a number of direct and indirect ways. The surface pressure and wind stress patterns for a mature low can be coherent over 600 kms., can persist for 3 to 4 days, and can directly drive a large-scale coastal current. Intense lows are frequently accompanied by trailing outbreaks of very cold polar air, causing sharp cold fronts which move southeastward over the southeastern states; and they can bring freezing weather and strong winds as far south as Florida. Smaller scale waves can develop along the polar front near the southeastern coast which exhibit highly variable stress

Table 1

Meteorological Stations

Station	Latitude	Longitude
Cape Hatteras, N.C.	35°16'N	75°33'W
Wilmington, N.C.	34°14'N	77°57'W
Charleston, S.C.	32°46'N	79°56'W
Savannah, Ga.	32°05'N	81°06'W

Table 2

Sea Level Stations

Station	Latitude	Longitude
Beaufort, N.C.	34°43.2'N	76°40.2'W
Beaufort Inlet, N.C.	34°41.6'N	76°42.7'W
Wilmington, N.C.	34°13.6'N	77°57.2'W
Frying Pan Shoals, N.C.	33°29.1'N	77°35.4'W
Charleston, S.C.	32°46'N	79°56'W

and precipitation patterns on the subsynoptic (10-100 km) scale (Bosart, Vando, and Helsdon, 1972; Bosart, 1973). Bosart and Cussen (1973) have found surface pressure fluctuations of 4-5 mb amplitude along the coast and have attributed these perturbations to atmospheric gravity wave generation by accompanying frontogenesis. Perhaps the most intense atmospheric pressure and surface wind stress patterns are associated with the large-scale tropical storms and hurricanes which develop primarily in August-October and occasionally migrate along the Southeast coast, visiting the Carolina coast with a frequency of about one severe storm every two years (U. S. Navy, 1970). The meteorological forcing on the Carolina Shelf is thus dominated in winter by transient extratropical storms with considerable variability in strength, structure, and persistence of the important meteorological fields. The predominant speeds reported to NOAA (1970) exceeding 8 m/sec (16 kts).

The summer meteorological regime along the Carolina coast is controlled by a strong weakening of the polar front and an intensification of the Azores-Bermuda high. The region of most intense cyclogenesis has shifted north of Cape Hatteras and while some active frontogenesis and cyclogenesis continues over the Southeast U. S. shelf, the atmospheric variability there is decreased in summer. The predominant winds are lighter and southerly to southwesterly. Some 60% of the NOAA-collected surface observations (NOAA, 1970) indicate wind speeds of less than 5 m/sec (10 kts), while 15% indicate wind speeds greater than 8 m/sec (16 kts). The standard deviation of the surface pressure shows both a strong seasonal fluctuation and a steady decrease with decreasing latitude south of Cape Hatteras (U. S. Navy, 1970). The standard deviation of the surface pressure at Charleston, S. C., is about one-half its mean winter value of 7 mb. Ward (1925) and his more recent co-workers suggest that a transition from a northern cyclonic-controlled climate to a more Gulf-like climate with higher temperatures and less dramatic weather occurs along the Southeast shelf near the latitude of Charleston.

On localized scales; an appreciable diurnal sea/land breeze, as well as an apparent semi-diurnal harmonic thereof, are in evidence along the North Carolina coast (Pietrafesa, it. al., 1977).

The recent work of Saunders (1977) suggests that there is a great deal of offshore as well as alongshore structure to the mean wind fields which gives rise to the need for meteorological buoys which would allow for an assessment of the curl and divergence of the wind field as well as a mass and heat air/sea interaction evaluation. Saunders also points out an offshore wind stress maximum which occurs during early fall; he finds no apparent reason for this but it seems likely that the air-sea temperature gradients may be largest during this time of the year, thereby increasing the drag coefficient and subsequently the relative stress field.

Another line of investigation has pursued the influence of meteorological forcing, albeit in a less systematic manner. In the summer season, near coastal winds with northward (alongshore) components are common and often persistent. Green (1944) and Taylor and Steward (1959) reported evidence for summer coastal upwelling of northeast North Carolina. Bumpus (1973) then inferred that wind-driven upwelling probably occurred throughout the South Atlantic Bight in the summer season. Wunsch, Hansen, and Zetler (1969) examined many years of sea level and meteorological data from the Florida Straits region; they found no evidence for a significant, systematic meteorological influence on the Florida Current.

The response of coastal surface elevation to continental atmospheric forcing has been examined, by a number of investigators. Miller (1957 and 1958) studied the New England and New Jersey coasts; Hamon (1962, 1963, 1966) studied the Australian coasts; Panshin (1967), Mooers and Smith (1968), Pietrafesa (1970), Cutchin and Smith (1973), Smith (1974), Kundu, Allen and Smith (1975) and Huyer, Hickey, Smith, Smith and Pillsbury (1975) have separately and in part investigated the effects of atmospheric forcing on sea level along the Pacific Northwest coast; Mysak and Hammon (1969) partially studied the North Carolina coast; Cragg and Sturges (1974) did an in depth study of the West Florida shelf while Brooks and Mooers (1977) considered sea level response along the East Florida shelf.

Sea surface elevations along coastlines are related to both alongshore and transshore winds. Simple Ekman theory (Ekman, 1905) and subsequent studies of both set-up and set-down (Hidaka, 1953; Welander, 1957) and shelf wave generation (Hamon, 1962, 1963, 1966; Mysak and Hamon, 1967; Cutchin and Smith, 1973; Huyer, et. al., 1975); have supported the evidence for sub-inertial frequency correlations between atmospheric forcing and sea level signature.

This review presents cross analyses of surface wind and atmospheric pressure which are then shown to provide the sea level response function to meteorological forcing. The implications which these results bear for shelf circulation investigations can then be inferred and supported with current meter data collected in the area of interest (Pietrafesa, et. al., 1978a and 1978b).

The literature cited suggests that variations in atmospheric pressure, wind speed and direction, currents and sub-inertial phenomena, such as shelf waves, can significantly affect the coastal sea level signature. Sea level response to variations in coastal meteorological pressure fields can be expressed in terms of a factor which is frequency dependent. It can be best appreciated as the relationship between the input to a filter and the subsequent convolved output. Generally, a one centimeter depression (rise) in sea level per one millibar increase (decrease) in barometric pressure is observed.

While the evidence for the existence of continental shelf waves has been at times inferred from the cross-statistical analyses of tidal and meteorological data, there have been few actual current meter observations made at sufficiently extensive longshore stations to corroborate the passage of these phenomena. Huyer, et. al. (1976) confirmed the existence of such phenomena along the Oregon-Washington coast and the ongoing Department of Energy current meter study between Cape Lookout and Savannah by Dr. T. N. Lee (of the University of Miami) and Dr. L. J. Pietrafesa (of North Carolina State University) could confirm the Mysak and Hamon (1969) contention of their existence. Pietrafesa, et. al. (1978) have produced current meter spectra from Onslow Bay, N. C. which show energy peaks at the 2.5-4, 5-7 and 8-11 day period bands, which could be associated with south/northward propagating wave phenomena. Nonetheless, without further corroboration, such as the Pietrafesa study may yield, the separation of free or forced Rossby wave sea level response from wind induced stationary sea level fluctuations is no more than speculation.

Wunsch, et. al. resolved that astronomical tides were responsible for most of the sea level variations. Herein, it is of note that low frequency fluctuations, within the 0.5-.08 cpd frequency range, are an observed feature of the Gulf Stream. Pillsbury (1890), Parr (1937), Duing, Mooers and Lee (1977), Duing (1975), Schmitz and Richardson (1968) and Lee and Mayer (1977) all independently observe such lateral, onshore-offshore periodicities of the current regime in the Gulf Stream off of the Florida Coast. Webster (1961) found a 0.14 cpd cross-shelf meander of the Gulf Stream front off of Onslow Bay, which seemed to be correlated with the cross-shelf wind component. Orlanski (1969), Niiler and Mysak (1971) and Orlanski and Cox (1973) independently suggest that inherent baroclinic instabilities of the Gulf Stream can be responsible for the energy which appears in the aforementioned frequency domain range. These instabilities would then force a shelf water response which could appear in the sea level signature. A contemporaneous description of coastal current, sea level, Gulf Stream dynamic character and atmospheric forcing needs to be accomplished; such a study is included in the aforementioned Lee and Pietrafesa field studies extending from Florida to Cape Hatteras, but in this report we shall simply report on some coastal meteorological and sea level relationships.

Meteorological stations and tide gauge stations chosen for this study are respectively: Cape Hatteras, Wilmington, Charleston and Savannah; Beaufort, Beaufort Inlet, Frying Pan Shoals, Wilmington, and Charleston. These are geographically depicted in Figure 1. Throughout this area the continental shelf tends to be shallow and generally broad with the major exception of a narrowing at Cape Hatteras and occasional incursions of shoals seaward of Capes Hatteras, Lookout and Fear (cf. Figure 1). The shelf break is typically at the 75 meter isobath. Though the topography in the vicinity of each gauge varies considerably, the similarity between the low frequency, low passed sea level records at the various stations supports the assumption that there is minimal location influence apparent in the spectral ranges considered, save for the Frying Pan Shoal and Wilmington data, which may be geographically and/or topographically influenced.

In this preliminary data report, two years of hourly heights, recorded to the nearest 2-3 centimeters were analyzed at each sea level station. Three hourly observations of atmospheric pressure and wind speed direction were obtained from the Savannah and Wilmington airports and Charleston

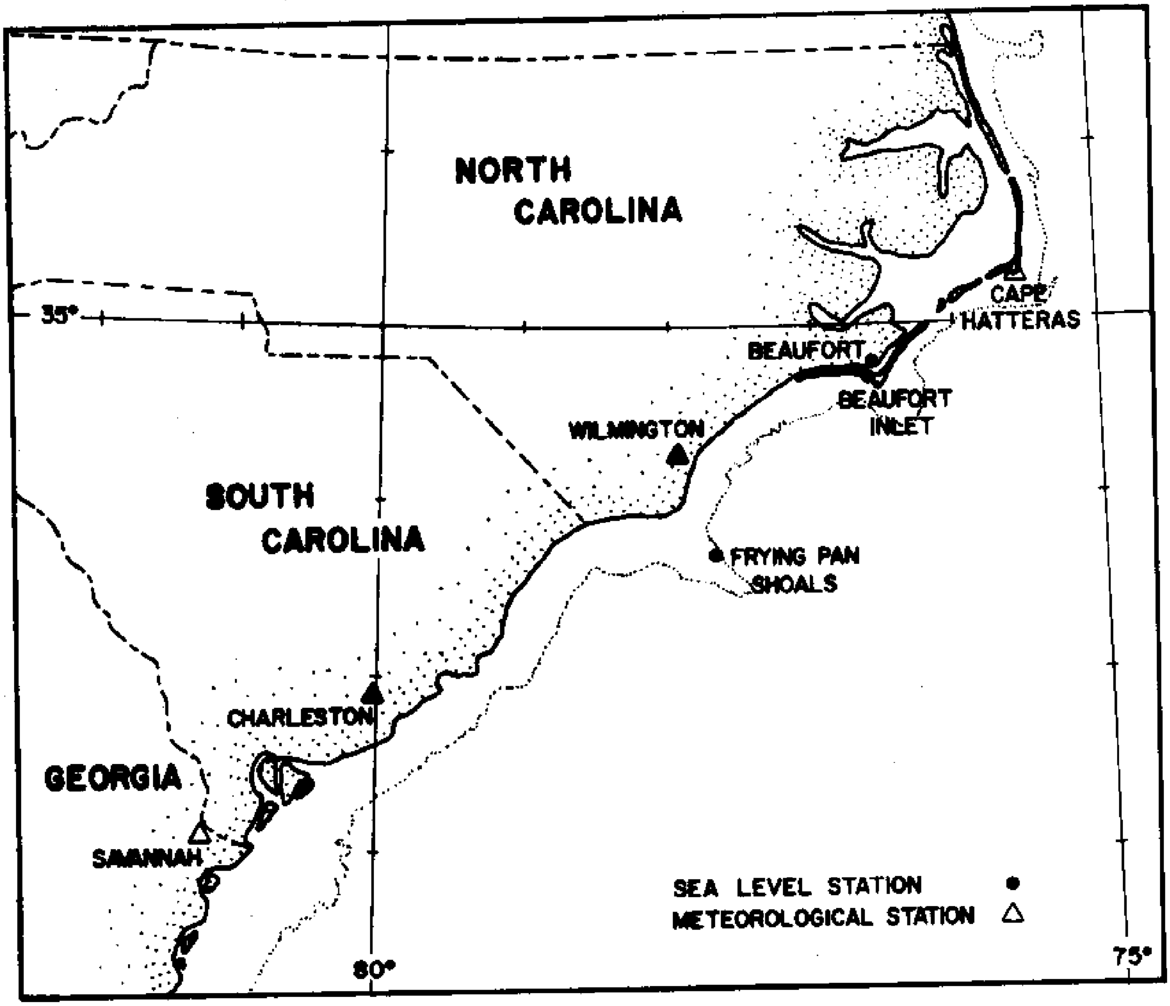

Figure 1 Location of meteorological and sea level stations

and Cape Hatteras coastal stations. The airport data are undoubtedly contaminated by topographic boundary layer effects and may thus show considerably diminished magnitudes, as well possible rotations in direction relative to the coastal stations. It is further appreciated that the coastal meteorological data may show both phase differences as well as magnitude and direction variations with the actual, at sea, marine atmospheric climatology. This contention is strongly suggested in the comparison of the Saunders (1977) offshore, at-sea meteorological statistics to the Ruzecki (1974) coastal, land based results.

The data analyzed are from coastal sea level, i.e. tide gauge, and meteorological stations located in Figure 1. Hourly values of sea level height for 1974-1975 were obtained from the National Ocean Survey, NOAA, Rockville, Maryland, for stations at Beaufort (BFT), Frying Pan Shoals (FPS) and Wilmington (WIL), North Carolina, and at Charleston (CHS), South Carolina. Three-hourly values of surface wind speed, wind direction, and atmospheric pressure for 1974-1975 were obtained from the National Climatic Center, NOAA, Asheville, North Carolina for stations at Cape Hatteras, N. C., (HAT), Wilmington, N. C. (WIL), Charleston, S. C. (CHS) and Savannah, Ga. (SAV).

The sea level data were low pass filtered using a Lanczos filter taper to attenuate the daily and semidaily tides and inertial fluctuations (the inertial periods at/are: SAV/22.64 hr; CHS/22.04 hr; WIL-FPS/21.46 hr; BFT/21.1 hr; and HAT/20.9 hr.). The envelope of the forty (40) hour low pass filter energy response functions are shown in Figure 2. Attenuation at diurnal and higher frequencies is greater than 10^6 and 10^5 respectively. After filtering, the sea level data were resampled at 8 and 6 hourly intervals, for the two separate filtering intervals, respectively.

The radial distances between these stations are approximately: SAV-CHS/130 km; SAV-WIL/380 km; SAV-BFT/480 km; SAV-HAT/620 km; CHS-WIL/240 km; CHS-BFT/340 km; CHS-HAT/480 km; WIL-BFT/100 km; WIL-HAT/240 km; and BFT-HAT/140 km.

Three-hourly wind stress vector components in a right-handed rotated coordinate system, such that the alongshore component is 55.6° East of North, were computed from the raw wind speed and direction data, with the positive vector sense in the direction toward which the wind blows. The stress components were computed using a quadratic drag law with the coefficient $C_D = 1.5 \times 10^{-3}$ (Pond, 1976). The wind stress components and atmospheric pressure time series were low pass filtered, using a filter with the response characteristics shown in Figure 2. The atmospheric data were then subsampled at 9-hour intervals and linearly interpolated to 8 and 6 hourly intervals to be commensurate with the respective sea level data.

The filtered atmospheric pressure time series indicates that the SAV, CHS, WIL, and HAT stations (Figure 1) are well correlated over most of the large and even small amplitude variations which is indicative of the

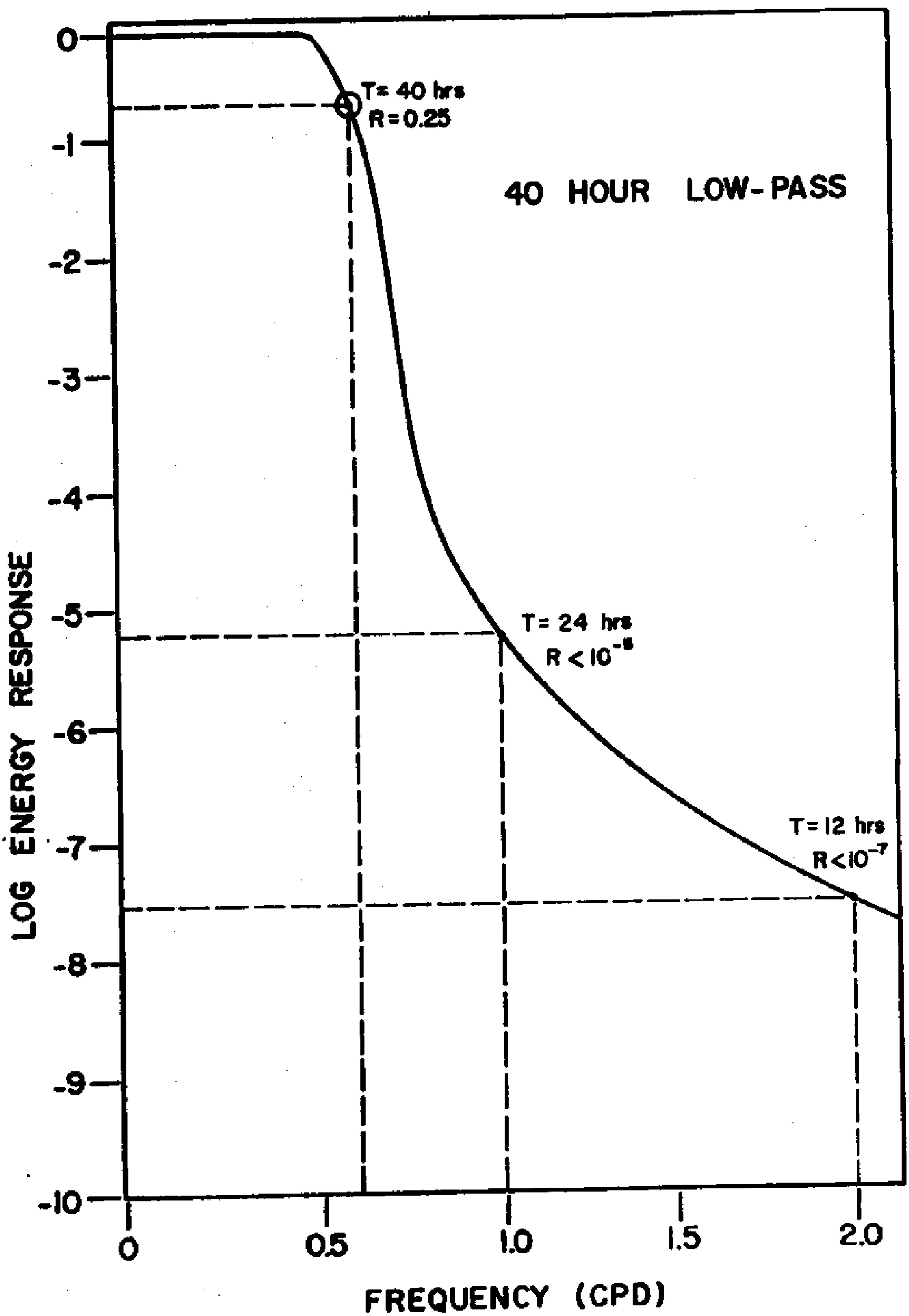

Figure 2 Filter energy response envelope, 40HRLP

ERRATA:

Page 9, line 11; clockwise should read counter-clockwise high degree of horizontal coherence over length scales of the pressure field much greater than the SAV-HAT radial separation distance which is 620 km. The large horizontal coherence distance presumably reflects the synoptic meteorological scales associated with mid-latitude atmospheric disturbances, especially during the fall, winter, spring periods. The alongshore wind stress components (Figures 3 thru 62) also show essential correlation over the SAV-HAT separation distance, but variations in intensity and structure between stations are more apparent than in the pressure time series. Vector representations or stacks of stick diagrams (Figures 51 - 62) of the wind stress during passage of cold front events indicate the counterclockwise rotation usually associated with the passage of such an event over the station(s). Here it is noted that HAT typically shows the largest stress magnitudes. Alongshore winds tend to dominate both in magnitude and duration relative to the cross-shelf components. Wind stress reversals, noted at all of the met stations, occurred on time scales of several days to several weeks, which is the typical periods of forcing within the atmospheric stress continuum.

HORIZONTAL WIND COHERENCE

Kinetic Energy Density (KED) spectra of alongshelf and transshelf wind components at stations WIL and HAT during the Summer, 1976; (Pietrafesa, et. al., 1978b; Figures 321-324 and 337-340), indicate that within the temporal period 2-14 days, there is a rise in the energy density as approximately the frequency to the minus three halves power, which is consistent with the findings of Oort and Taylor (1969) and Cragg and Sturges (1974) for other coastal regions and is attributed to the passages of cyclones and anticyclones. The KED curve flattens out at periods in excess of 14 days. Within the temporal ranges of interest of the continental shelf studies of Pietrafesa, the range from the order several days to a month, alongshore winds show a remarkably high degree of visual correlation, save for occasional several day departures, in the station time series shown in Figures 3 through 62. One can observe similarly good visual correlation between transshelf wind components between station pairs over the whole of the radial separation distance with occasional departures, in the same figure series as above.

Over the entire frequency range of 0.5-0.05 cpd, alongshore winds are more energetic than cross-shelf winds. Figures 321-324 and 337-340 (in Pietrafesa, et. al., 1978b) show this in the KED's for WIL and HAT. Note the strong diurnal signal in the on/off direction.

During the April-July, 1974 subset, alongshore wind components between station pairs are in general more coherent than off/on shore winds at frequencies below 0.23 cpd and vice versa at frequencies above 0.23 cpd. The exceptions are WIL-HAT where C^2 is always higher for alongshore vs. transshore winds and WIL-HAT where alongshore winds are more coherent below 0.3 cpd and transshore winds are more coherent above 0.3 cpd. The Sept.-Dec., 1974 subset offers greater complexity in that, with minor variations, alongshore winds are generally more coherent than cross-shore winds at frequencies below 0.12 cpd, higher between 0.14 and 0.28 cpd at the northerly stations. C^2's between station pair components vary above 0.28 cpd. Figures 204 through 247 depict the various cross-correlations. Alongshore wind pairs display less phase shifts, which are typically less than a few hours, than cross-shelf wind pairs. This is evident from both the time series and the cross-correlations. Additionally, it is noted that alongshore winds over radial separation distances as large as 630 km have C^2's always in excess of 0.5 and occasionally higher than 0.65 at frequencies below 0.3 cpd but tend to become less coherent at a C^2 rate of 0.1 per 150 km increase in station pair separation distance.

It can therefore be concluded that winds recorded at any one of the coastal stations could, at least qualitative, be representative of the wind fields at any of the other stations, with appropriate reservation. The adequacy of representation is an event, season, location sensitive variable, but for events within the frequency band 0.3 to 0.05 cpd the contention is not without evidential basis. What is suggested herein is that the divergence of the alongshore wind stress may not be large, and furthermore that possibly the curl of the cross-shore wind stress may not be large but the data indicates little of a definitive nature about the curl of $\tau^{(y)}$ or the divergence of $\tau^{(x)}$ and moreover nothing about the offshore wind field structure, which is the actual mechanical forcing function

ATMOSPHERIC PRESSURE COHERENCE

Forty hour low-passed atmospheric pressure from the met stations indicate a high degree of coherence with daily pressures rarely differing by more than several millibars between stations. The Phase shifts are nearly zero at all frequencies save for shifts of the order of 0-20 degrees over radial distances the order of 100-650 kms (egs. HAT/WIL, Figure 174; HAT/SAV, Figure 178; CHS/SAV, Figure 176). The southerly met stations typically lead the more northerly stations (eg. CHS leads HAT) for the entire separate series lengths of years 1974 and 1975. Considering the 4 month block, April-July 1974, though: HAT lags WIL only at frequencies greater than 0.2 cpd, below that the pair are in 0 degree phase; WIL leads CHS from 0.1-0.2 cpd, lags above and is in 0 degree phase below; CHS leads SAV from below 0.2 cpd and lags above 0.2 cpd; HAT leads CHS between 0.2-0.1 cpd, lags above and is in phase below; HAT leads SAV between 0.2-0.1 cpd and lags below. During the period Sept.-Dec., 1974, the southerly stations consistently lead the more northerly station pair, over all frequencies, with no exceptions. It certainly appears, herein, from the cross-correlations between station pairs that the pressure spectrum at any individual station is reasonably representative of that at any other with minor adjustments in phase as a function of the pairing and the frequency. Coherence squared (C^2) is typically in excess of 0.9 over station radial separation distances the order of 200 km and drops off from 0.95 to 0.5 at distances in excess of 400 km in the 0.1-0.5 cpd band. Exceptions to the rule are noted for: WIL-CHS, C^2 of 0.5 at 0.4 cpd during April-July, 1974; HAT-CHS, C^2 of 0.3 at 0.4 cpd during April-July, 1974; HAT-SAV, C^2 of 0.25 at 0.4 cpd during Sept.-Dec., 1974; and WIL-CHS, C^2 of 0.75 at 0.4 cpd during Sept.-Dec., 1974.

SEA LEVEL

As described earlier, the sea level data were low pass filtered using a Lanczos filter taper to attenuate the diurnal and semi-diurnal tides and inertial fluctuations (cf. Figure 2).

Among factors which significantly affect sea level, particular note is made to the variations in atmospheric pressure, atmospheric winds, oceanic currents and long, shelf wave phenomena. The response of the level of the sea surface to varying atmospheric pressure is more correctly expressed in terms of a frequency dependent barometric factor, i.e., a transfer function for the pressure and sea level system. Herein, the sea level data was "adjusted" (as well as left "unadjusted") for the so-called "barometric effect". For frequencies below 1 cpd, the sea surface responds to changes in atmospheric pressure in a reasonably regular, nearly instantaneous fashion. The adjustment suggested over nearly the entire frequency range of interest in this study (eg. Roden, 1960; Mysak and Hamon, 1969) for sea level fluctuations due to varying barometric pressure is about 1.0 cm/m bar, i.e., a one millibar increase (decrease) in pressure depresses (elevates) the sea surface approximately 1 centimeter.

Spectral analyses of alongshore and cross-shore winds, separately, and sea level are shown in the series of Figures 87 through 122. Remarkably high C^2 results between sea level and alongshore winds, especially at frequencies below 0.35 cpd, over the 1974 and 1975 yearly series, as well as the 4 month series blocks, April-July and Sept.-Dec., 1974. The cross-coast wind vs. sea level comparisons, at coincident or nearby sites, indicate more selective coherence bands. Some of the potential hazards which should be noted in this preliminary comparison are that the Wilmington tide gauge is located 27 miles from the mouth of the Cape Fear River Estuary, a tidally influenced coastal plain estuary which undoubtedly has a sea level response signature very different from that of an open, coastal station. Consequently, any intercomparisons of sea level at WIL and any coastal station, (save for one at the mouth of the Cape Fear River Estuary), as was done by Brooks (1977) to confirm the existence and southerly propagation of continental shelf waves, must be done so with appropriate reservation. Likewise, the intercomparisons of HAT atmospheric data and BFT sea level must be done so with recognition of the 140 km radial separation of the two stations.

C^2's the order of 0.7 to 0.95 between wind and sea level appear over period bands 3-4 days and 5-10 days in the alongshore wind intercomparisons (eg. CHS v stress vs. CHS ADJ SEALVL APR-JUL 74, Figure 110 and SEP-DEC 74, Figure 122). The overall C^2 level is much lower in the transshelf wind cases, with C^2's in excess of 0.5 at periods of 3-4 days.

These spectra imply that there is a substantial and coherent coupling between the sea level response variable and the wind input variable, particularly at selective frequencies, i.e., in simplistic terms the membrane responds to the forcing within the band of the forcing frequencies. In fact the KED's of sea level demonstrate the same rise of energy to the minus three-halfs power of frequency over periods of several days to several weeks which is shown in the wind spectra (Figures 248, 249 and 250).

It is of note herein that the KED's indicate a rise in energy levels from north to south, i.e., from BFT to FPS to CHS (Figures 248-250) over the entire frequency range. This is consistent, at the semi-diurnal period of 12-41 hours, with the motion of the semi-diurnal tide propagating as a Poincare wave which increases in amplitude as the shelf widens, as it does from Cape Hatteras to Savannah. A doublet spike at the diurnal period appears in all of the sea level KED's; there is no immediate explanation for this phenomenon.

It was deemed necessary, at this point, to proceed in the data analysis of the met/sea level time series by computing multiple coherences between pressure, wind components and sea level and to compute in phase transfer functions between the atmospheric variables and sea level. Since pressure and wind are coherent over varying frequency bands, between each other, as well as separately with sea level, it is enlightening to input one atmospheric variable, then another and finally another and watch the C^2's with sea level be either augmented, enhanced or reduced. It is useful to compute the ratio of the co-spectrum of sea level and alongshore or cross-shore winds or pressure to the auto-spectrum of the respective atmospheric variable; a uniform (nonuniform) ratio over some spectral range would then be indicative of no preferential (of a preferential) frequency band within which air-sea momentum transfers are more efficient which is further indicative of no resonance (of resonance) between the atmosphere and sea level.

These latter kinds of data products are buried in the data presented but need to be formally accomplished.

Considering the alongshore and cross-shelf wind stress components (heretofore $\tau^{(y)}$ and $\tau^{(x)}$) and adjusted sea level, it is noted that sea level consistently, without exception, lags $\tau^{(x)}$ but leads $\tau^{(y)}$. Additionally, it should be noted that $\tau^{(y)}$ leads $\tau^{(x)}$ over the most coherent bands, between the two, and in fact the two components tend to be in quadrature. This is entirely consistent with the scenario of sea level falling at the coast due to increasing offshore or southwesterly, alongshore winds and rising with increased onshore or northeasterly winds.

It appears that sea level (SL) from CHS to BFT responds, to some measure, in a conventional Ekman sense, i.e., SL fluctuates up or down in direct response to wind stress both in the alongshore and transshore directions. Southwesterly (northeasterly) winds produce a setdown (setup) of SL at the coast and offshore (on shore) winds produce a setdown (setup) of SL at the coast. A clear example of this is shown in the time series of sea level at CHS and the wind stress field at CHS from 5-20 January, 1974 (days 5-20 in Figures 63 and 27). The coastal Ekman scenario follows so well that even a relaxation in the magnitude of the stress field, which was directed to the northeast on days 9 and 10 was mirrored in a slight increase in sea level. BFT-SL is entirely consistent with the CHS Ekman scenario during this period given the agreement of the HAT, WIL and CHS winds. The southwesterly to northeasterly wind reversal which occurred during day 11 (11 Jan., 1974), consistent with the clockwise wind stress vector rotation of a cold front, Figure 51, from $\tau^{(y)} \sim 0.6$ dynes/cm^2 to $\tau^{(y)} \sim -0.5$ dynes/cm^2 resulted a drop in sea level of approximately 55 cm.

It is of note here that the sea level data, particularly intercomparisons of the BFT/FPS time series because they imply that not only transshelf but also alongshelf slopes of sea surface, consistent with a piling up of the surface waters in the direction of the wind, exist. On 1 December 1974 a large southwesterly wind event occurred and not only dropped sea level at FPS and BFT, which were both at 130 cm height at the event onset, but created a 50 cm rise in sea level from FPS to BFT, a radial distance of 150 km. This is evident in Figures 20 and 68 which shows evidence for the existence of longshore pressure gradients, which were hypothesized to exist by Garvine (1971) and used in a mathematical model of coastal dynamics by Pietrafesa (1973) to drive a cross-shelf interior flow thereby eliminating the necessity of a bottom, frictional layer to balance the offshore Ekman transport. In a barotropic geostrophic sense the cross-shelf flow induced by this longshore pressure gradient, using the relation $u = (gf^{-1})\zeta_y$ is of the order of 23 cm/sec. The longshore variations in sea level observed between Capes Lookout and Fear, which define Onslow Bay in the alongshore direction, are certainly no proof of the existence of Garvine's contention nor a justification of Pietrafesa's use of the longshore pressure gradient in his model, since both of these investigators were dealing with straight coastlines having no longitudinal constraints and the cape shoals do constrain the hydrodynamics within. CHS vs. SAV sea level intercomparisons would offer a more generic look at the question of existence of a ζ_y in concert with an imposed $\tau^{(y)}$ at the surface.

A simplified balance in the alongshore direction could be written as $\zeta_y \sim \tau^{(y)}$ g $\dot{D}$ where D is the depth of the direct wind induced layer (the layer within which the wind is piled up). The example presented above of a $\Delta\zeta$ of 50 cm from BFT to FPS, a distance of 150 km, with a $|\tau^{(y)}|$ of 0.9 dynes/cm^2 indicates a D of 2.8 meters.

A great deal of visual correlation is obvious in the time series of filtered sea level (Figures 63 through 86). The Kinetic Energy Density representations (Figures 248-250) also indicate that BFT, FPS and CHS contain the similar energetics, save for the fact that the energy level rises from north to south, especially in the shape of the curve, as we described earlier in the text.

The cross analyses of sea level, including most of the pairing combinations, between CHS, BFT, WIL and FPS are shown in Figures 179 thru 203. Consider several subsets, not including WIL in the discussion because of the aforementioned fact that WIL is 27 miles (45 km) from the mouth of the tidal, wind and river runoff influenced Cape Fear River Estuary.

During the Sept.-Dec., 1974 subset, (Figure 197) BFT and CHS are coherent (above the 95% confidence level, which loses some credible meaning at C^2's too low) over the entire frequency range. There are several highly significant period bands which should be noted: at 2.25 days, $C^2 \sim 0.8$ and CHS leads BFT by 4½ hours; at 3.6 days, $C^2 \sim 0.85$, CHS leads BFT by 4 1/3 hours; at periods above 10 days the two stations are essentially in phase. During this same period: CHS $\tau^{(y)}$ and $\tau^{(x)}$ (Figure 228) are most coherent at periods encompassing 3 and 6-7 days and are close to quadrature (60-90°) with $\tau^{(y)}$ leading $\tau^{(x)}$; SAV $\tau^{(y)}$ and $\tau^{(x)}$ (Figure 229) are more broadly coherent, over the period range 2.8 - 10 days and also indicate $\tau^{(y)}$ leading $\tau^{(x)}$ by approximately 60°-80°; HAT $\tau^{(y)}$ leads $\tau^{(x)}$ (Figure 226) at 2+, 3 and 10 day periods by 90°-110°. WIL $\tau^{(x)}$ and $\tau^{(y)}$ relationships (Figure 227) closely follow those of SAV with the two components being very close to quadrature. The phase relationships between these wind components and to sea level indicate a lowering of sea level with increasing positive $\tau^{(y)}$ and $\tau^{(x)}$ wind stress with the offshore propagation of an anticyclone cold front whereby, from the coast seaward a southeasterly wind would begin to rotate clockwise, while sea level dropped to some maximum low as the wind became southwesterly, then began to rise as the wind rotated to be northwesterly to northerly and so-on.

During this same Sept.-Dec., 1974 period: FPS was coherent with BFT (Figure 200) at 2 and 5-8 day periods, with minimal coherence (90% confidence level) at 3 day periods, with FPS leading BFT at the 3 and 5-8 day periods by about 15 hours and 25-40 hours; FPS and CHS (Figure 202) are coherent at 2 and 3-9 day periods (esp. at 6-8 days) with FPS leading CHS by 0.45 days, at 0.275 cpd and 0.4 days between 0.16 and 0.12 cpd frequencies suggesting an event propagation speed of 5 m/sec. from Frying Pan Shoals to Charleston.

One could investigate the phase differences between wind stress components and adjusted sea level by adjusting the two time series so that the phase lag between the two is eliminated and then reconsider the correlation between the two time series. One could also consider the average ratio of sea level amplitude to wind speed magnitude, a value to be compared to the magnitude of the average of the ratio of the co-spectrum of sea level and wind component to the auto-spectrum of the wind component. These calculations will be done in a report to follow.

Monthly to seasonal to annual variations in sea level, due to the thermal variability of the water column and the changes in the atmospheric, marine climatology will be investigated in the report to follow. Seasonal to annual harmonics could be eliminated from the time series, thereby suppressing the long period contamination of the short period correlations.

By extracting data which represents a change in only one of the atmospheric variables, while the other variables remain below some greatest lower bound, one could plot the sea level response to changes in that variable alone. There, a functional relationship between sea level and atmospheric pressure and wind could be obtained in an empirical fashion.

This type of procedure could be done for winds blowing in any direction and should result in a curve which indicates the changes in sea level as a function of wind direction, station by station.

Because of the problems which were encountered in obtaining tide gauge data from NOAA/NOS, we do not have all of the data which is probably available for both the years and area of interest. We did not receive the Frying Pan Shoal sea level data until recently and so were not able to fully incorporate this invaluable data set into our analysis to date. Fortunately though, this is a preliminary assessment of the atmospheric climatology and sea level in the Carolina Capes region of the South Atlantic Bight and the report to follow this initial effort will be more inclusive and extensive and will incorporate the moored current, temperature, pressure, conductivity data as has been done by other investigators (eg: Smith, 1974; Cragg and Sturges, 1974).

DATA PRODUCTS

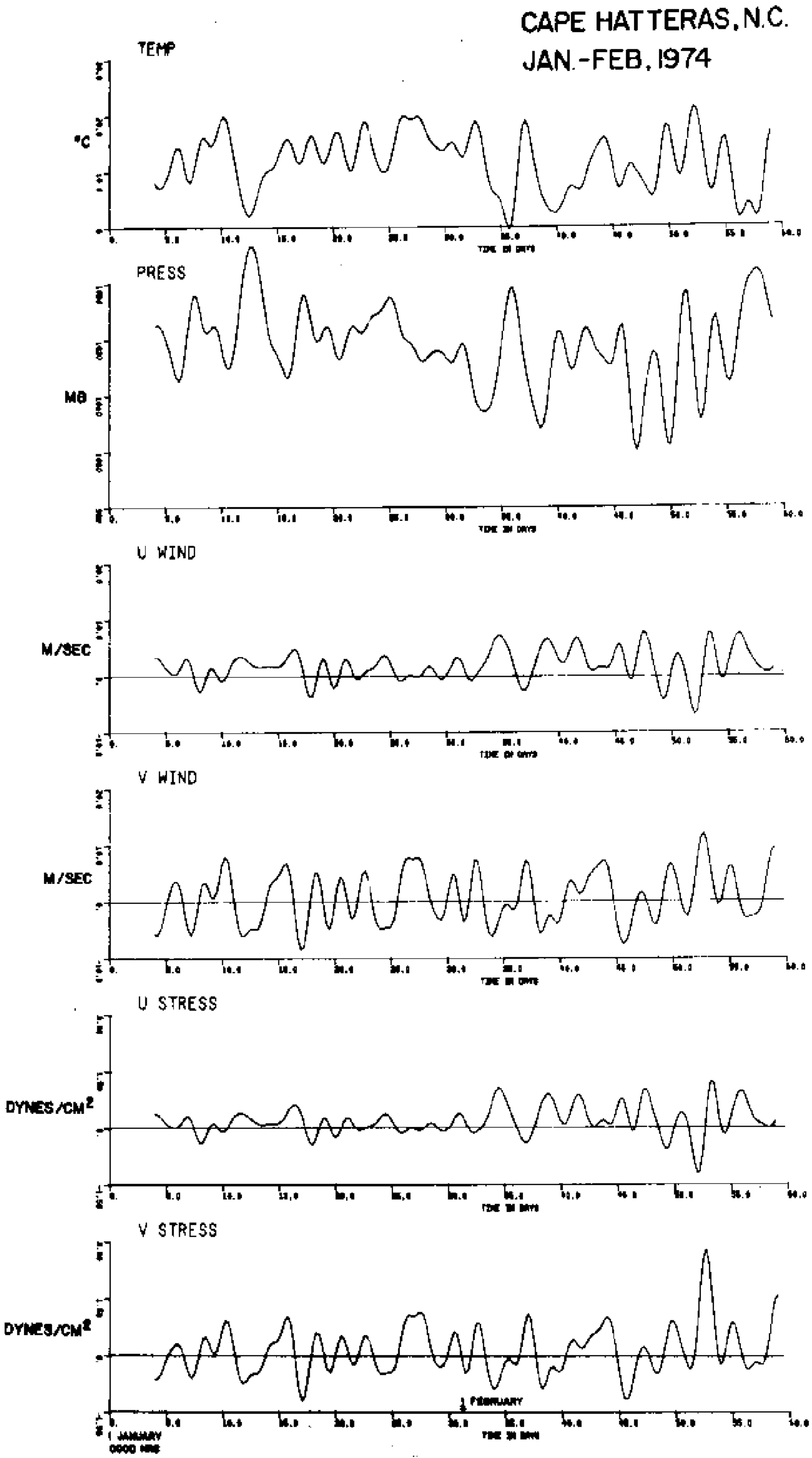

Figure 3 Temperature, pressure, wind velocity components and wind stress components at Cape Hatteras, N. C., Jan. through Feb., 1974

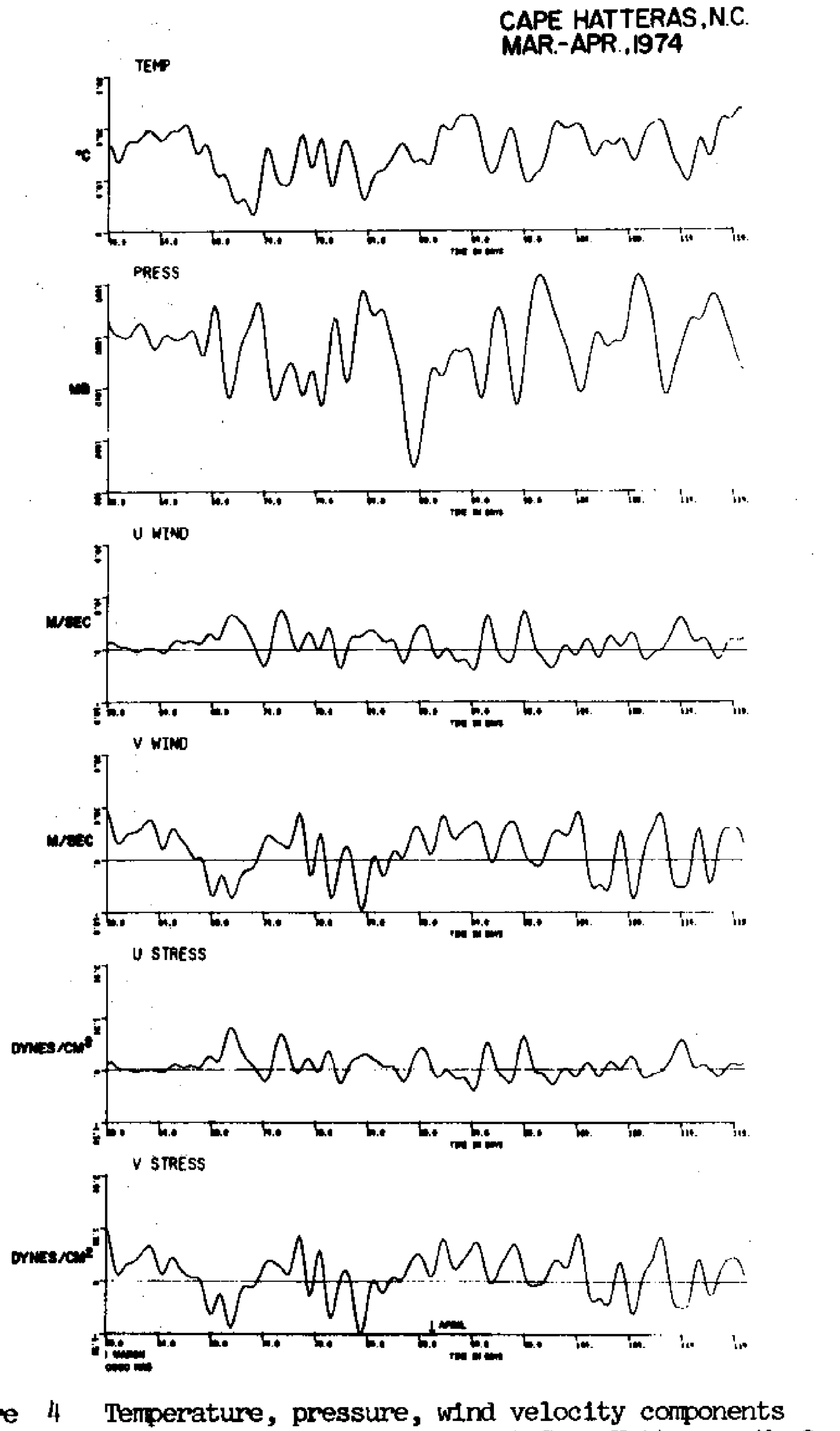

Figure 4 Temperature, pressure, wind velocity components and wind stress components at Cape Hatteras, N. C., Mar. through Apr., 1974

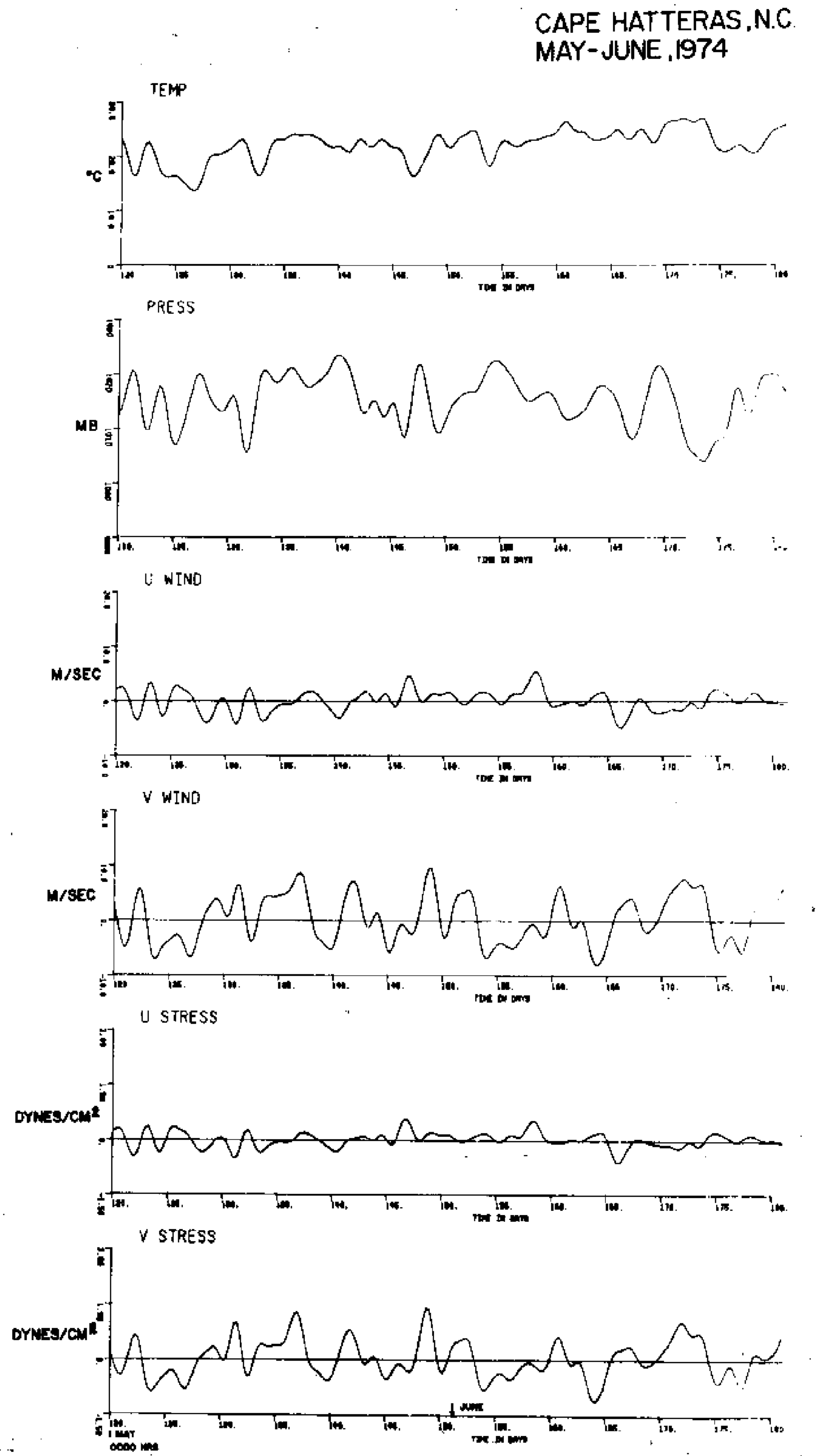

Figure 5 Temperature, pressure, wind velocity components and wind stress components at Cape Hatteras, N. C., May through June, 1974

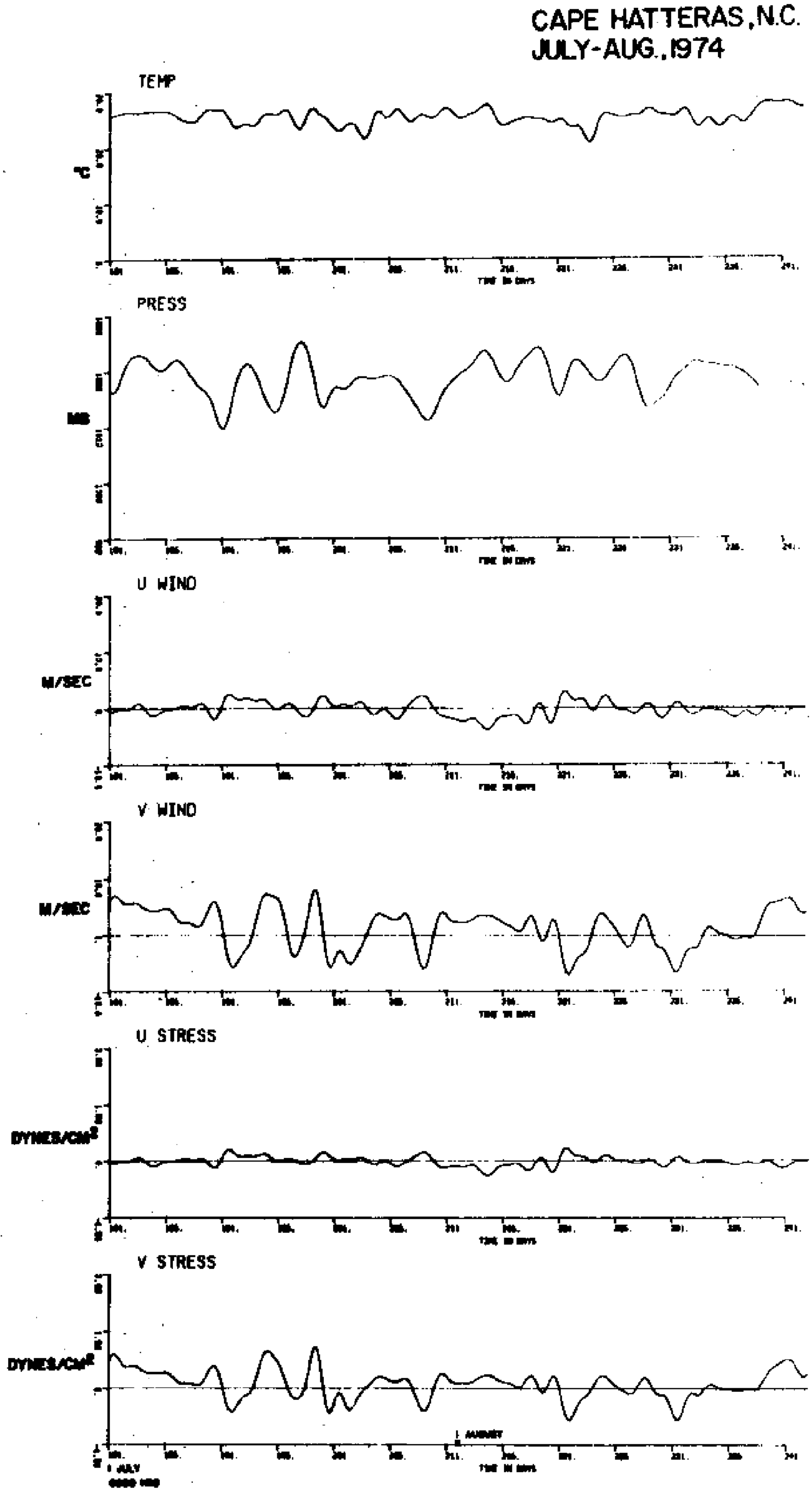

Figure 6 Temperature, pressure, wind velocity components and wind stress components at Cape Hatteras, N. C., July through Aug., 1974

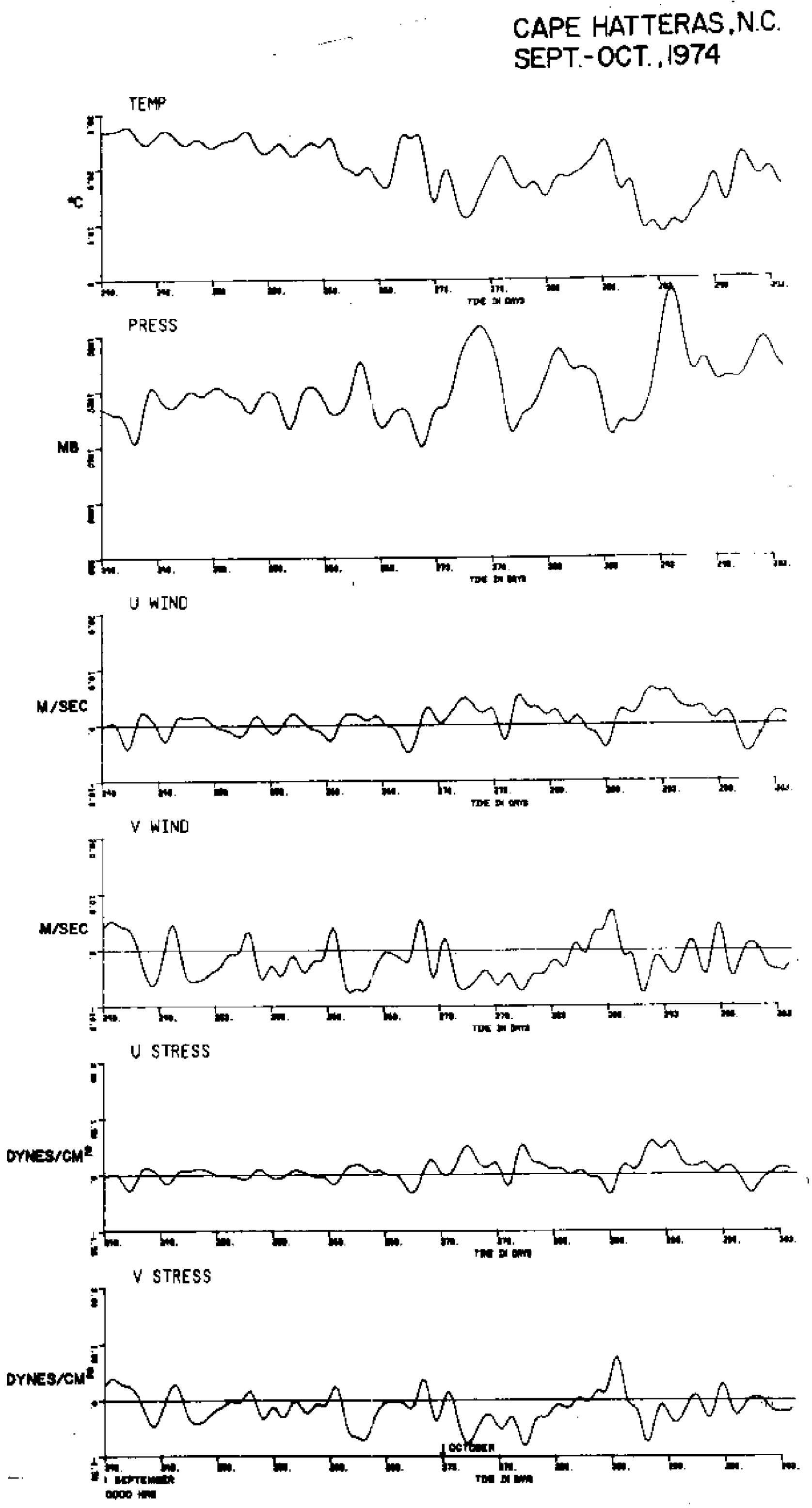

Figure 7 Temperature, pressure, wind velocity components and wind stress components at Cape Hatteras, N. C., Sept. through Oct., 1974

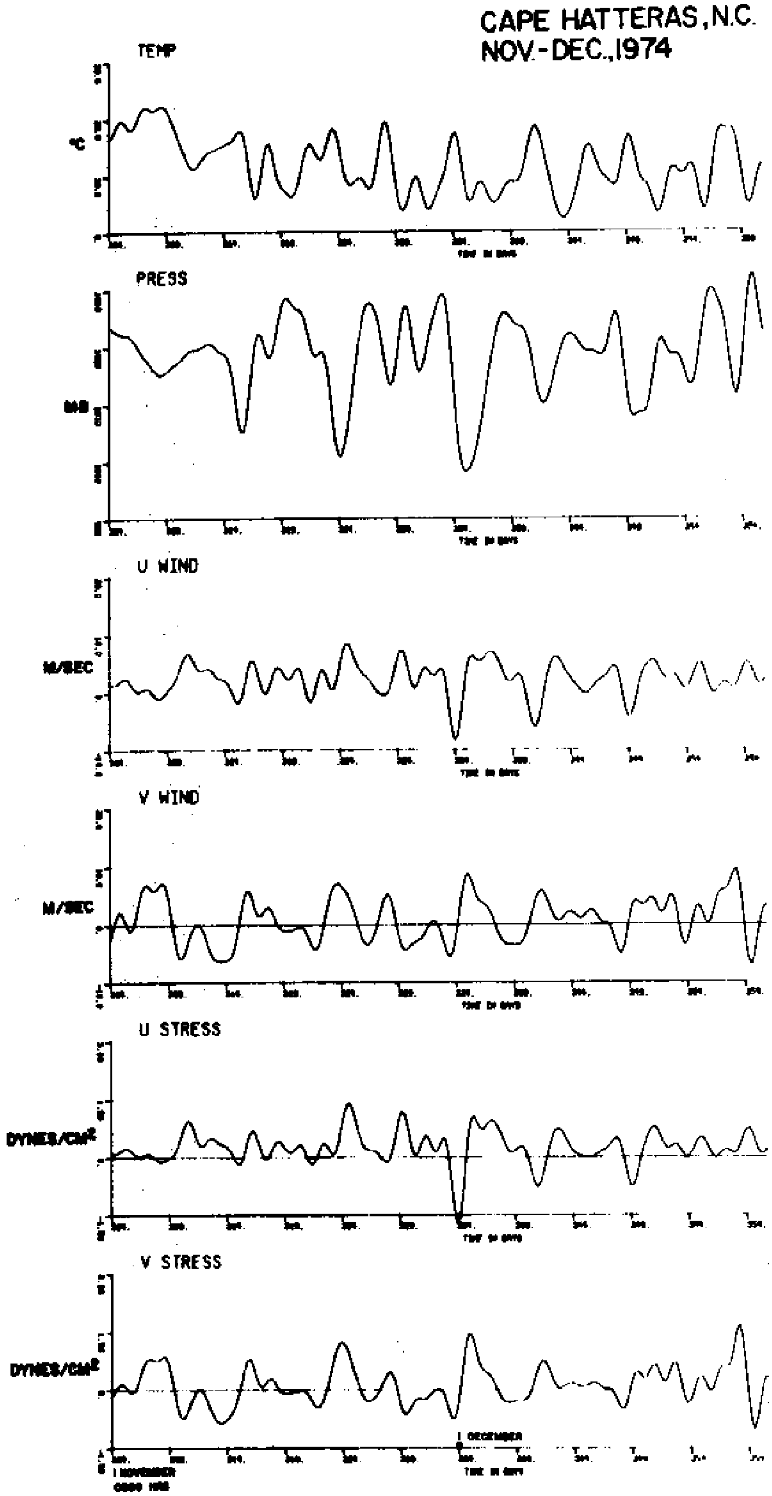

Figure 8 Temperature, pressure, wind velocity components and wind stress components at Cape Hatteras, N. C., Nov. through Dec., 1974

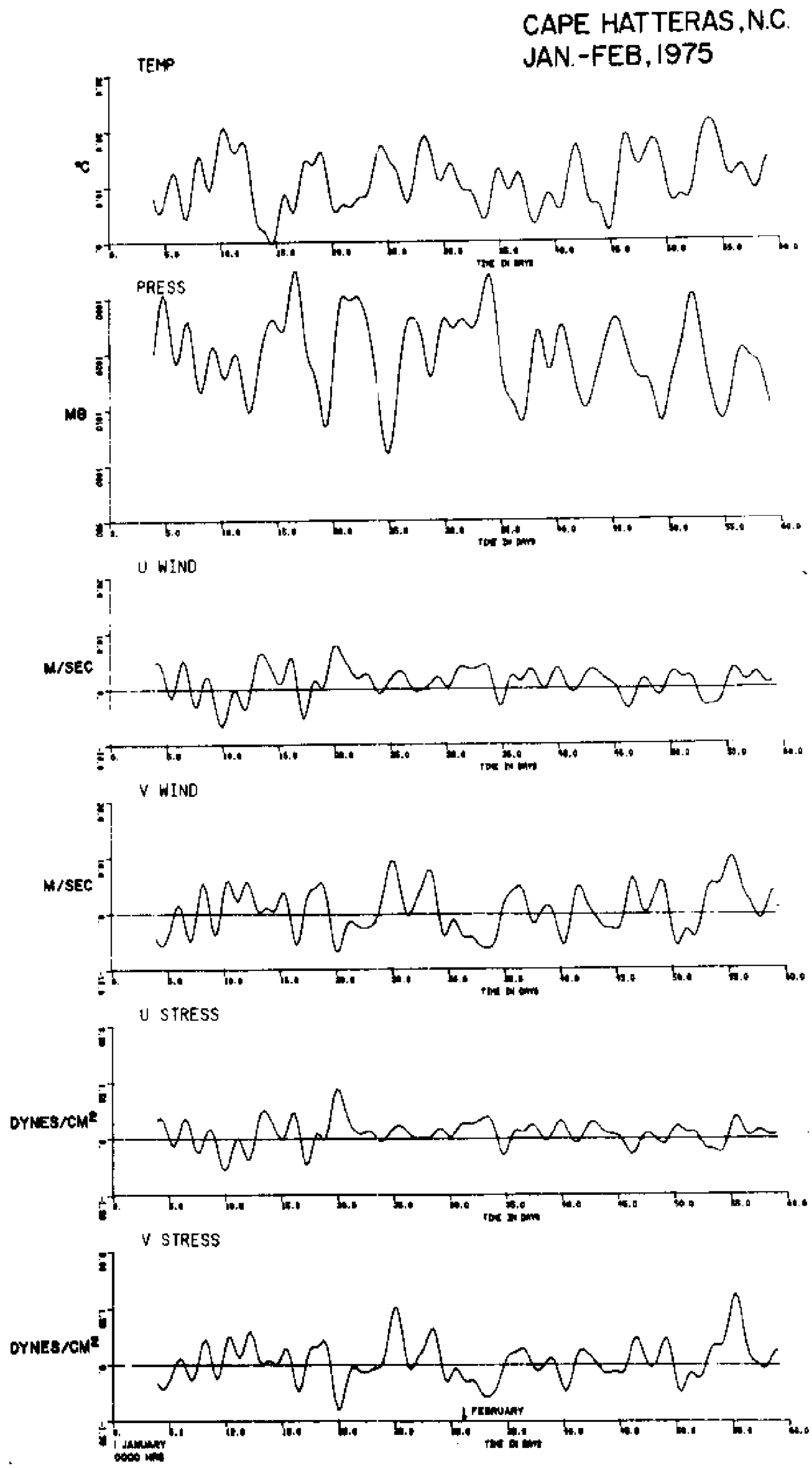

Figure 9 Temperature, pressure, wind velocity components and wind stress components at Cape Hatteras, N. C., Jan. through Feb., 1975

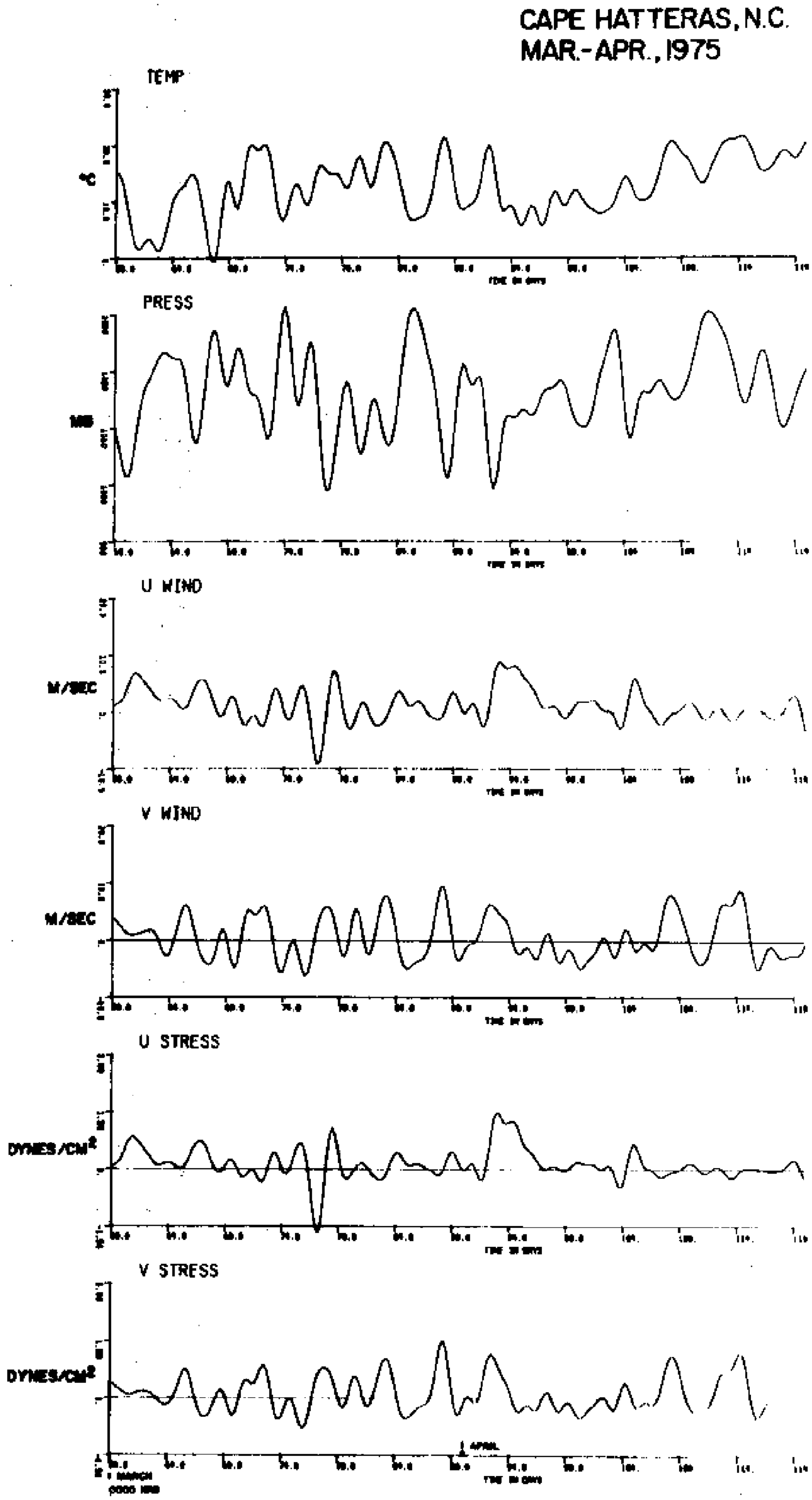

Figure 10 Temperature, pressure, wind velocity components and wind stress components at Cape Hatteras, N. C., Mar. through Apr. 1975

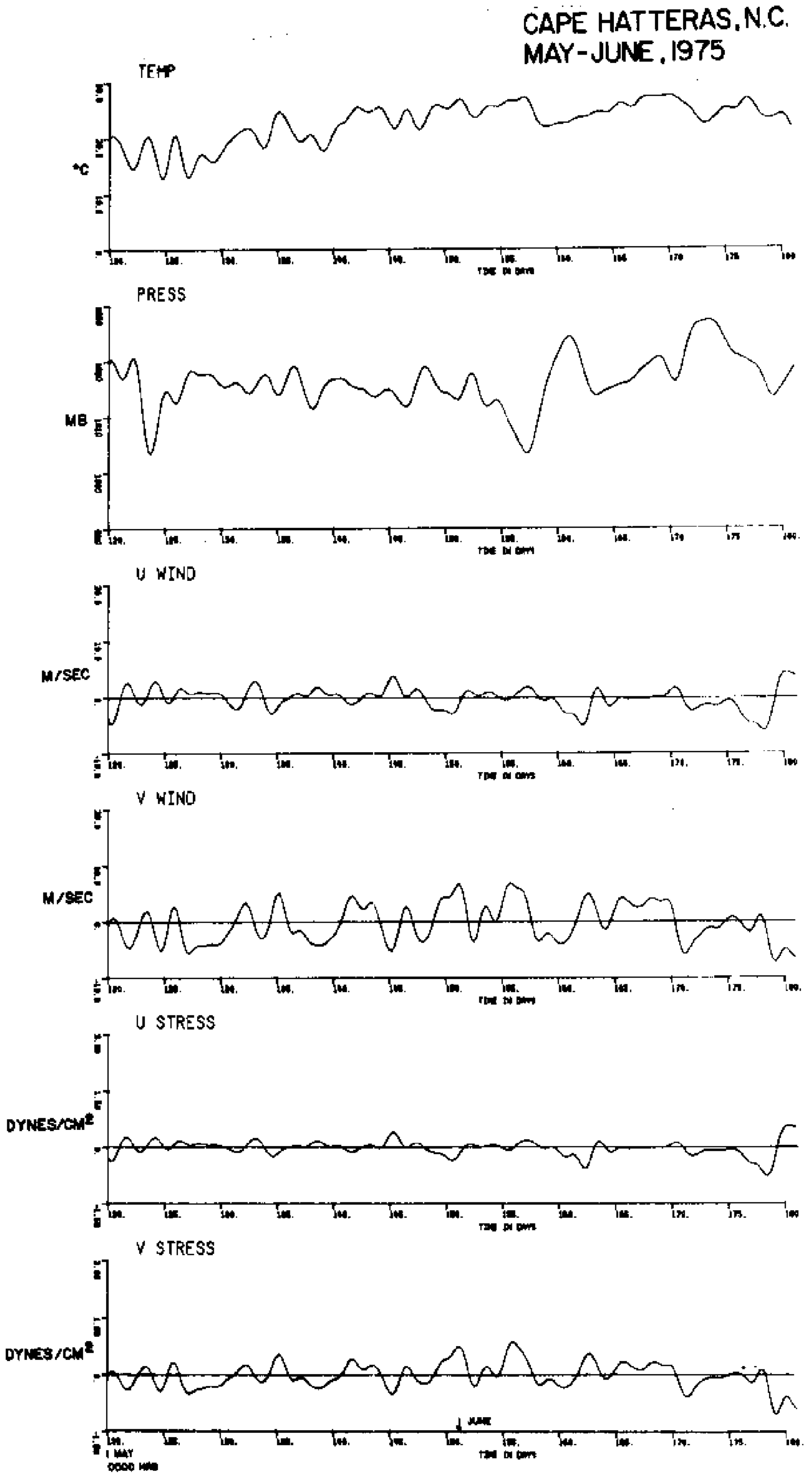

Figure 11 Temperature, pressure, wind velocity components and wind stress components at Cape Hatteras, N. C., May through June, 1975

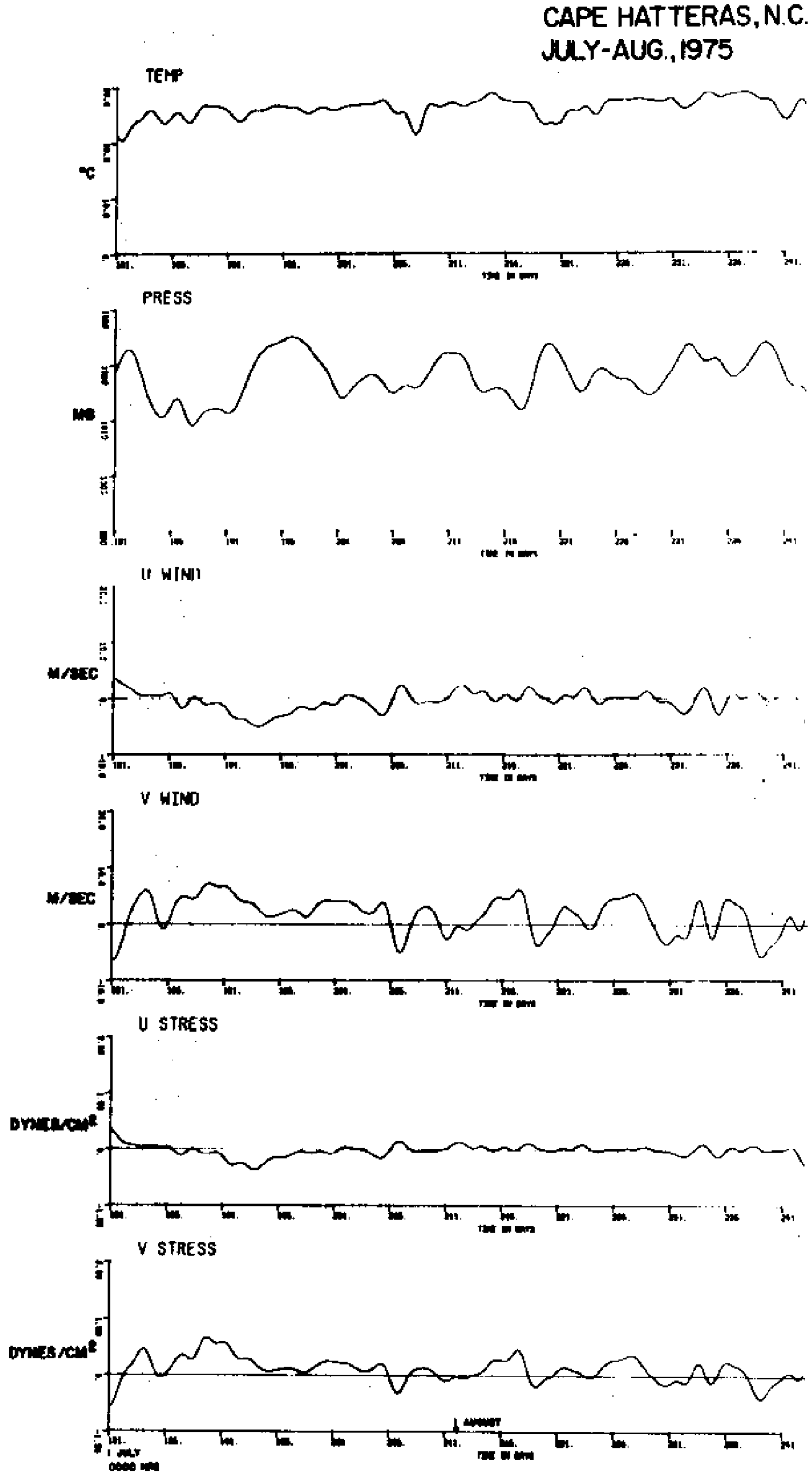

Figure 12 Temperature, pressure, wind velocity components and wind stress components at Cape Hatteras, N. C., July through Aug., 1975

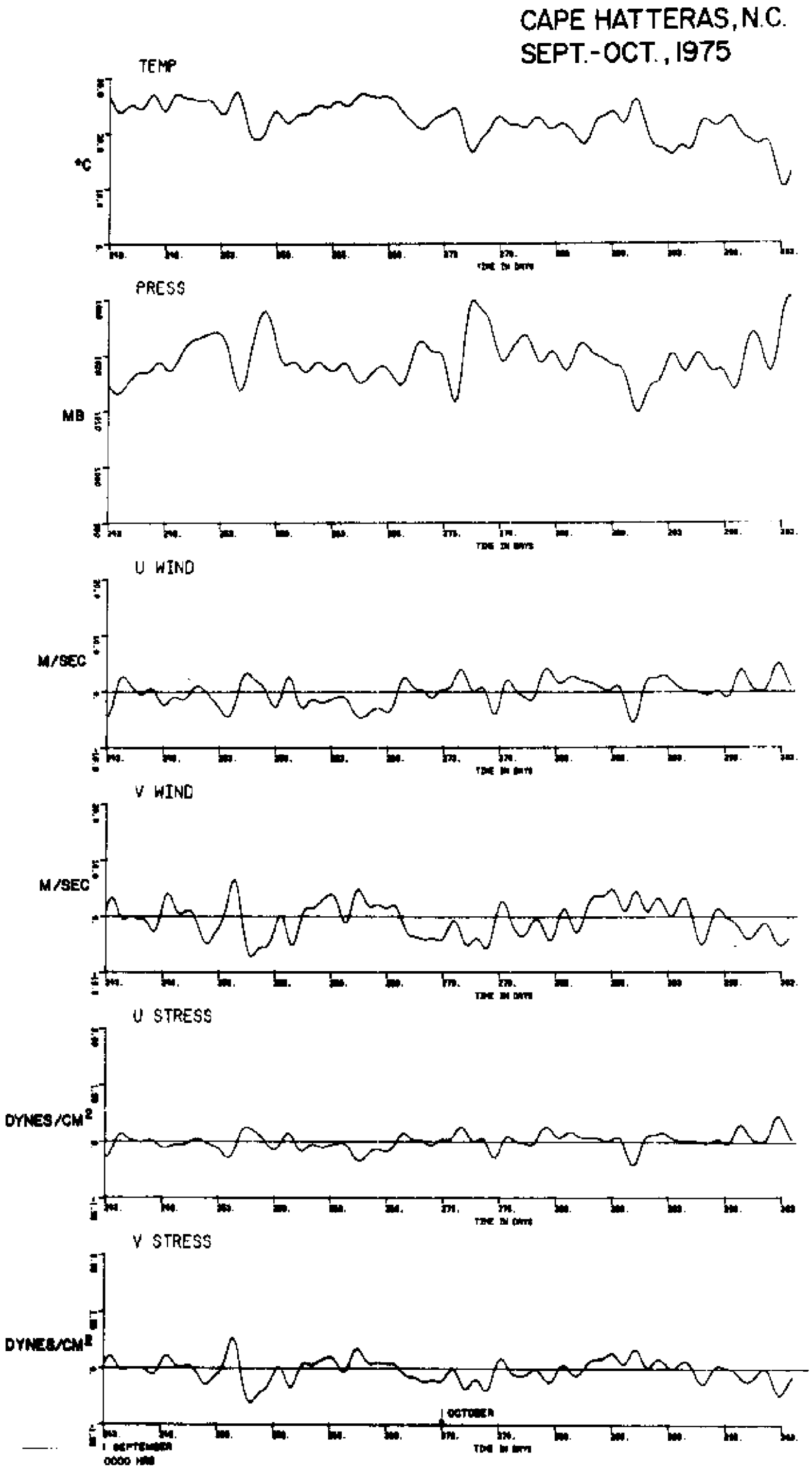

Figure 13 Temperature, pressure, wind velocity components and wind stress components at Cape Hatteras, N. C., Sept. through Oct., 1975

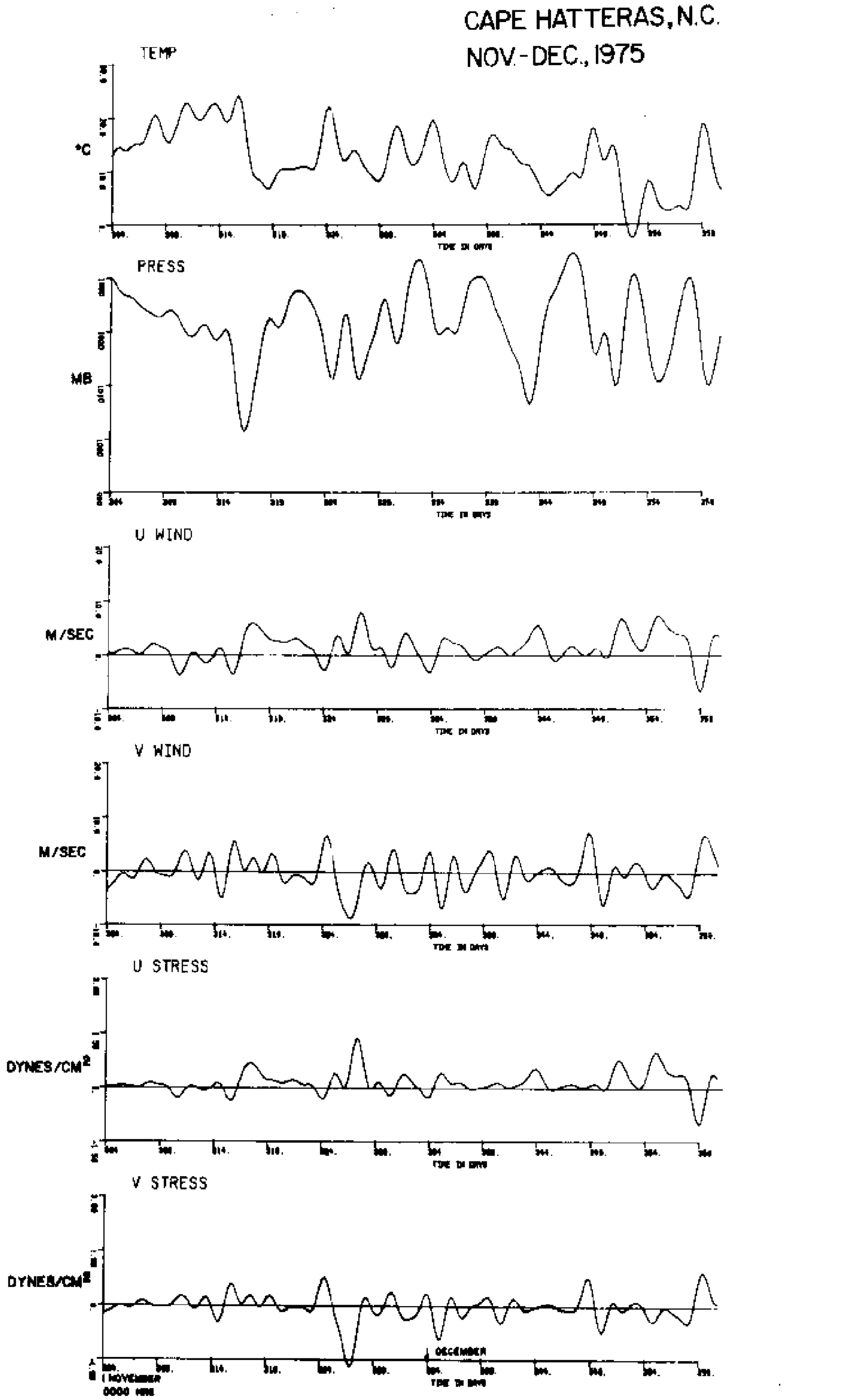

Figure 14 Temperature, pressure, wind velocity components and wind stress components at Cape Hatteras, N. C., Nov. through Dec., 1975

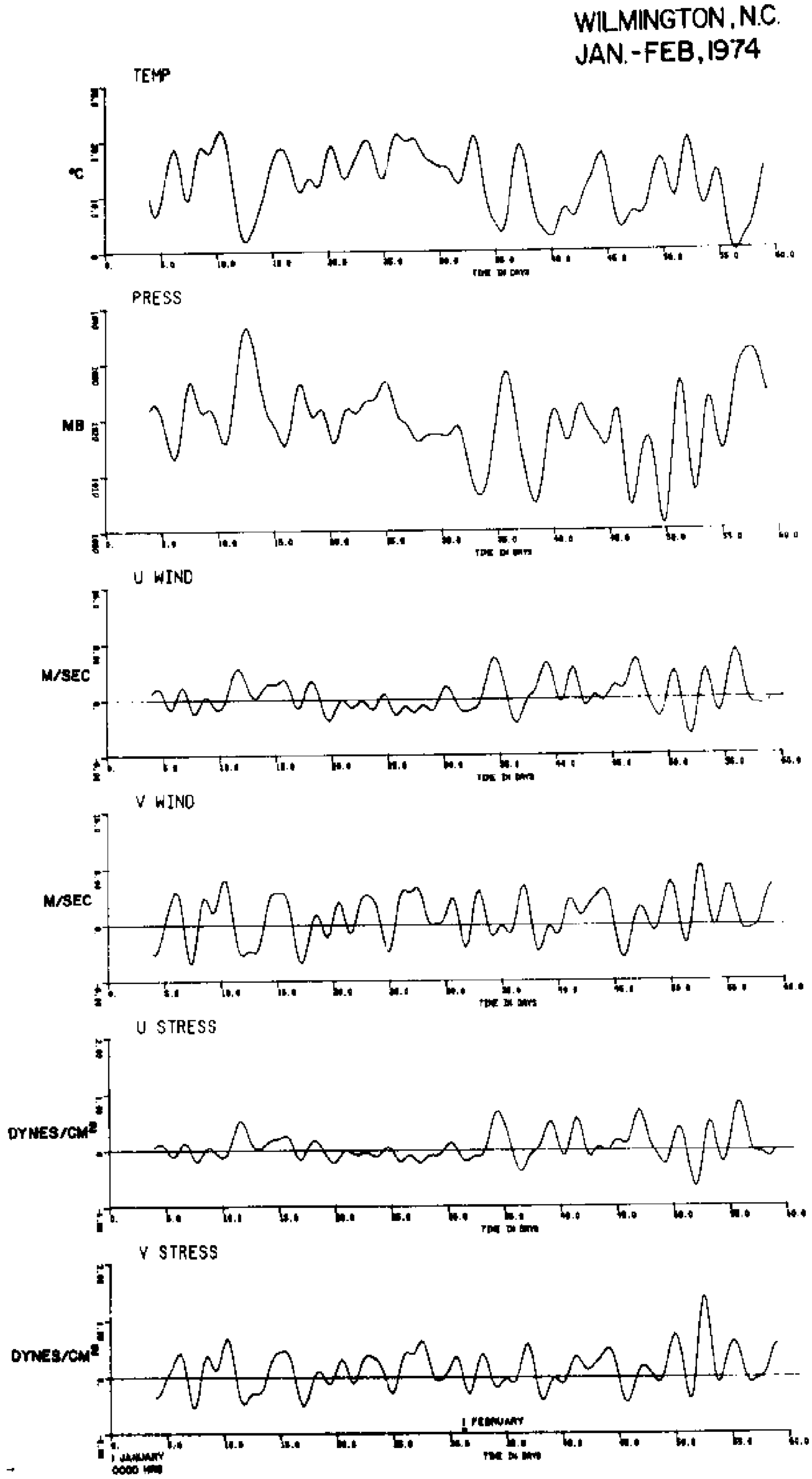

Figure 15 Temperature, pressure, wind velocity components and wind stress components at Wilmington, N. C., Jan. through Feb., 1974

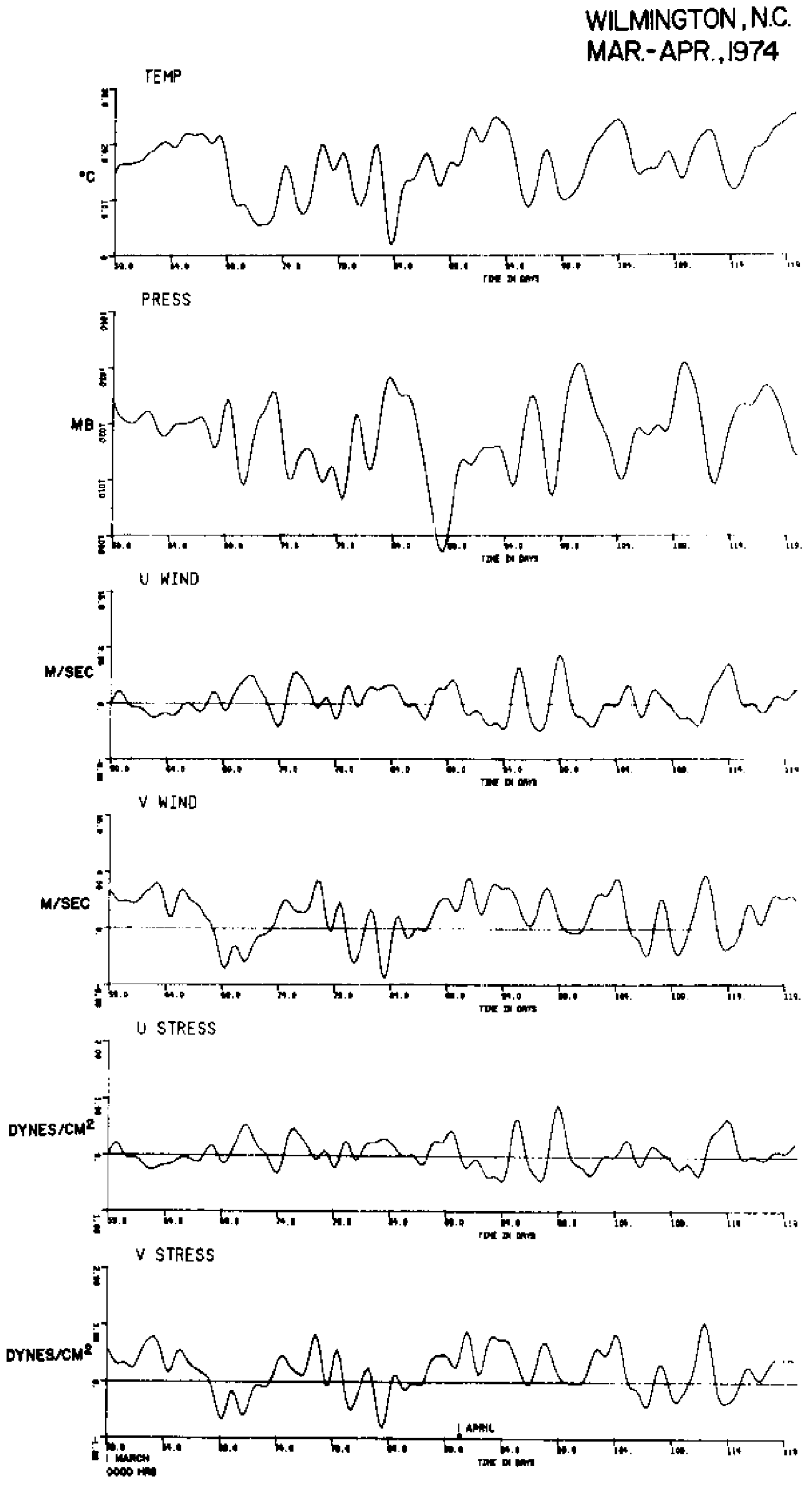

Figure 16 Temperature, pressure, wind velocity components and wind stress components at Wilmington, N. C., Mar. through Apr., 1974

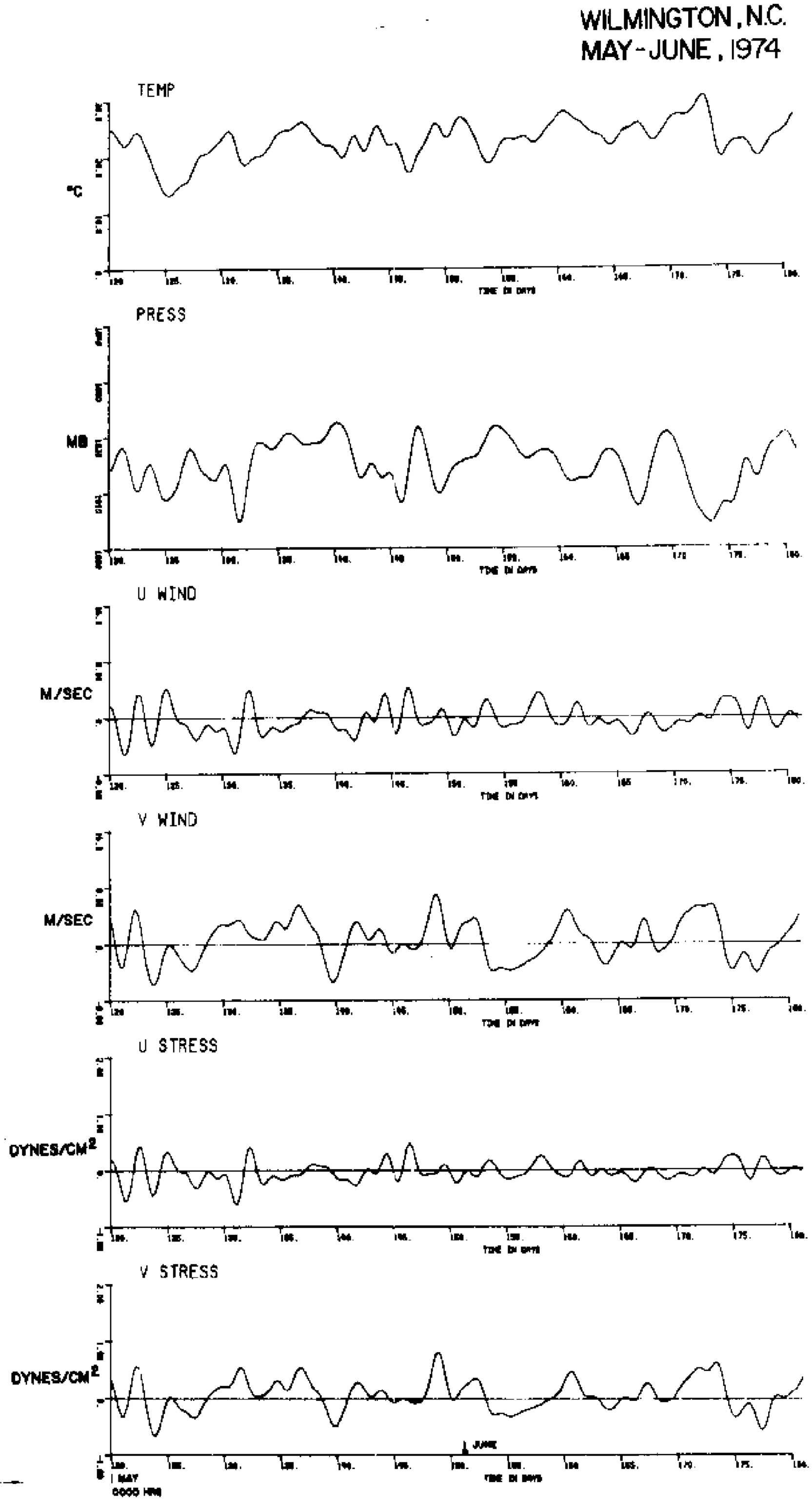

Figure 17 Temperature, pressure, wind velocity components and wind stress components at Wilmington, N. C., May through June, 1974

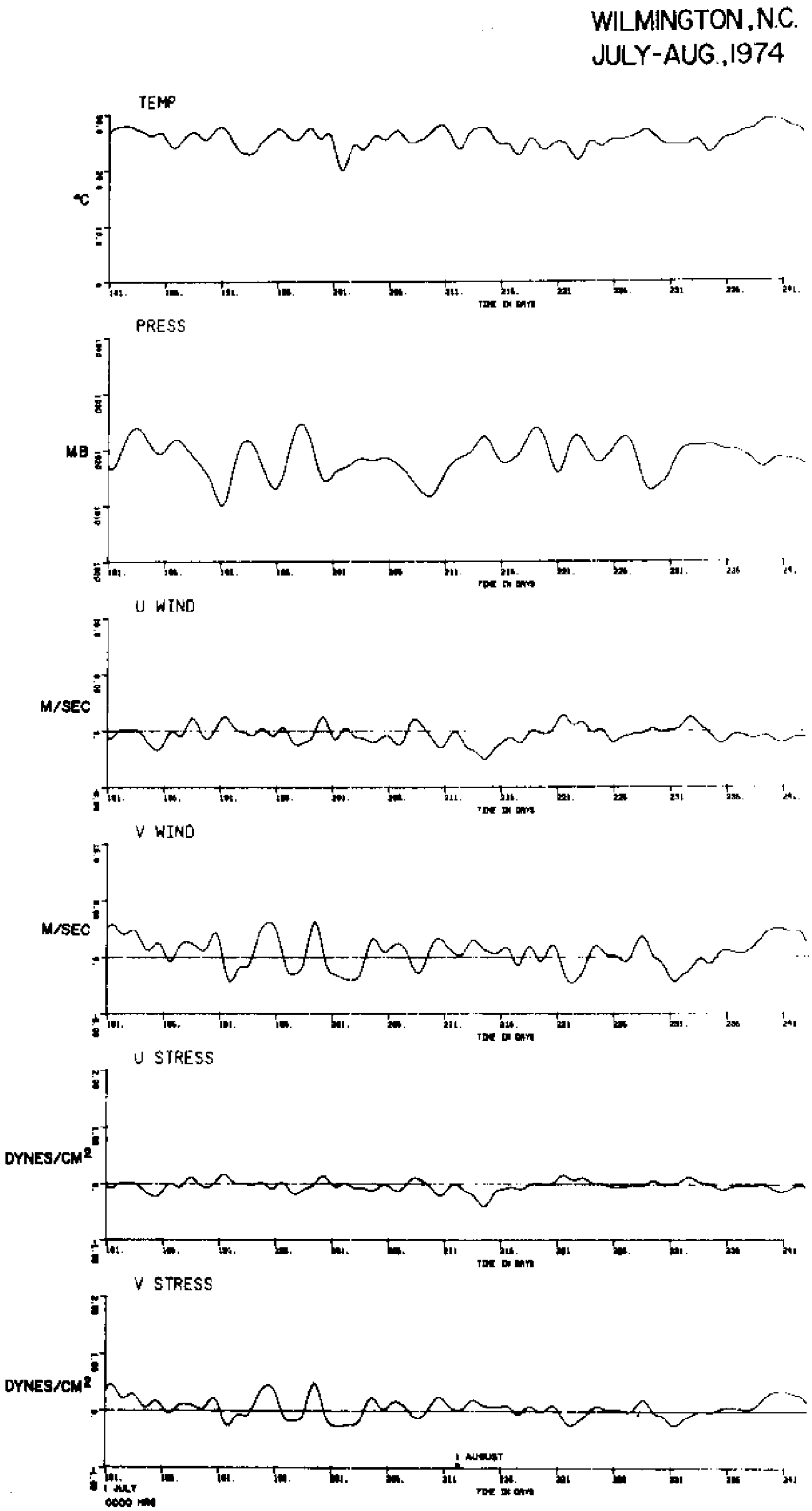

Figure 18 Temperature, pressure, wind velocity components and wind stress components at Wilmington, N. C., July through Aug., 1974

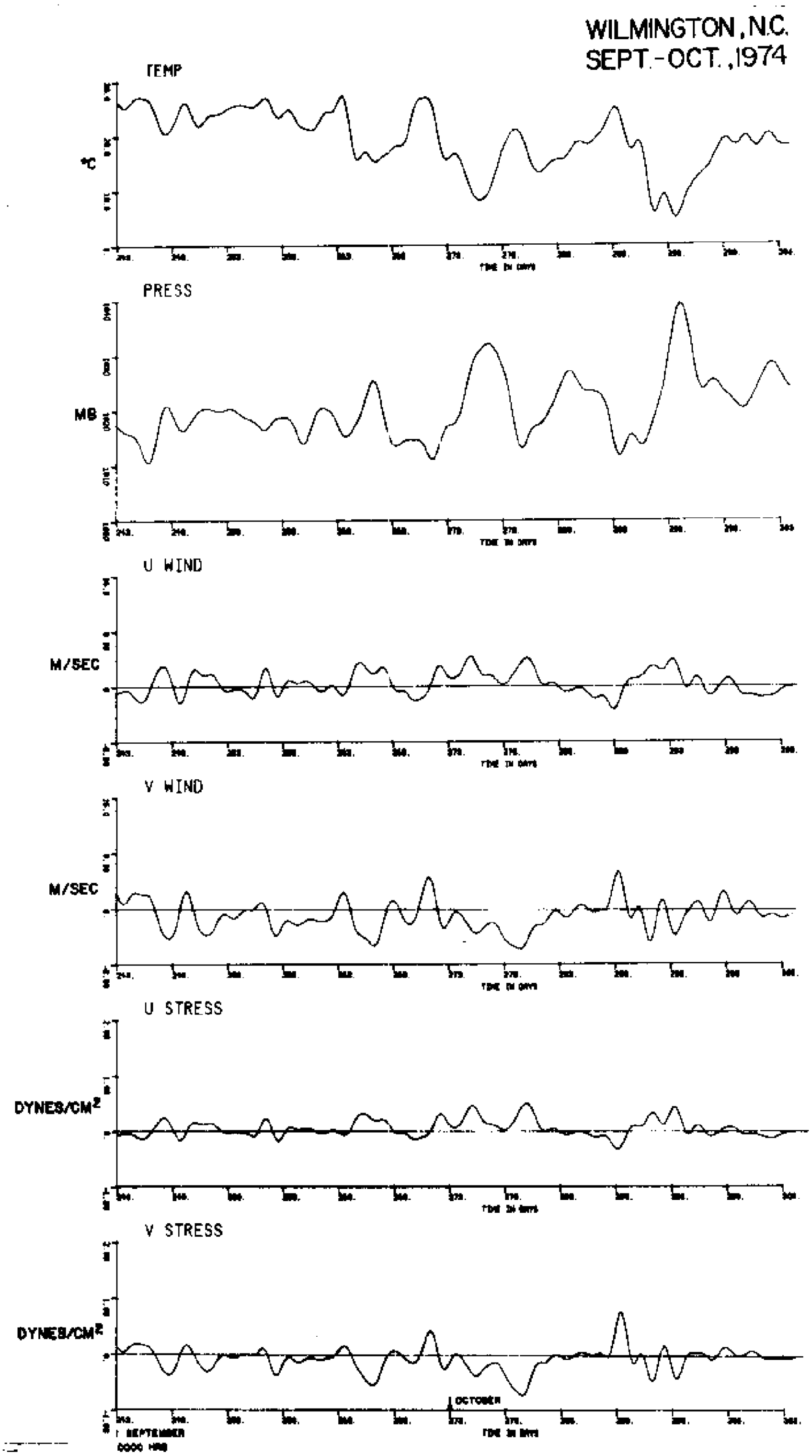

Figure 19 Temperature, pressure, wind velocity components and wind stress components at Wilmington, N. C., Sept. through Oct., 1974

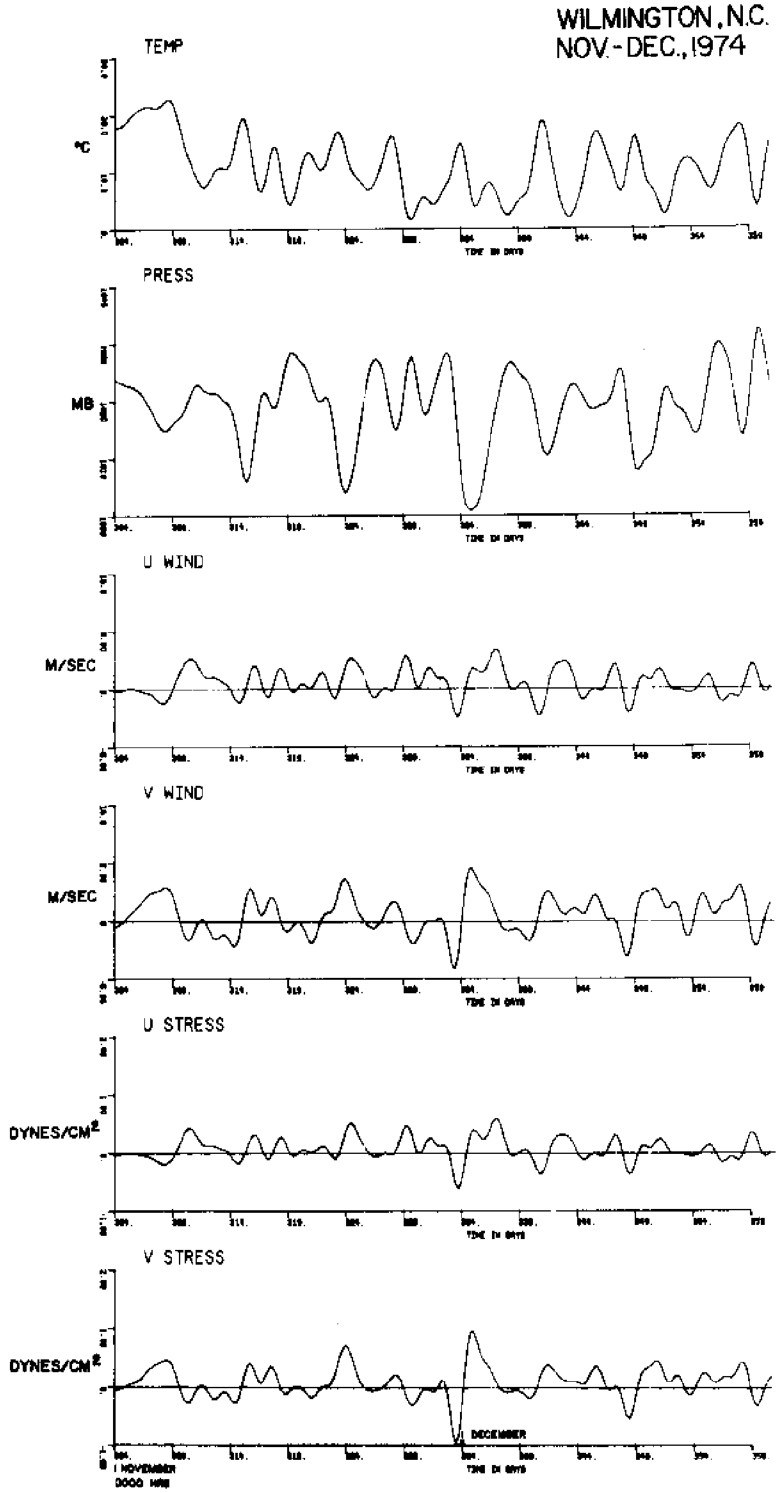

Figure 20 Temperature, pressure, wind velocity components and wind stress components at Wilmington, N. C., Nov. through Dec., 1974

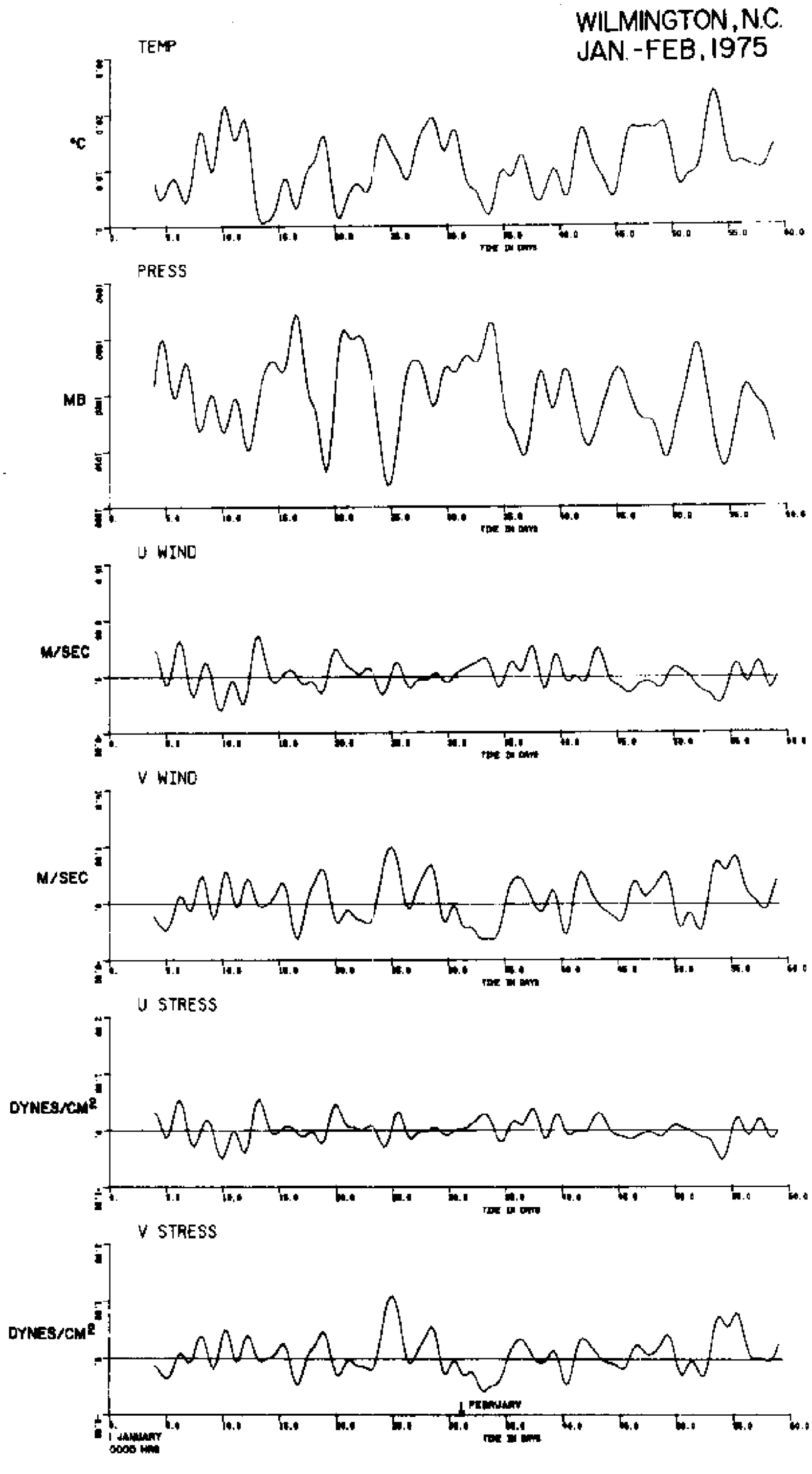

Figure 21 Temperature, pressure, wind velocity components and wind stress components at Wilmington, N. C., Jan. through Feb., 1975

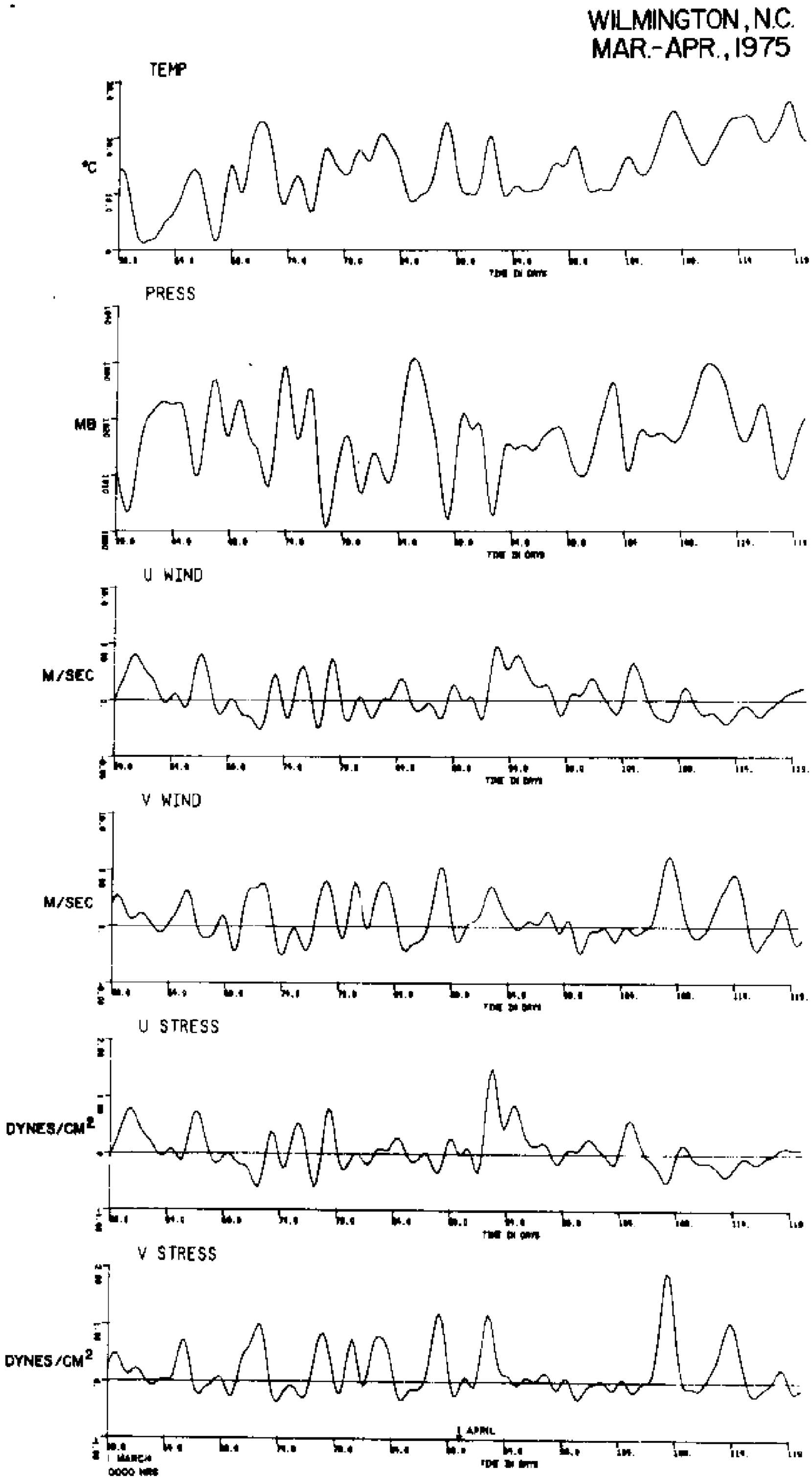

Figure 22 Temperature, pressure, wind velocity components and wind stress components at Wilmington, N. C., Mar. through Apr., 1975

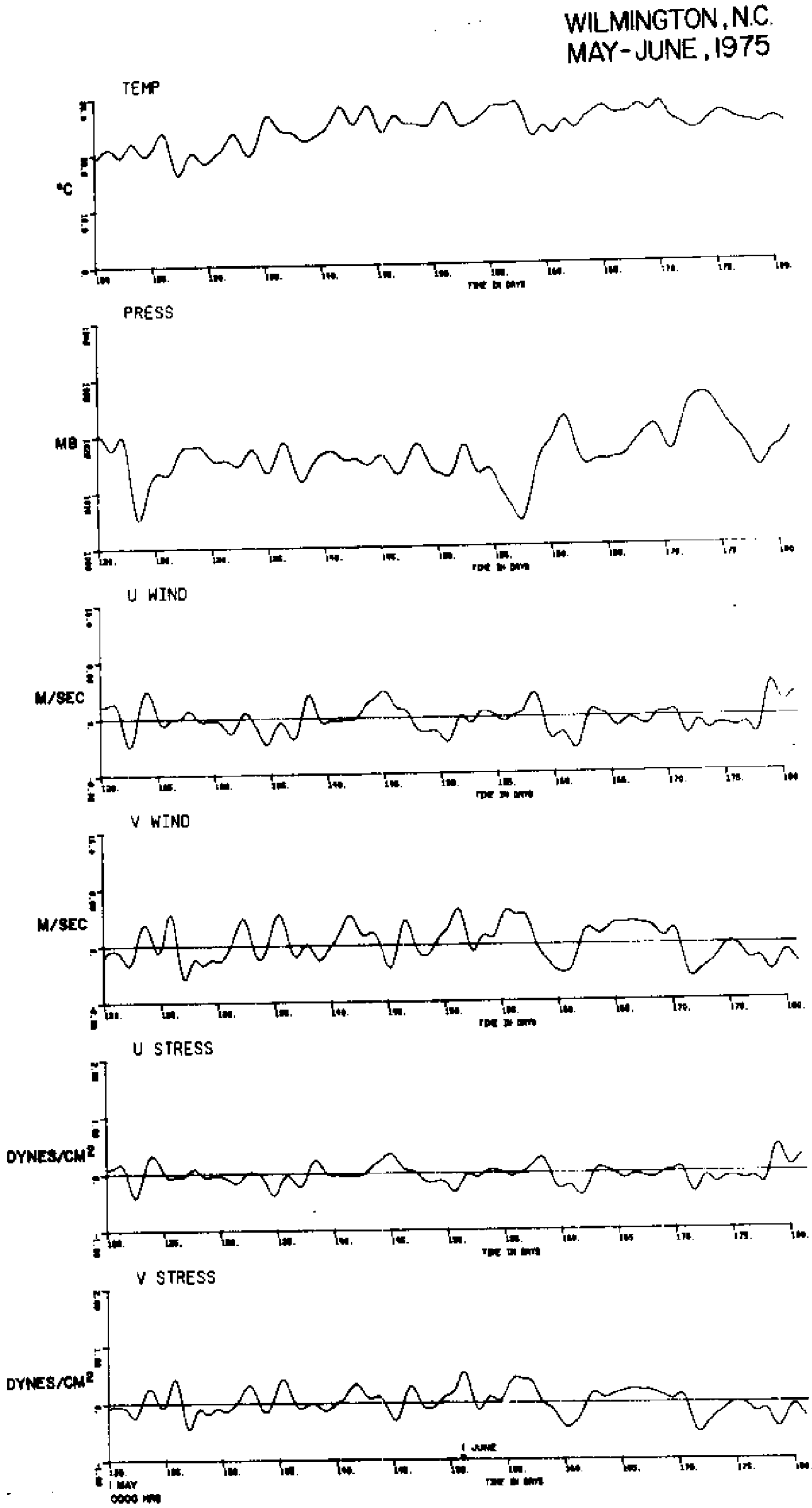

Figure 23 Temperature, pressure, wind velocity components and wind stress components at Wilmington, N. C., May through June, 1975

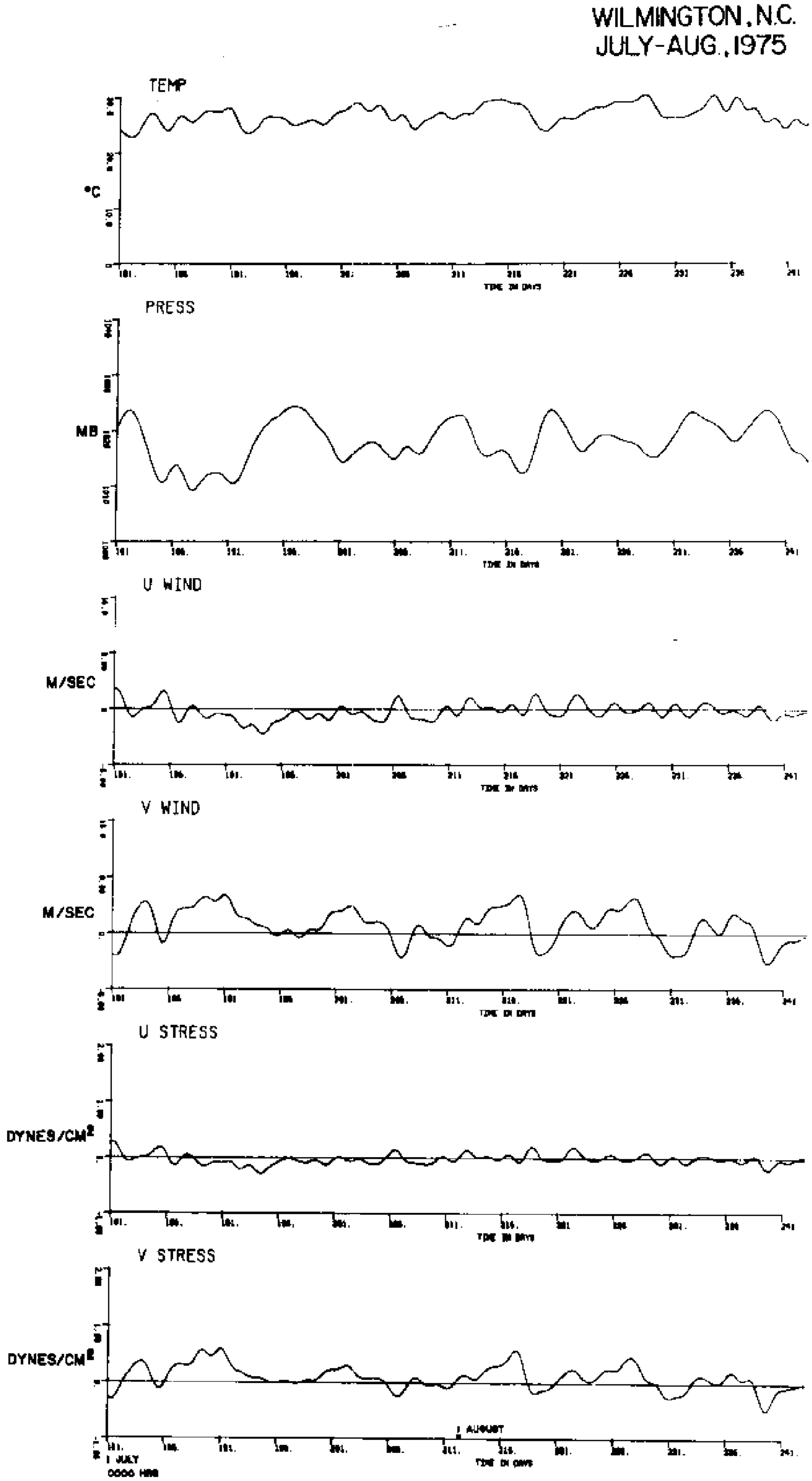

Figure 24 Temperature, pressure, wind velocity components and wind stress components at Wilmington, N. C., July through Aug., 1975

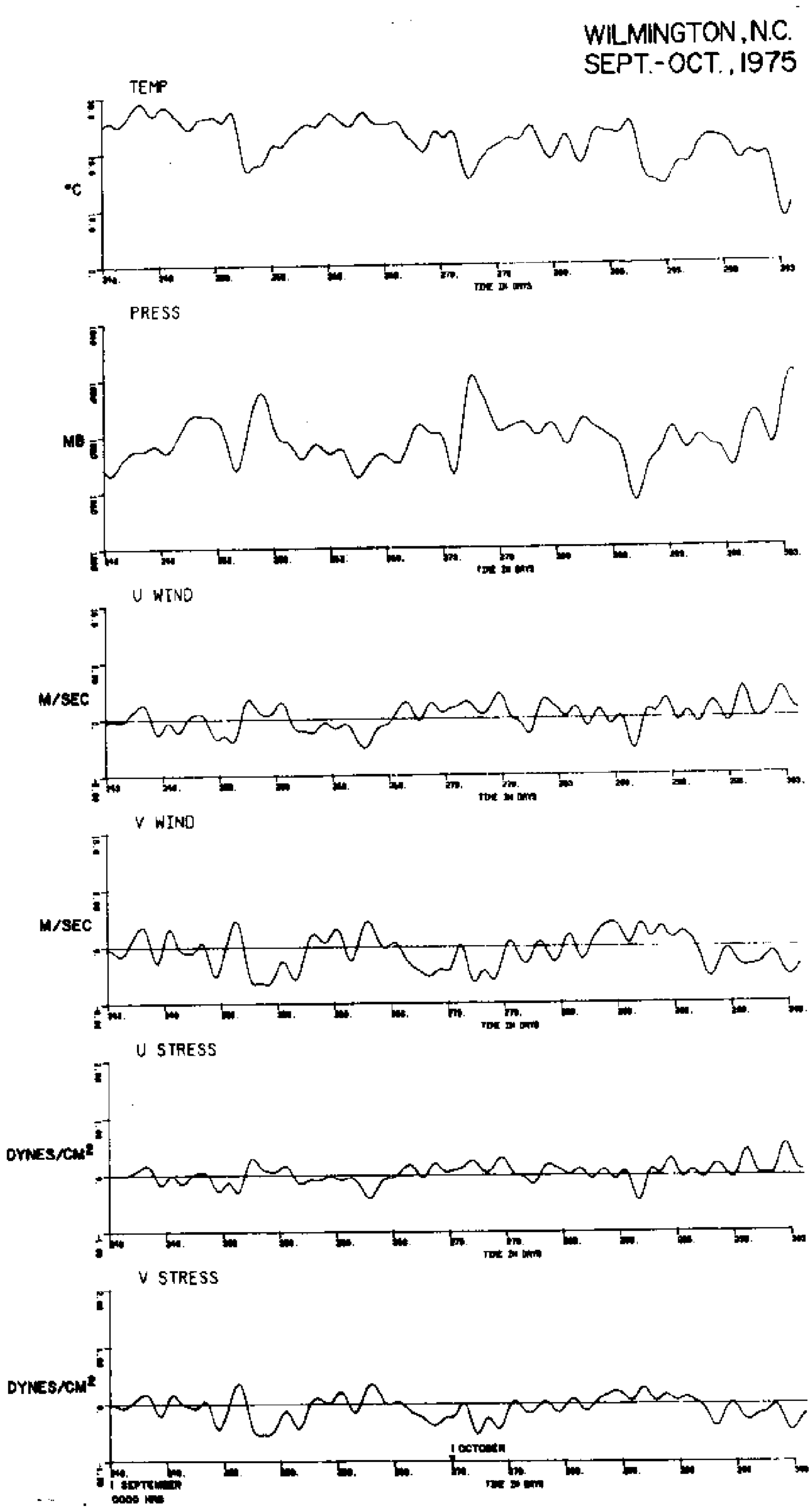

Figure 25 Temperature, pressure, wind velocity components and wind stress components at Wilmington, N. C., Sept. through Oct., 1975

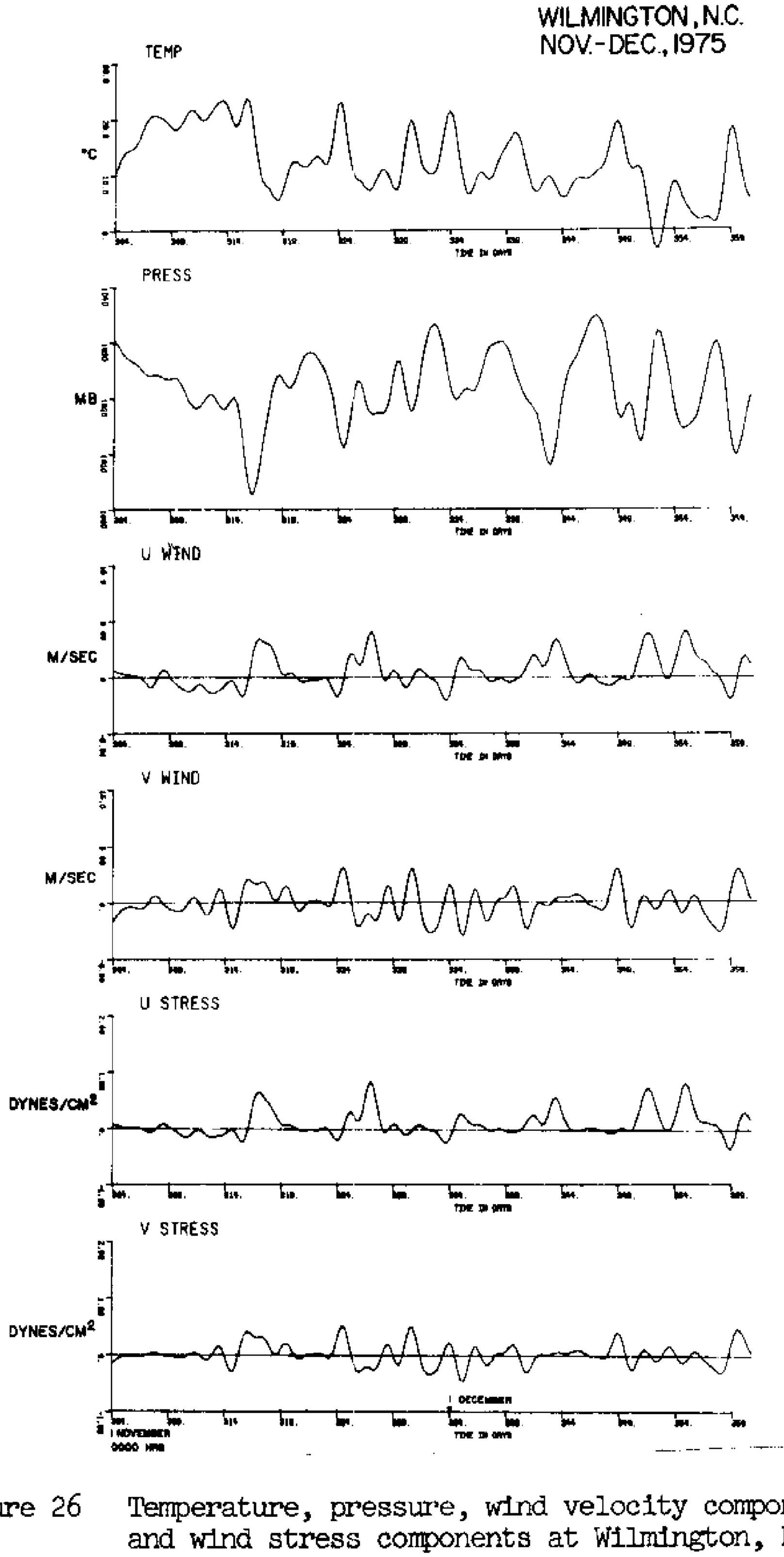

Figure 26 Temperature, pressure, wind velocity components and wind stress components at Wilmington, N. C., Nov. through Dec., 1975

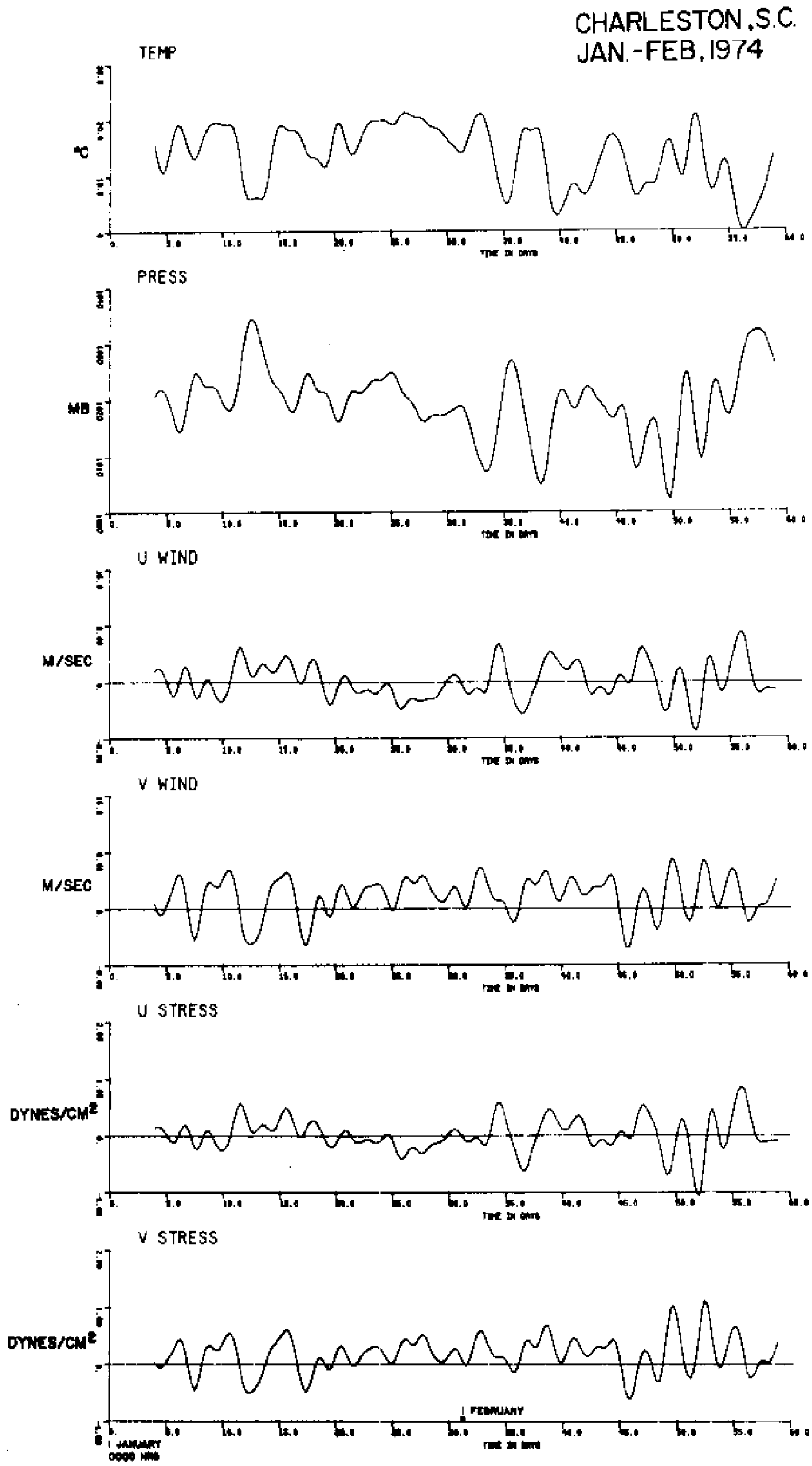

Figure 27 Temperature, pressure, wind velocity components and wind stress components at Charleston, S. C., Jan. through Feb., 1974

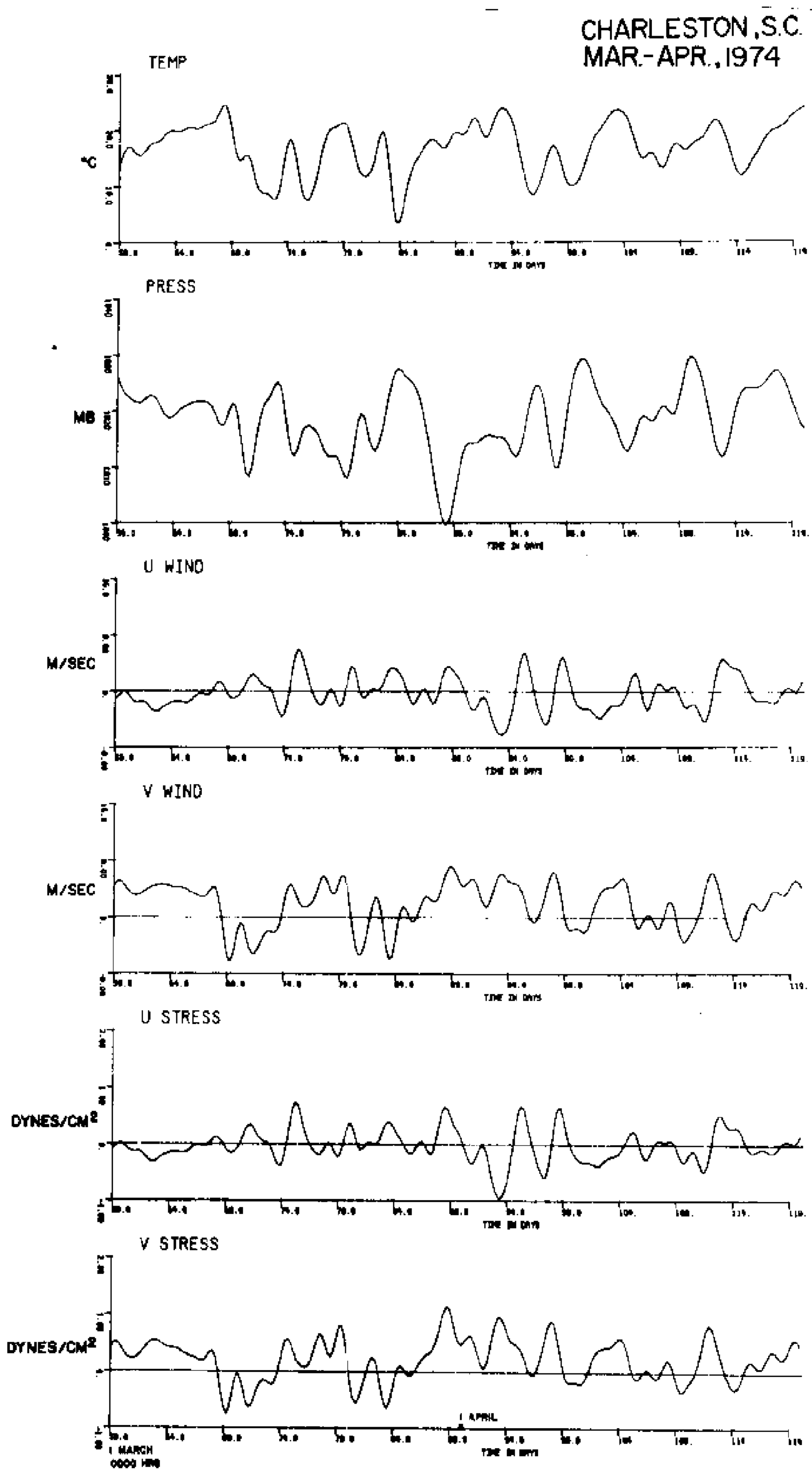

Figure 28 Temperature, pressure, wind velocity components and wind stress components at Charleston, S. C., Mar. through Apr., 1974

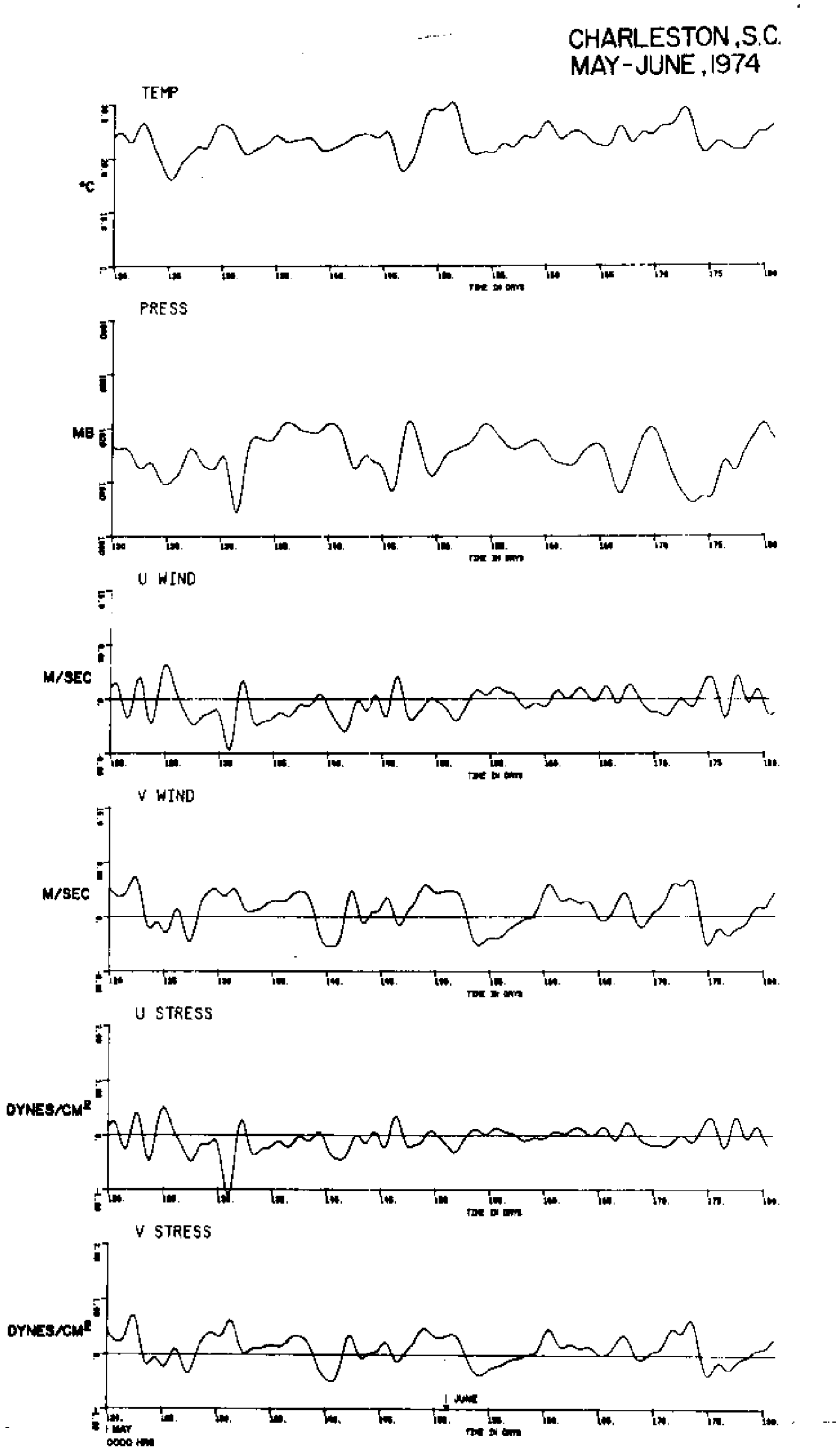

Figure 29 Temperature, pressure, wind velocity components and wind stress components at Charleston, S. C., May through June, 1974

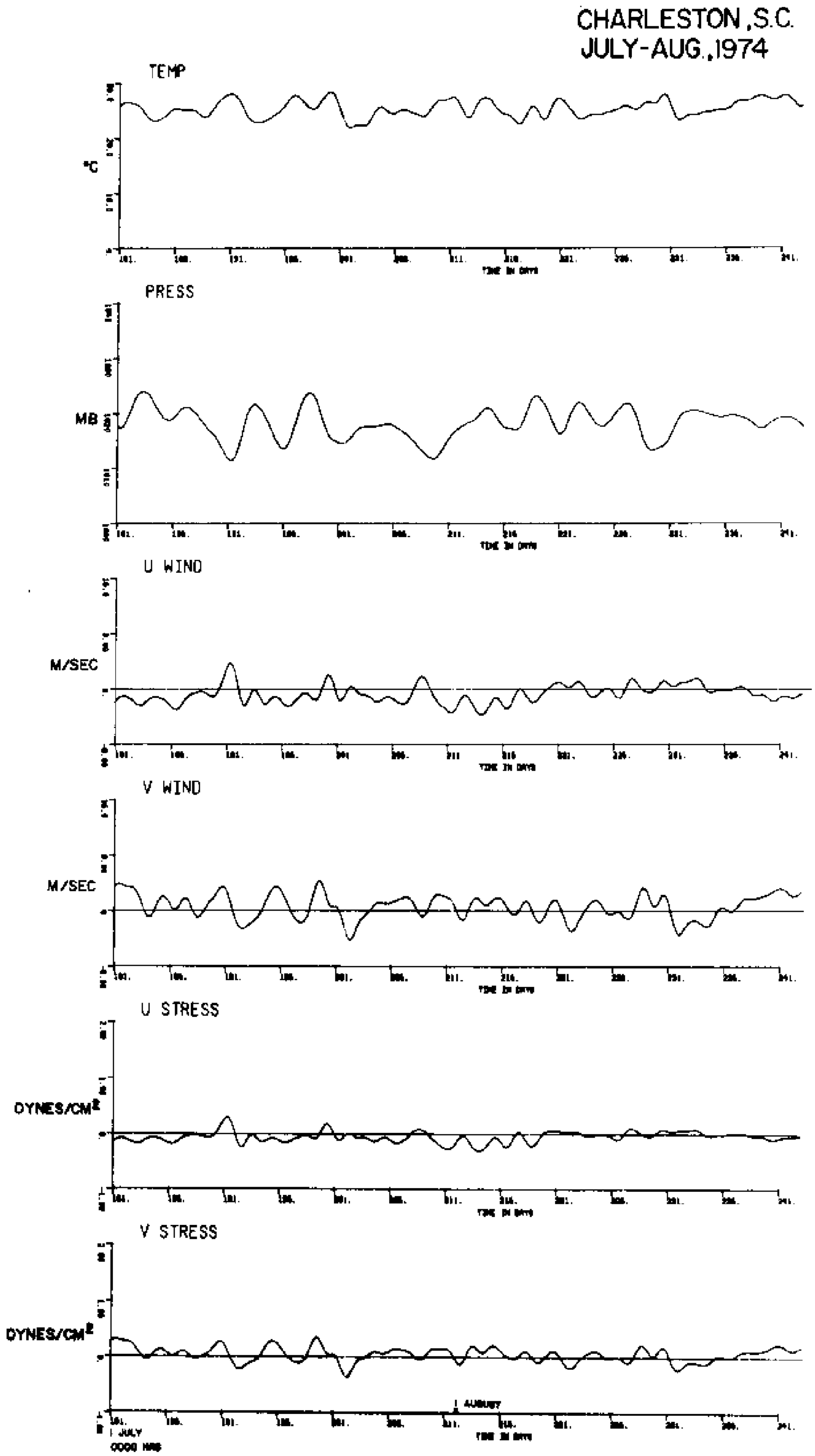

Figure 30 Temperature, pressure, wind velocity components and wind stress components at Charleston, S. C., July through Aug., 1974

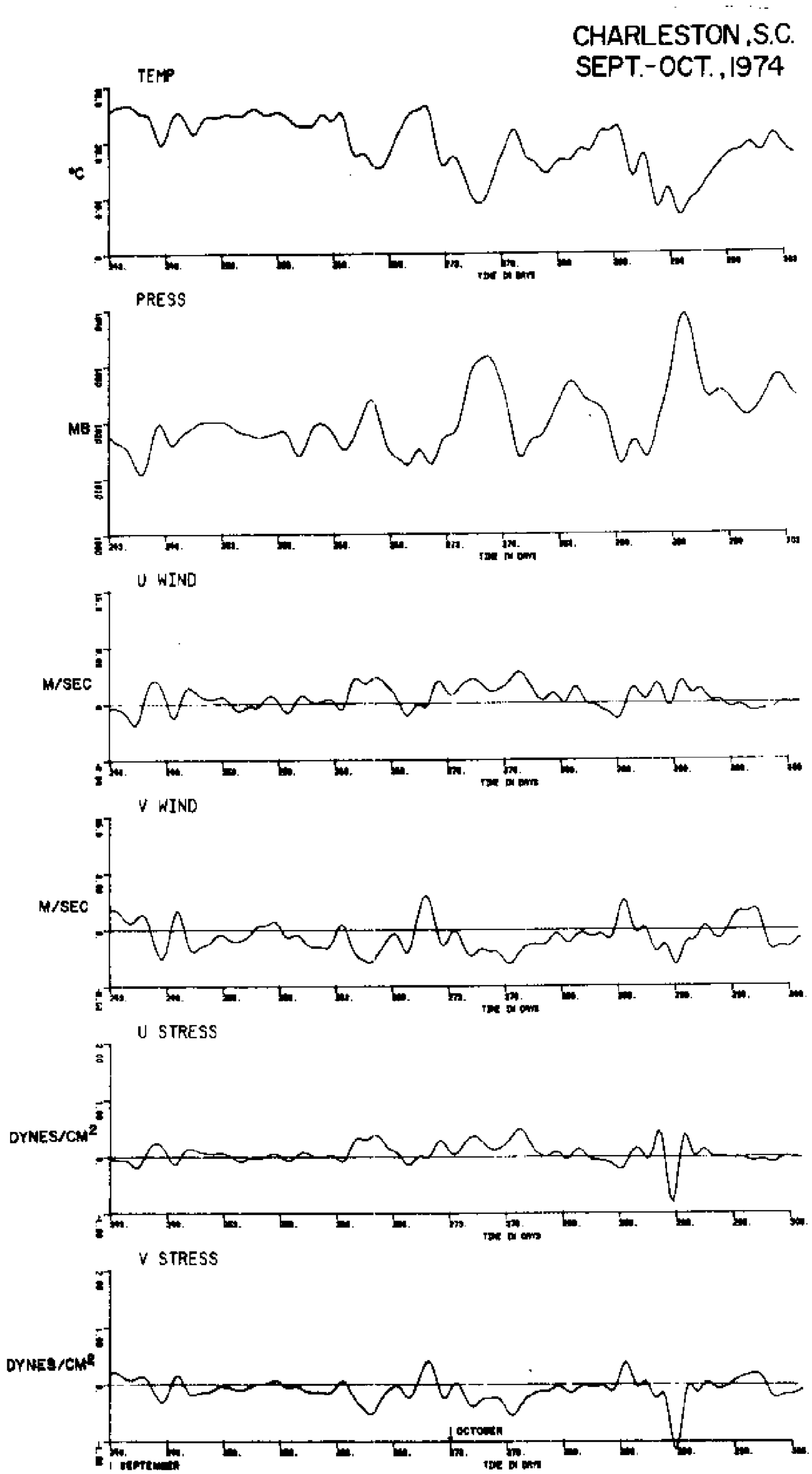

Figure 31 Temperature, pressure, wind velocity components and wind stress components at Charleston, S. C., Sept. through Oct., 1974

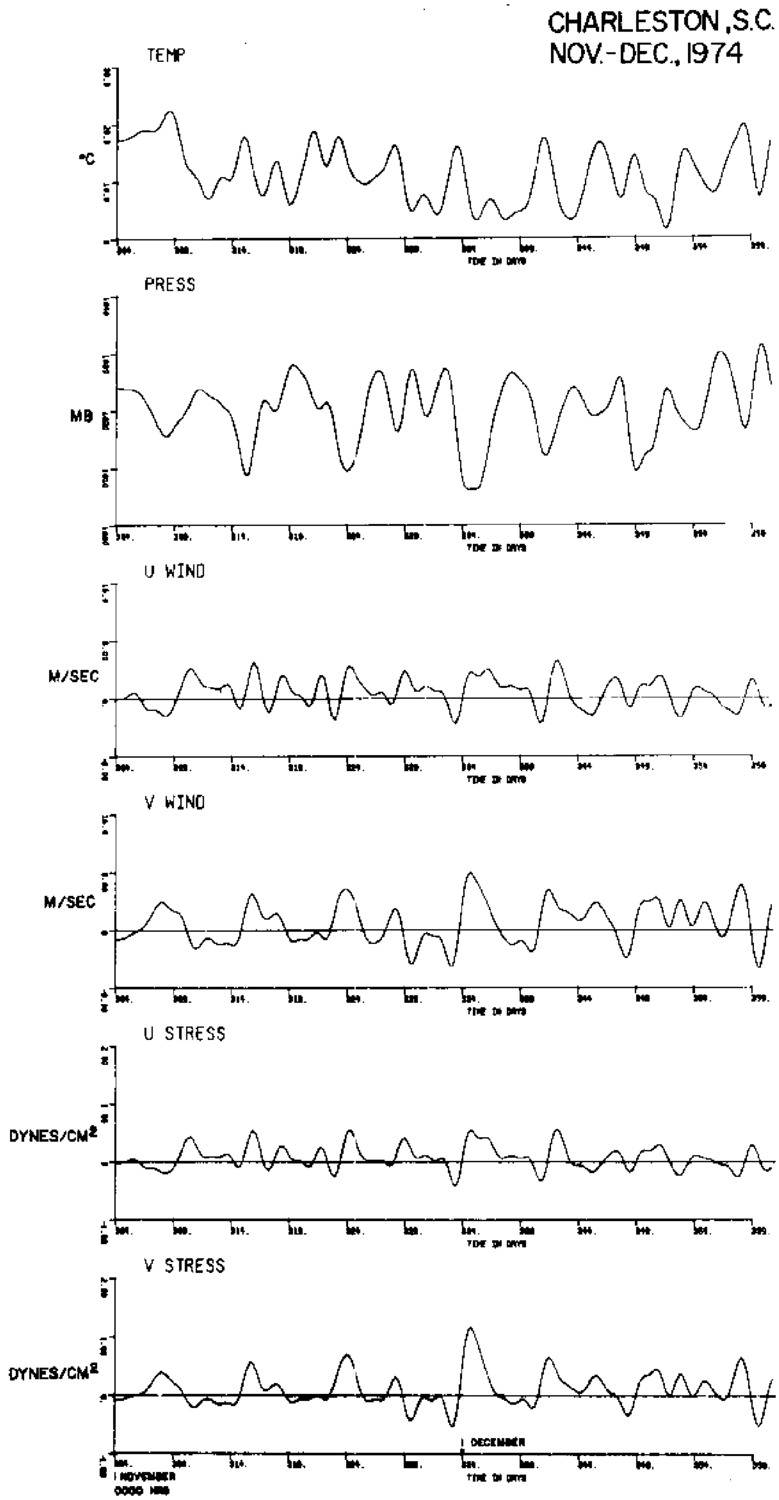

Figure 32 Temperature, pressure, wind velocity components and wind stress components at Charleston, S. C., Nov. through Dec., 1974

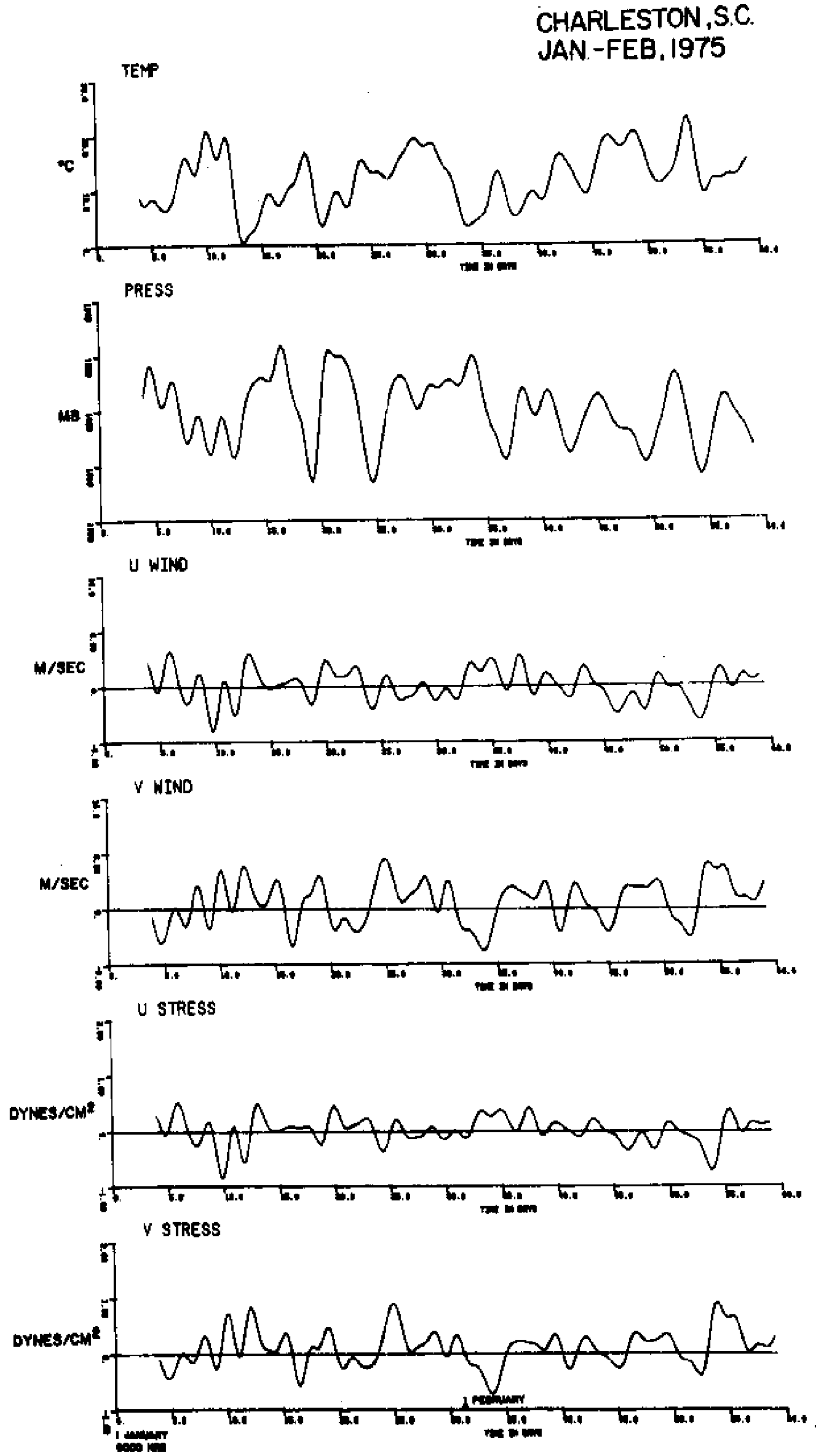

Figure 33 Temperature, pressure, wind velocity components and wind stress components at Charleston, S. C., Jan. through Feb., 1975

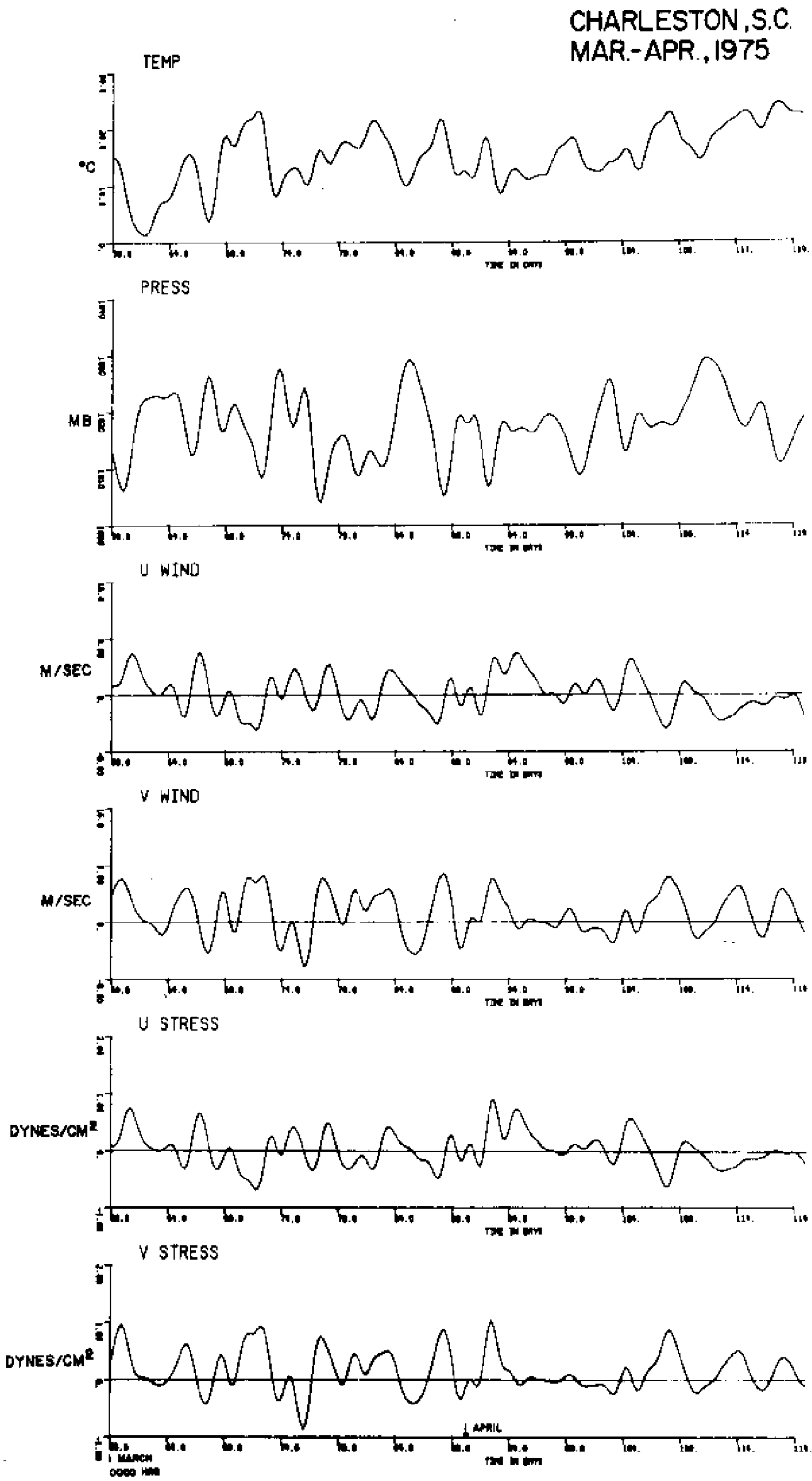

Figure 34 Temperature, pressure, wind velocity components and wind stress components at Charleston, S. C., Mar. through Apr., 1975

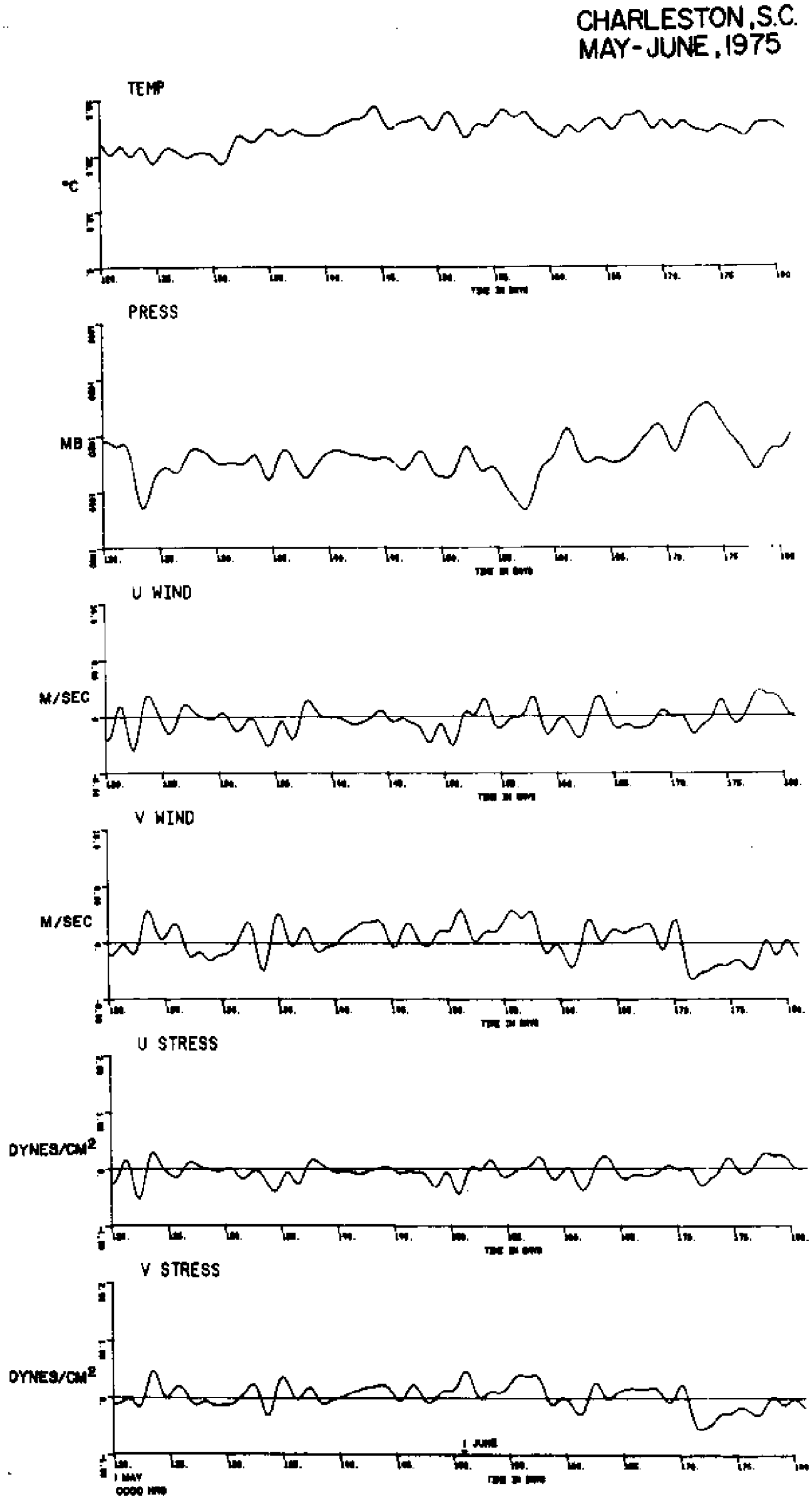

Figure 35 Temperature, pressure, wind velocity components and wind stress components at Charleston, S. C., May through June, 1975

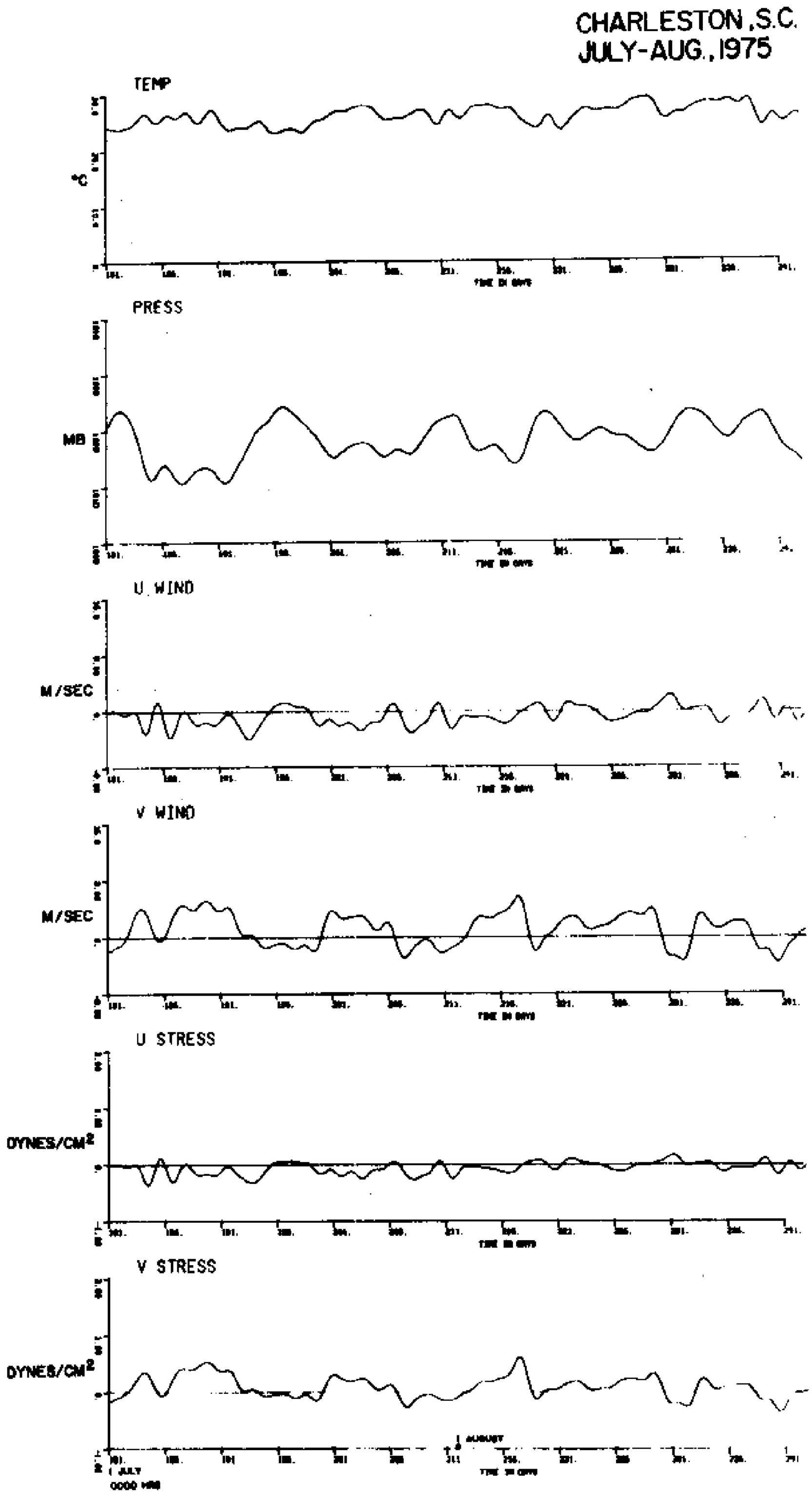

Figure 36 Temperature, pressure, wind velocity components and wind stress components at Charleston, S. C., July through Aug., 1975

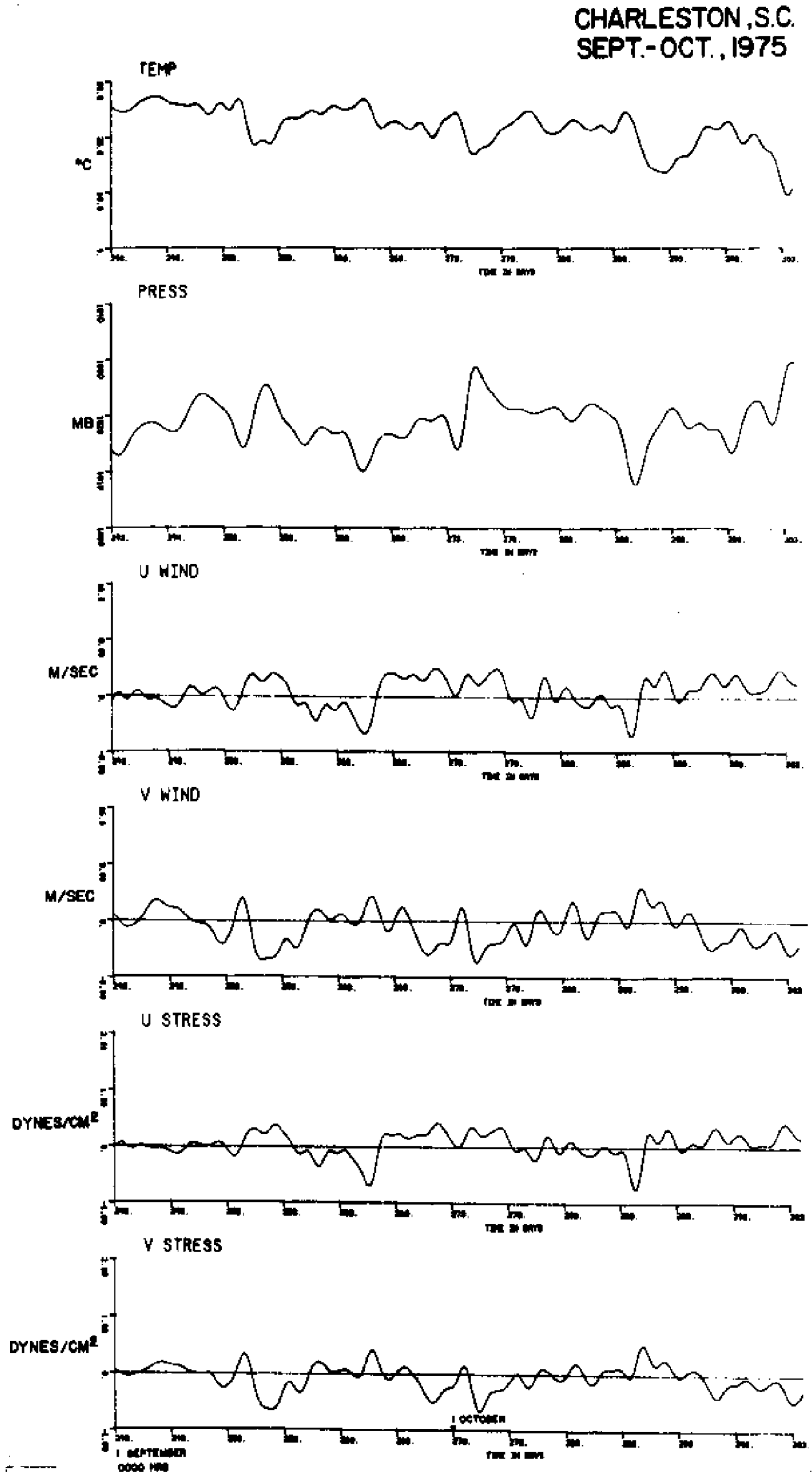

Figure 37 Temperature, pressure, wind velocity components and wind stress components at Charleston, S. C., Sept. through Oct., 1975

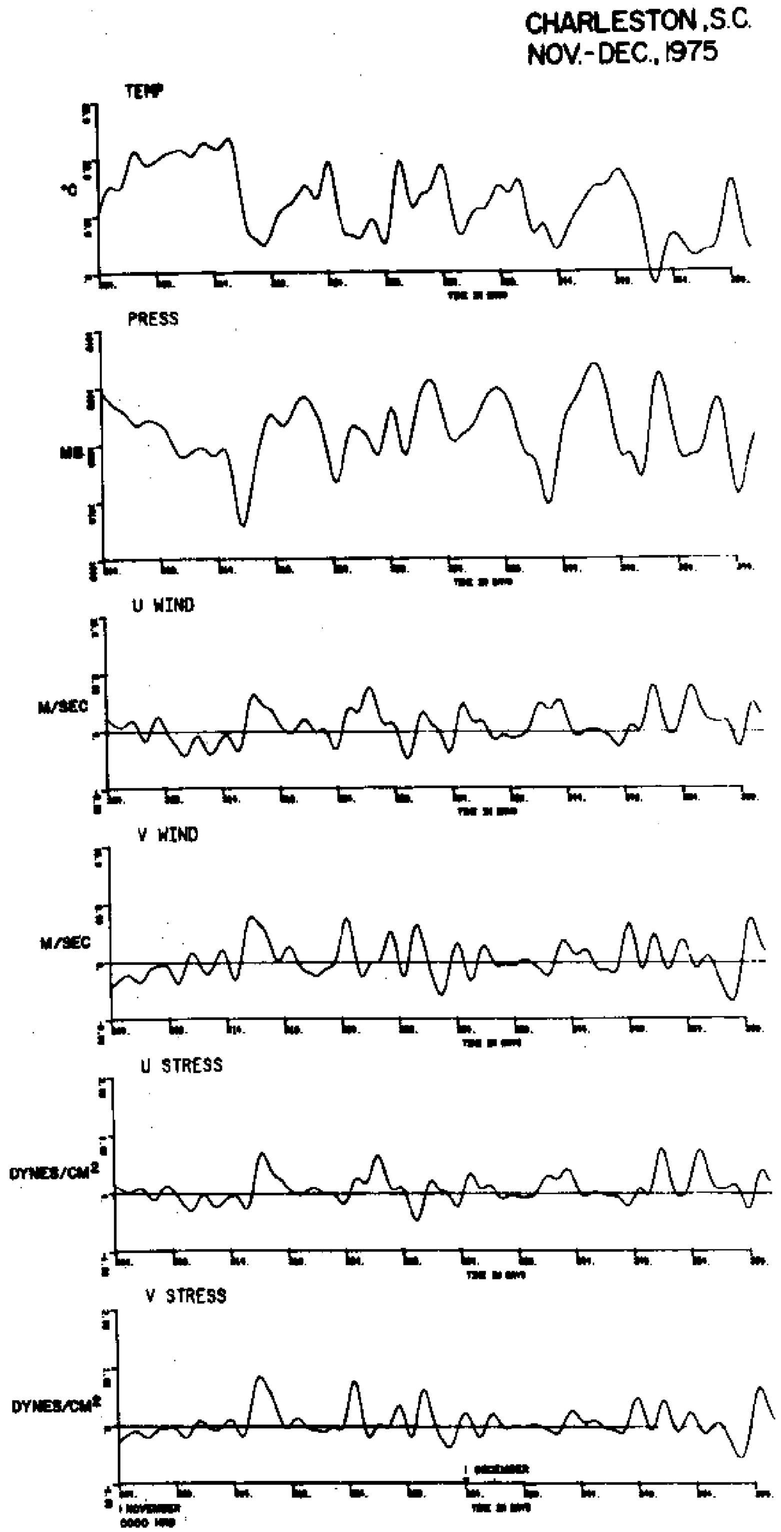

Figure 38 Temperature, pressure, wind velocity components and wind stress components at Charleston, S. C., Nov. through Dec., 1975

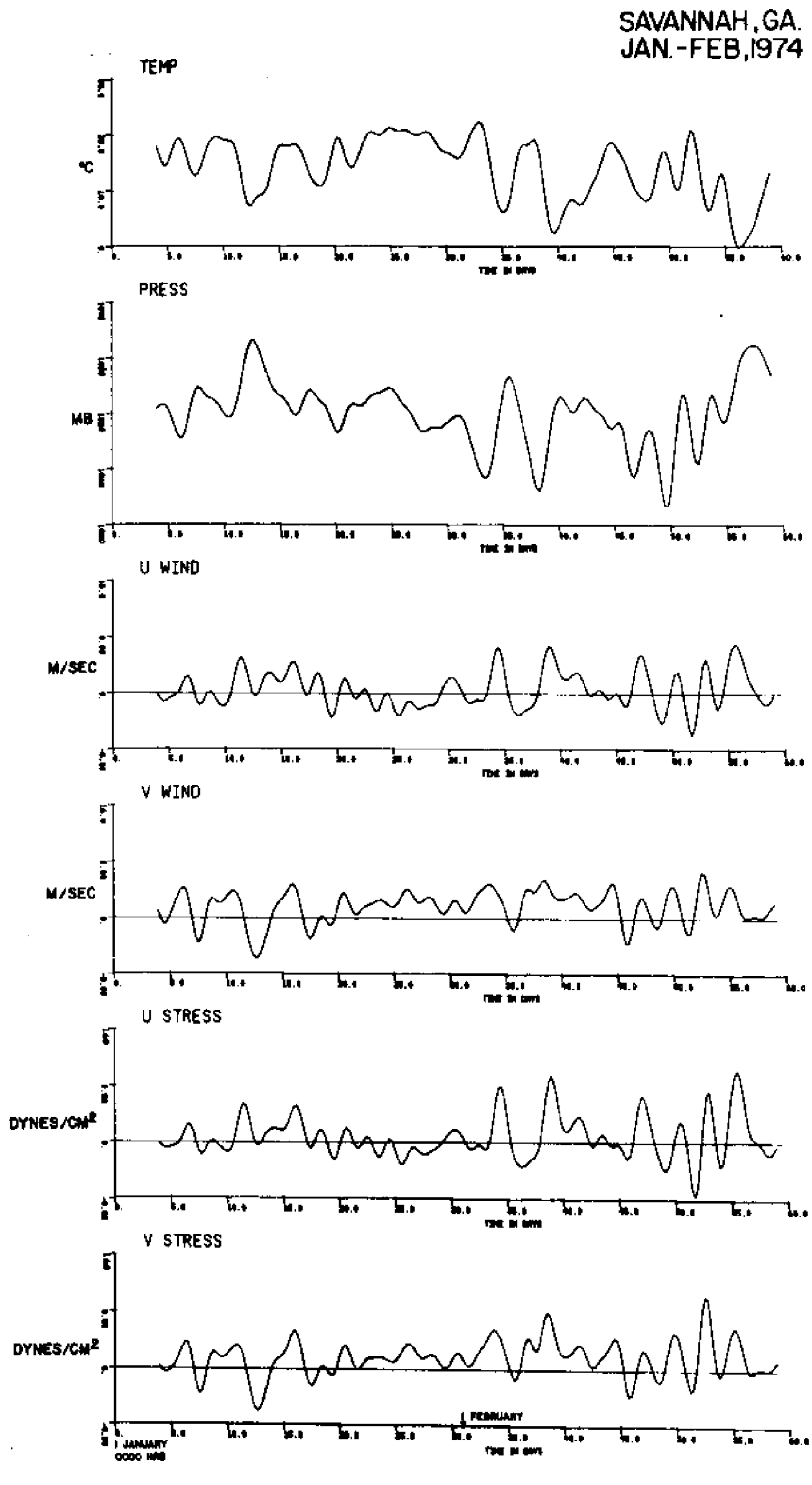

Figure 39 Temperature, pressure, wind velocity components and wind stress components at Savannah, Ga., Jan. through Feb., 1974

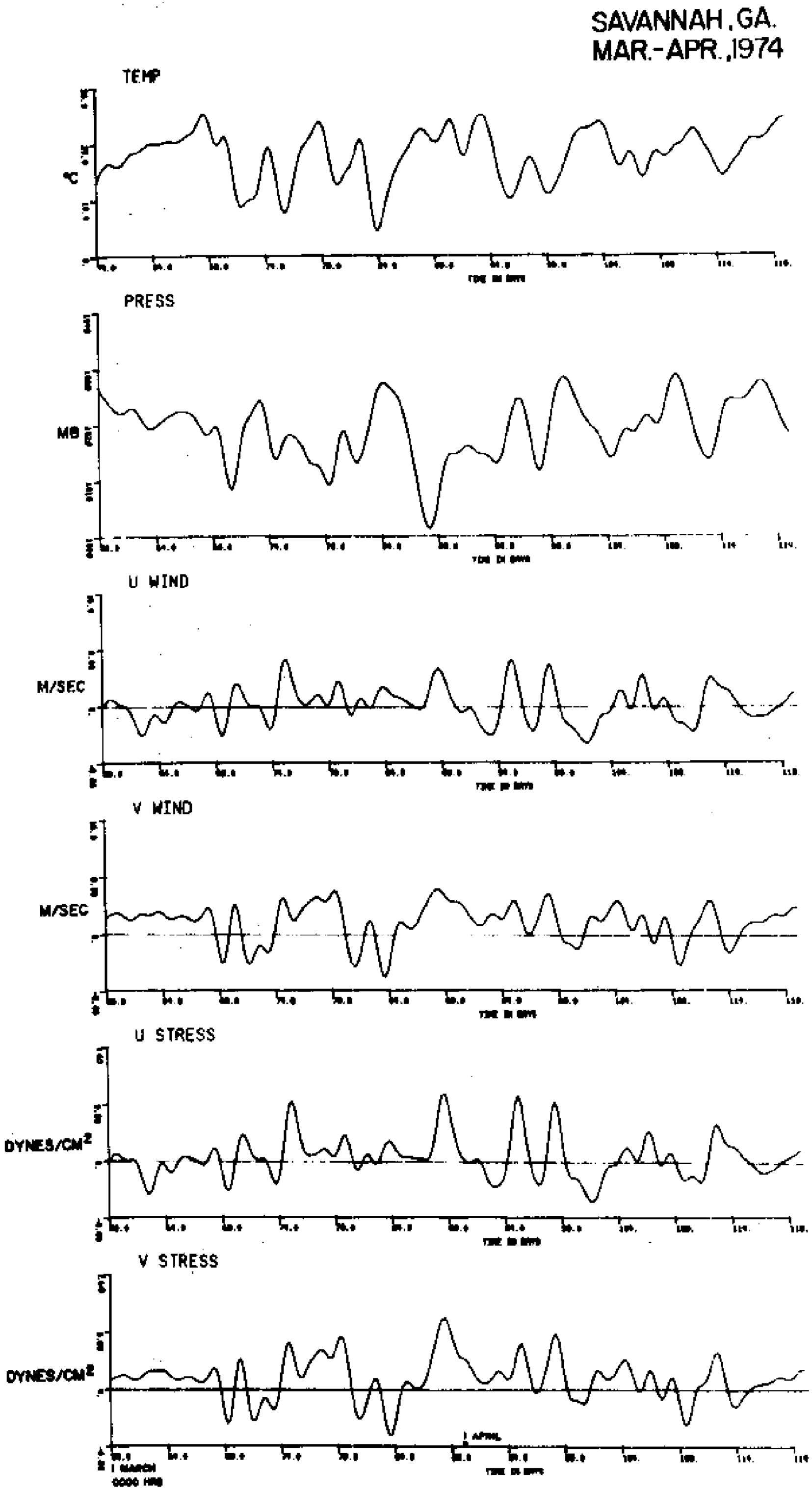

Figure 40 Temperature, pressure, wind velocity components and wind stress components at Savannah, Ga., Mar. through Apr., 1974

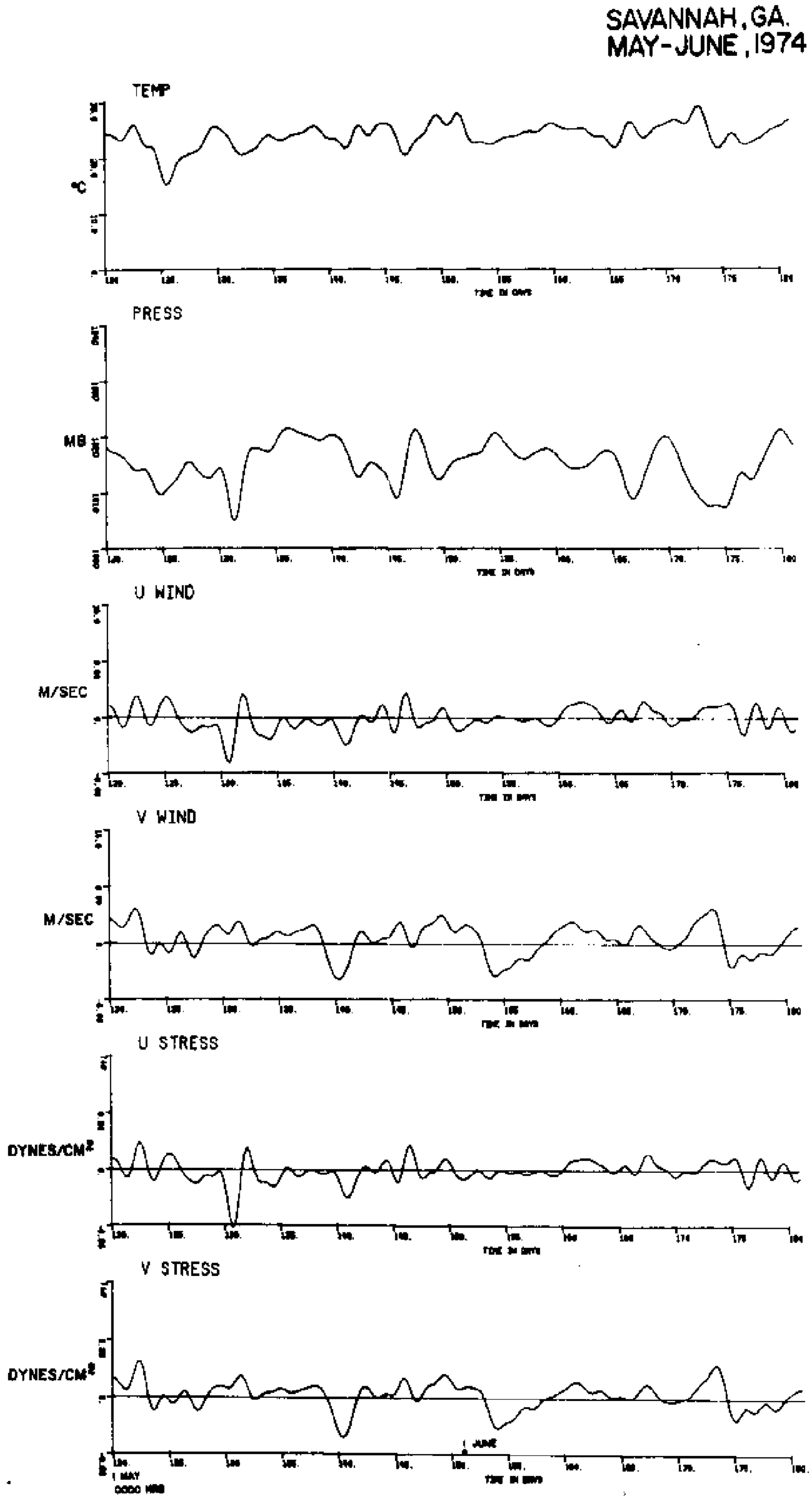

Figure 41 Temperature, pressure, wind velocity components and wind stress components at Savannah, Ga., May through June, 1974

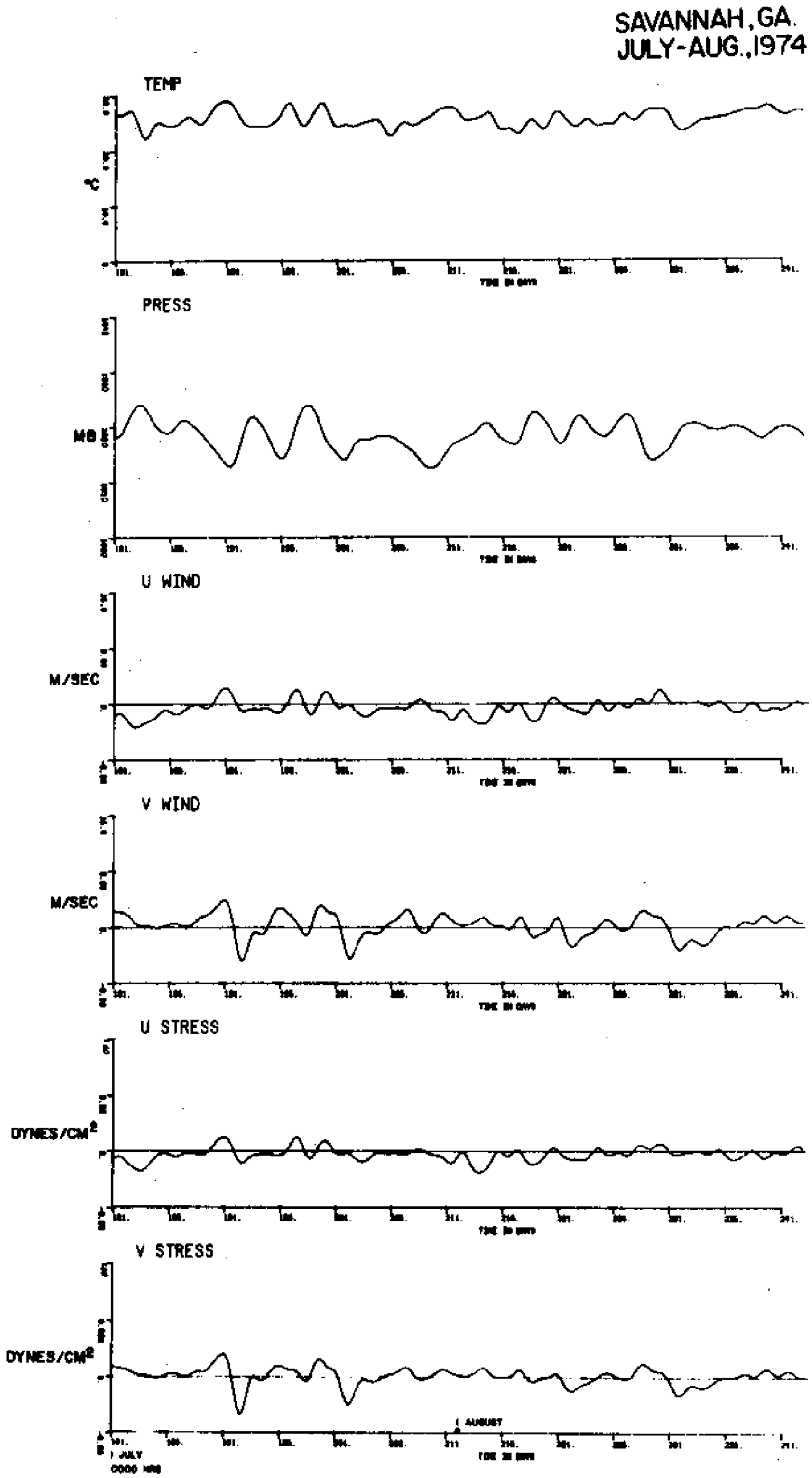

Figure 42 Temperature, pressure, wind velocity components and wind stress components at Savannah, Ga., July through Aug., 1974

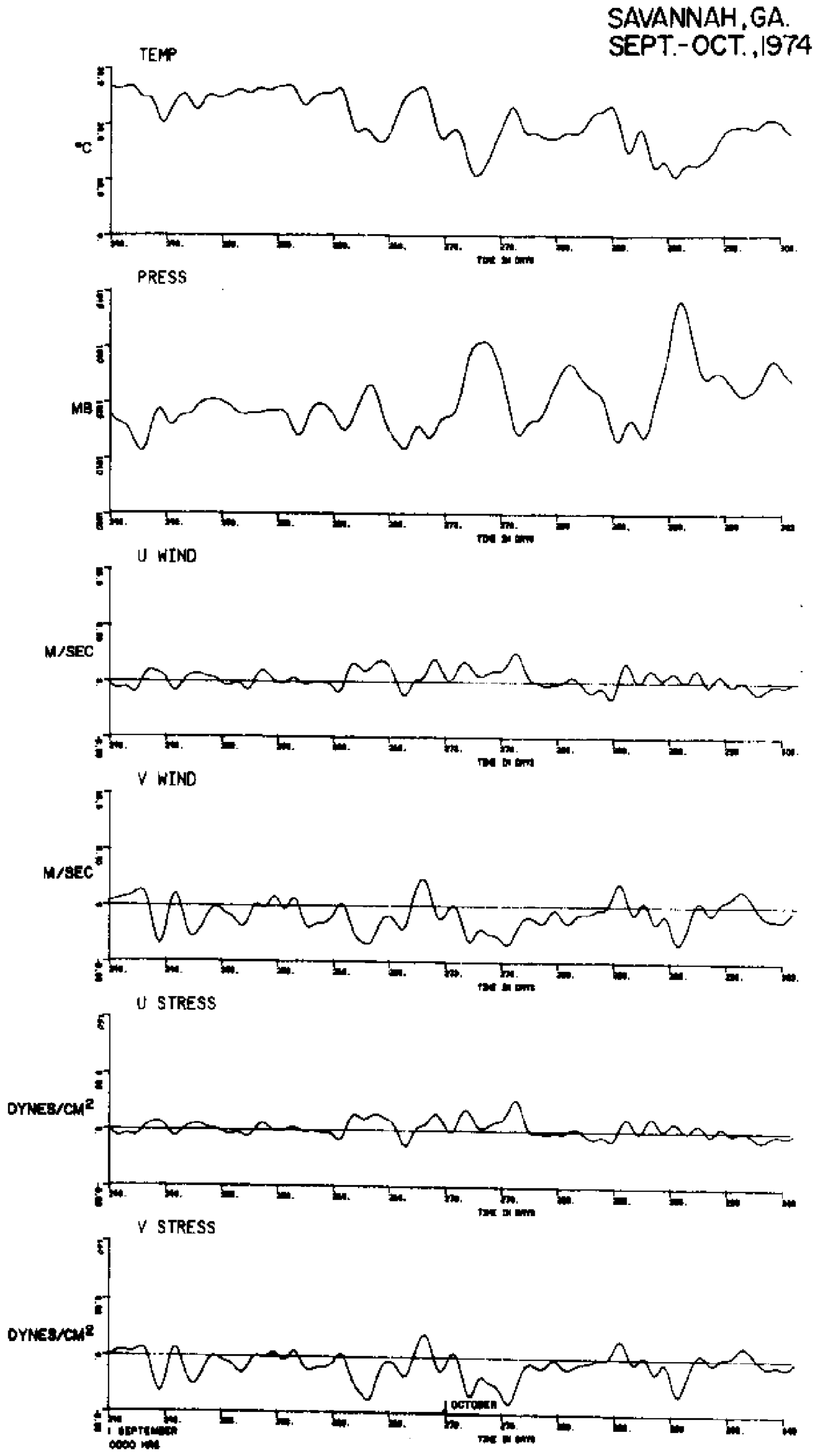

Figure 43 Temperature, pressure, wind velocity components and wind stress components at Savannah, Ga., Sept. through Oct., 1974

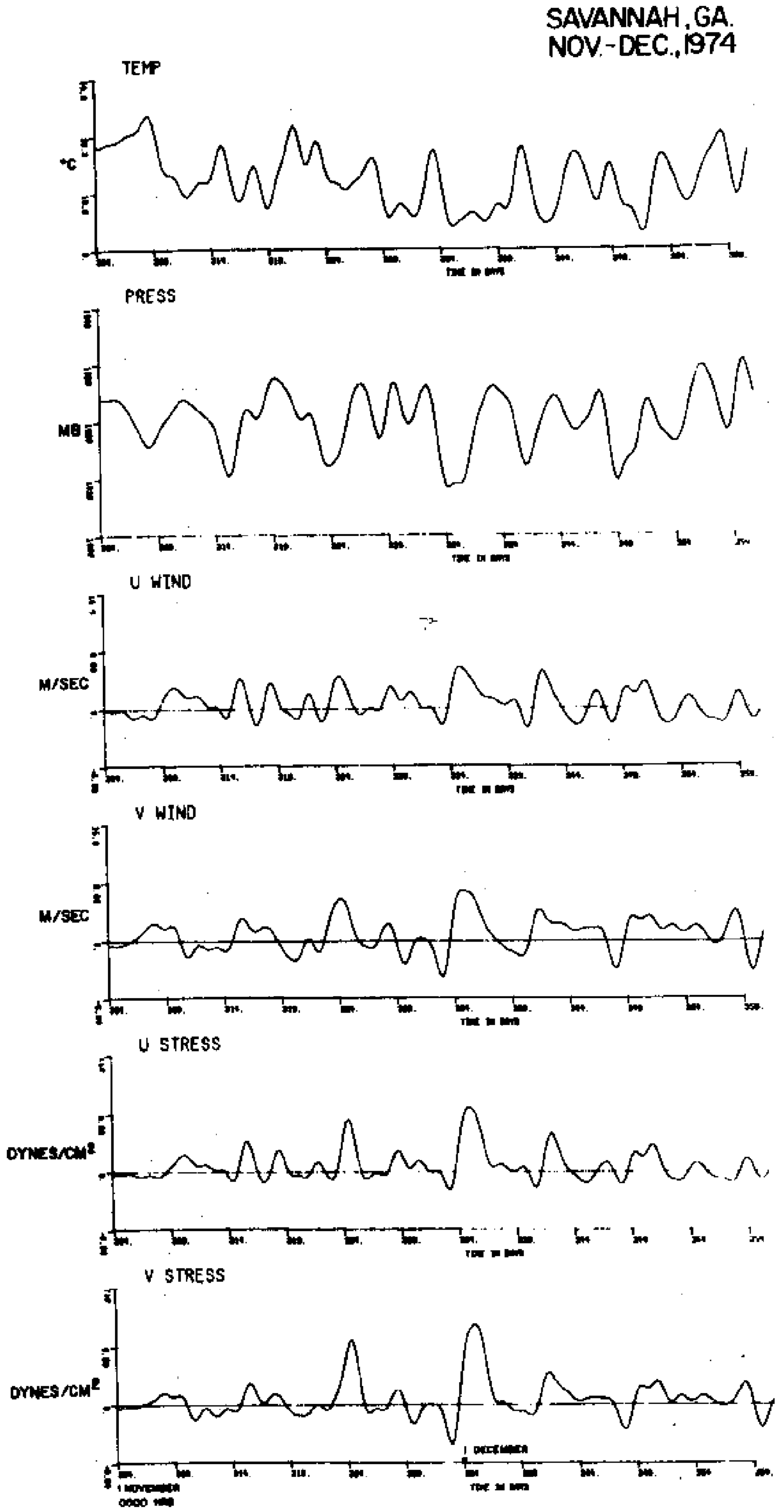

Figure 44 Temperature, pressure, wind velocity components and wind stress components at Savannah, Ga., Nov. through Dec., 1974

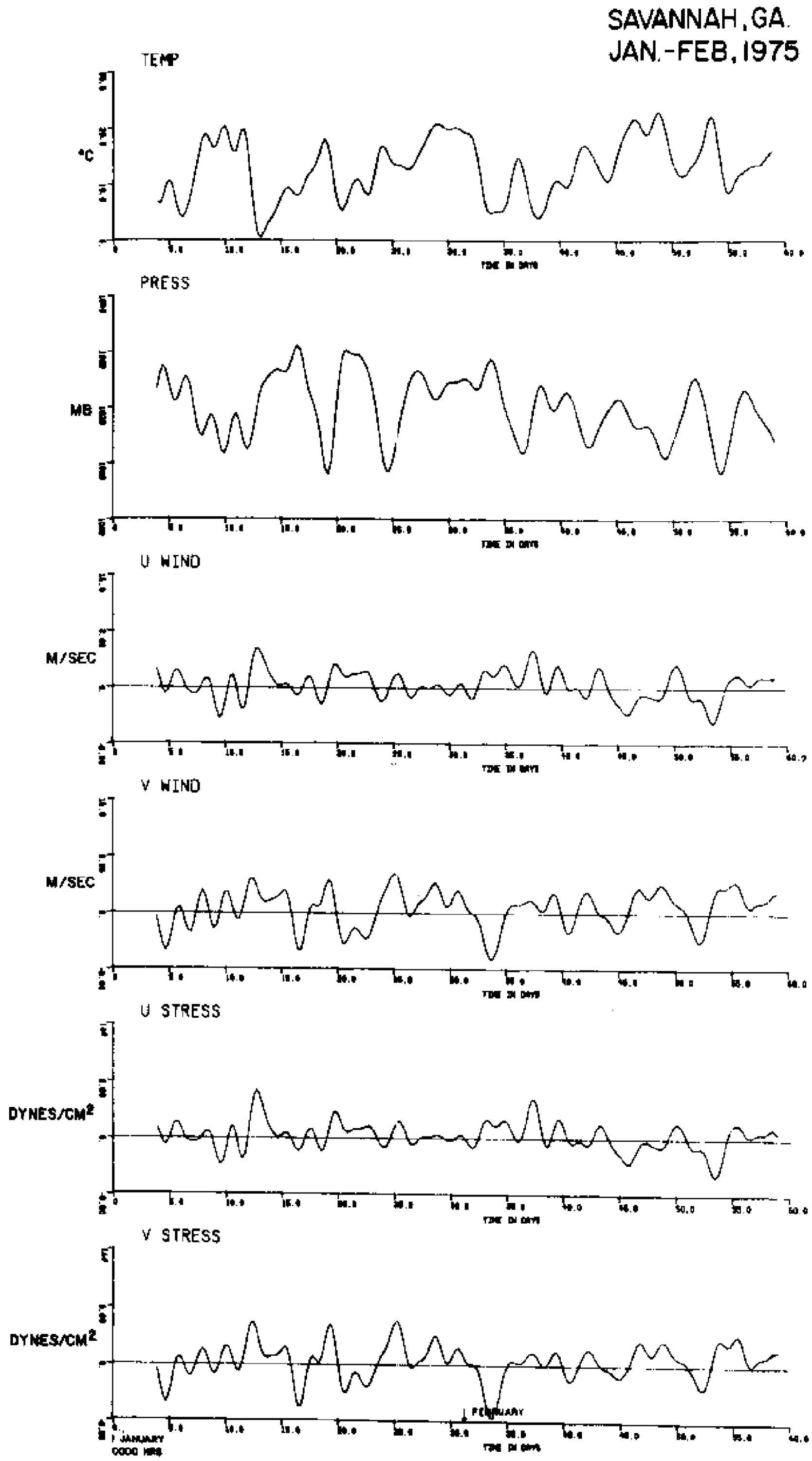

Figure 45 Temperature, pressure, wind velocity components and wind stress components at Savannah, Ga., Jan. through Feb., 1975

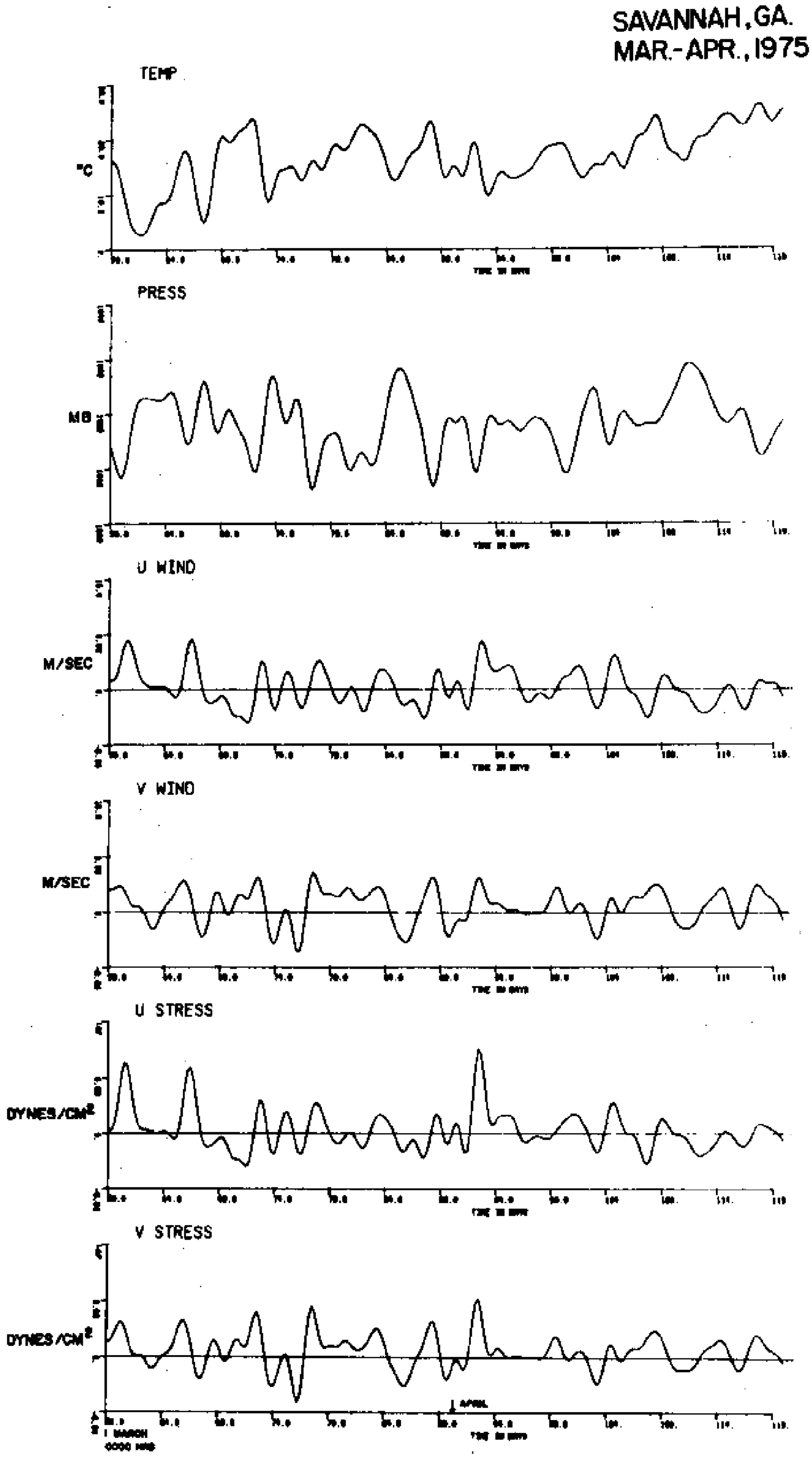

Figure 46 Temperature, pressure, wind velocity components and wind stress components at Savannah, Ga., Mar. through Apr., 1975

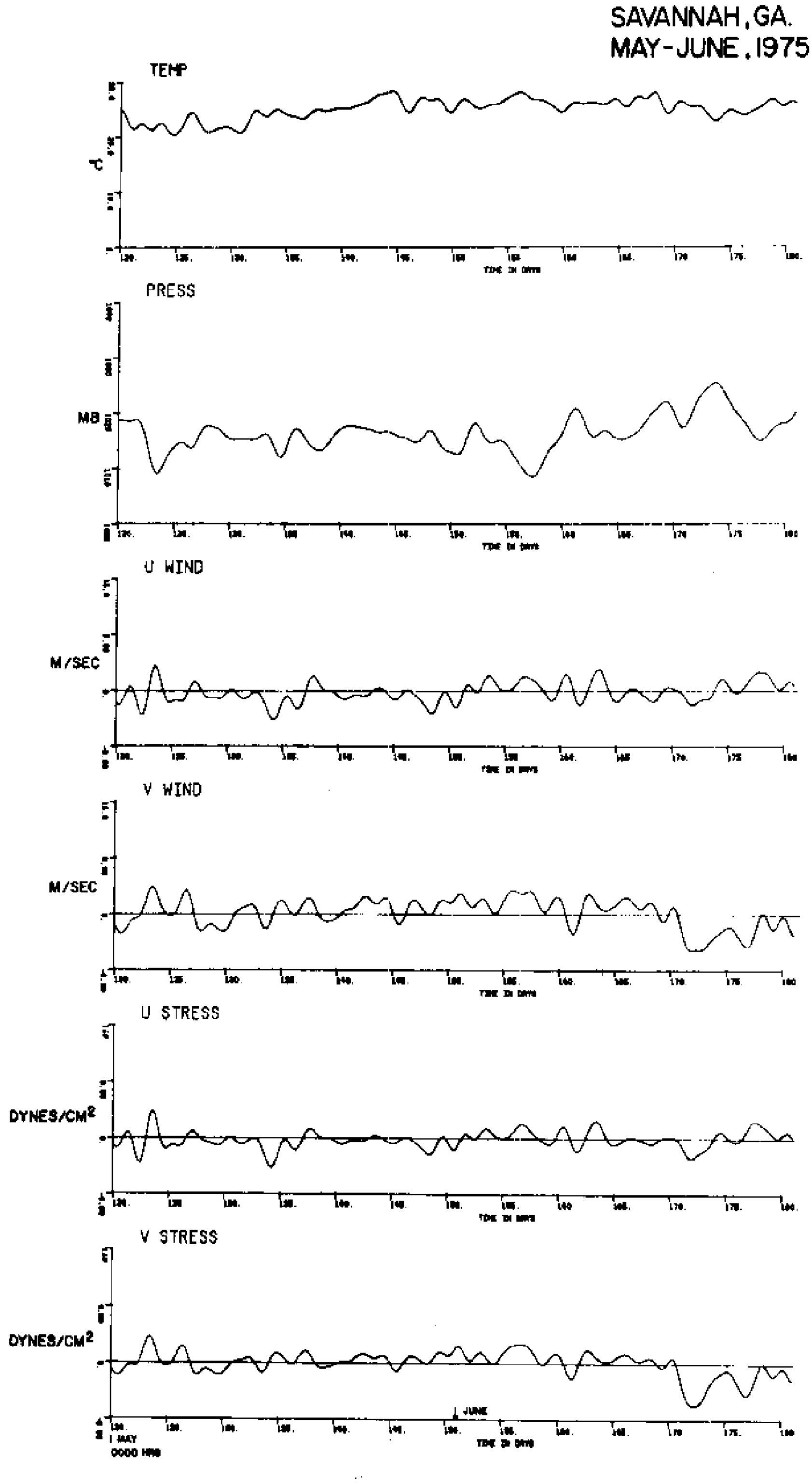

Figure 47 Temperature, pressure, wind velocity components and wind stress components at Savannah, Ga., May through June, 1975

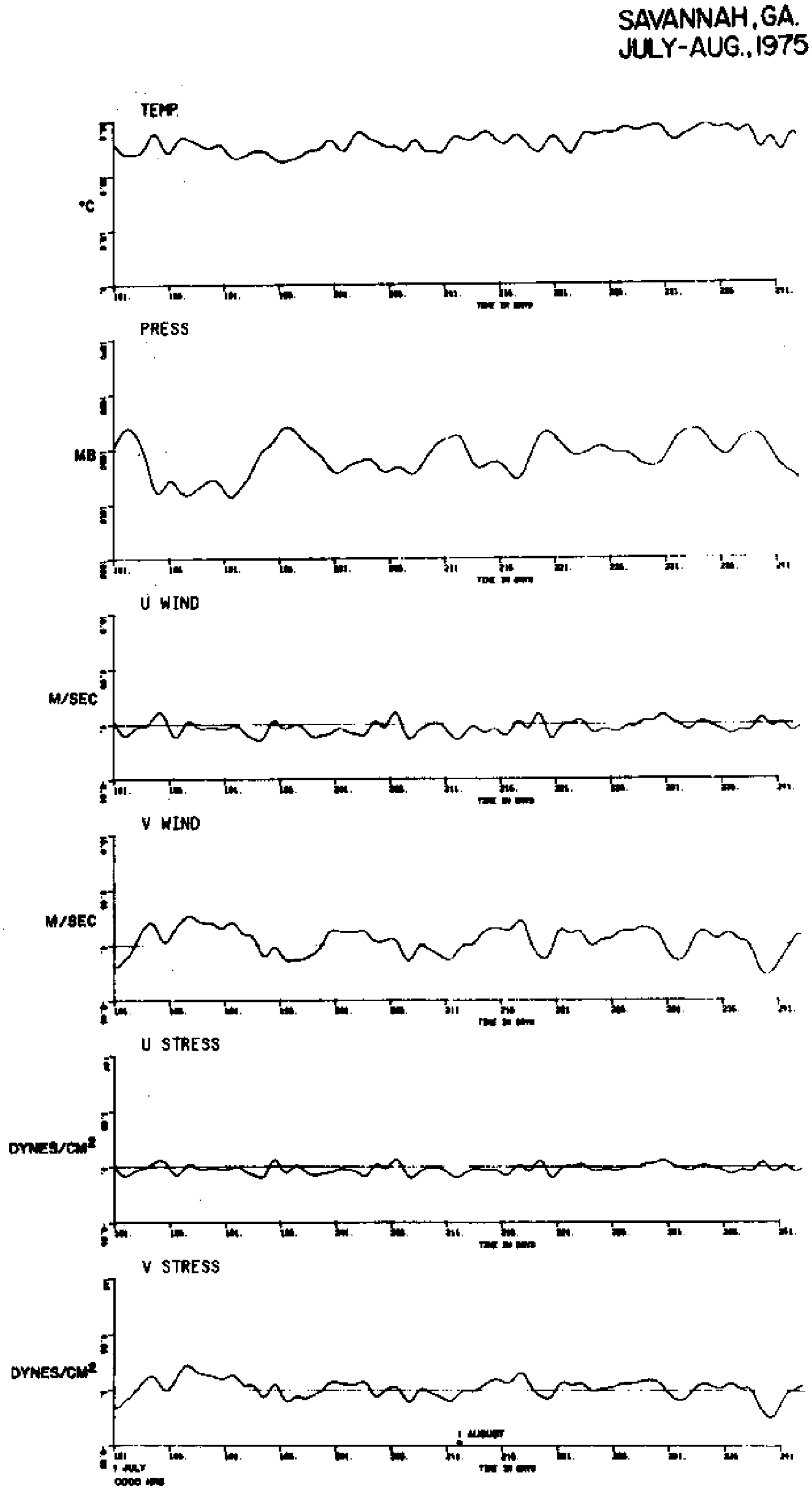

Figure 48 Temperature, pressure, wind velocity components and wind stress components at Savannah, Ga., July through Aug., 1975

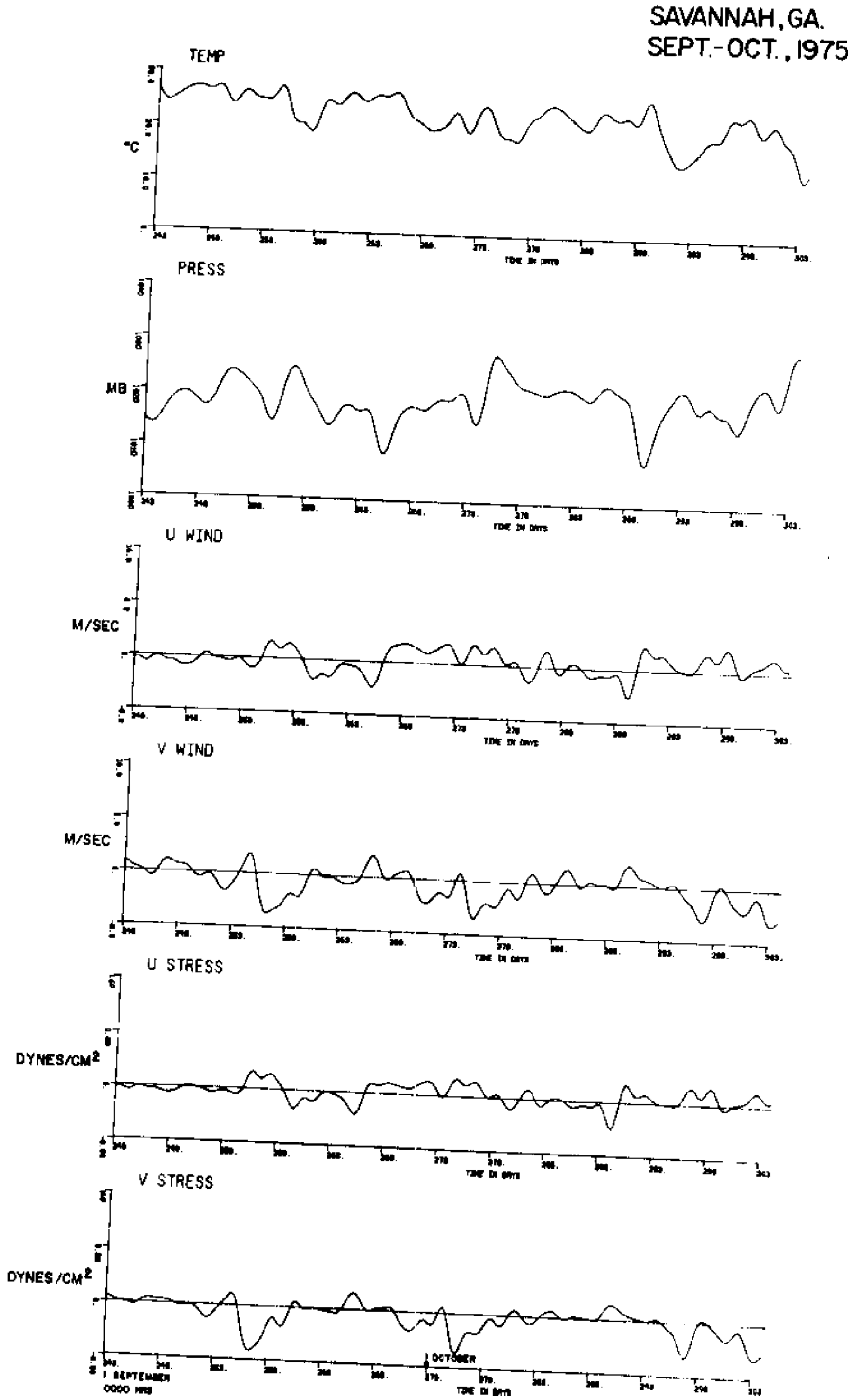

Figure 49 Temperature, pressure, wind velocity components and wind stress components at Savannah, Ga., Sept. through Oct., 1975

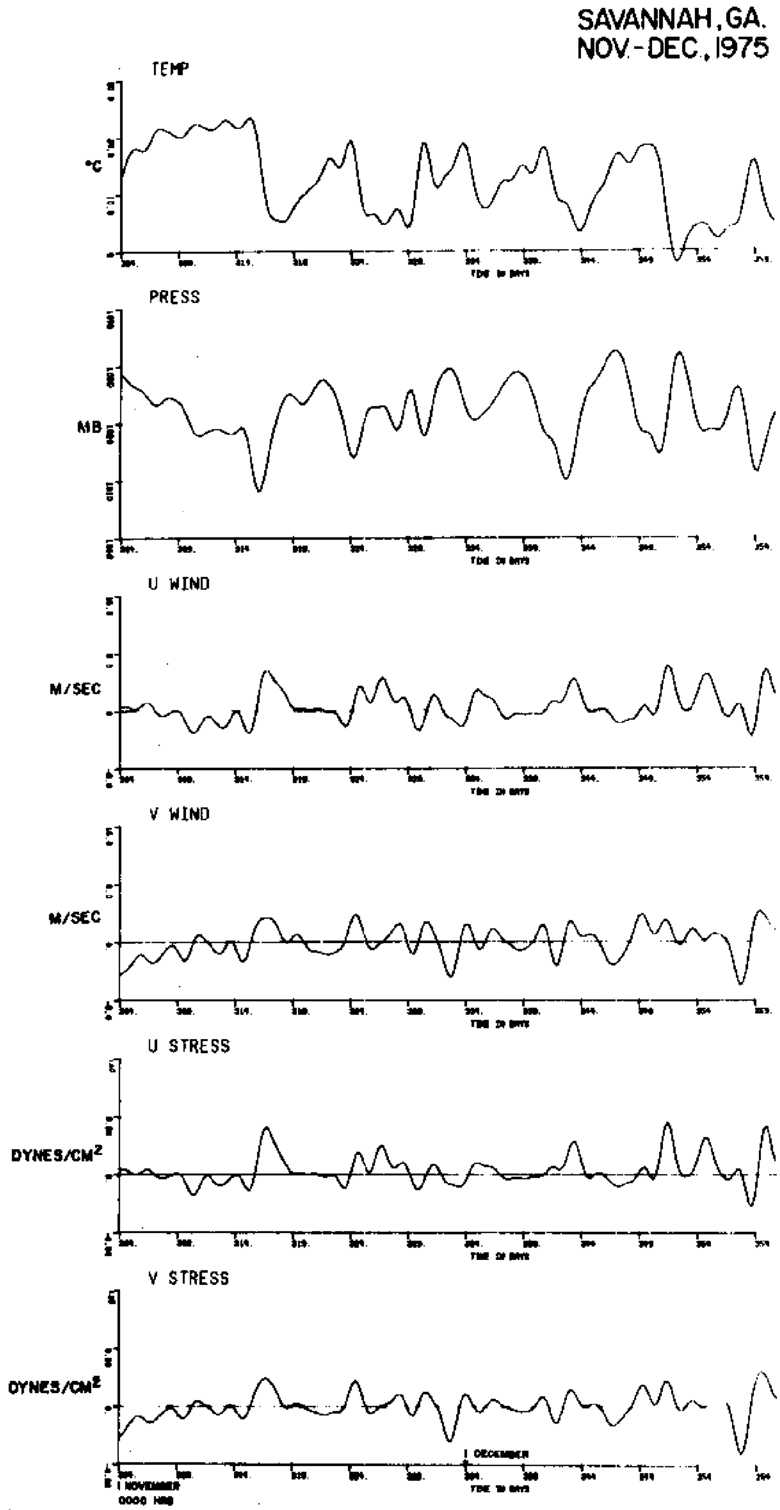

Figure 50 Temperature, pressure, wind velocity components and wind stress components at Savannah, Ga., Nov. through Dec., 1975

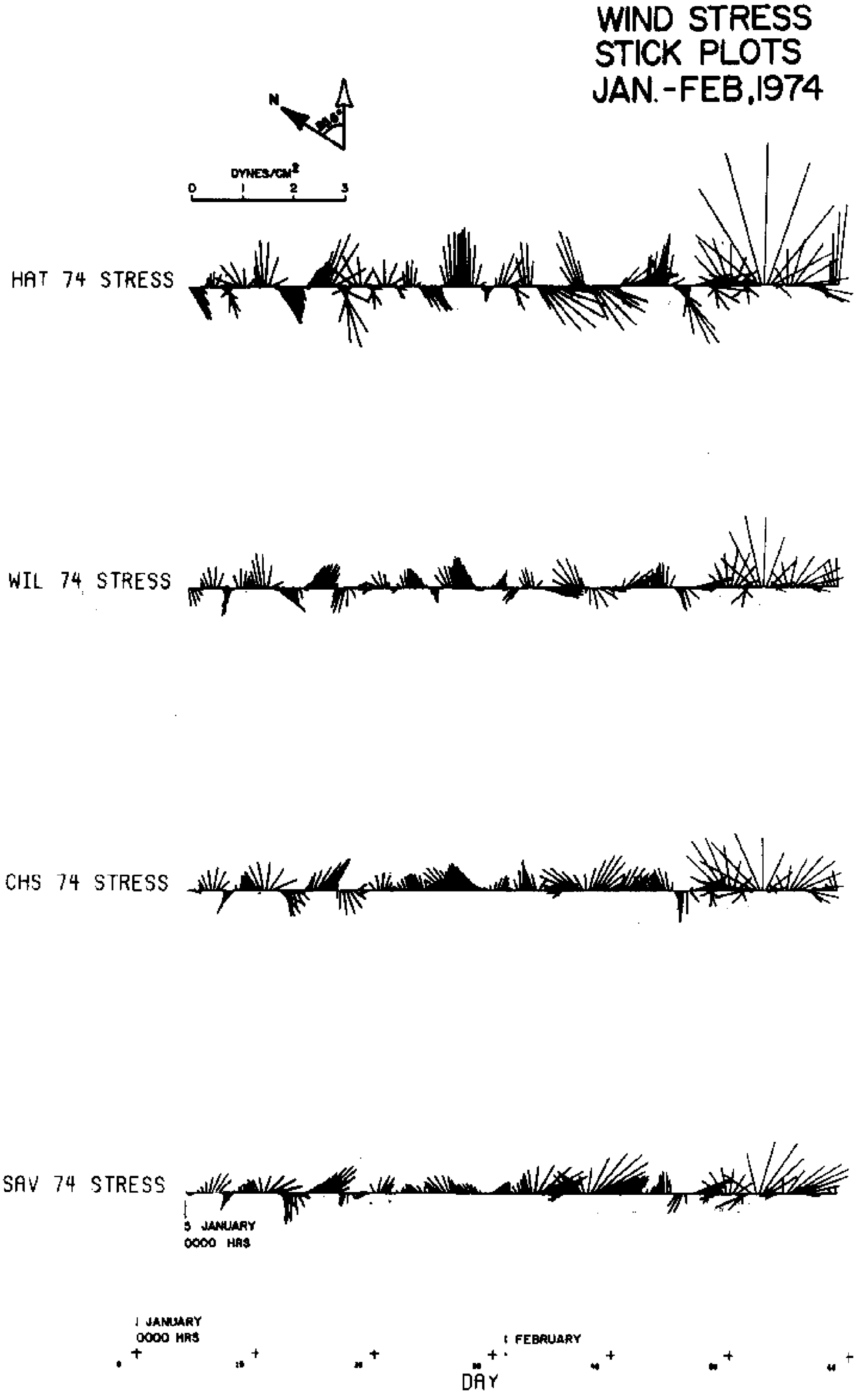

Figure 51 Wind stress vectors at Cape Hatteras, N. C., Wilmington, N. C., Charleston, S. C. and Savannah, Ga., Jan through Feb., 1974

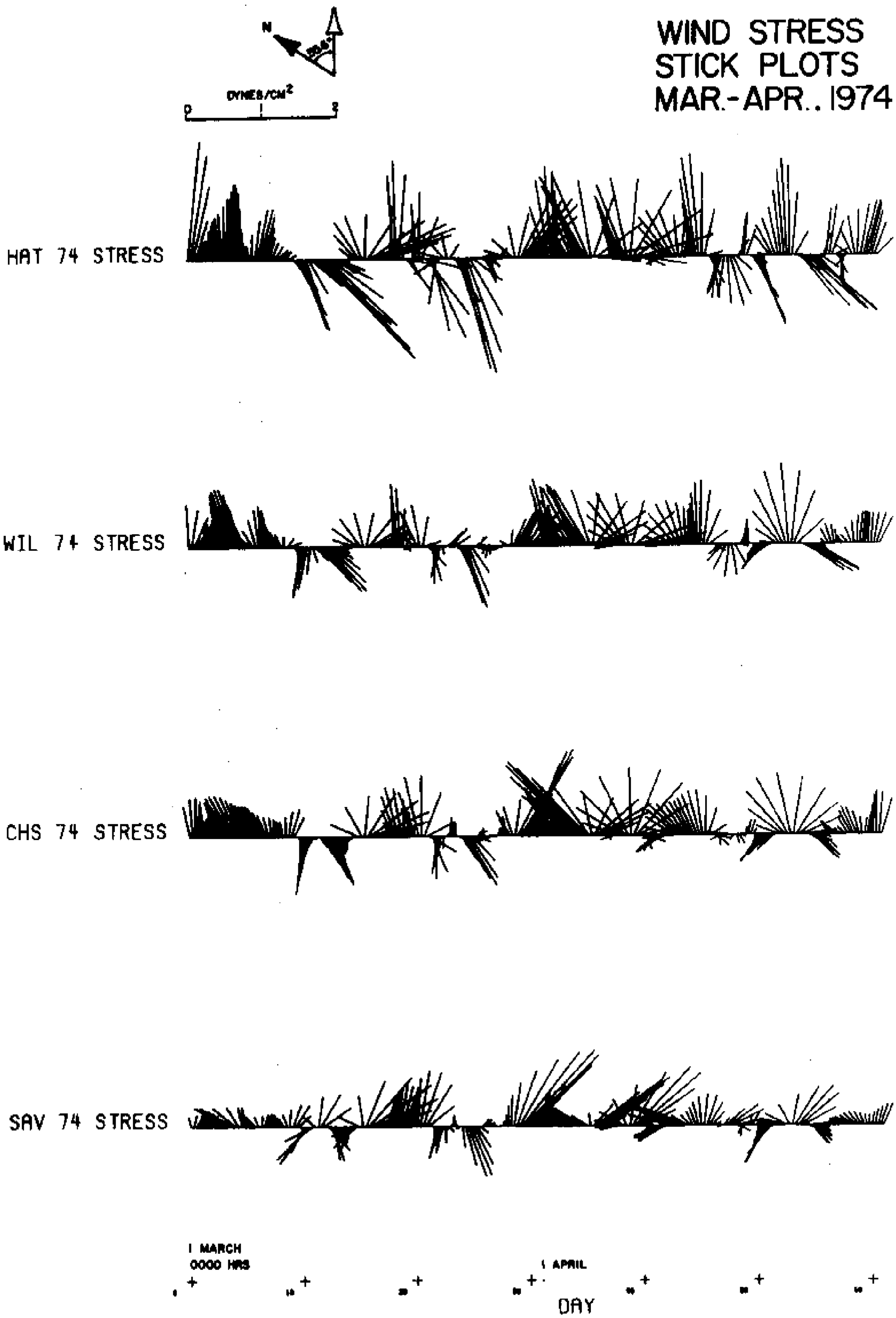

Figure 52 Wind stress vectors at Cape Hatteras, N. C., Wilmington, N. C., Charleston, S. C., and Savannah, Ga., Mar. through Apr., 1974

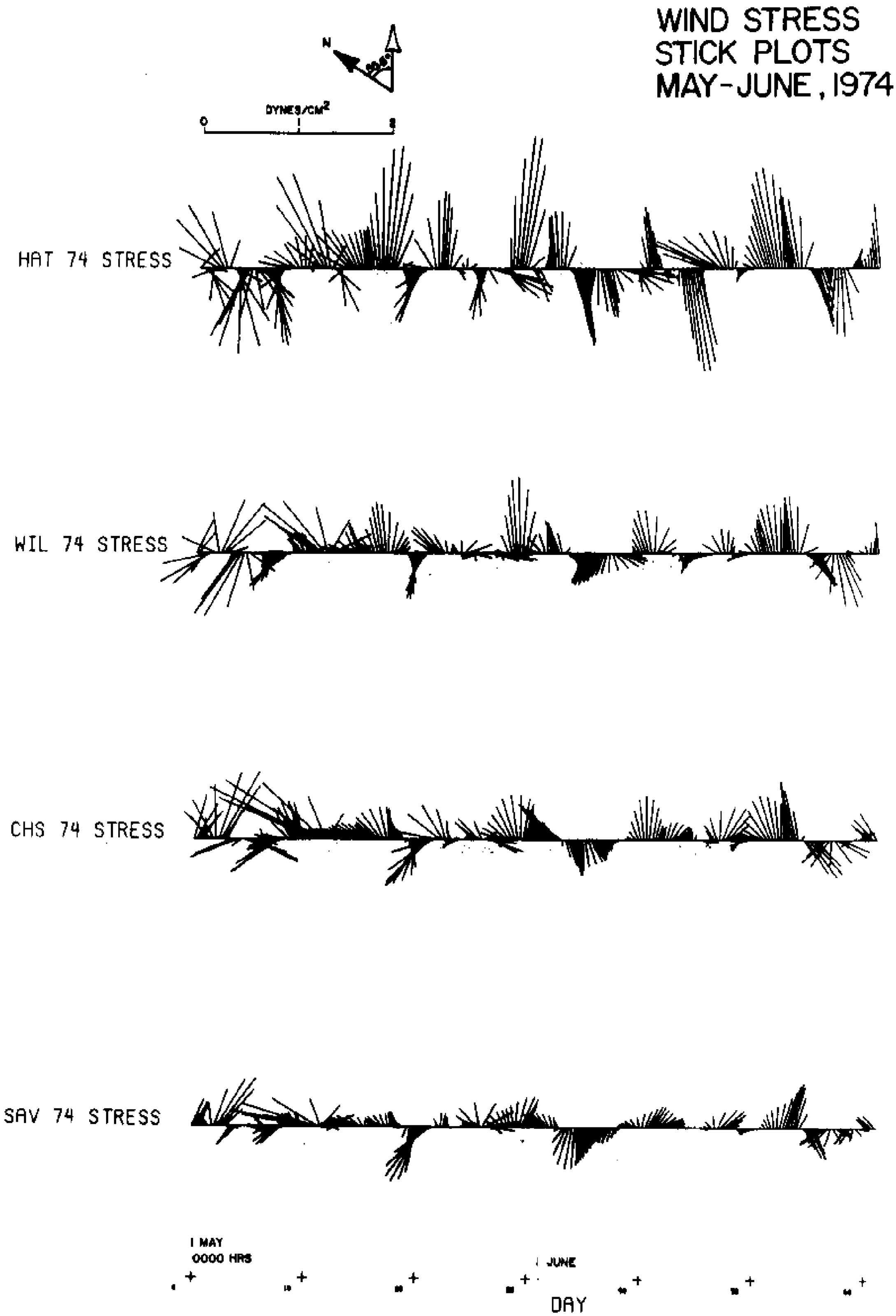

Figure 53 Wind stress vectors at Cape Hatteras, N. C., Wilmington, N. C., Charleston, S. C. and Savannah, Ga., May through June, 1974

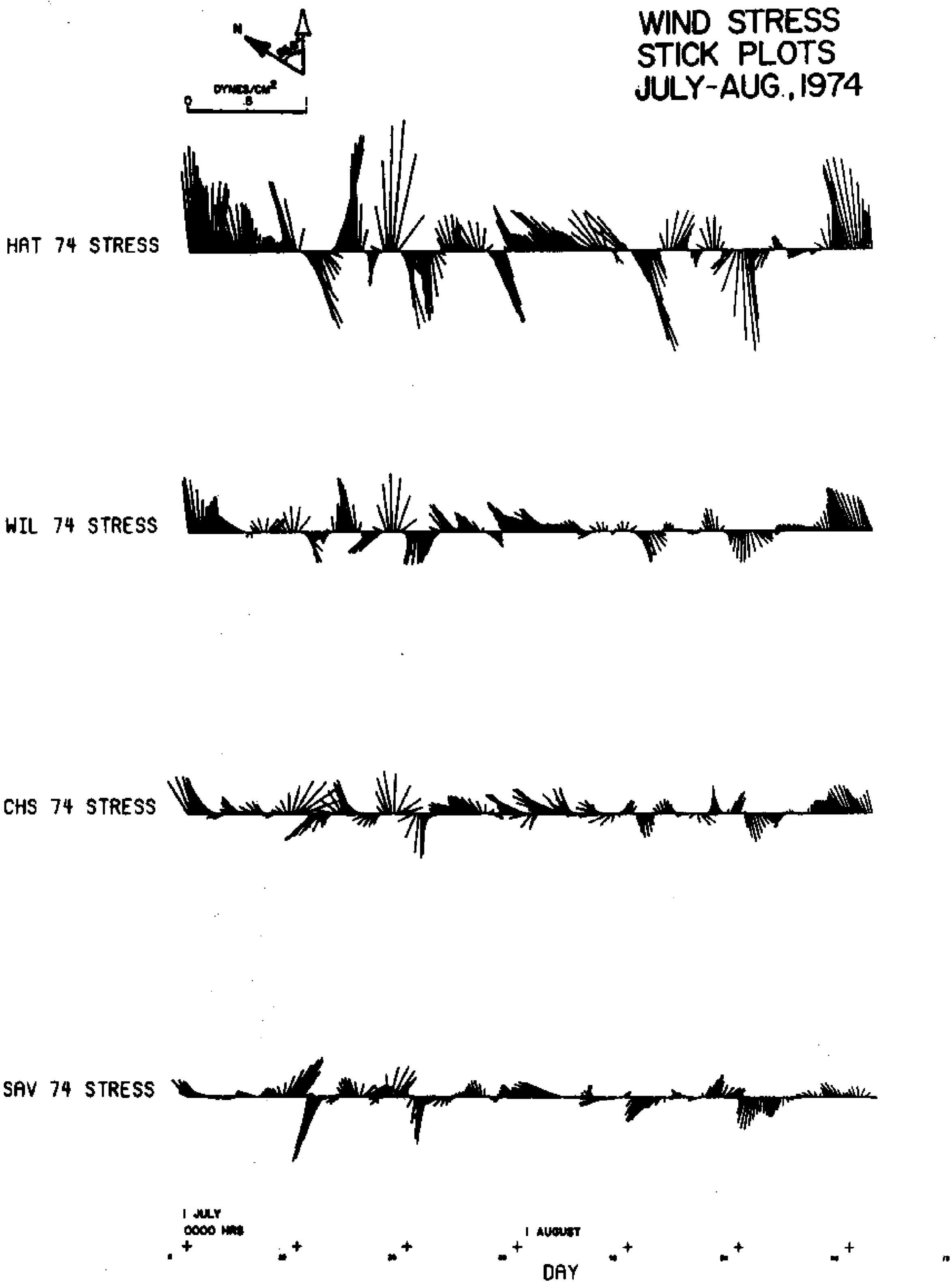

Figure 54 Wind stress vectors at Cape Hatteras, N. C., Wilmington, N. C., Charleston, S. C., and Savannah, Ga., July through Aug., 1974

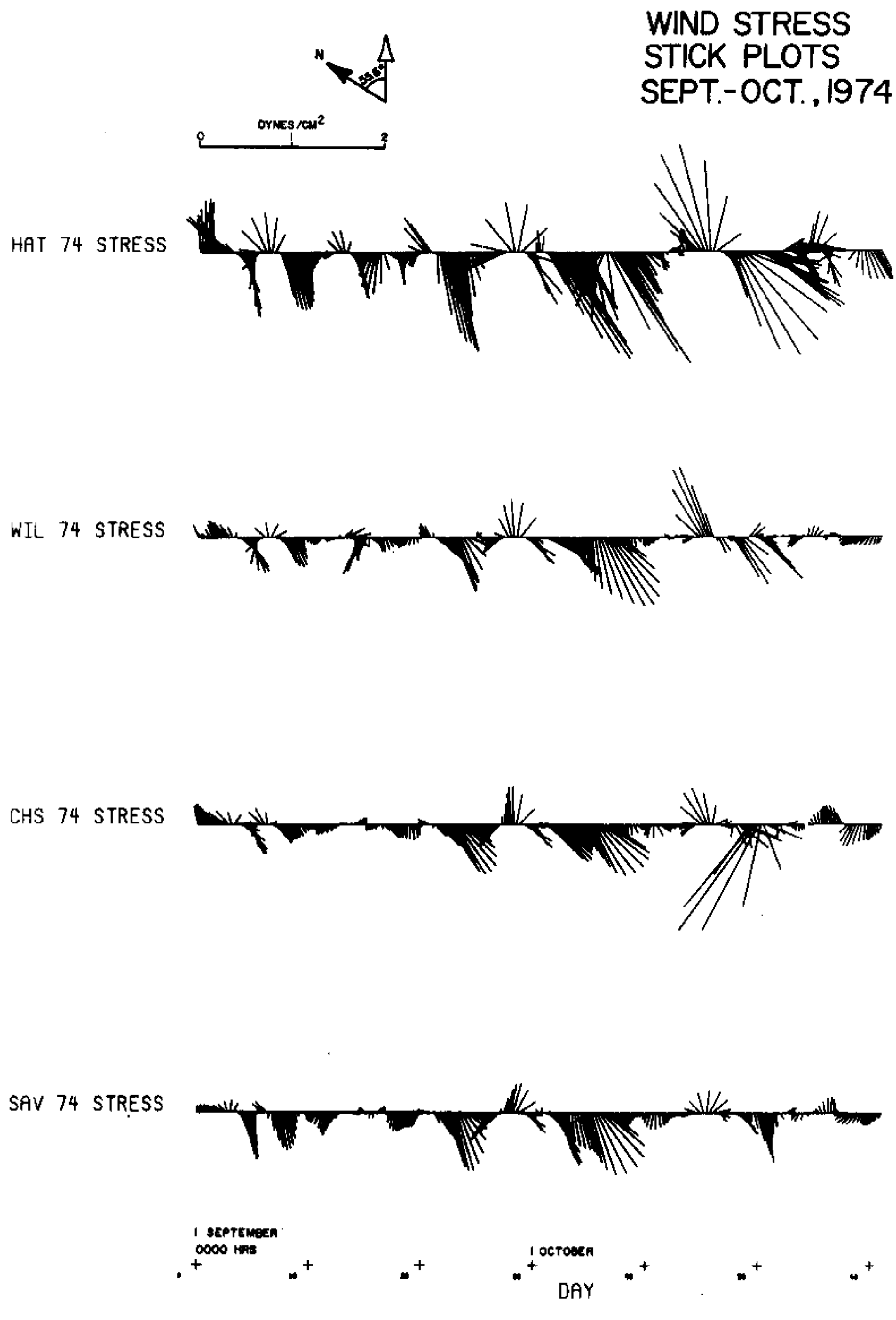

Figure 55 Wind stress vectors at Cape Hatteras, N. C., Wilmington, N. C., Charleston, S. C. and Savannah, Ga., Sept. through Oct., 1974

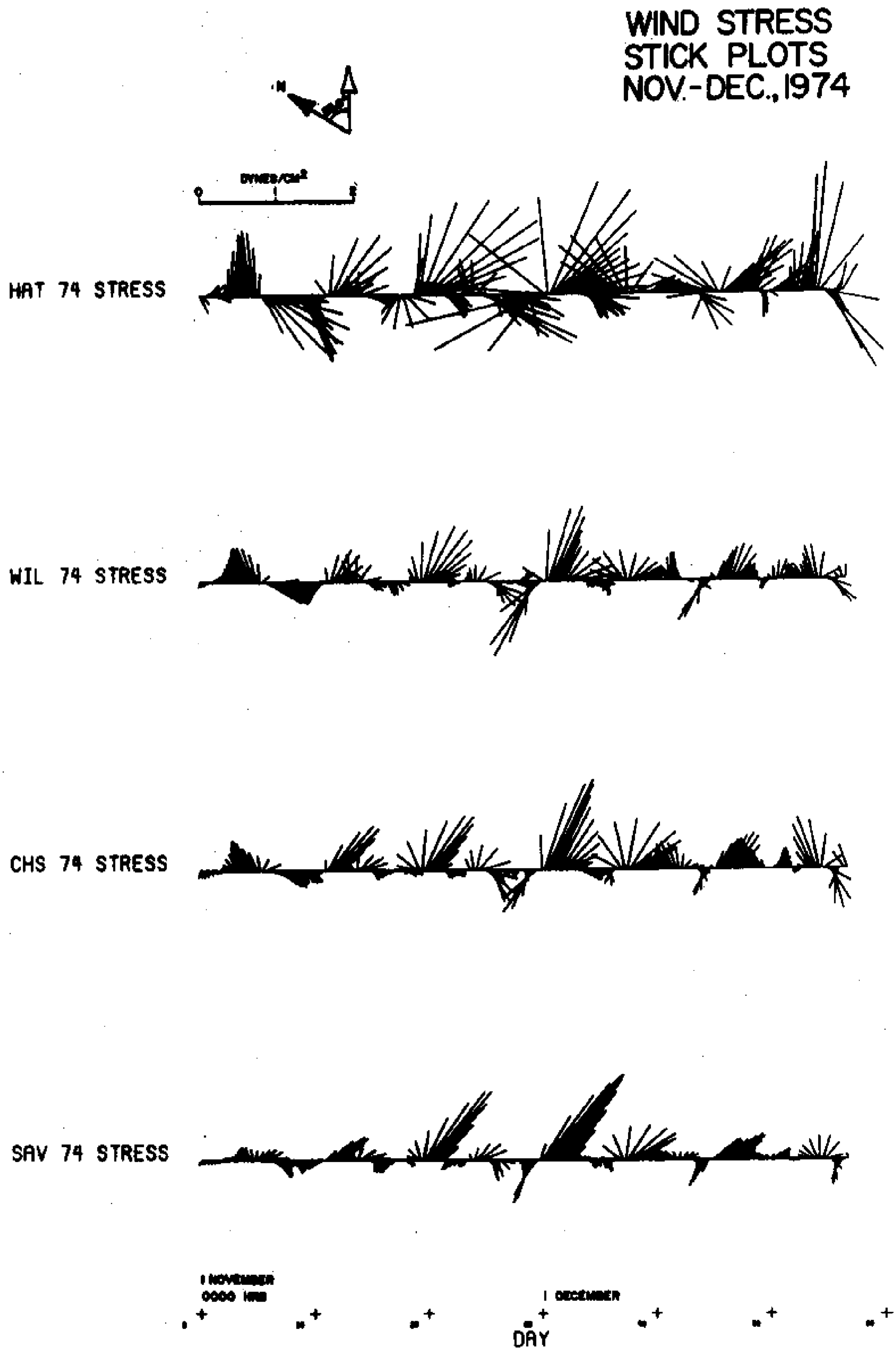

Figure 56 Wind stress vectors at Cape Hatteras, N. C., Wilmington, N. C., Charleston, S. C. and Savannah, Ga., Nov. through Dec., 1974

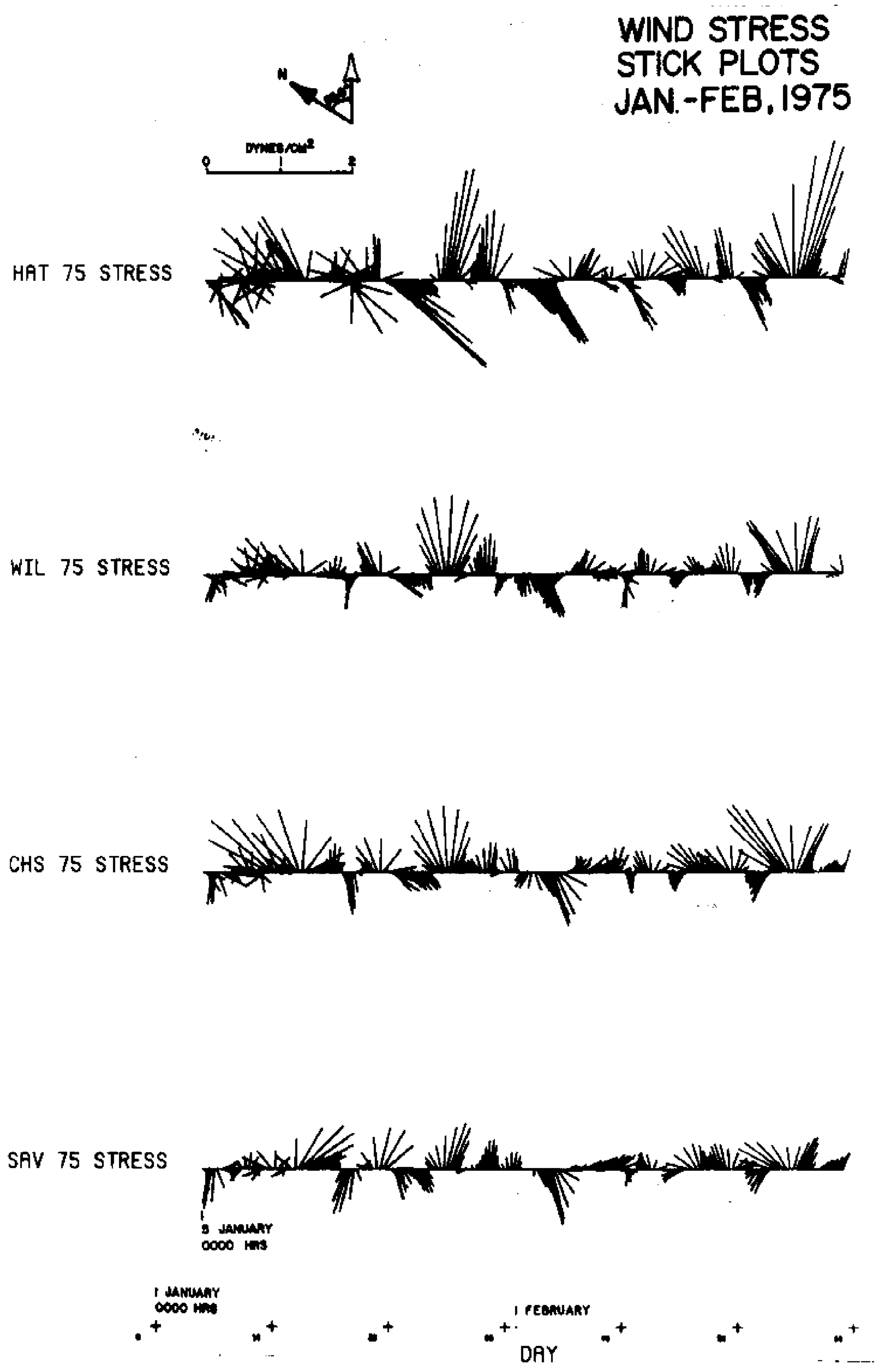

Figure 57 Wind stress vectors at Cape Hatteras, N. C., Wilmington, N. C., Charleston, S. C. and Savannah, Ga., Jan. through Feb., 1975

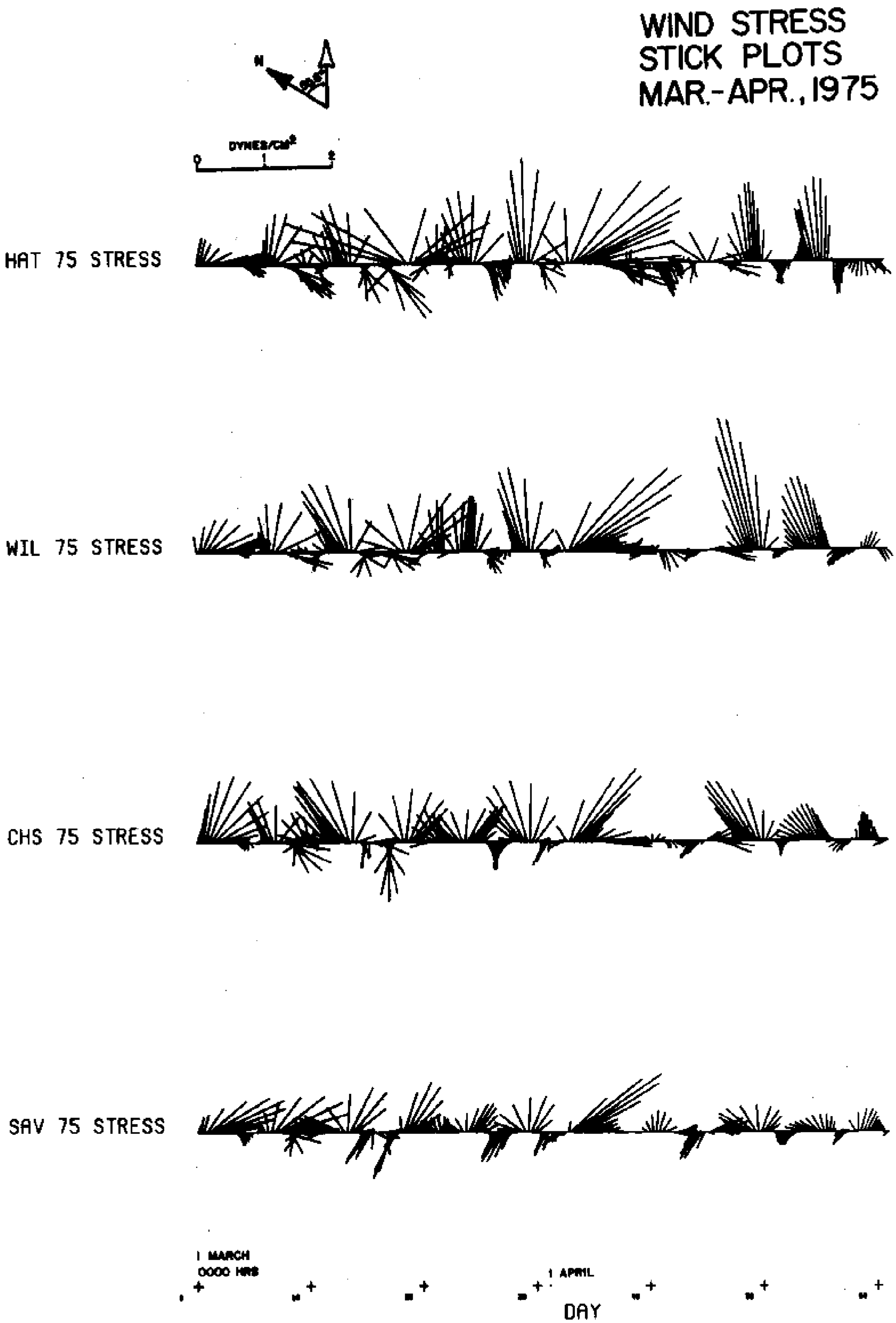

Figure 58 Wind stress vectors at Cape Hatteras, N. C., Wilmington, N. C., Charleston, S. C. and Savannah, Ga., Mar. through Apr., 1975

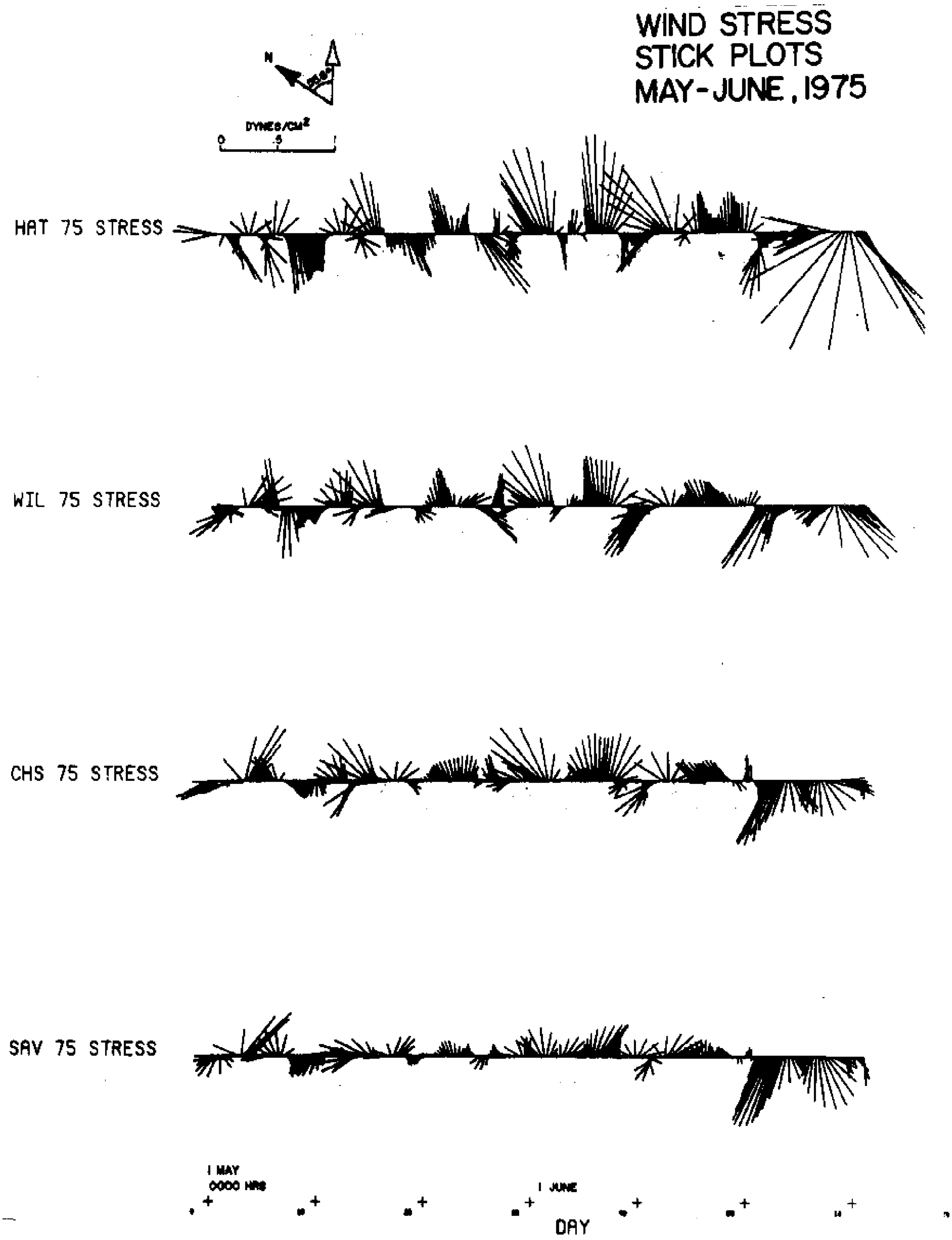

Figure 59 Wind stress vectors at Cape Hatteras, N. C., Wilmington, N. C., Charleston, S. C. and Savannah, Ga., May through June, 1975

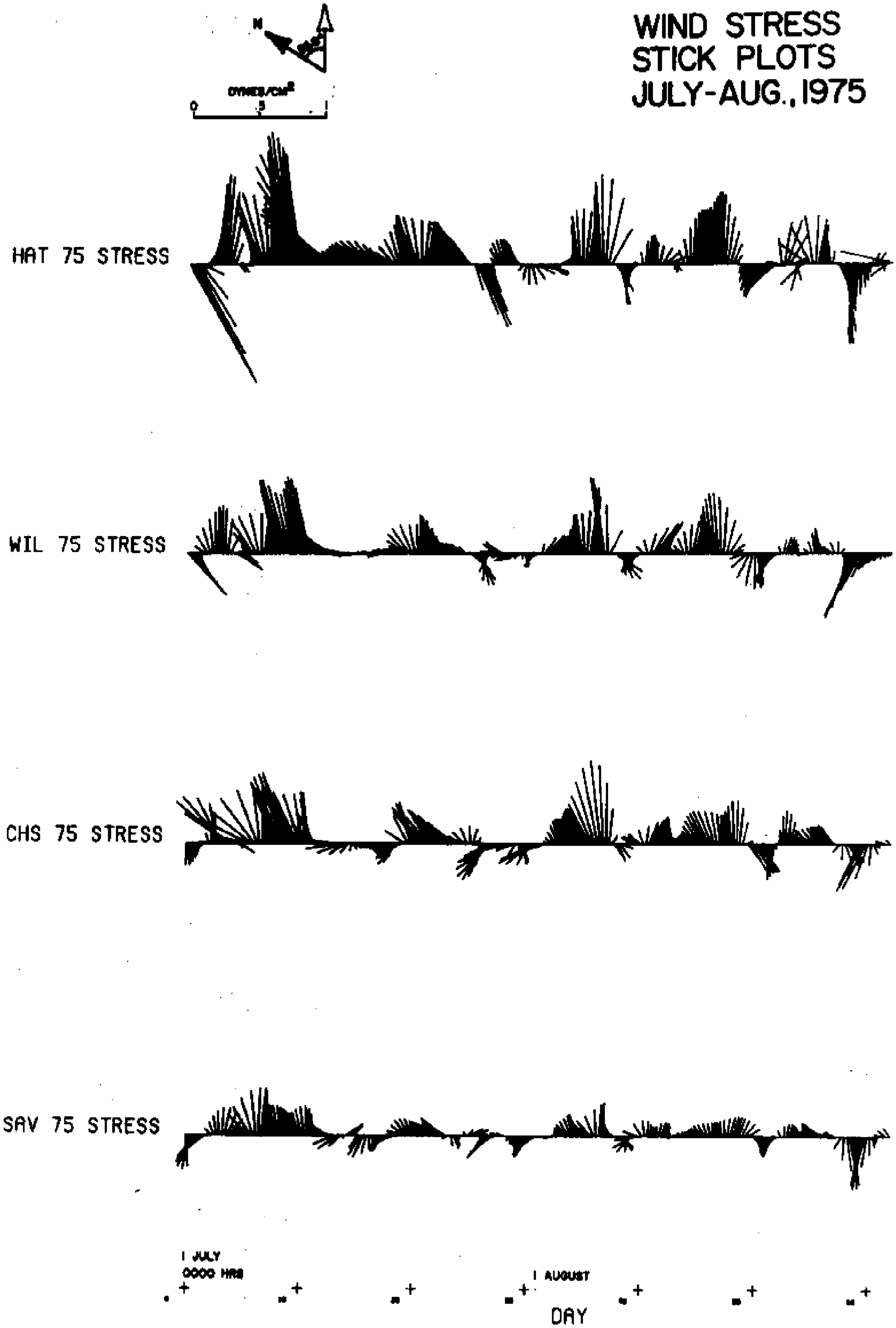

Figure 60 Wind stress vectors at Cape Hatteras, N. C., Wilmington, N. C., Charleston, S. C. and Savannah, Ga., July through Aug., 1975

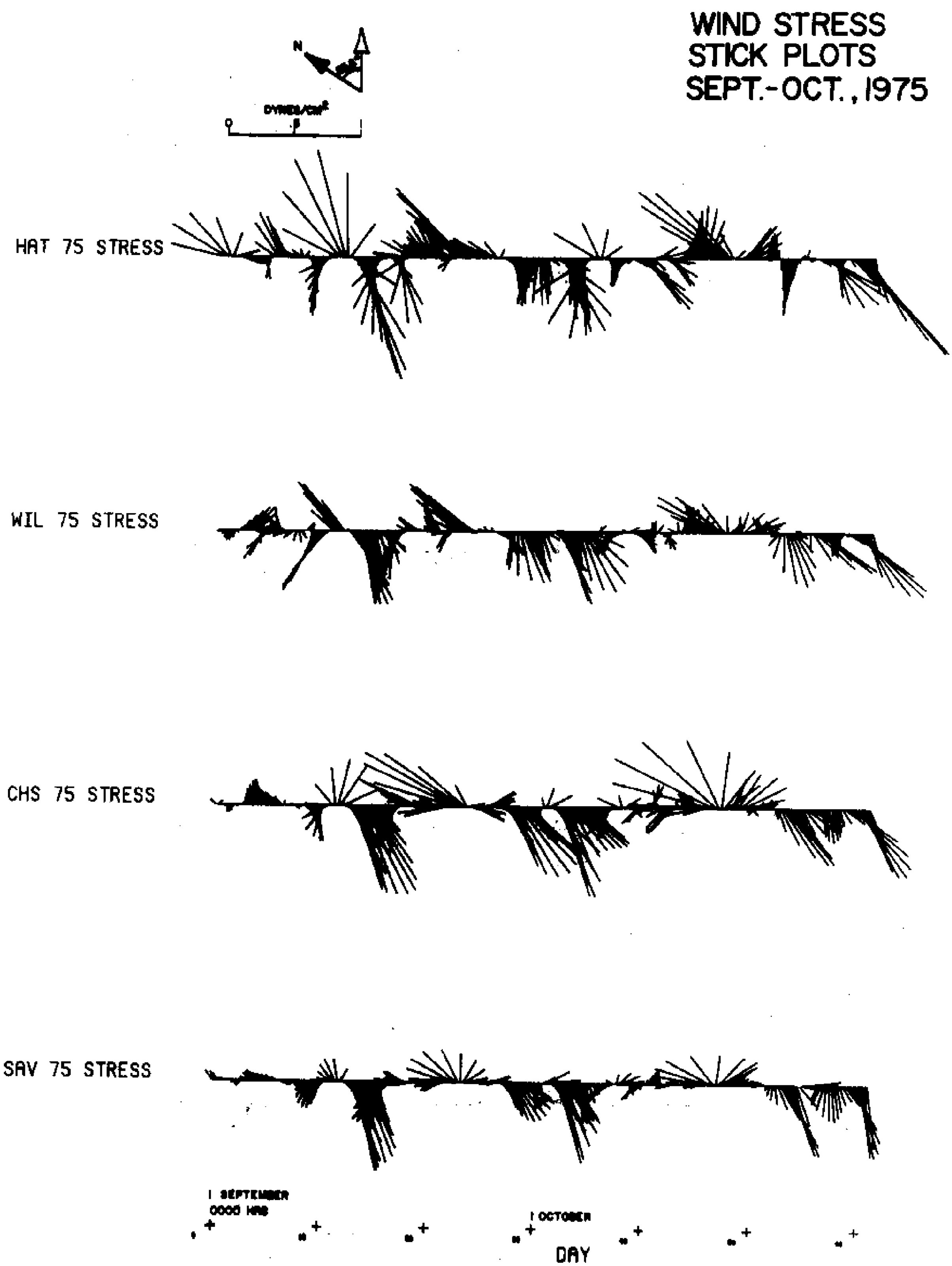

Figure 61 Wind stress vectors at Cape Hatteras, N. C., Wilmington, N. C., Charleston, S. C. and Savannah, Ga., Sept. through Oct., 1975

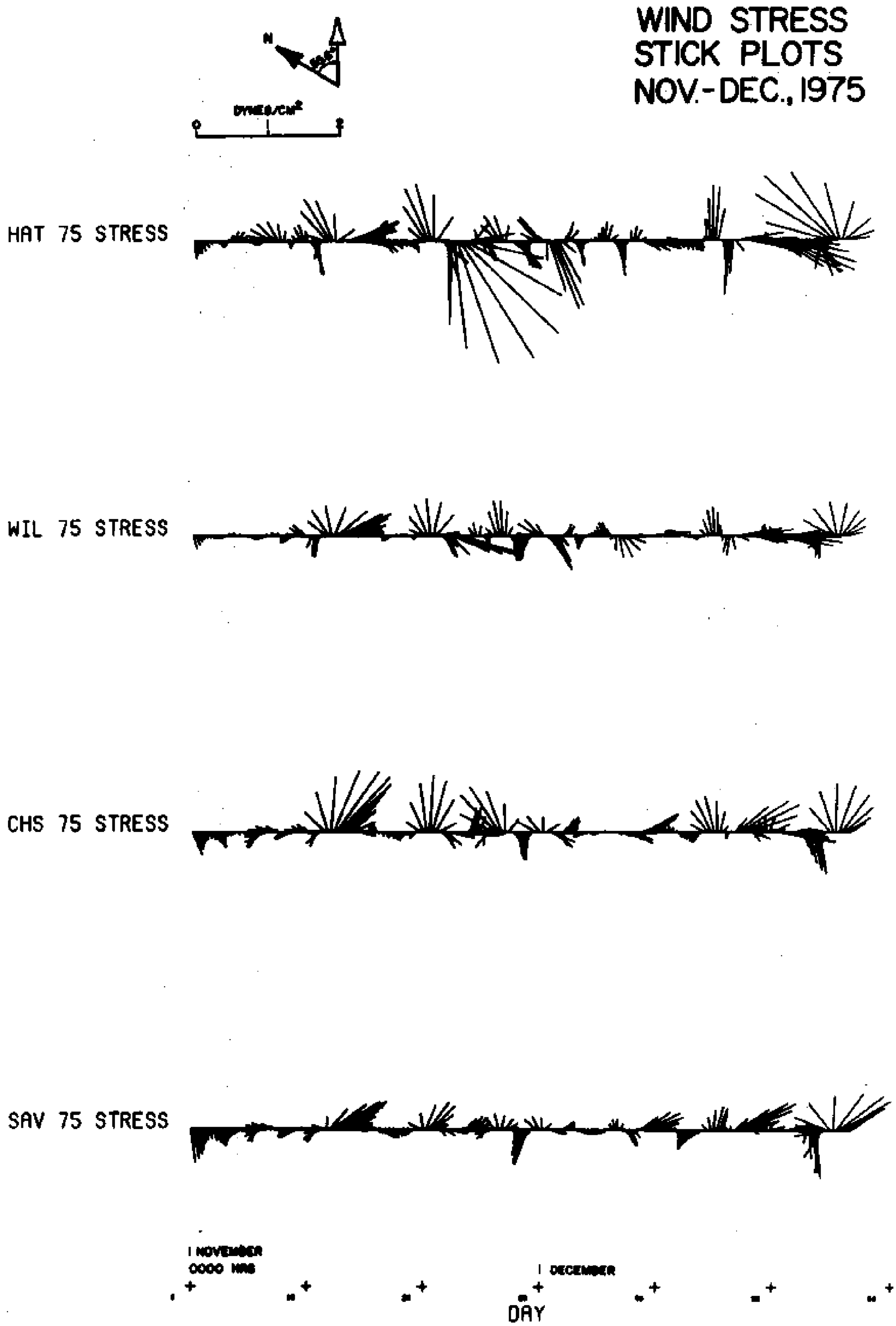

Figure 62 Wind stress vectors at Cape Hatteras, N. C., Wilmington, N. C., Charleston, S. C. and Savannah, Ga., Nov. through Dec., 1975

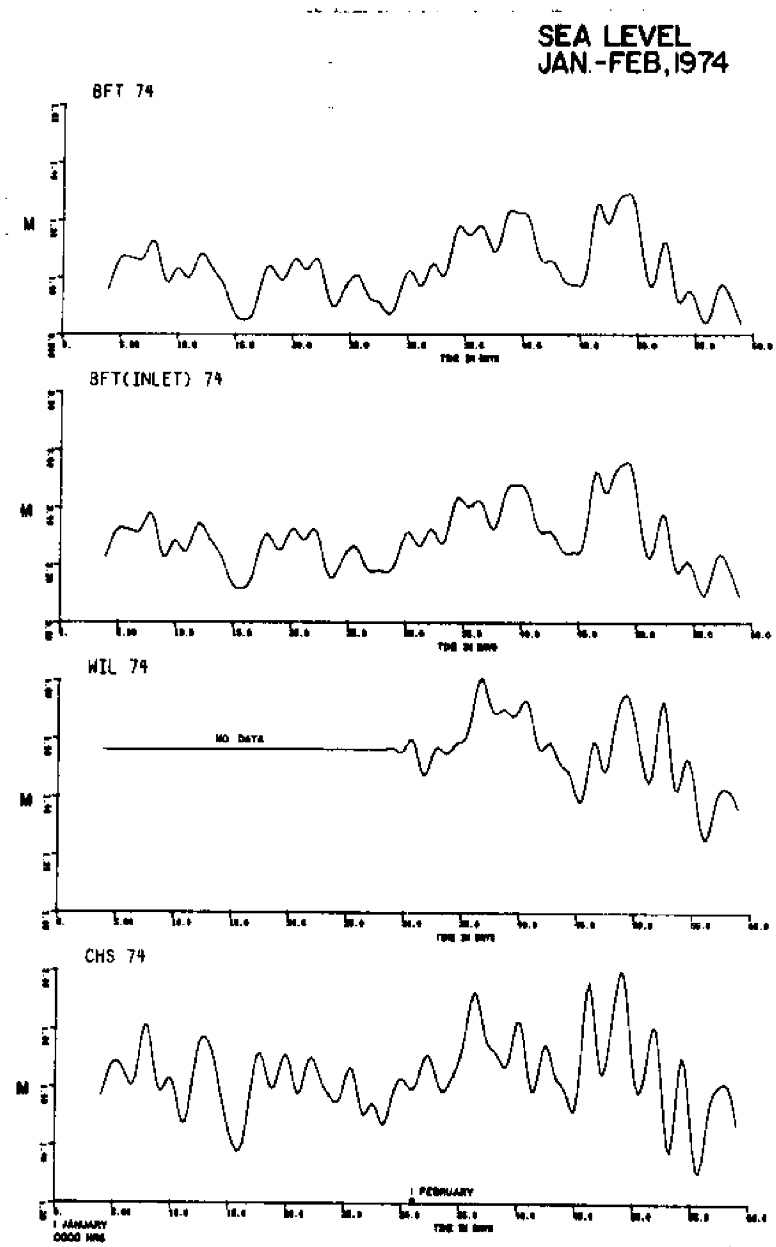

Figure 63 Sea level measurements at Beaufort, N. C., Beaufort Inlet, N. C., Wilmington, N. C. and Charleston, S. C., Jan. through Feb., 1974

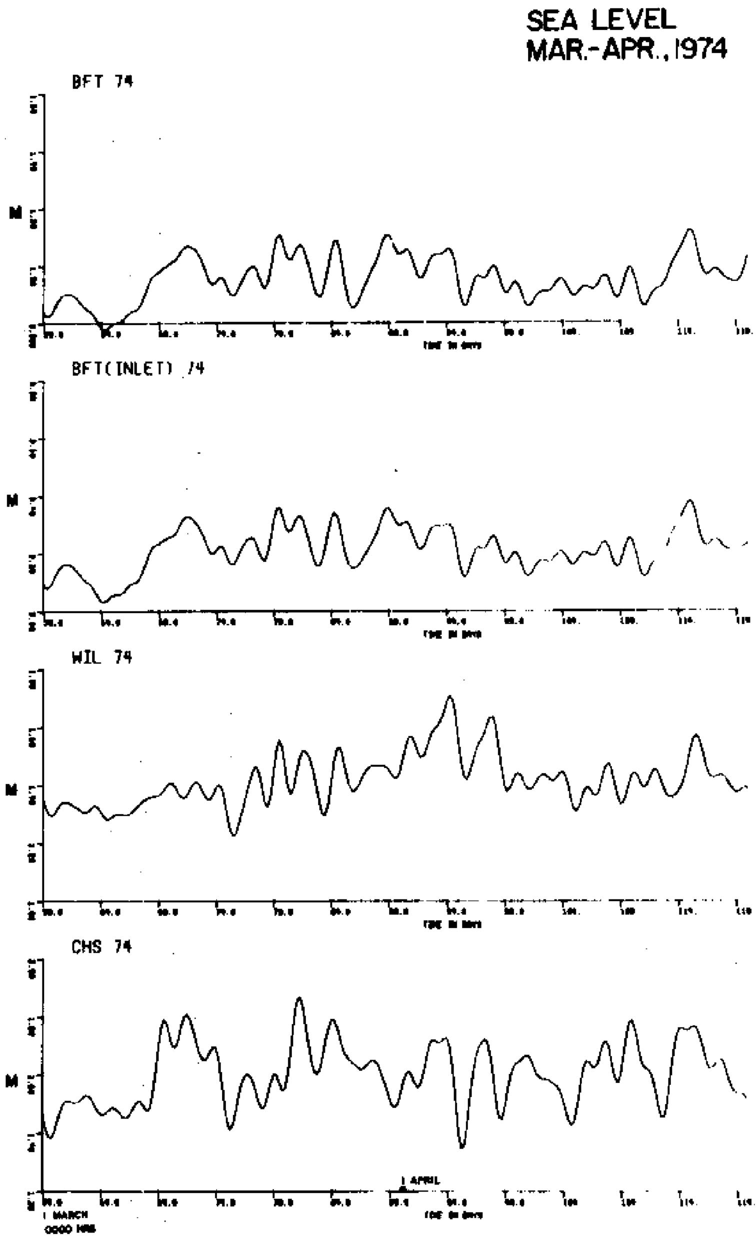

Figure 64 Sea level measurements at Beaufort, N. C., Beaufort Inlet, N. C., Wilmington, N. C. and Charleston, S. C., Mar. through Apr., 1974

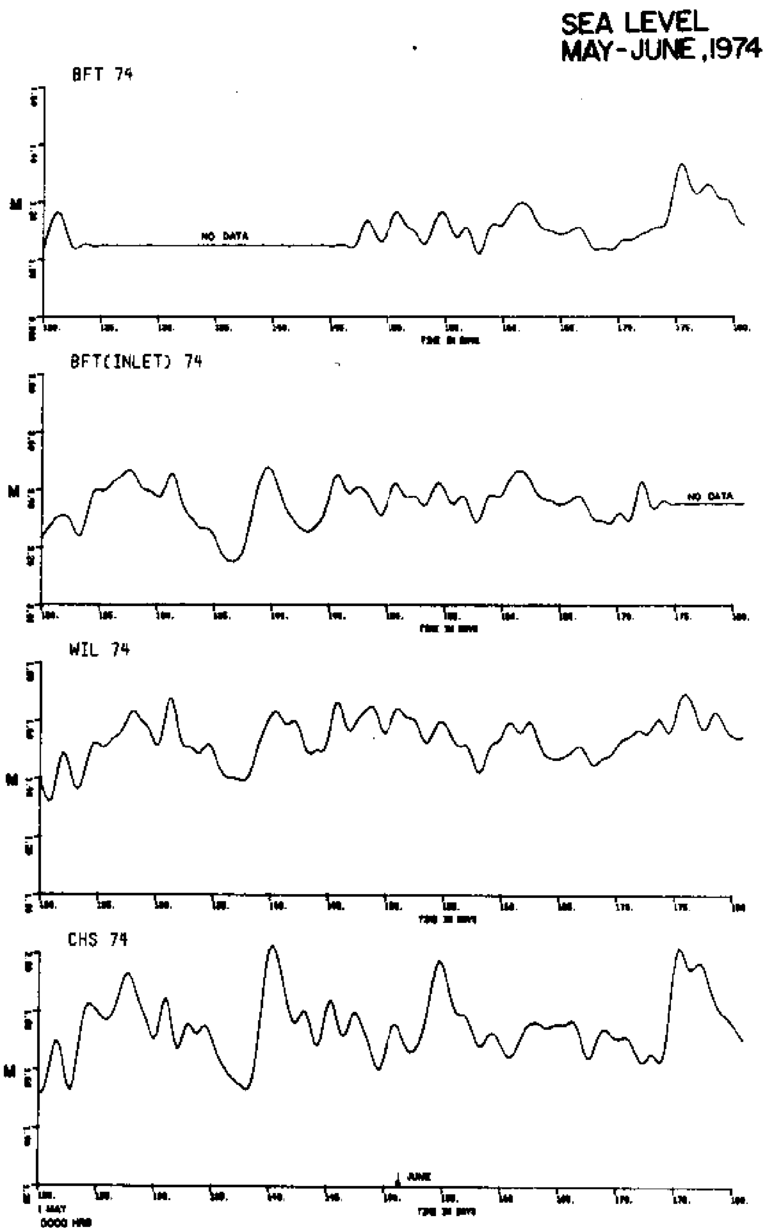

Figure 65 Sea level measurements at Beaufort, N. C., Beaufort Inlet, N. C., Wilmington, N. C. and Charleston, S. C., May through June, 1974

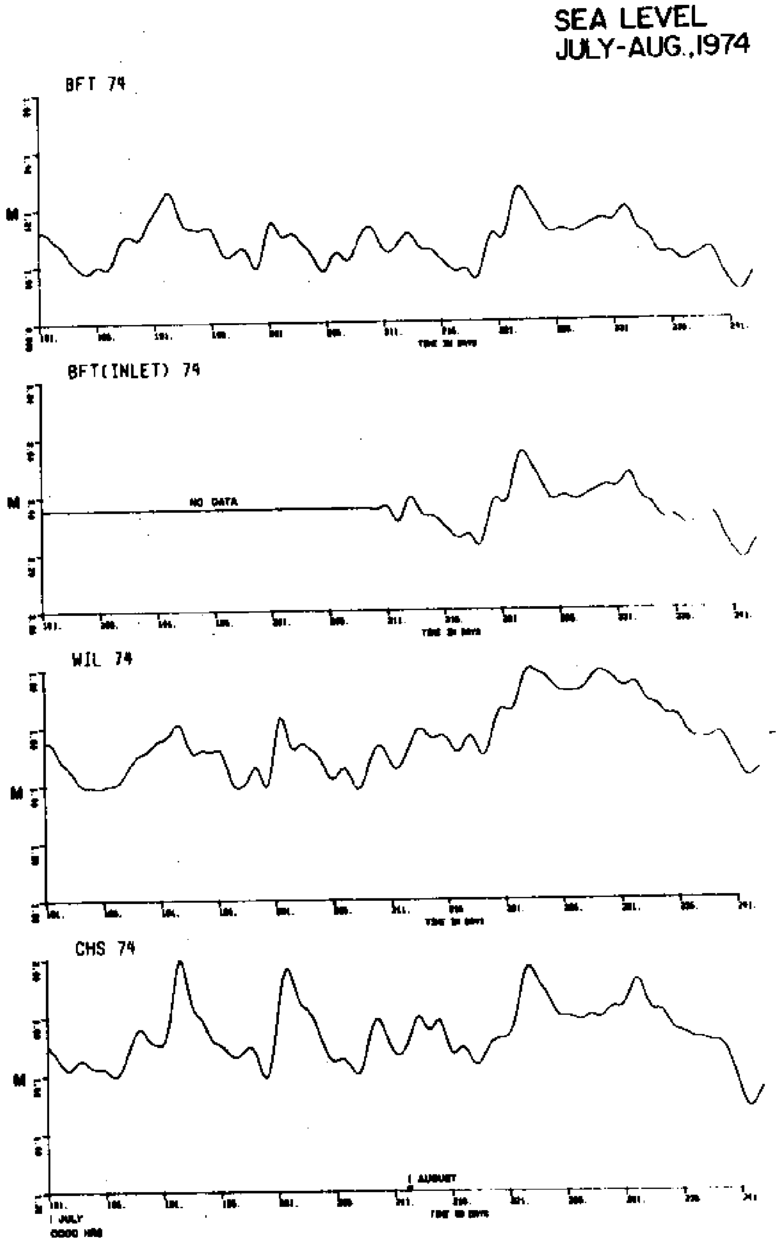

Figure 66 Sea level measurements at Beaufort, N. C., Beaufort Inlet, N. C., Wilmington, N. C. and Charleston, S. C., July through Aug., 1974

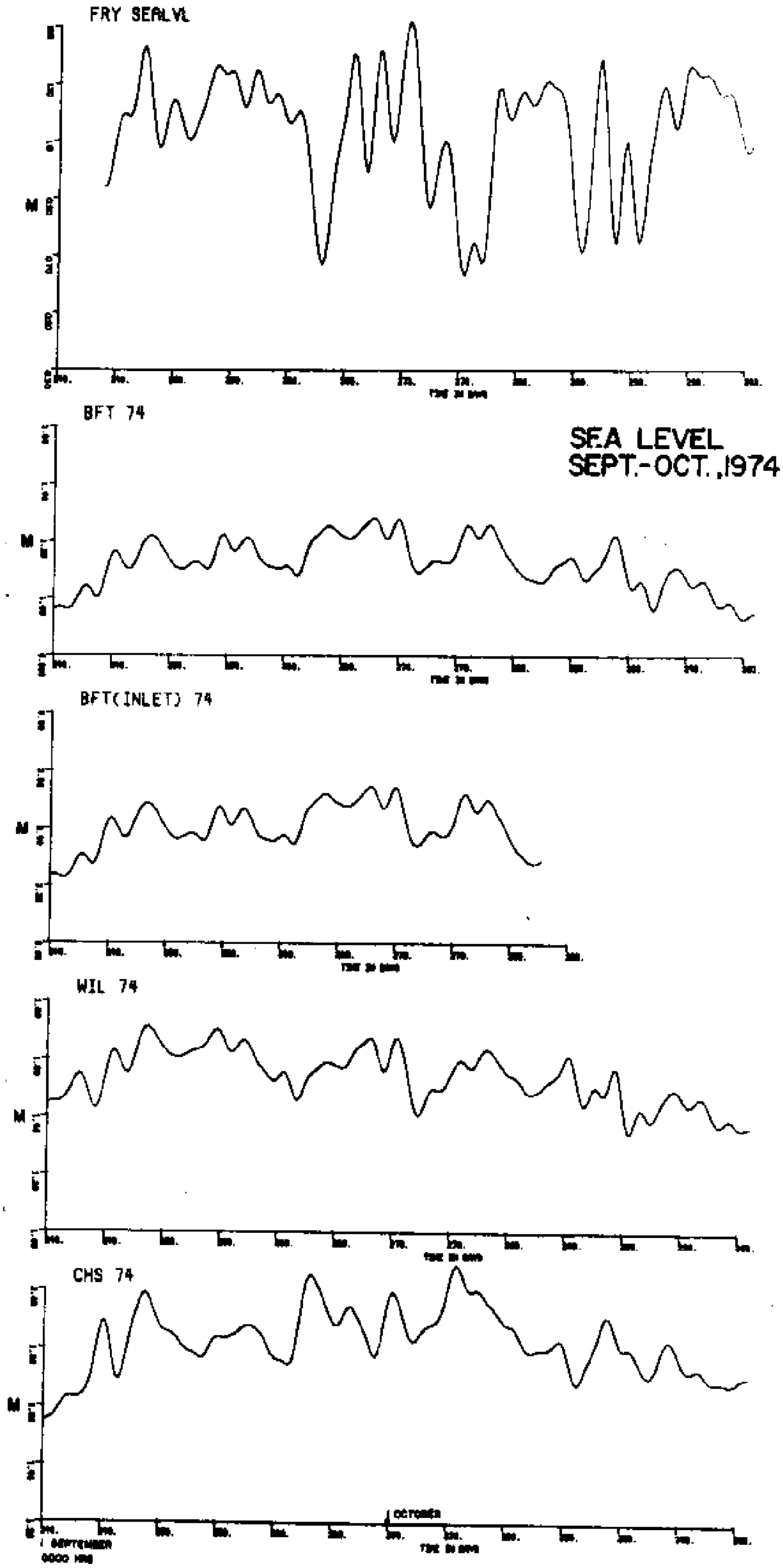

Figure 67 Sea level measurements at Frying Pan Shoals, N. C., Beaufort, N. C., Beaufort Inlet, N. C., Wilmington, N. C. and Charleston, S. C., Sept. through Oct., 1974

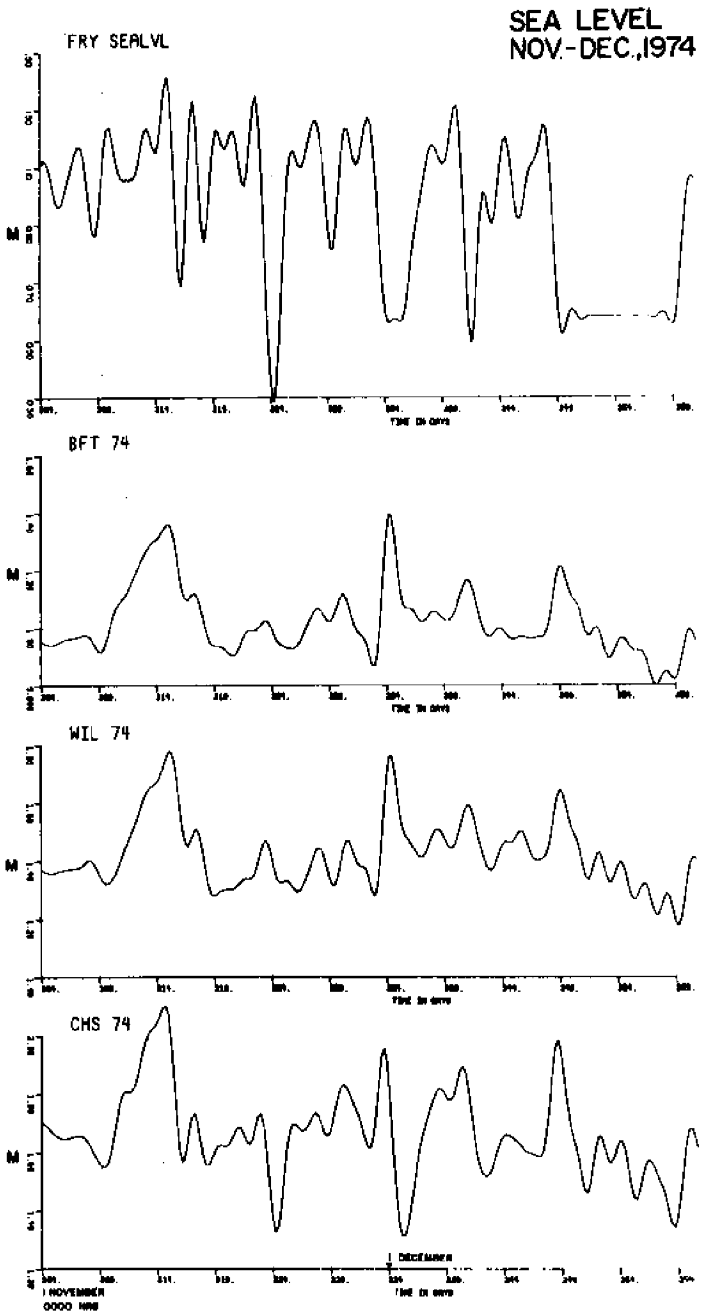

Figure 68 Sea level measurements at Frying Pan Shoals, N. C., Beaufort, N. C., Wilmington, N. C. and Charleston, S. C., Nov. through Dec. 1974

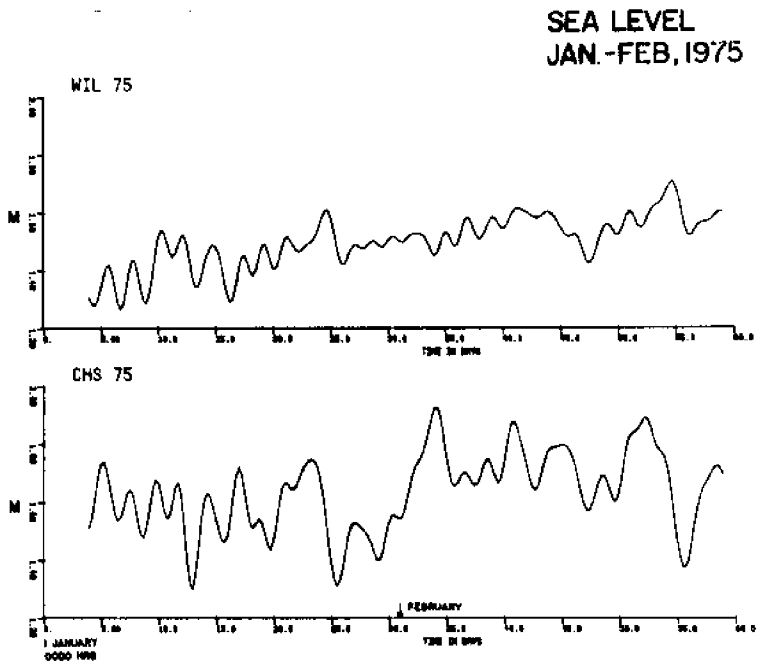

Figure 69 Sea level measurements at Wilmington, N. C. and Charleston, S. C., Jan. through Feb., 1975

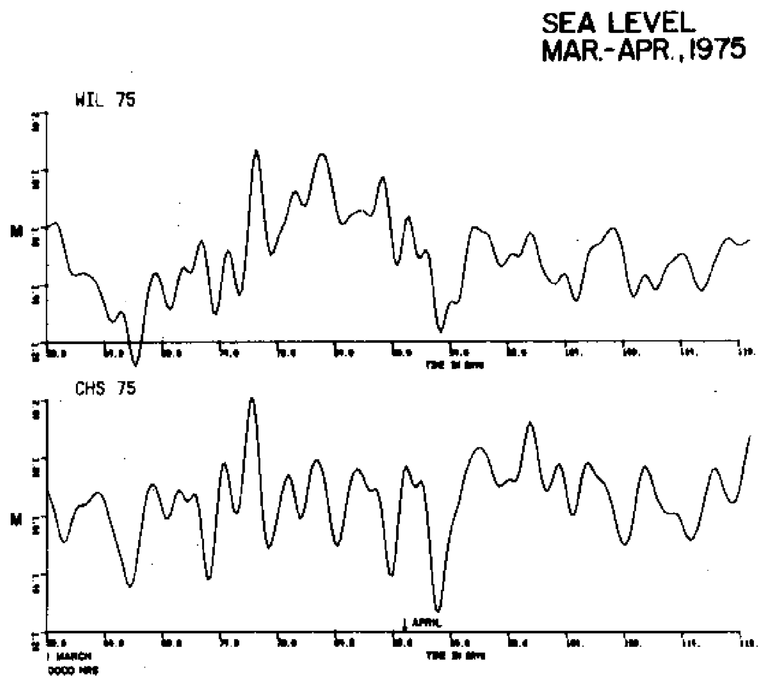

Figure 70 Sea level measurements at Wilmington, N. C. and Charleston, S. C., Mar. through Apr., 1975

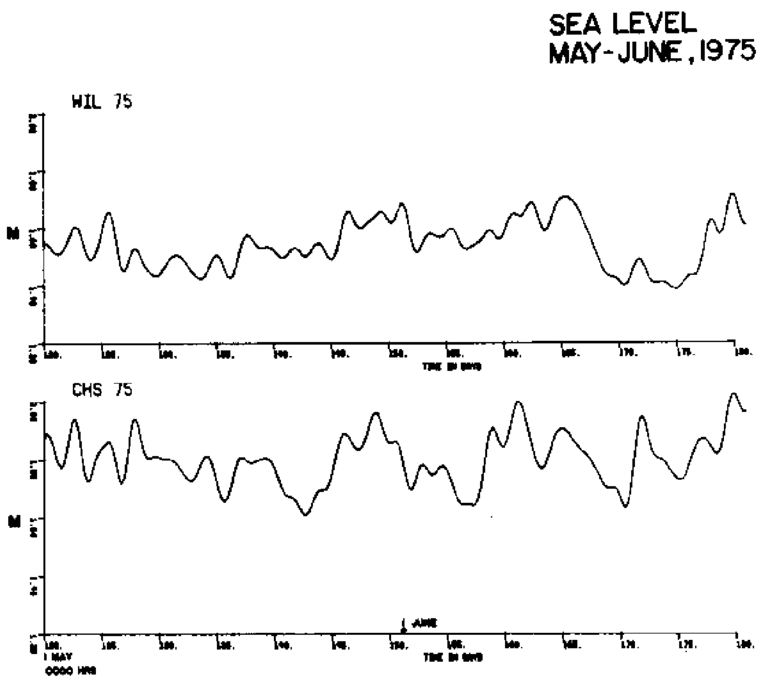

Figure 71 Sea level measurements at Wilmington, N. C. and Charleston, S. C., May through June, 1975

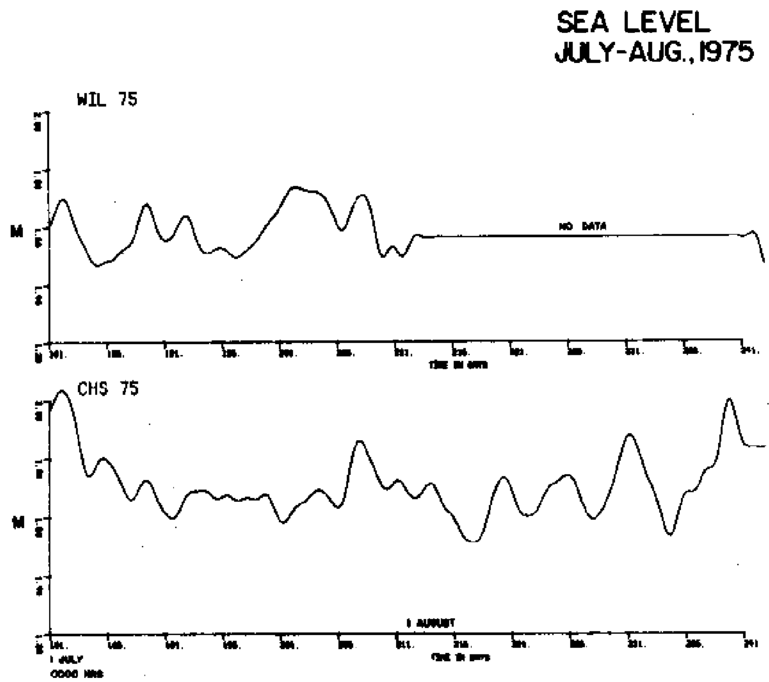

Figure 72 Sea level measurements at Wilmington, N. C. and Charleston, S. C., July through Aug., 1975

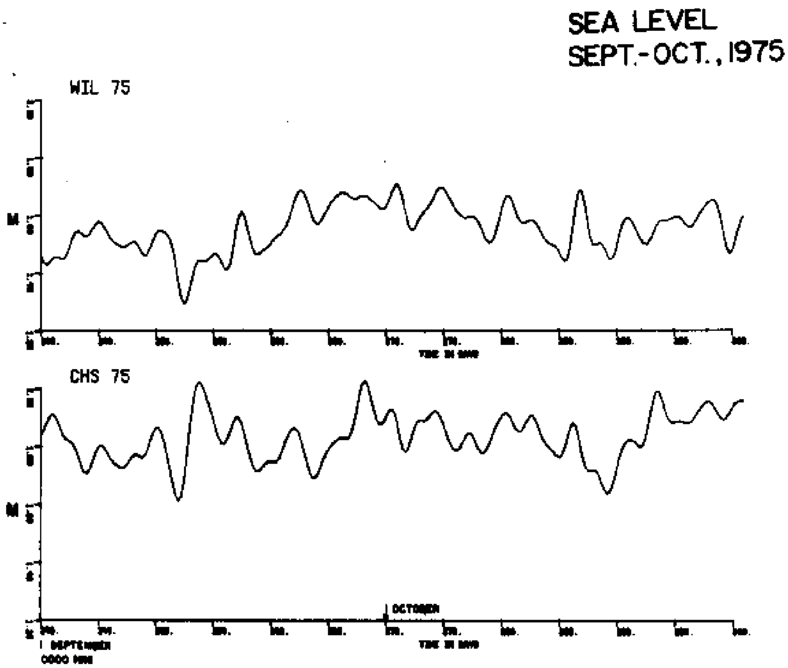

Figure 73 Sea level measurements at Wilmington, N. C., and Charleston, S. C., Sept. through Oct., 1975

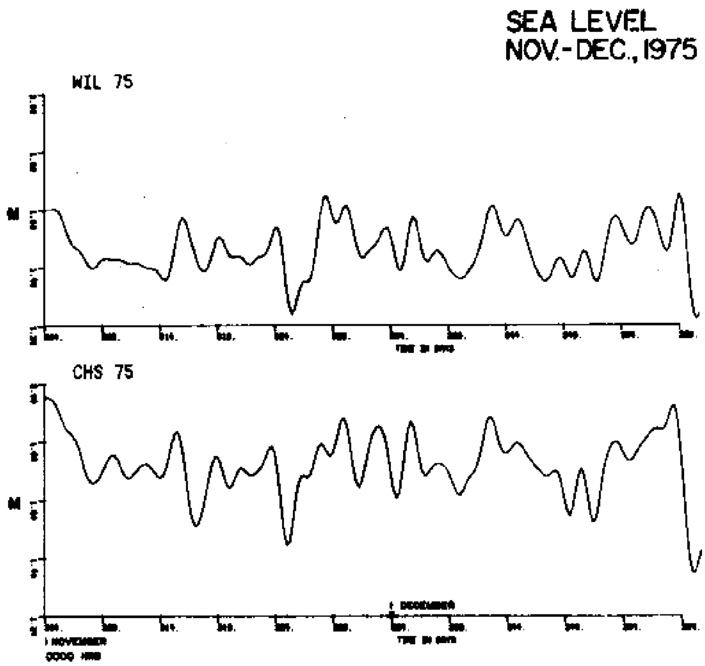

Figure 74 Sea level measurements at Wilmington, N. C. and Charleston, S. C., Nov. through Dec., 1975

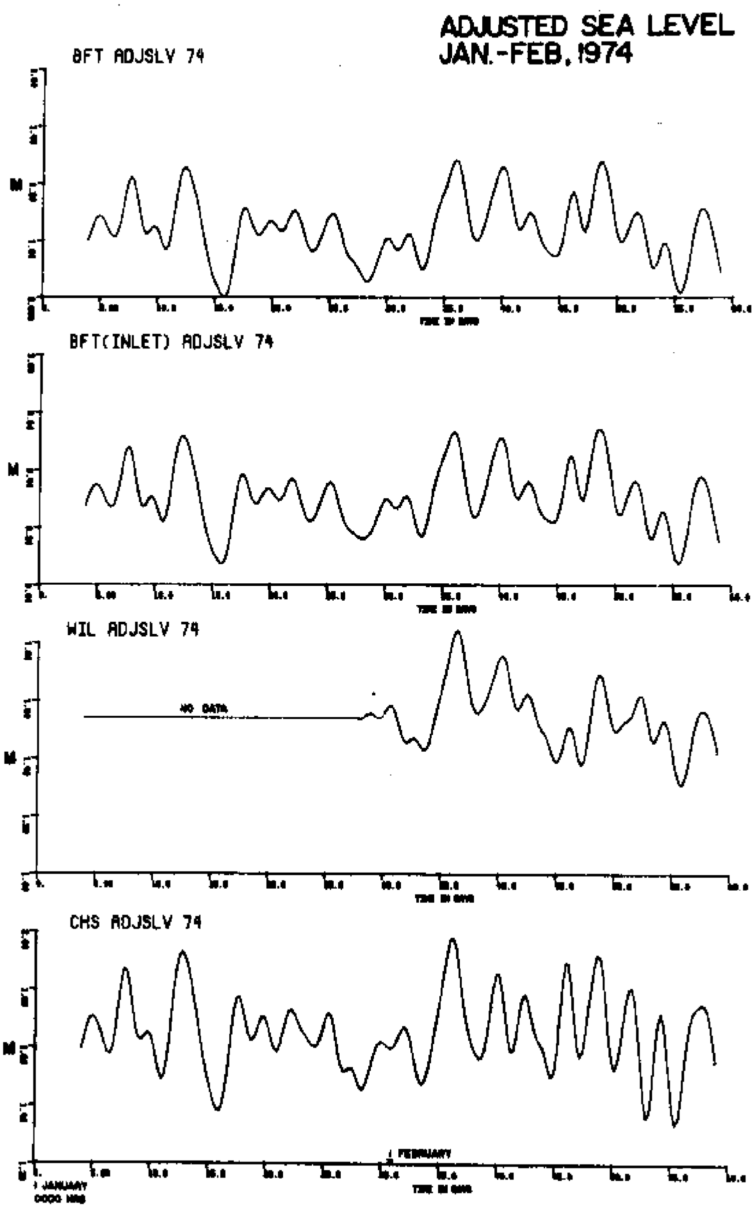

Figure 75 Adjusted sea level measurements at Beaufort, N. C., Beaufort Inlet, N. C., Wilmington, N. C. and Charleston, S. C., Jan. through Feb., 1974

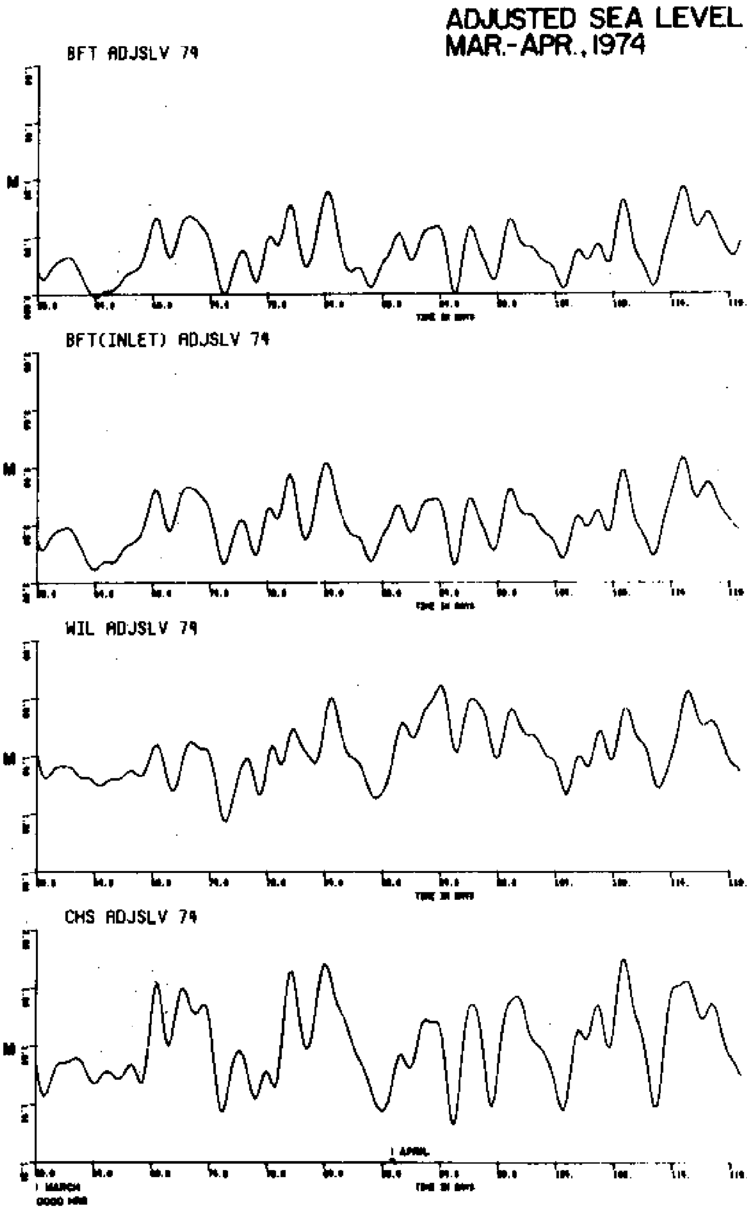

Figure 76 Adjusted sea level measurements at Beaufort, N. C., Beaufort Inlet, N. C., Wilmington, N. C. and Charleston, S. C., Mar. through Apr., 1974

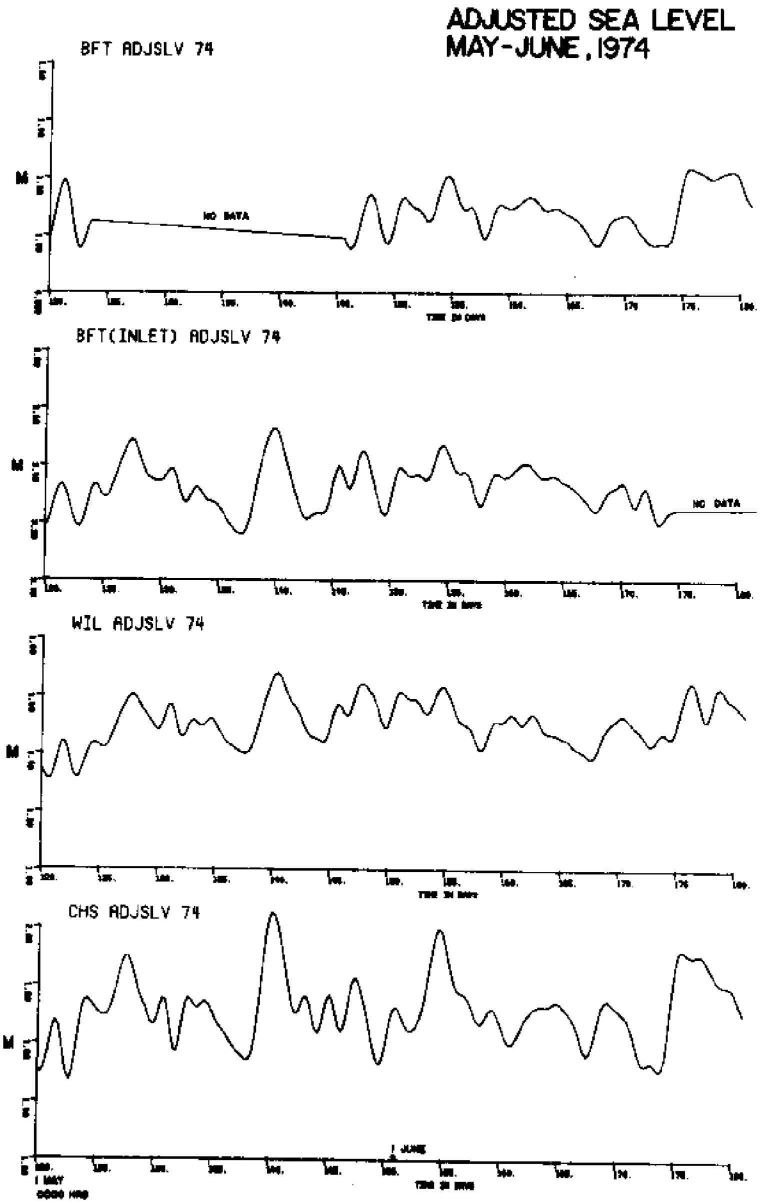

Figure 77 Adjusted sea level measurements at Beaufort, N. C., Beaufort Inlet, N. C., Wilmington, N. C. and Charleston, S. C., May through June, 1974

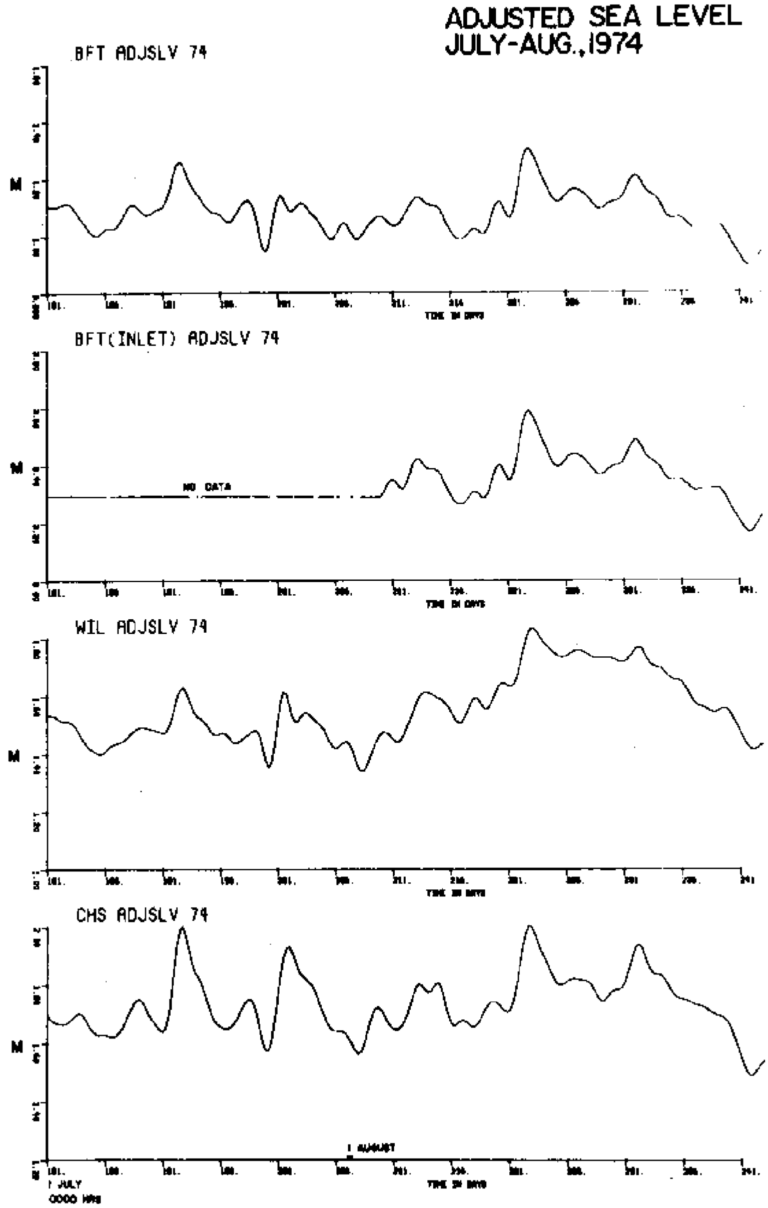

Figure 78 Adjusted sea level measurements at Beaufort, N. C., Beaufort Inlet, N. C., Wilmington, N. C. and Charleston, S. C., July through Aug., 1974

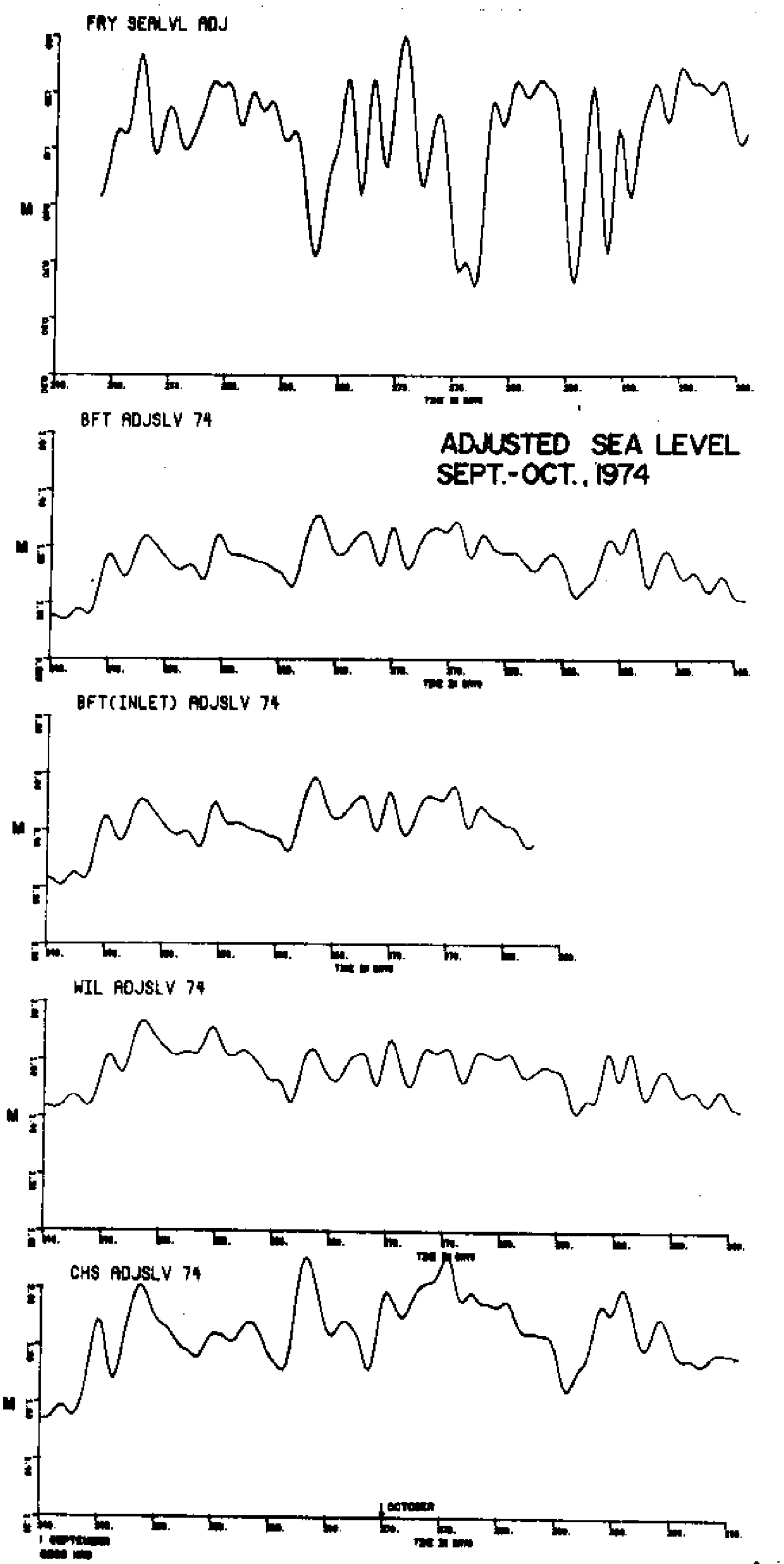

Figure 79 Adjusted sea level measurements at Frying Pan Shoals, N. C., Beaufort, N. C. Beaufort Inlet, N. C., Wilmington, N. C. and Charleston, S. C., Sept. through Oct., 1974

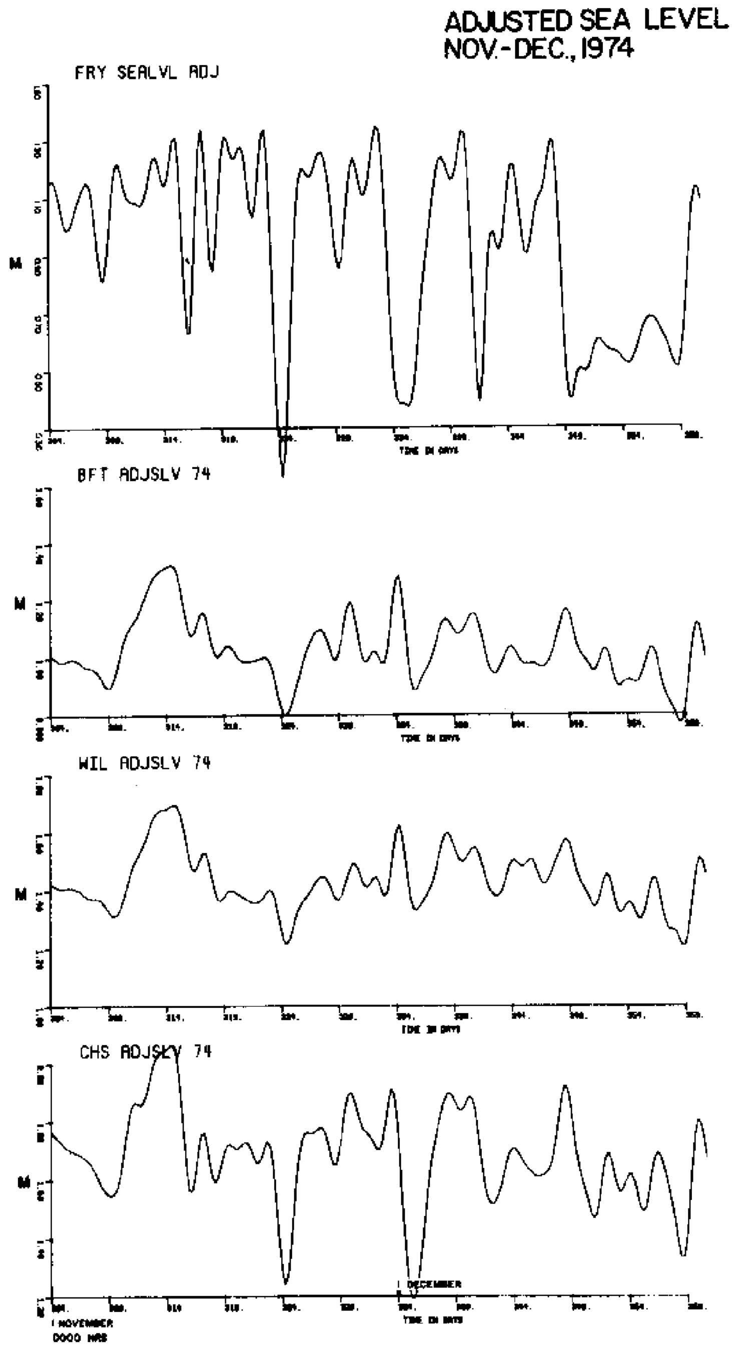

Figure 80 Adjusted sea level measurements at Frying Pan Shoals, N. C., Beaufort, N. C., Wilmington, N. C. and Charleston, S. C., Nov. through Dec., 1974

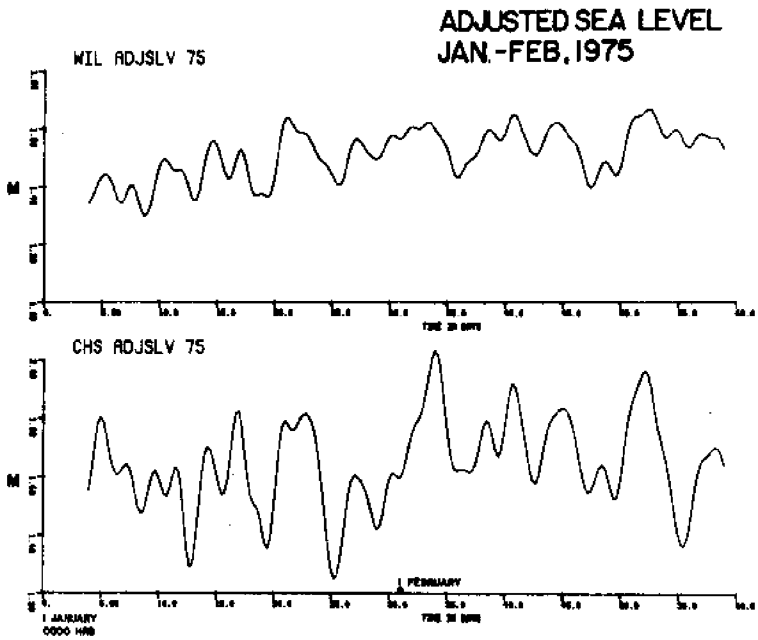

Figure 81 Adjusted sea level measurements at Wilmington, N. C. and Charleston, S. C., Jan. through Feb., 1975

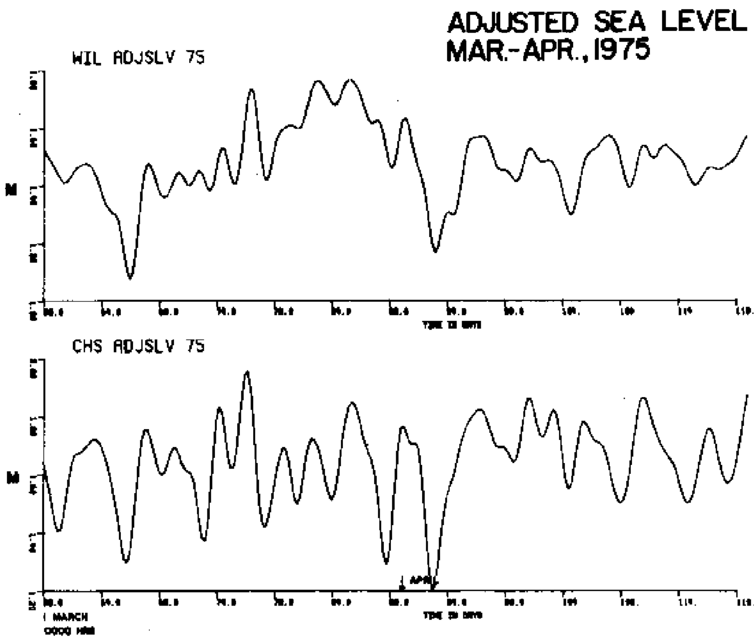

Figure 82 Adjusted sea level measurements at Wilmington, N. C. and Charleston, S. C., Mar. through Apr., 1975

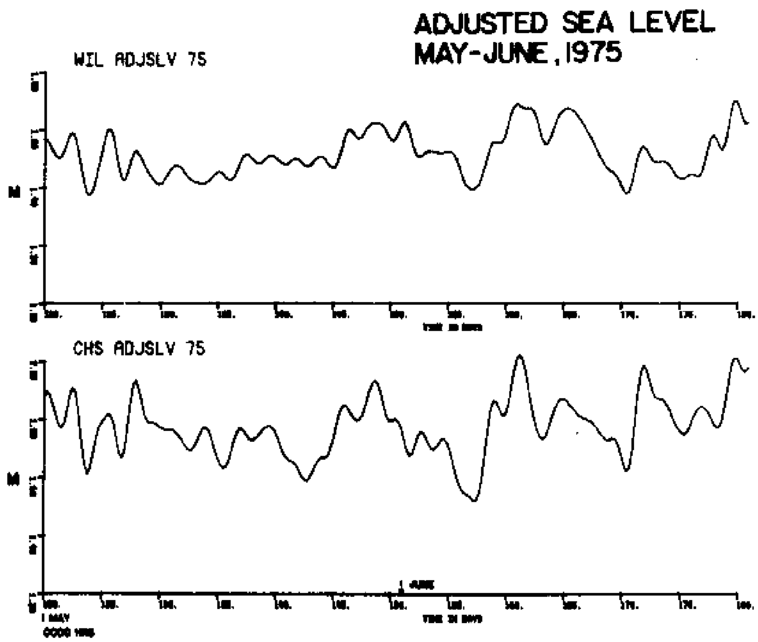

Figure 83 Adjusted sea level measurements at Wilmington, C. C. and Charleston, S. C., May through June, 1975

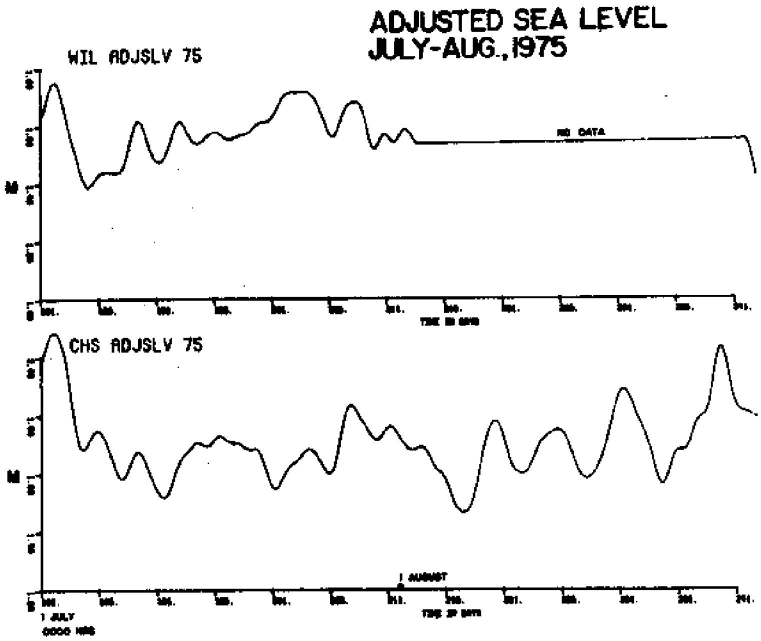

Figure 84 Adjusted sea level measurements at Wilmington, N. C. and Charleston, S. C., July through Aug., 1975

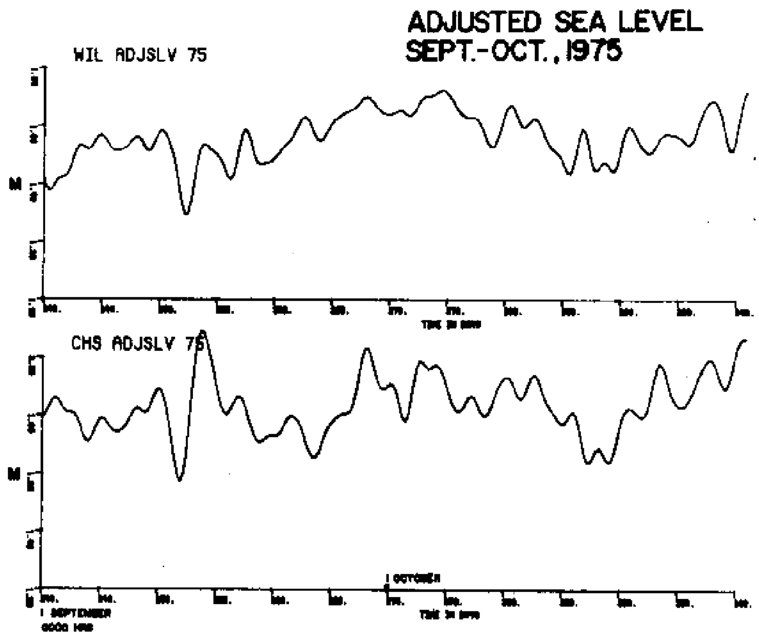

Figure 85 Adjusted sea level measurements at Wilmington, N. C. and Charleston, S. C., Sept. through Oct., 1975

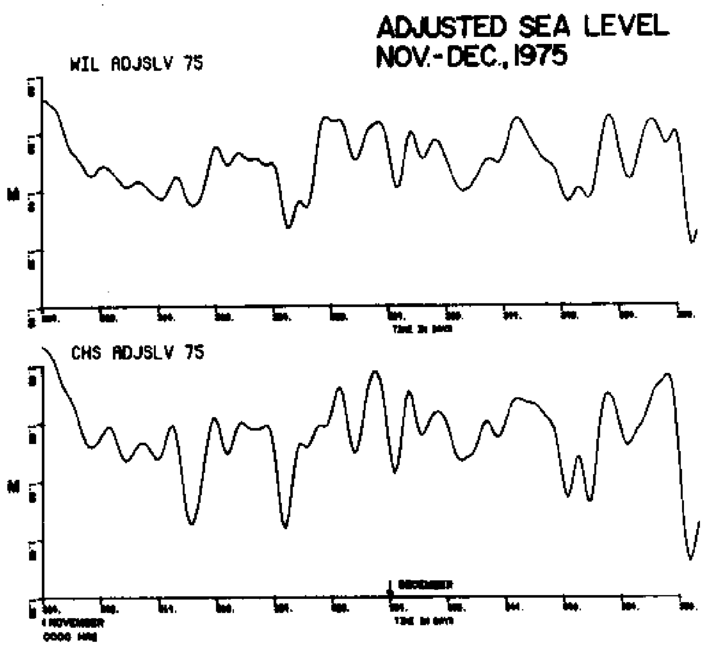

Figure 86 Adjusted sea level measurements at Wilmington, N. C. and Charleston, S. C., Nov. through Dec., 1975

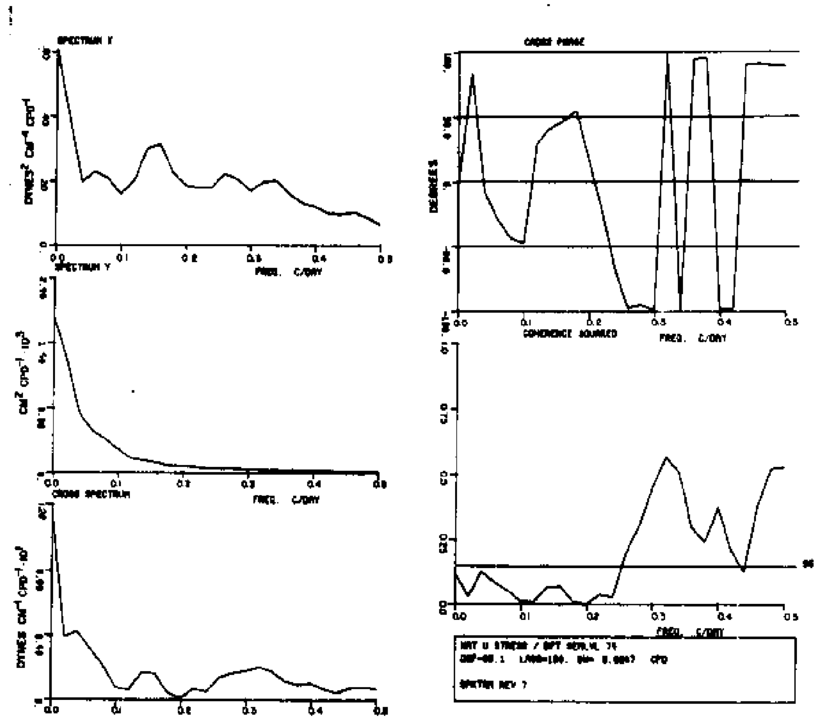

Figure 87 Spectra of wind stress u component at Cape Hatteras, N. C. vs. the sea level at Beaufort, N. C., 1974

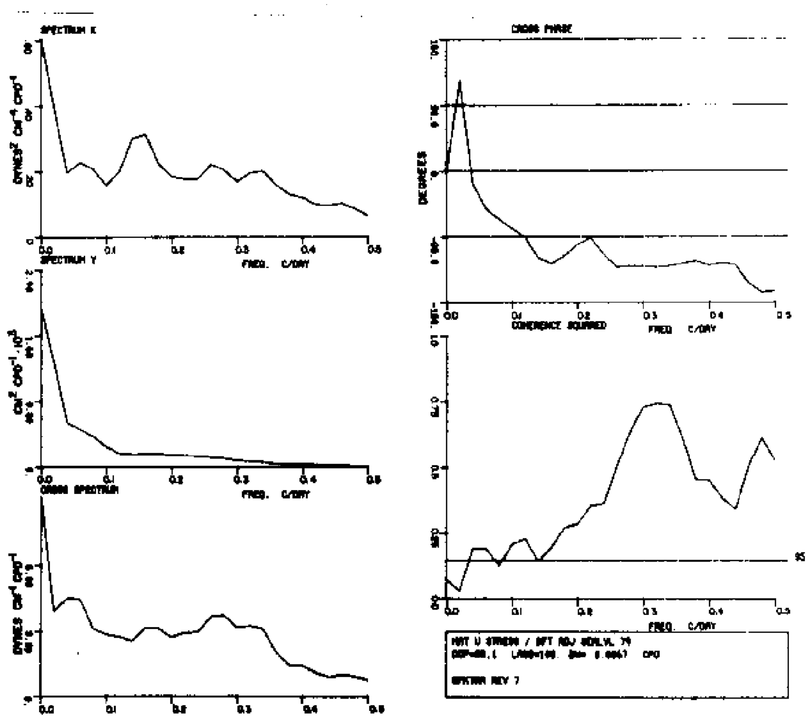

Figure 88 Spectra of wind stress u component at Cape Hatteras, N. C. vs. the adjusted sea level at Beaufort, N. C., 1974

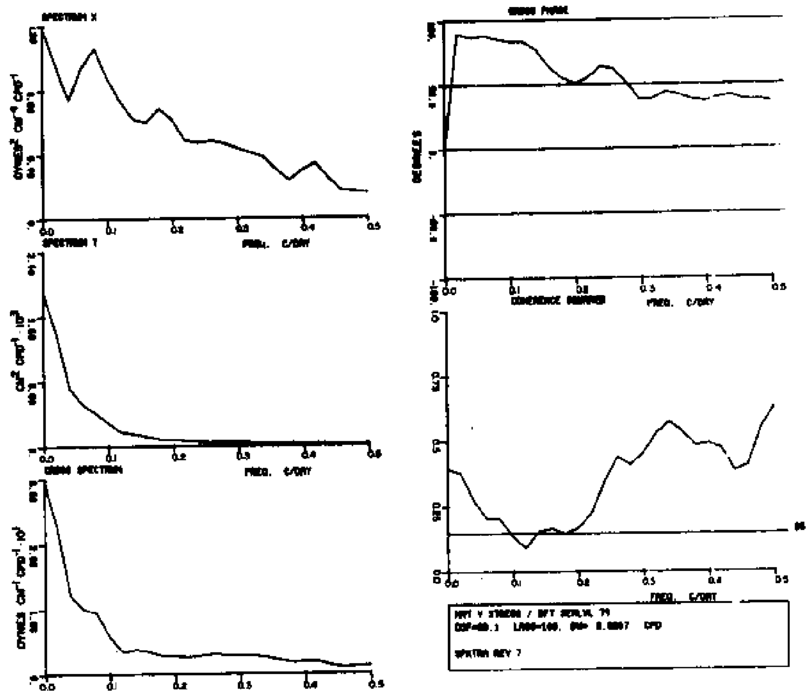

Figure 89 Spectra of wind stress v component at Cape Hatteras, N. C. vs. the sea level at Beaufort, N. C., 1974

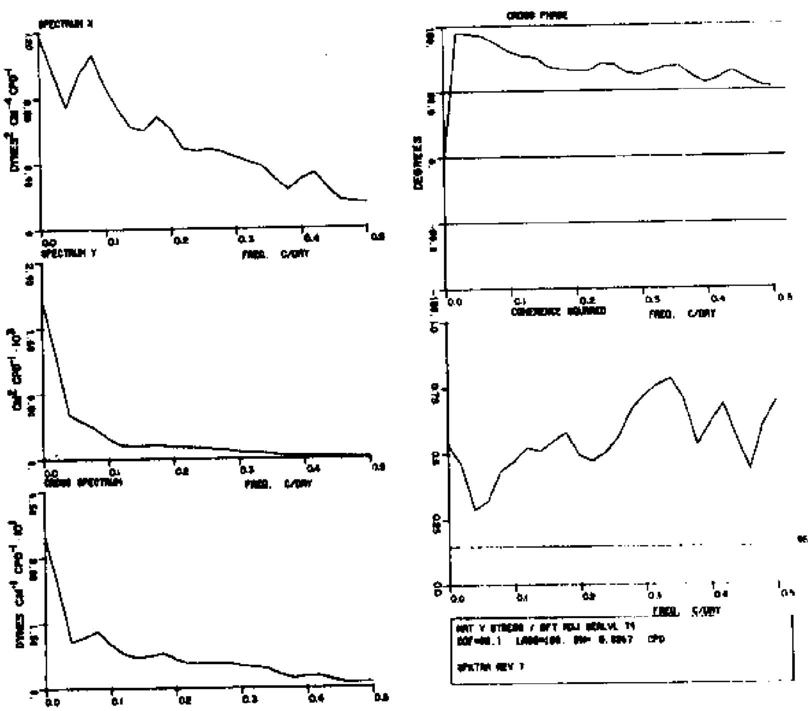

Figure 90 Spectra of wind stress v component at Cape Hatteras, N. C. vs. the adjusted sea level at Beaufort, N. C., 1974

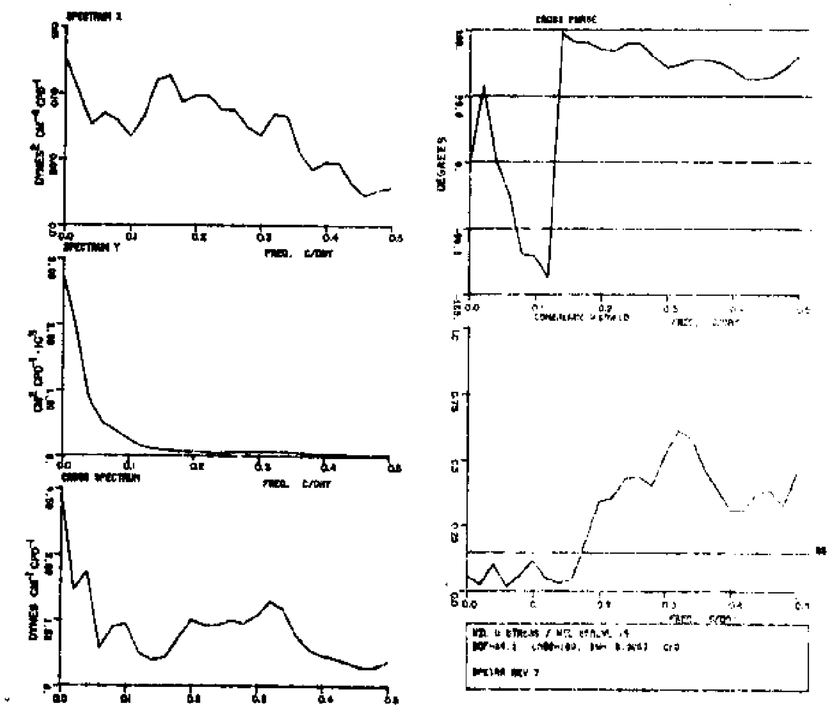

Figure 91 Spectra of wind stress u component at Wilmington, N. C. vs. the sea level at Wilmington, N. C., 1974

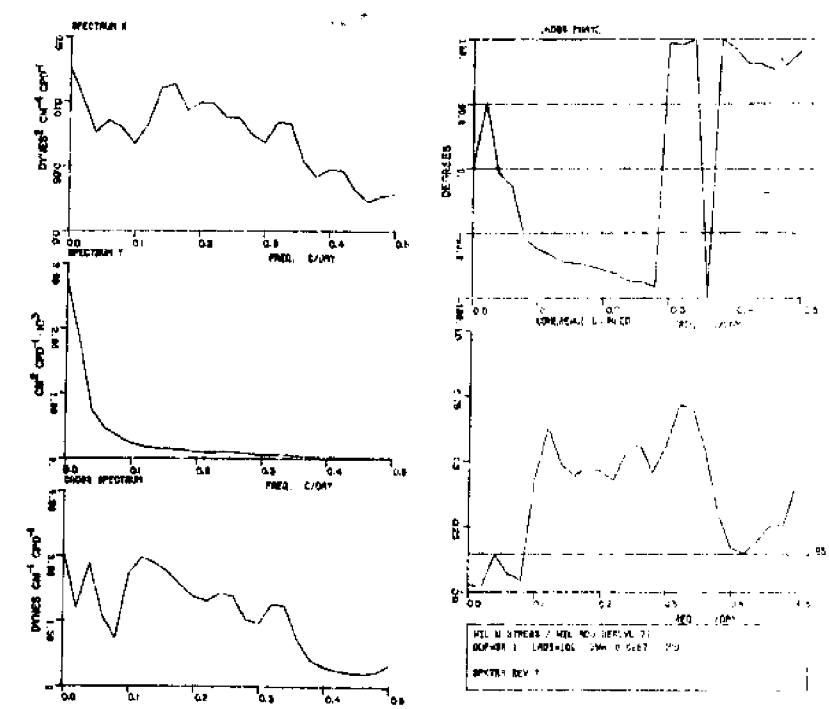

Figure 92 Spectra of wind stress u component at Wilmington, N. C. vs. the adjusted sea level at Wilmington, N. C., 1974

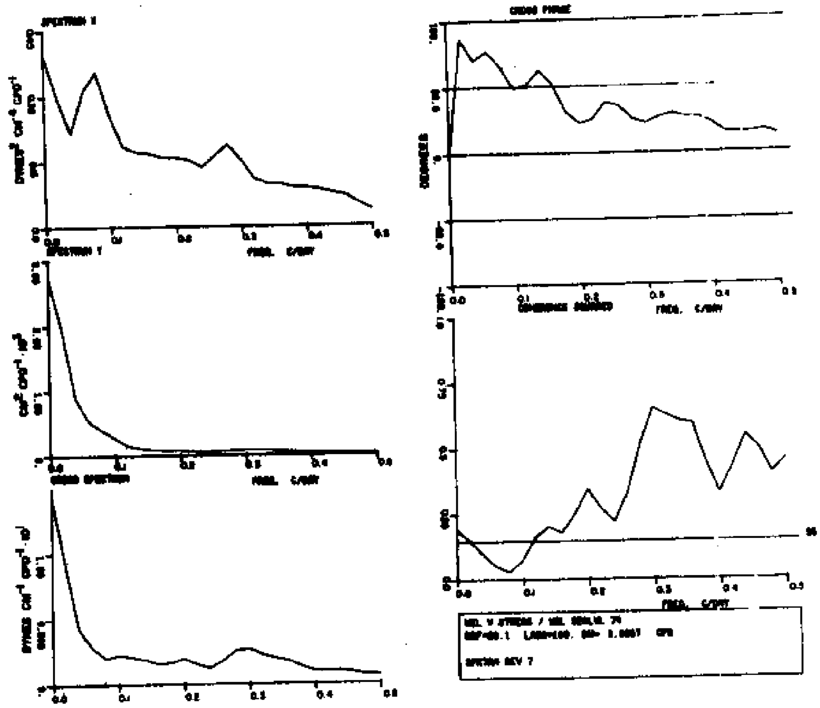

Figure 93 Spectra of wind stress v component at Wilmington, N. C. vs. the sea level at Wilmington, N. C., 1974

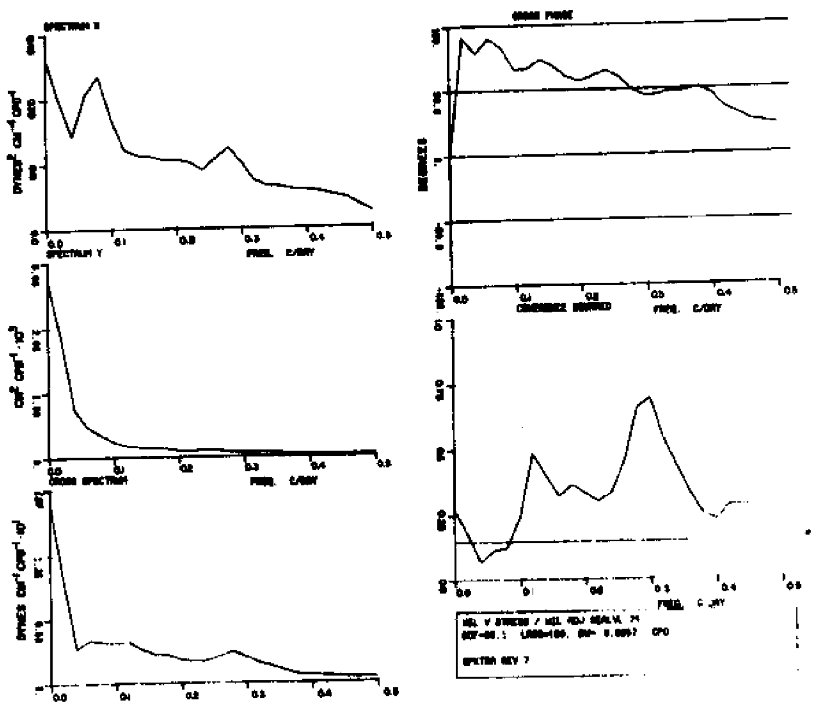

Figure 94 Spectra of wind stress v component at Wilmington, N. C. vs. the adjusted sea level at Wilmington, N. C., 1974

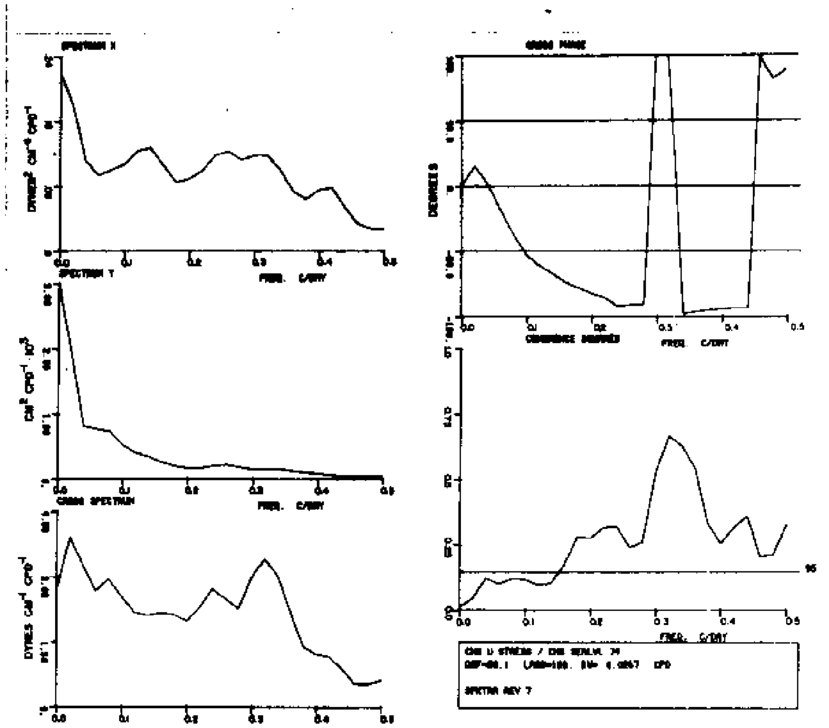

Figure 95 Spectra of wind stress u component at Charleston, S. C. vs. the sea level at Charleston, S. C., 1974

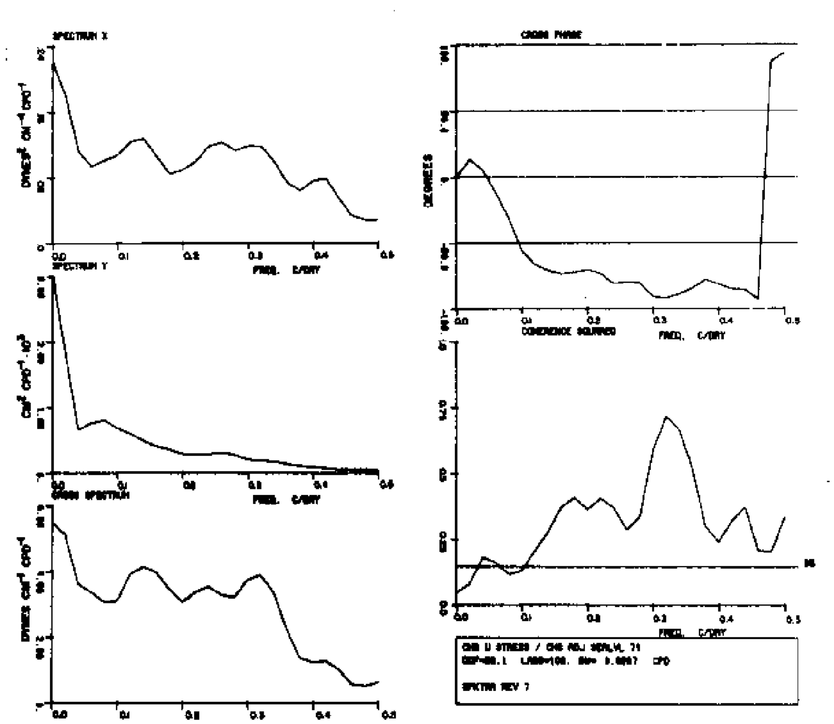

Figure 96 Spectra of wind stress u component at Charleston, S. C. vs. the adjusted sea level at Charleston, S. C., 1974

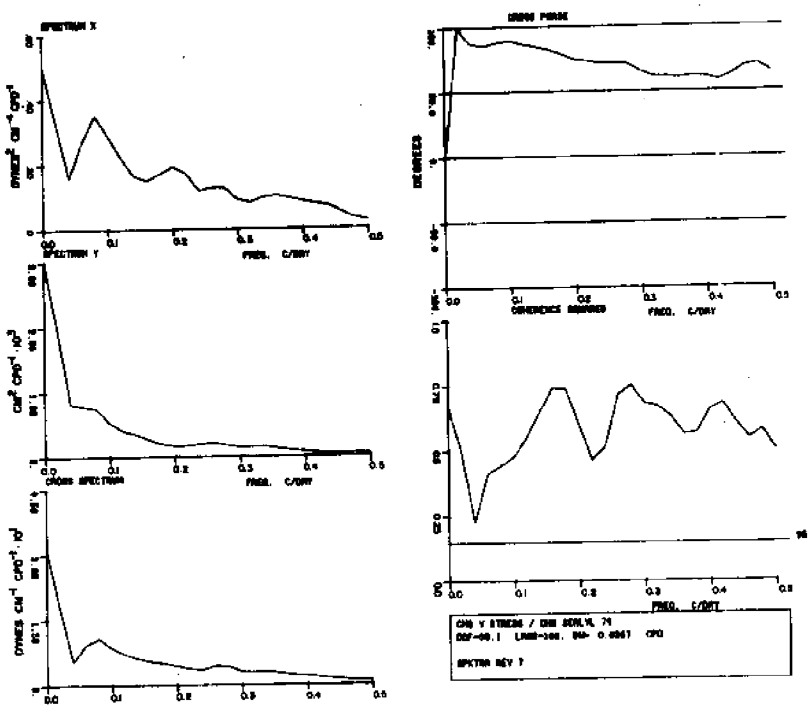

Figure 97 Spectra of wind stress v component at Charleston, S. C. vs. the sea level at Charleston, S. C., 1974

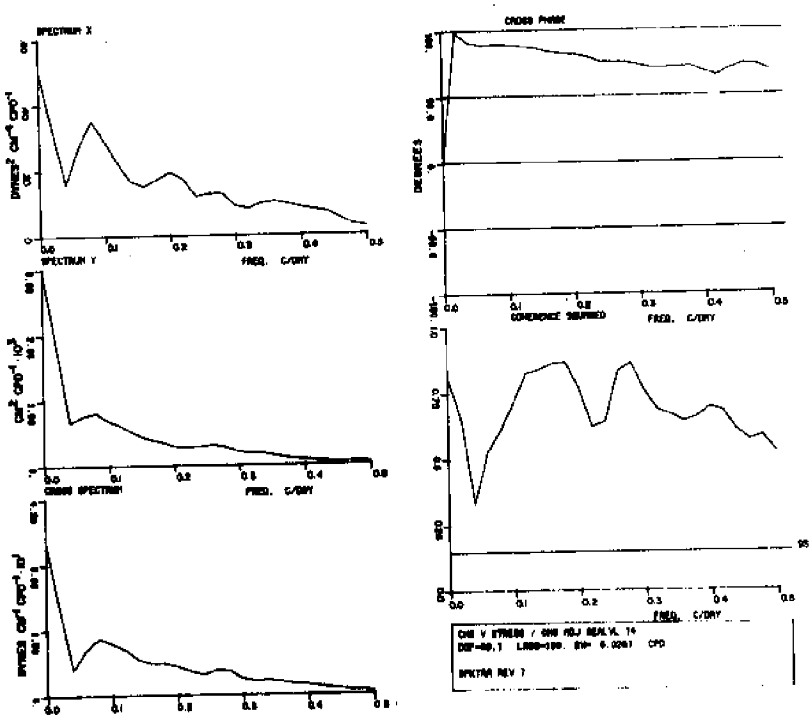

Figure 98 Spectra of wind stress v component at Charleston, S. C. vs. the adjusted sea level at Charleston, S. C., 1974

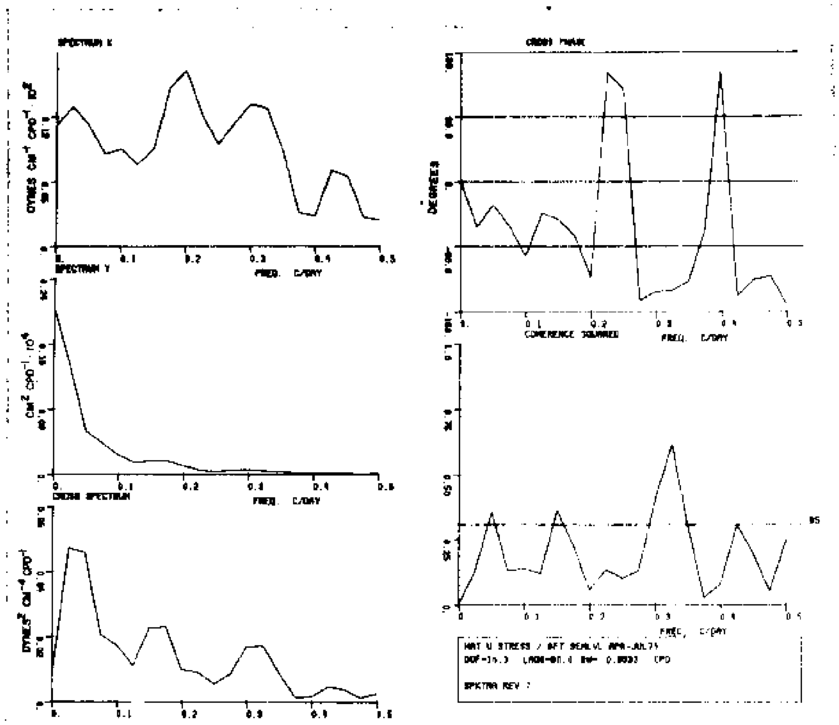

Figure 99 Spectra of wind stress u component at Cape Hatteras, N. C. vs. the sea level at Beaufort, N. C. April–July 1974

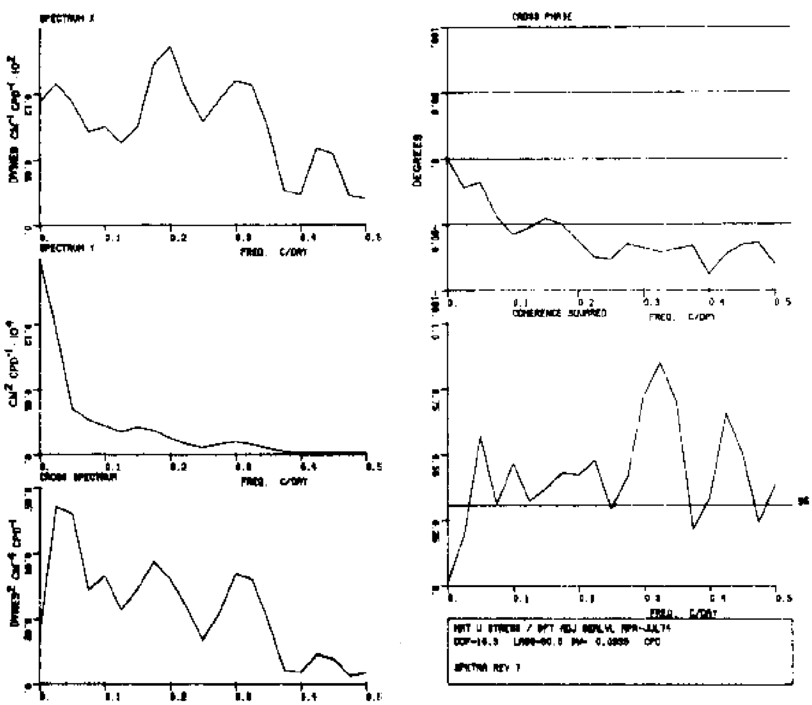

Figure 100 Spectra of wind stress u component at Cape Hatteras, N. C. vs. the adjusted sea level at Beaufort, N.C. April–July 1974

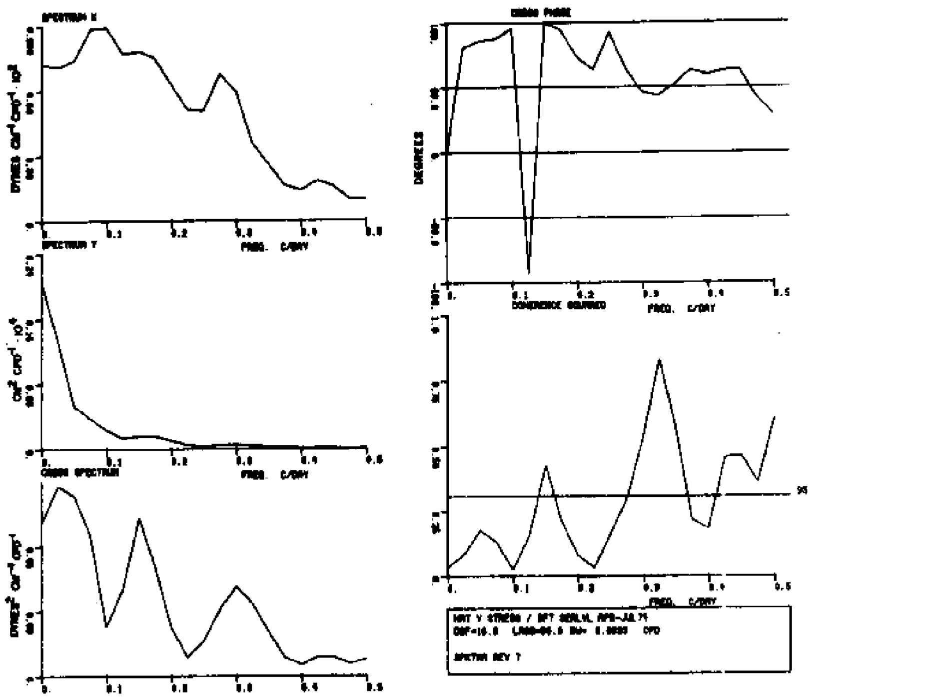

Figure 101 Spectra of wind stress v component at Cape Hatteras, N. C. vs. the sea level at Beaufort, N. C. April–July 1974

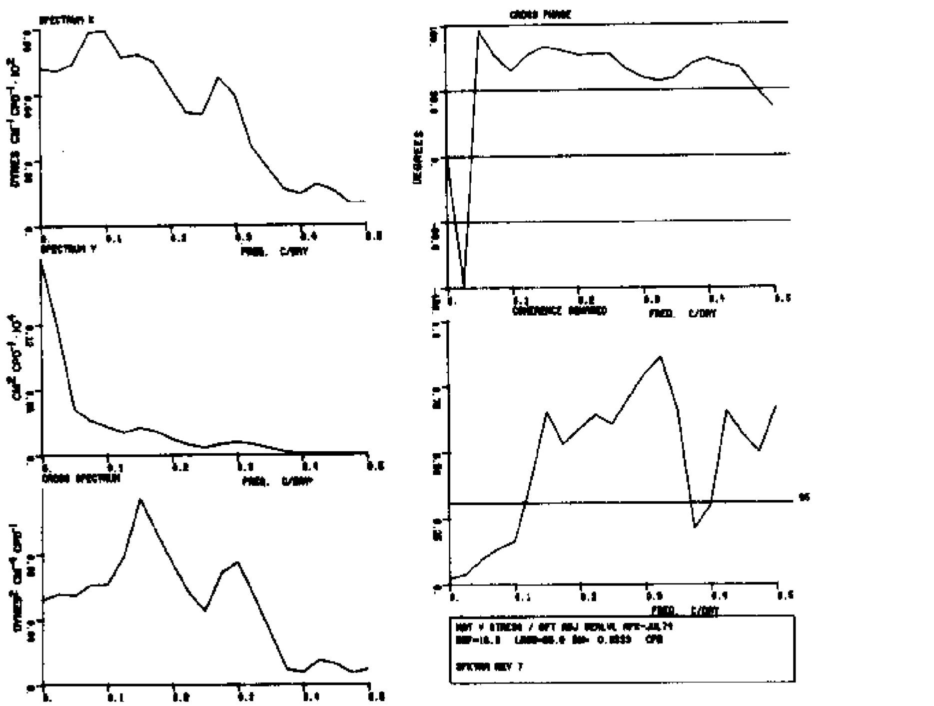

Figure 102 Spectra of wind stress v component at Cape Hatteras, N. C. vs. the adjusted sea level at Cape Hatteras, N. C., April–July 1974

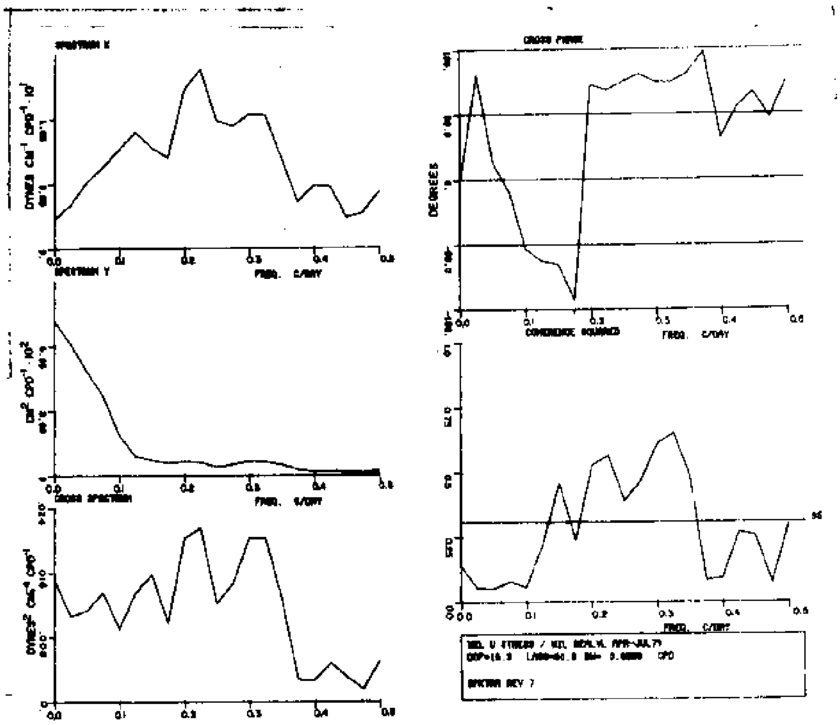

Figure 103 Spectra of wind stress u component at Wilmington, N. C., vs. the sea level at Wilmington, N. C., April-July 1974

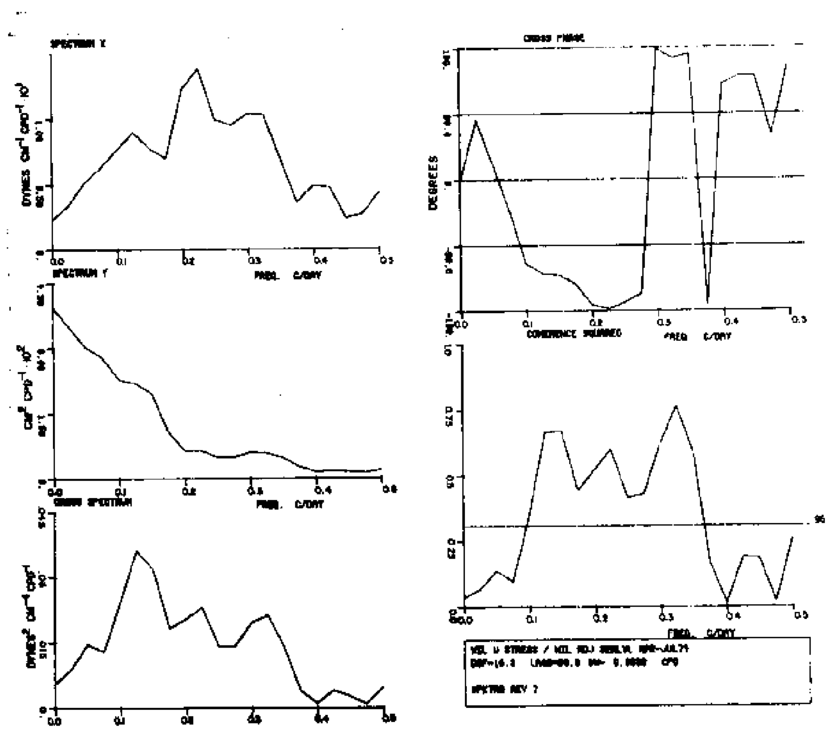

Figure 104 Spectra of wind stress u component at Wilmington, N. C. vs. the adjusted sea level at Wilmington, N. C., April-July 1974

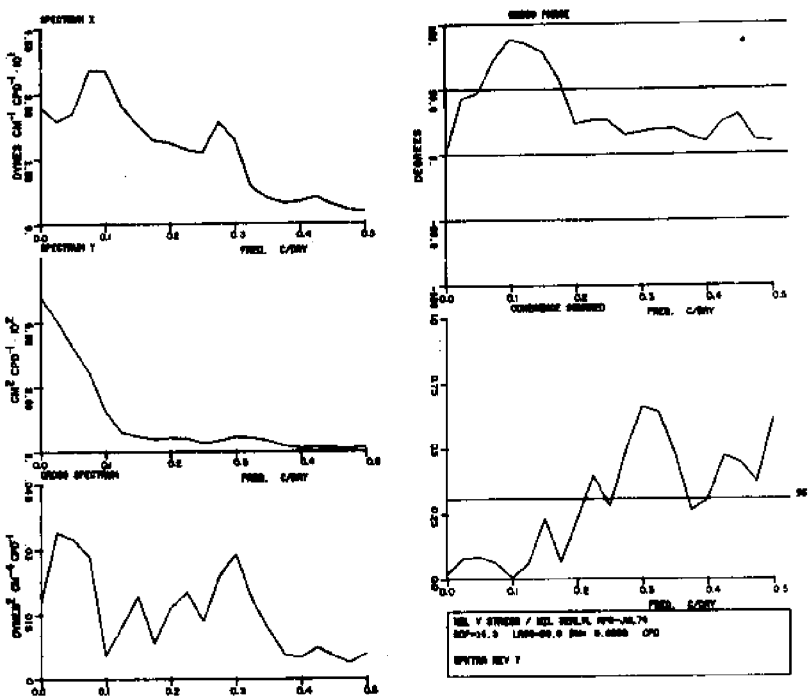

Figure 105 Spectra of wind stress v component at Wilmington, N. C. vs. the sea level at Wilmington, N. C. April-July 1974

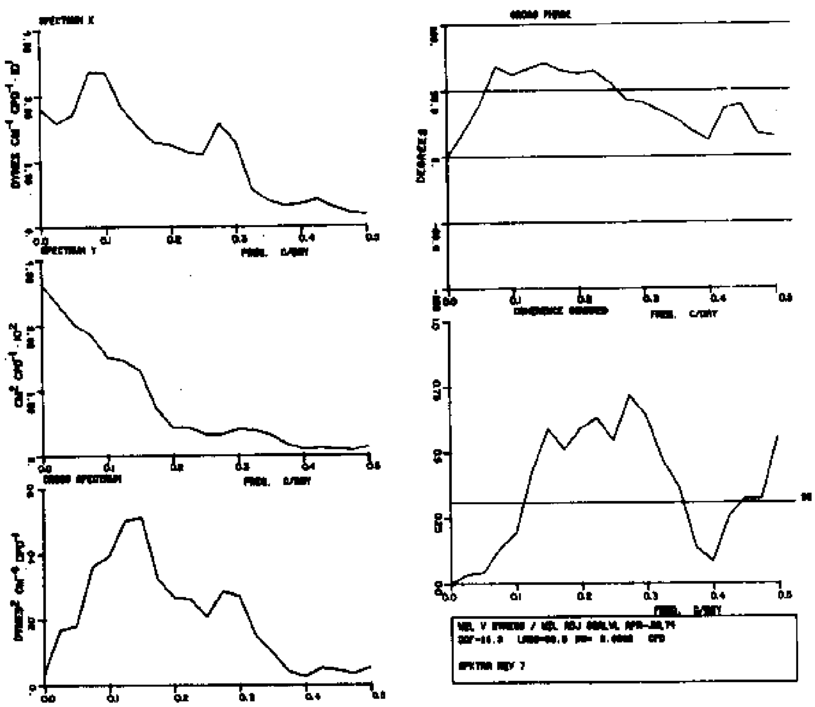

Figure 106 Spectra of wind stress v component at Wilmington, N. C. vs. the adjusted sea level at Wilmington, N. C., April-July 1974

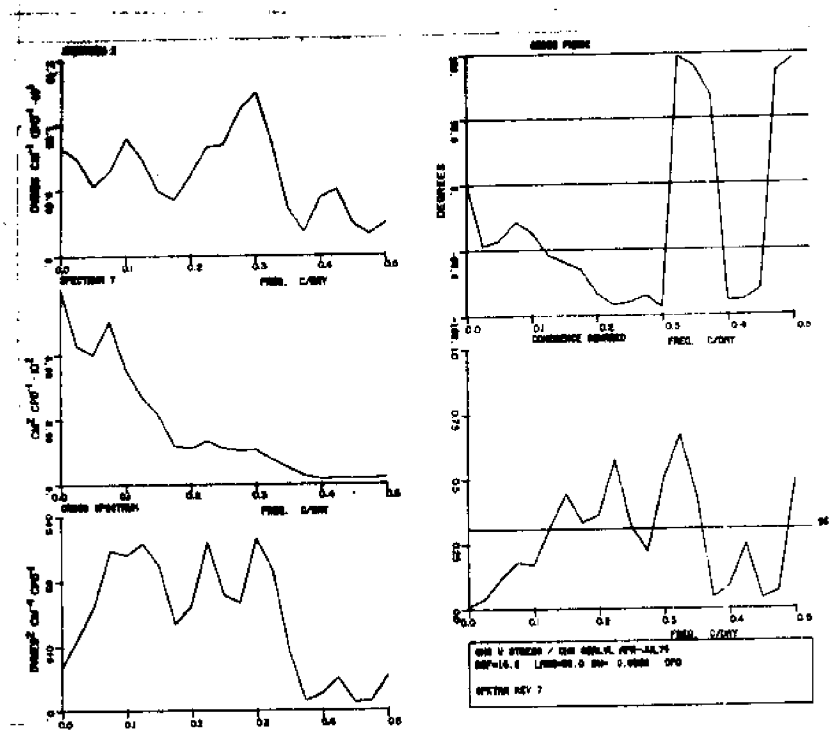

Figure 107 Spectra of wind stress u component at Charleston, S. C. vs. the sea level at Charleston, S. C. April-July 1974

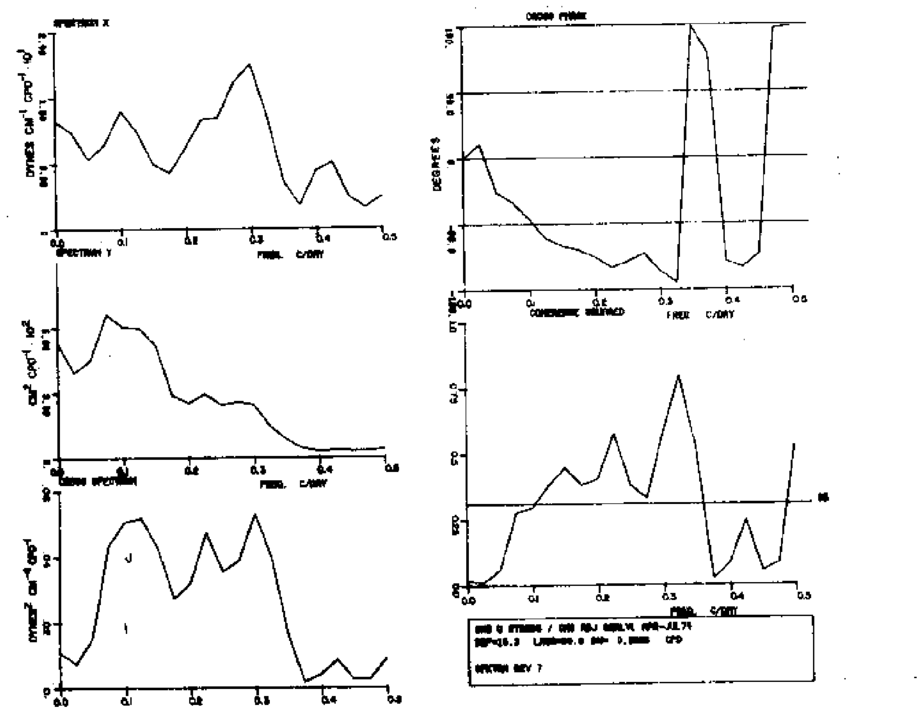

Figure 108 Spectra of wind stress u component at Charleston, S. C. vs. the adjusted sea level at Charleston, S. C., April-July 1974

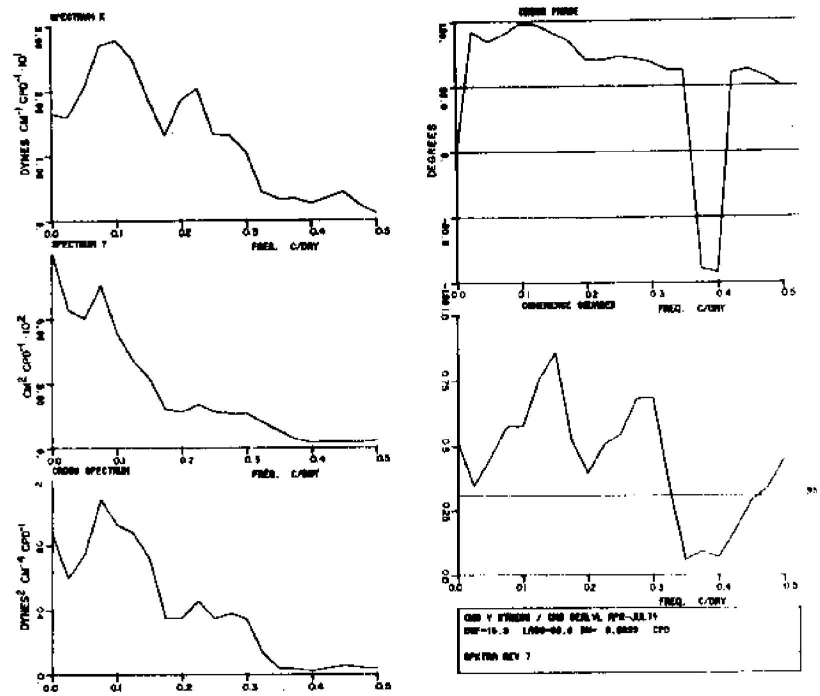

Figure 109 Spectra of wind stress v component at Charleston, S. C. vs. the sea level at Charleston, S. C. April-July 1974

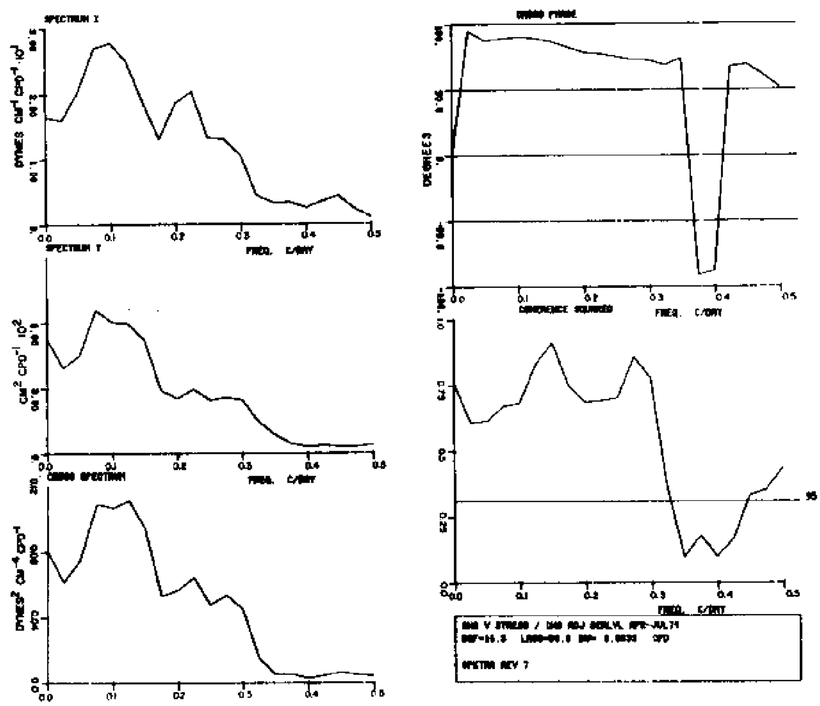

Figure 110 Spectra of wind stress v component at Charleston, S. C. vs. the adjusted sea level at Charleston, S. C., April-July 1974

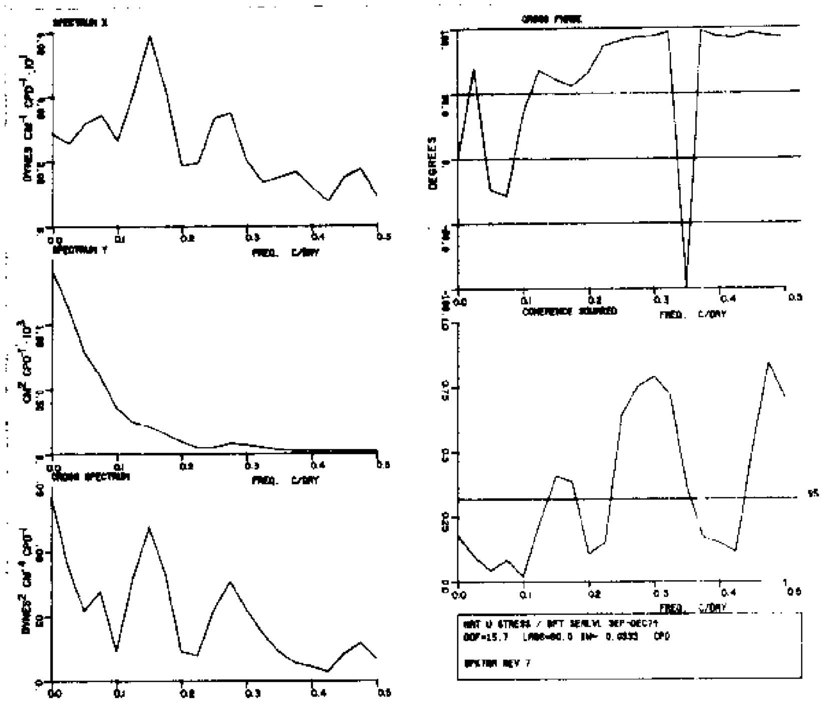

Figure 111 Spectra of wind stress u component at Cape Hatteras, N. C. vs. the sea level at Beaufort, N. C. Sept.-Dec 1974

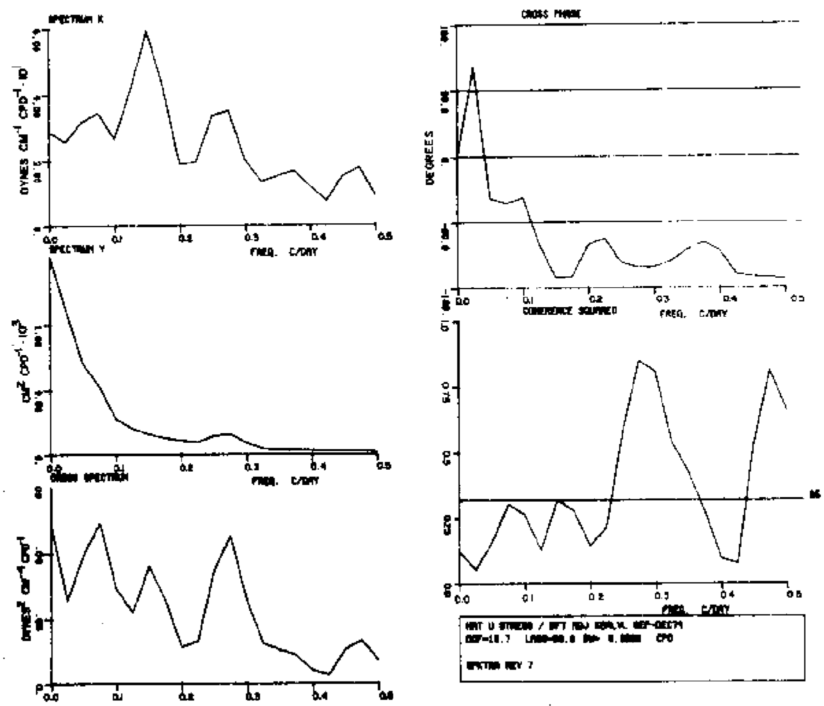

Figure 112 Spectra of wind stress u component at Cape Hatteras, N. C. vs. the adjusted sea level at Beaufort, N. C. Sept.-Dec. 1974

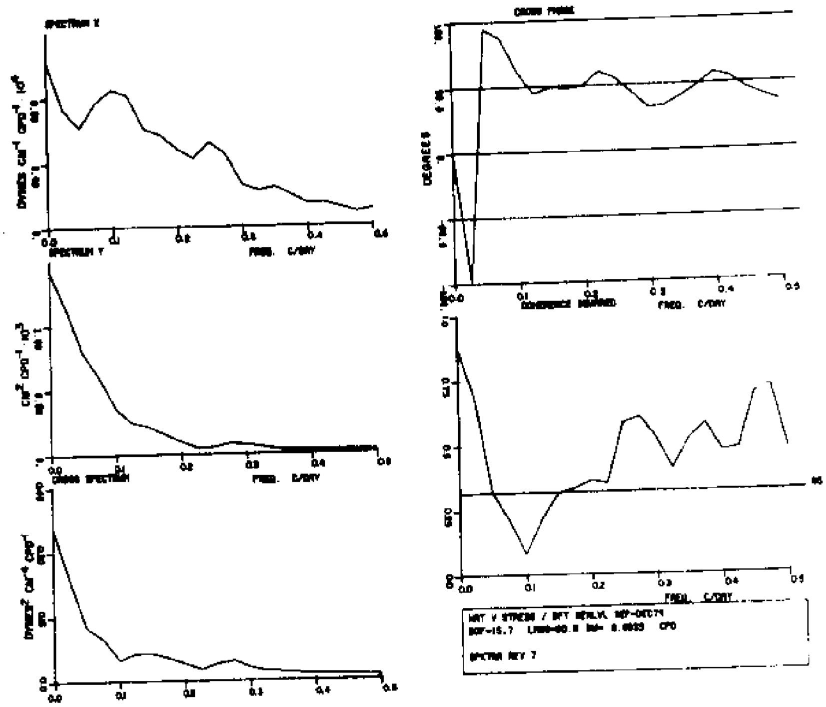

Figure 113 Spectra of wind stress v component at Cape Hatteras, N. C. vs. the sea level at Beaufort, N. C. Sept.-Dec. 1974

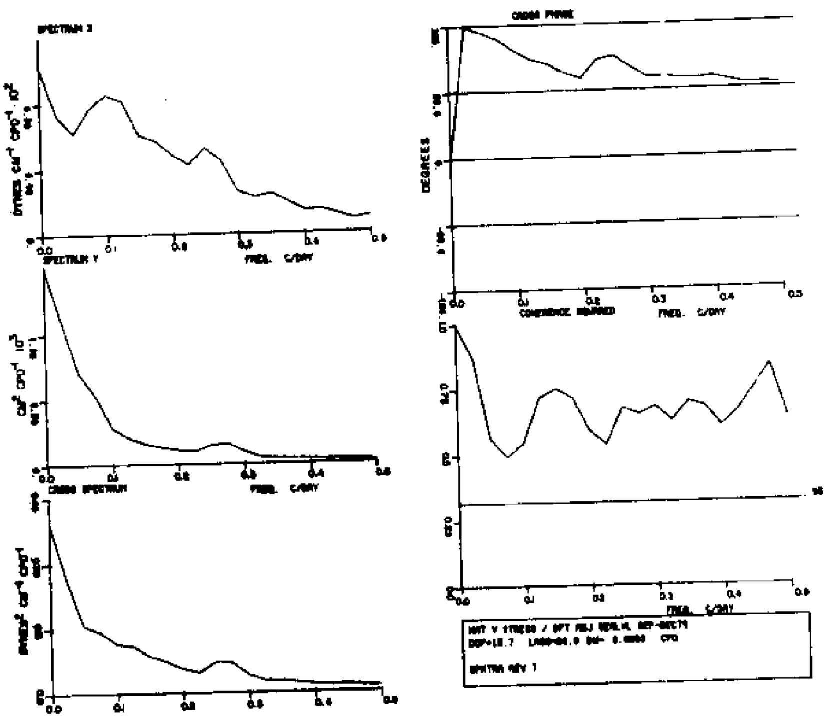

Figure 114 Spectra of wind stress v component at Cape Hatteras, N. C. vs. the adjusted sea level at Beaufort, N. C. Sept.-Dec. 1974

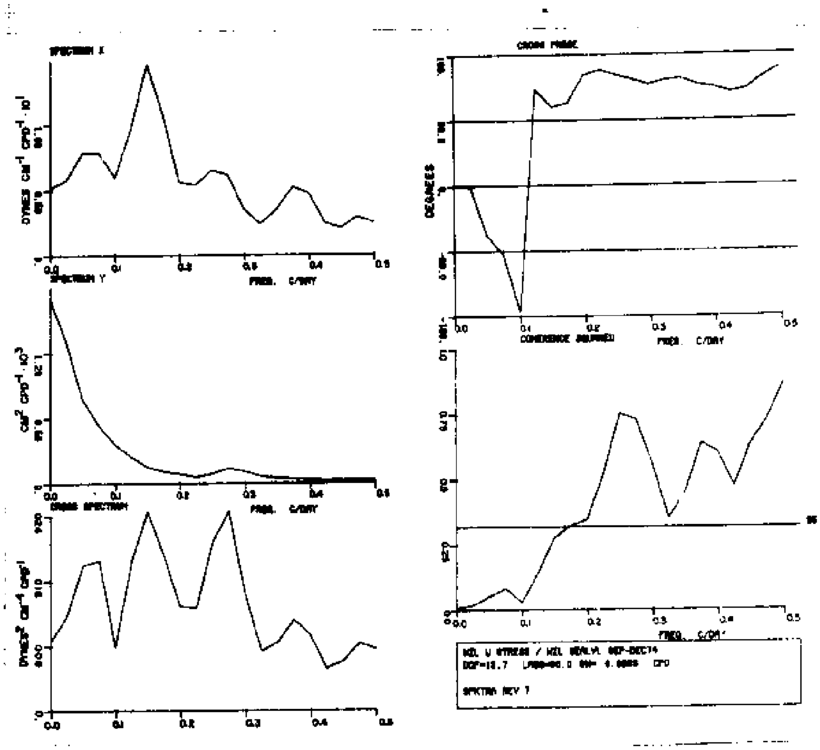

Figure 115 Spectra of wind stress u component at Wilmington, N. C. vs. the sea level at Wilmington, N. C. Sept.-Dec. 1974

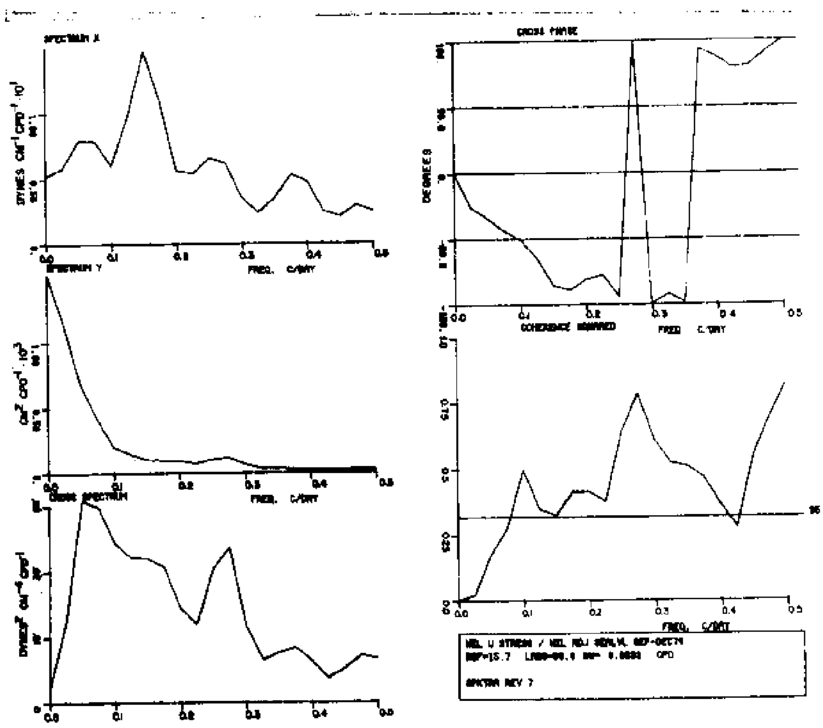

Figure 116 Spectra of wind stress u component at Wilmington, N. C. vs. the adjusted sea level at Wilmington, N. C. Sept.-Dec. 1974

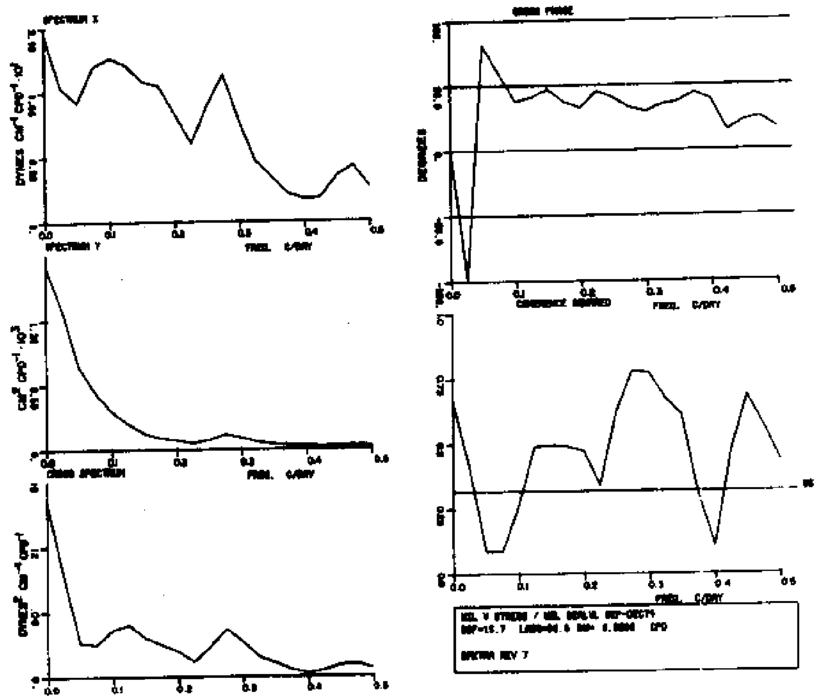

Figure 117 Spectra of wind stress v component at Wilmington, N. C. vs. the sea level at Wilmington, N. C., Sept.-Dec. 1974

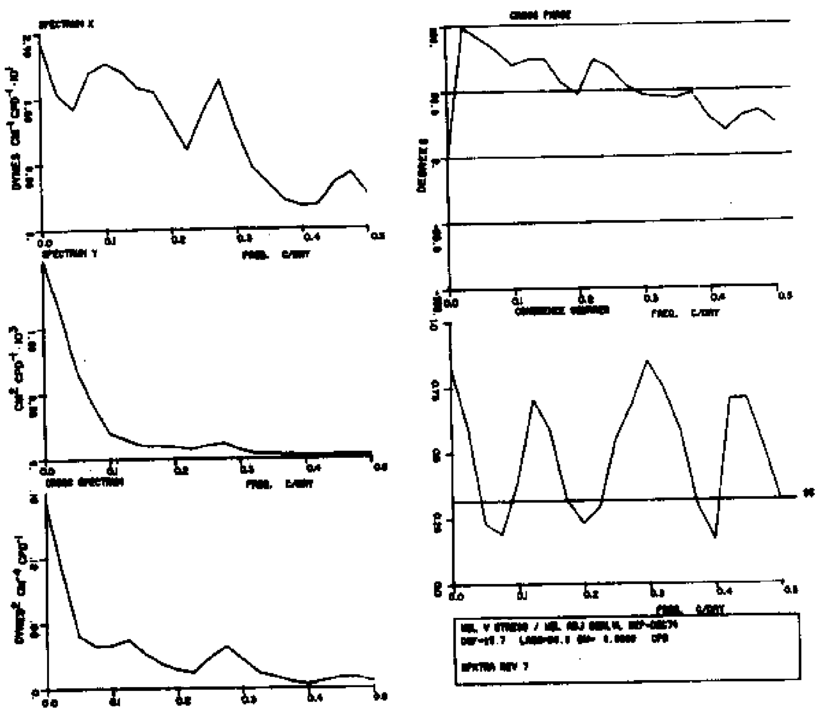

Figure 118 Spectra of wind stress v component at Wilmington, N. C. vs. the adjusted sea level at Wilmington, N. C., Sept.-Dec. 1974

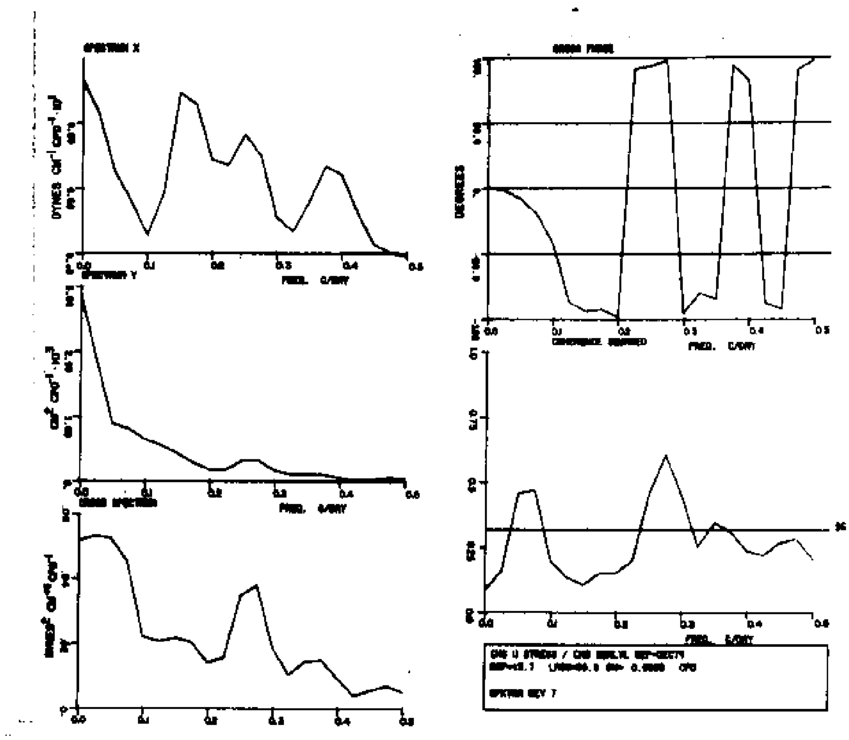

Figure 119 Spectra of wind stress u component at Charleston, S. C. vs. the sea level at Charleston, S. C., Sept.-Dec. 1974

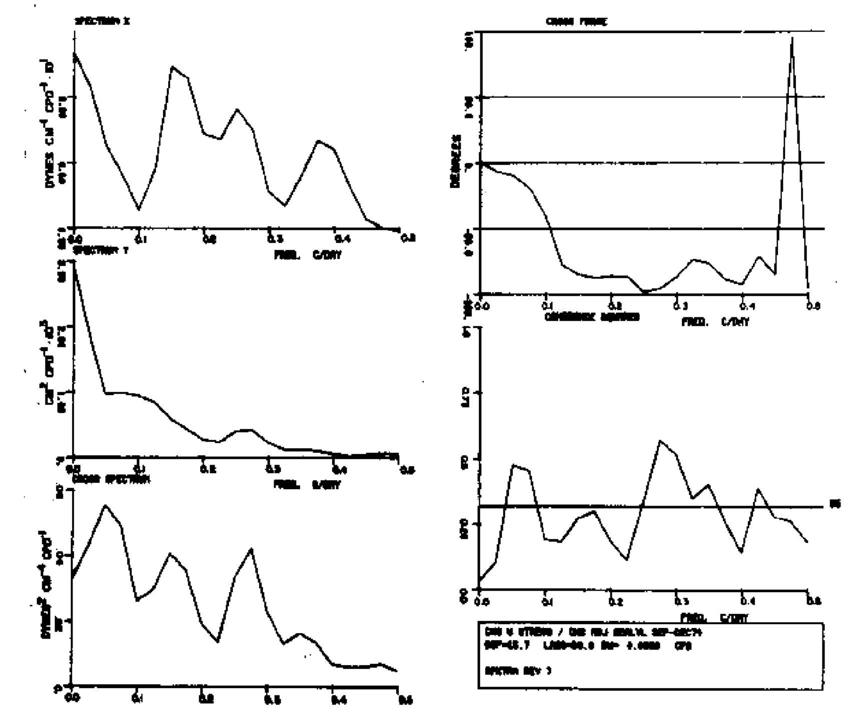

Figure 120 Spectra of wind stress u component at Charleston, S. C. vs. the adjusted sea level at Charleston, S. C., Sept.-Dec. 1974

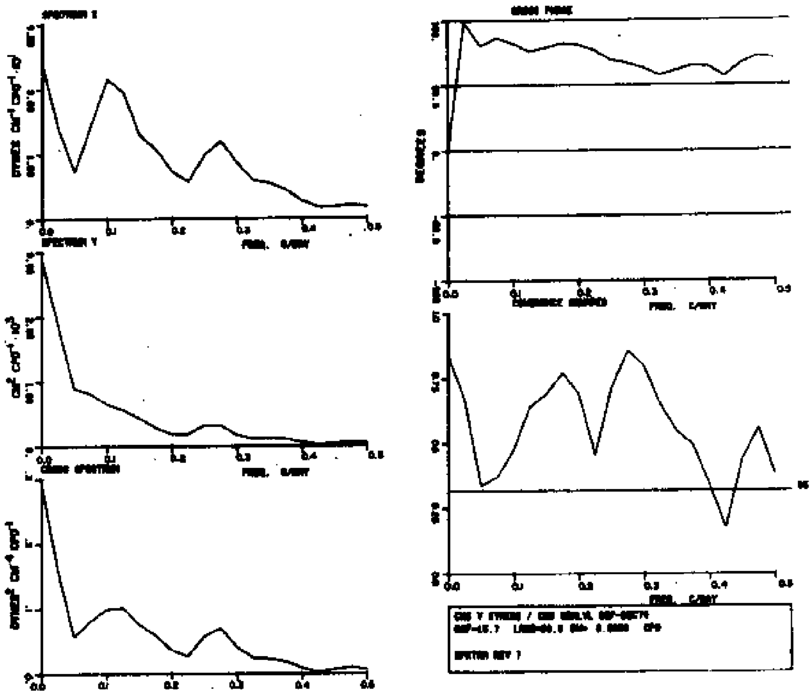

Figure 121 Spectra of wind stress v component at Charleston, S. C. vs. the sea level at Charleston, S. C., Sept.-Dec. 1974

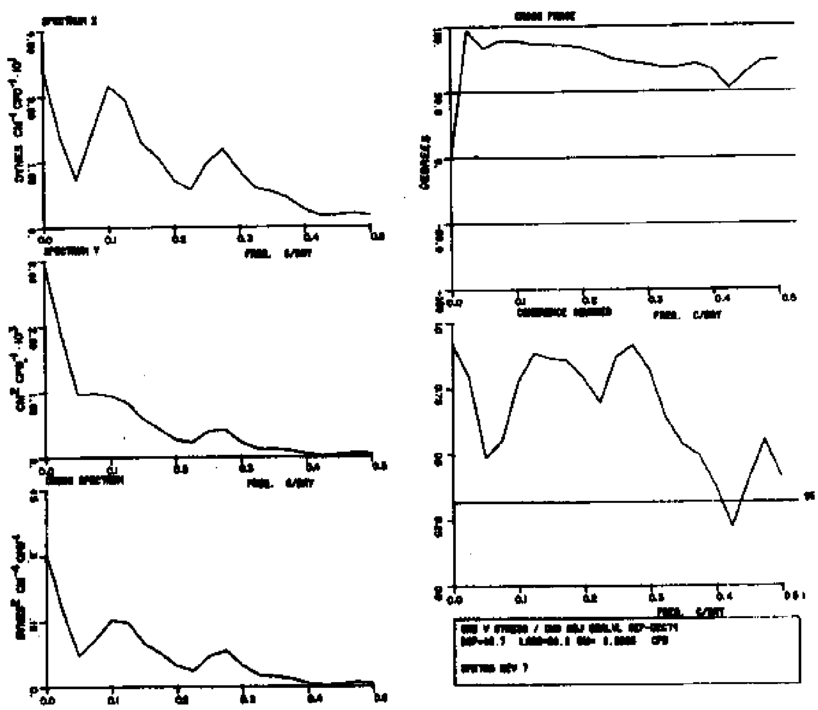

Figure 122 Spectra of wind stress v component at Charleston, S. C. vs. the adjusted sea level at Charleston, S. C., Sept.-Dec. 1974

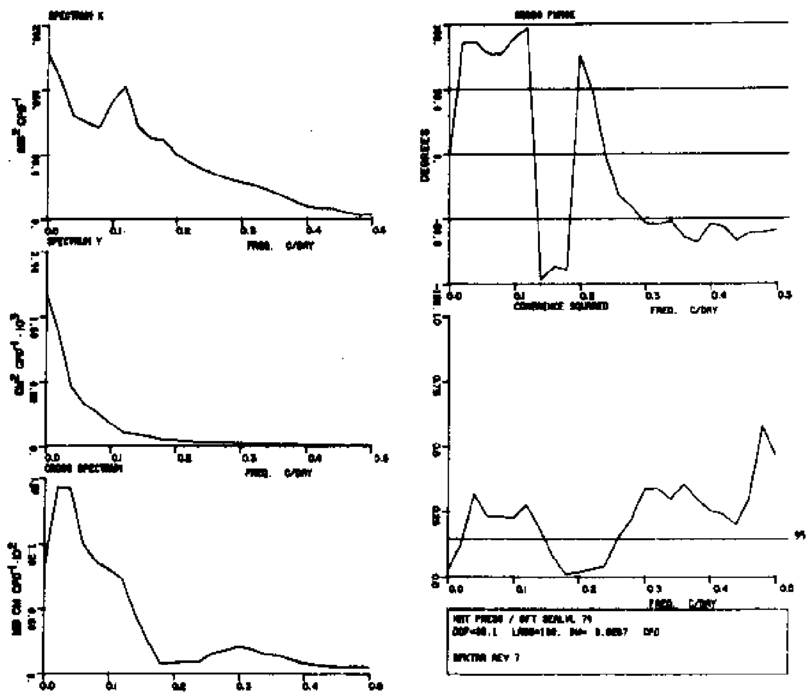

Figure 123 Spectra of pressure at Cape Hatteras, N. C. vs. sea level at Beaufort, N. C., 1974

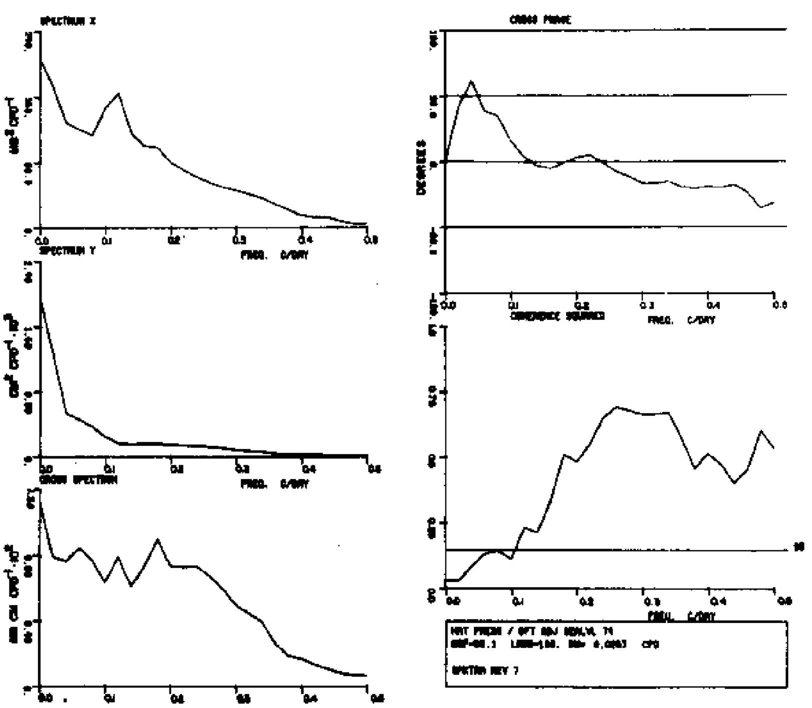

Figure 124 Spectra of pressure at Cape Hatteras, N. C. vs. adjusted sea level at Beaufort, N. C., 1974

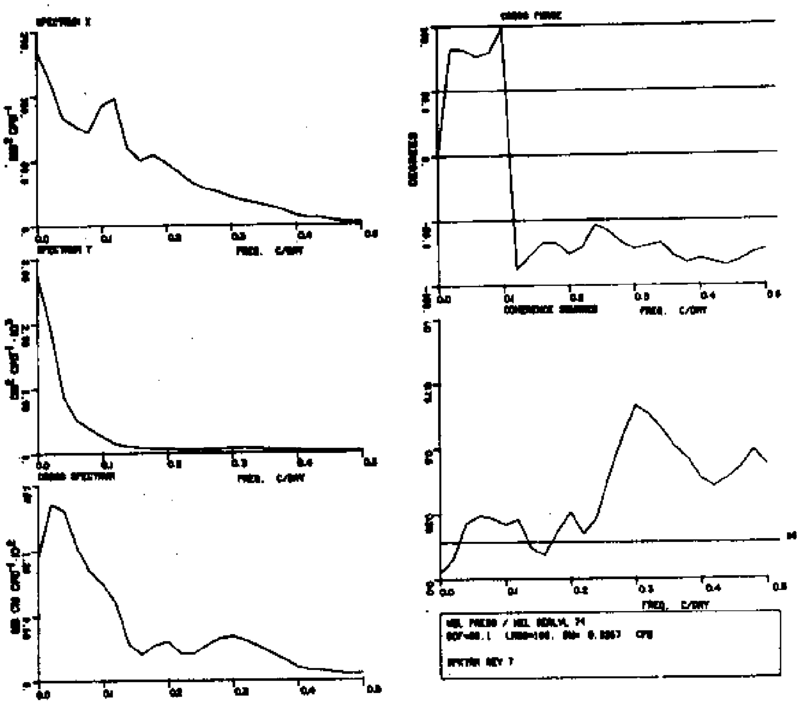

Figure 125 Spectra of pressure at Wilmington, N. C. vs. sea level at Wilmington, N. C., 1974

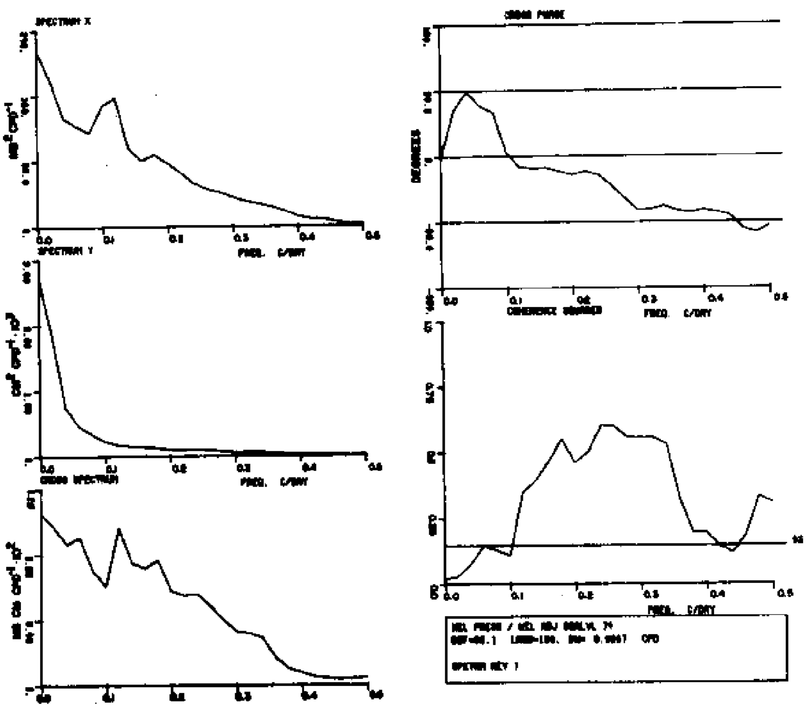

Figure 126 Spectra of pressure at Wilmington, N. C. vs. adjusted sea level at Wilmington, N. C., 1974

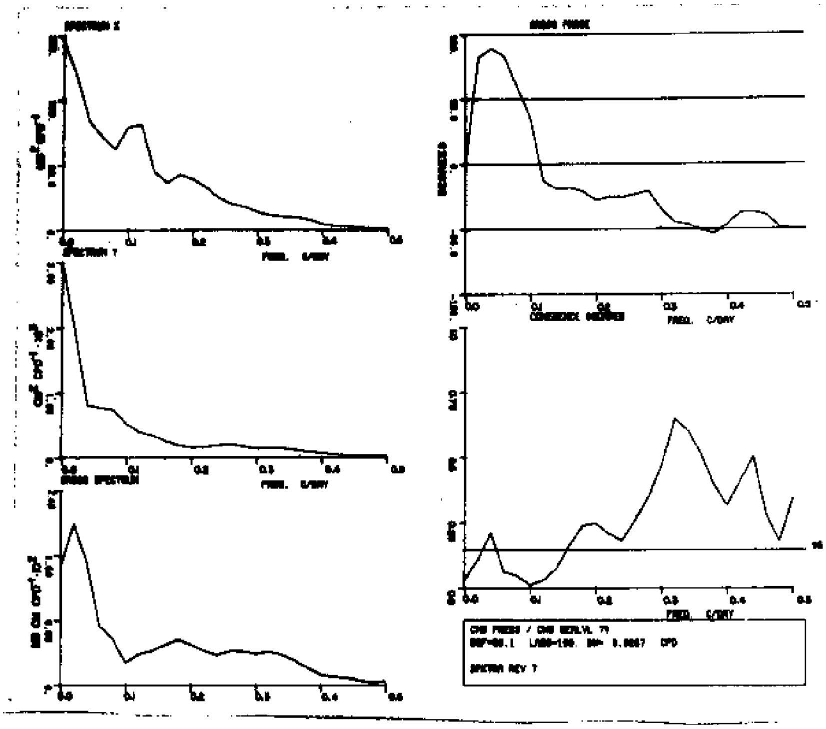

Figure 127 Spectra of pressure at Charleston, S. C. vs. sea level at Charleston, S. C., 1974

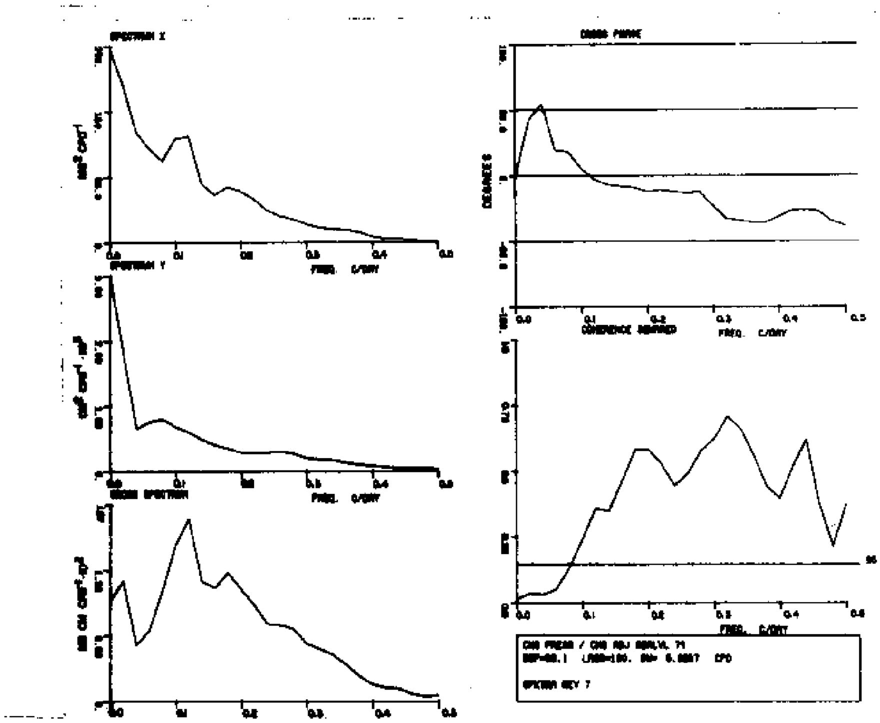

Figure 128 Spectra of pressure at Charleston, S. C. vs. adjusted sea level at Charleston, S. C., 1974

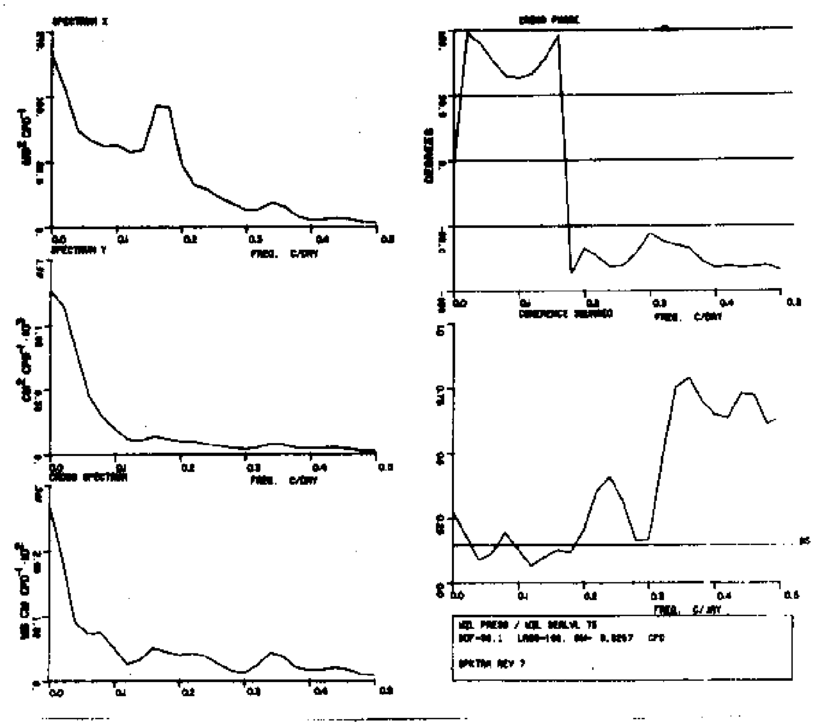

Figure 129 Spectra of pressure at Wilmington, N. C. vs. sea level at Wilmington, N. C., 1975

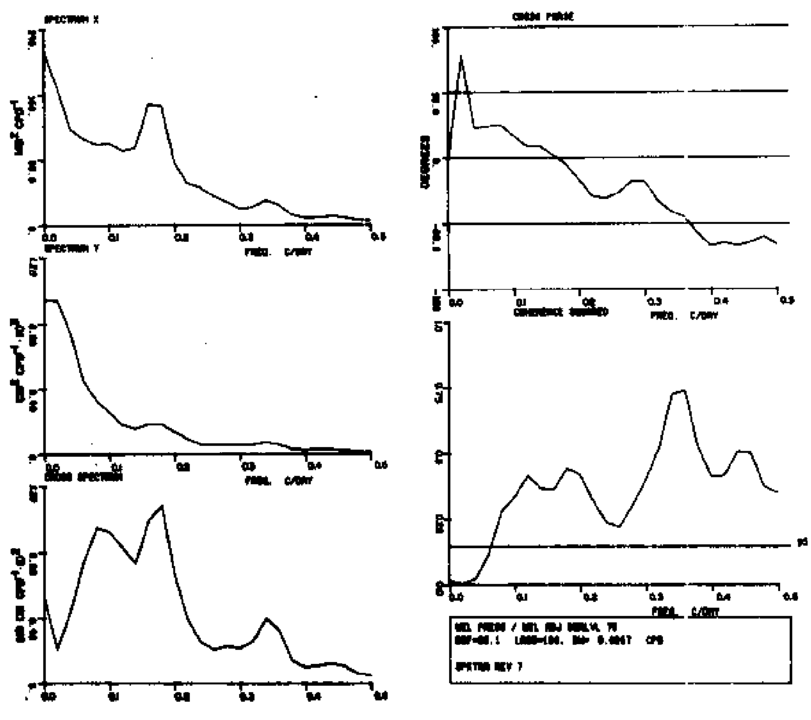

Figure 130 Spectra of pressure at Wilmington, N. C. vs. adjusted sea level at Wilmington, N. C., 1975

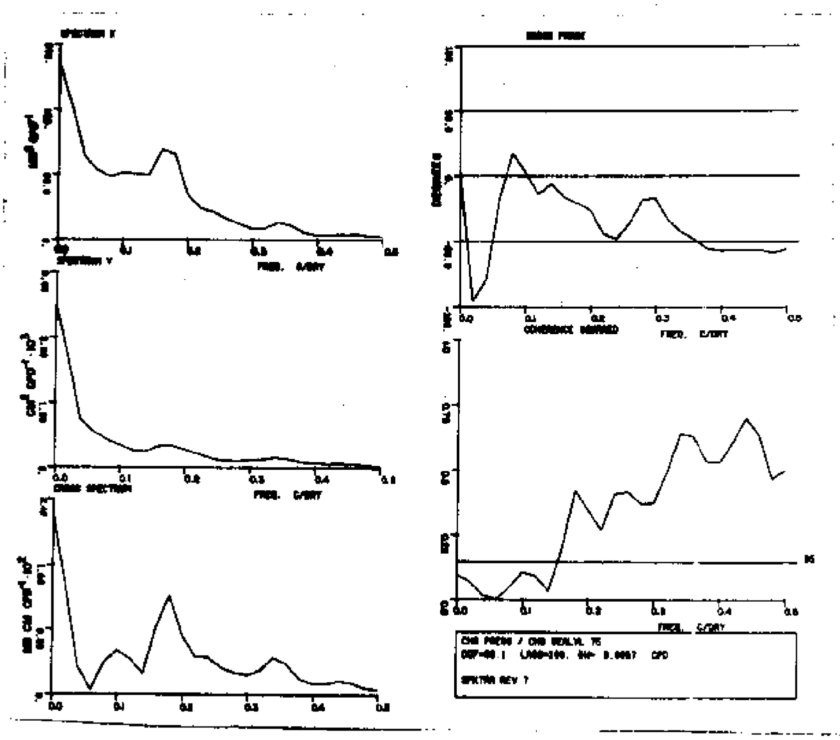

Figure 131 Spectra of pressure at Charleston, S. C. vs. sea level at Charleston, S. C., 1975

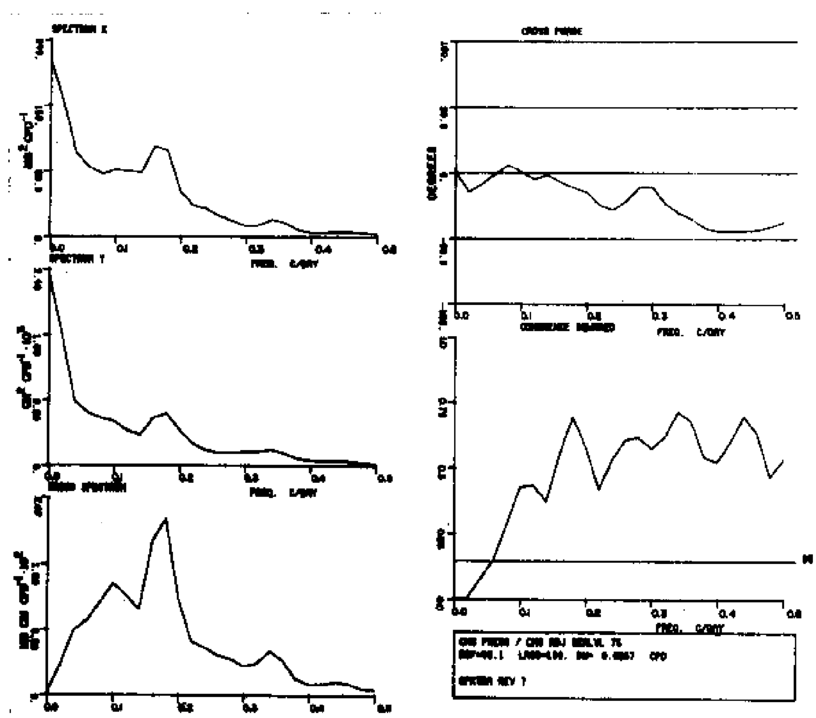

Figure 132 Spectra of pressure at Charleston, S. C. vs. adjusted sea level at Charleston, S. C., 1975

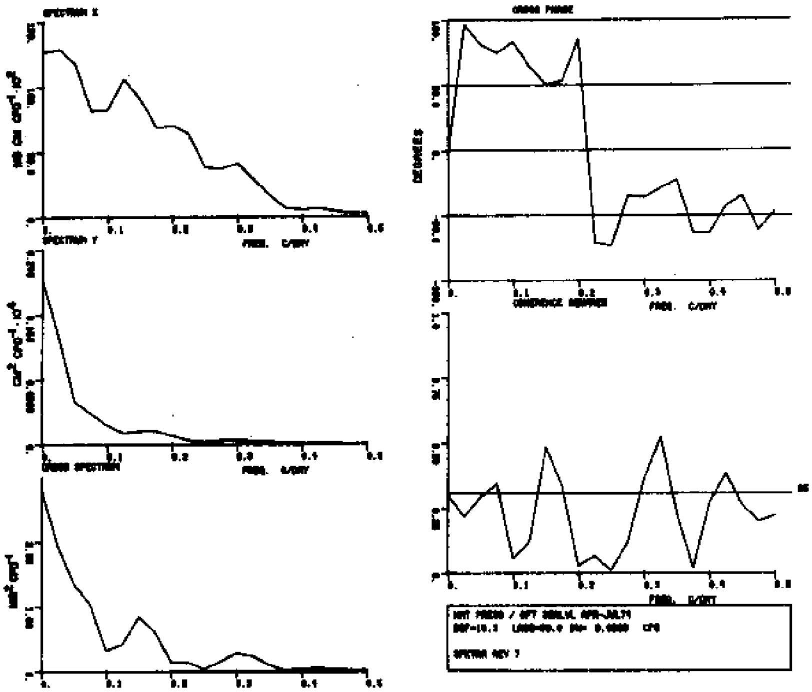

Figure 133 Spectra of pressure at Cape Hatteras, N. C. vs. sea level at Beaufort, N. C., April-July 1974

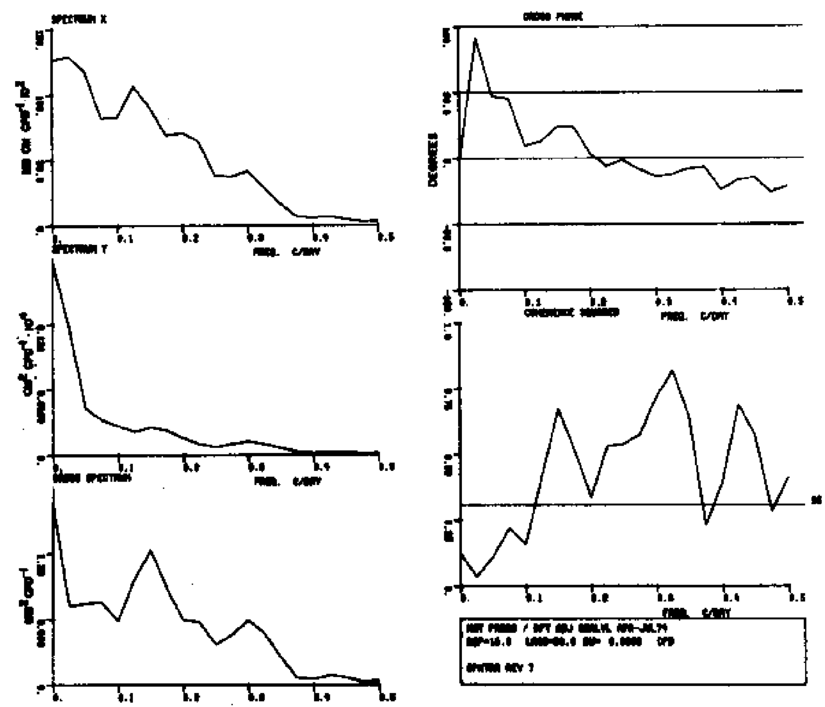

Figure 134 Spectra of pressure at Cape Hatteras, N. C. vs. adjusted sea level at Beaufort, N. C., April-July 1974

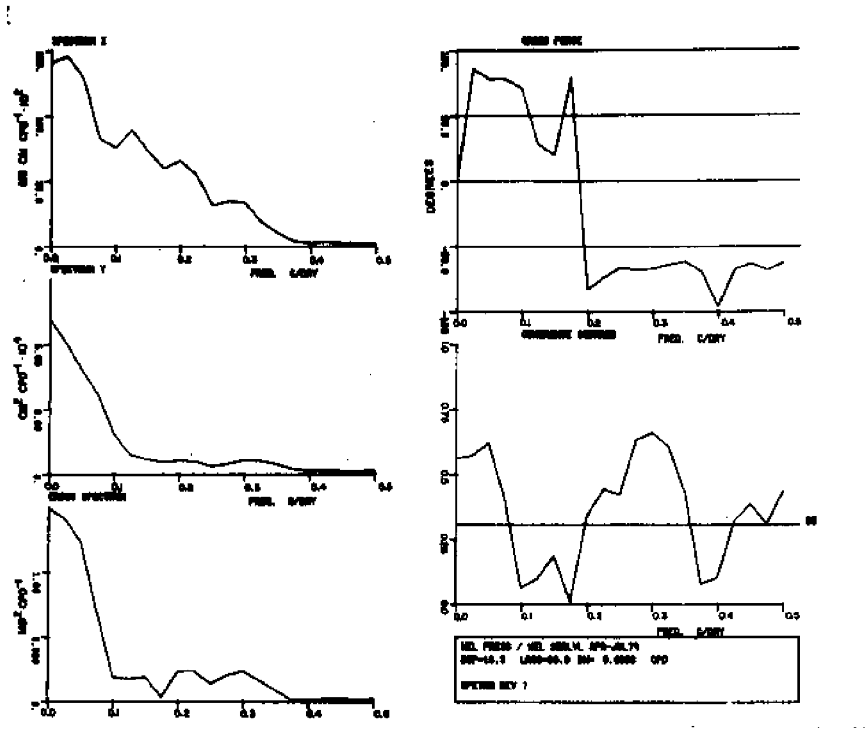

Figure 135 Spectra of pressure at Wilmington, N. C. vs. sea level at Wilmington, N. C., April-July 1974

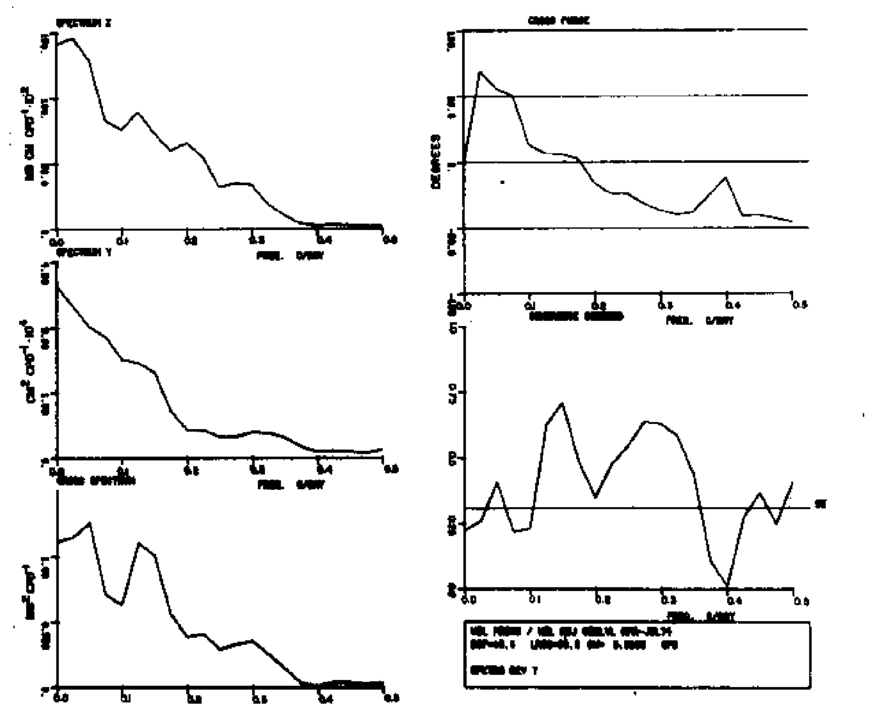

Figure 136 Spectra of pressure at Wilmington, N. C. vs. adjusted sea level at Wilmington, N. C., April-July 1974

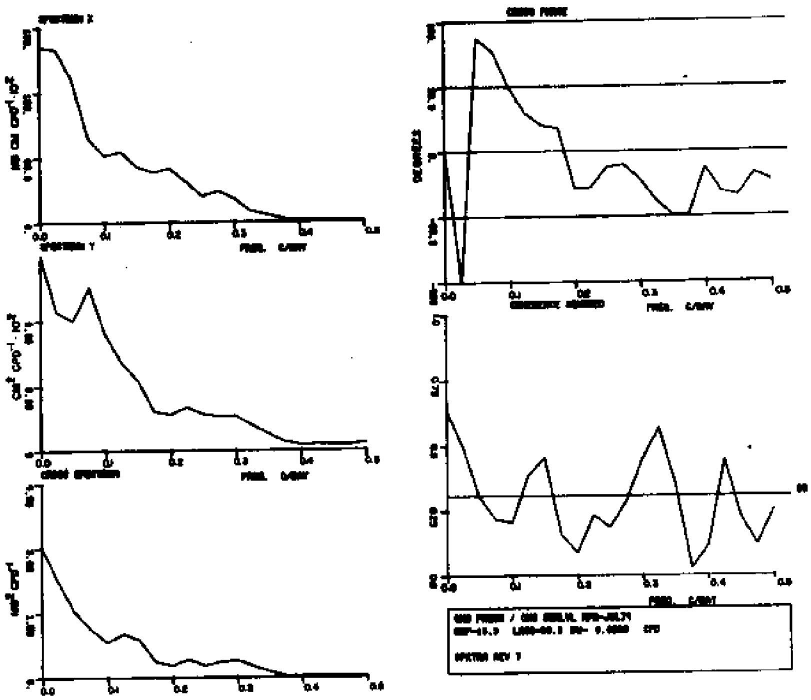

Figure 137 Spectra of pressure at Charleston, S. C. vs. sea level at Charleston, S. C., April-July 1974

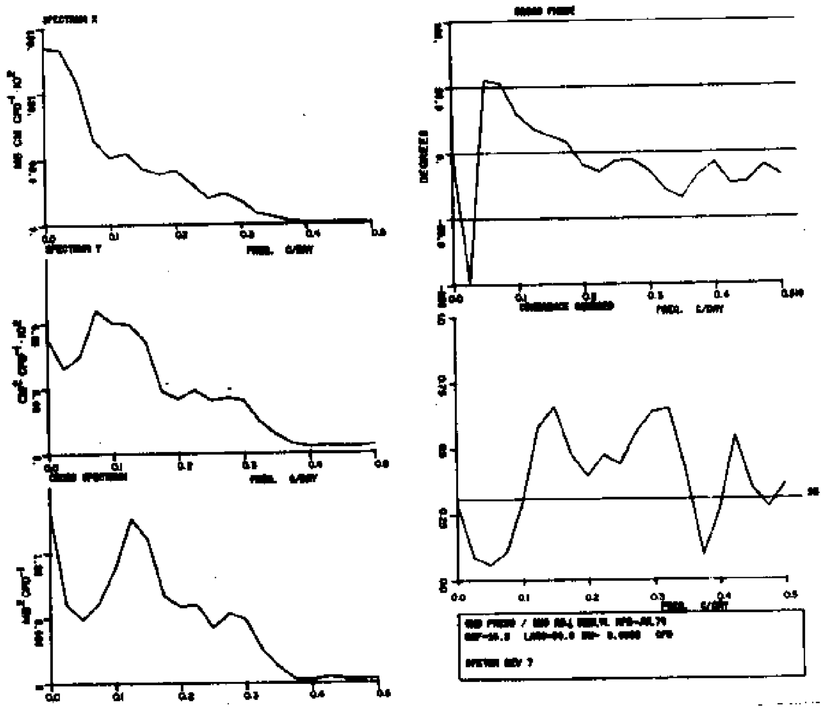

Figure 138 Spectra of pressure at Charlesotn, S. C. vs. adjusted sea level at Charleston, S. C., April-July 1974

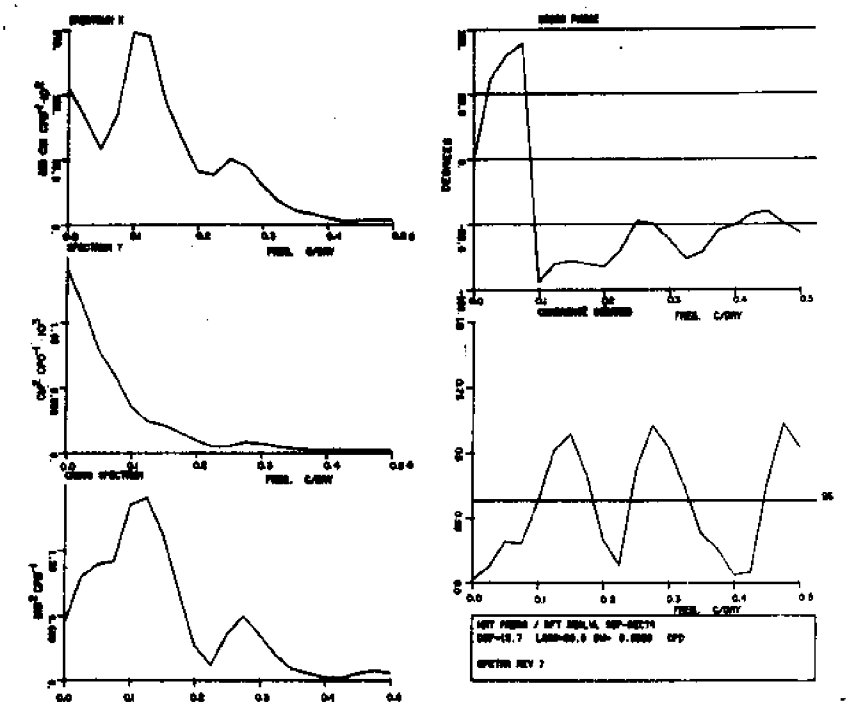

Figure 139 Spectra of pressure at Cape Hatteras, N. C. vs. sea level at Beaufort, N.C., Sept.-Dec. 1974

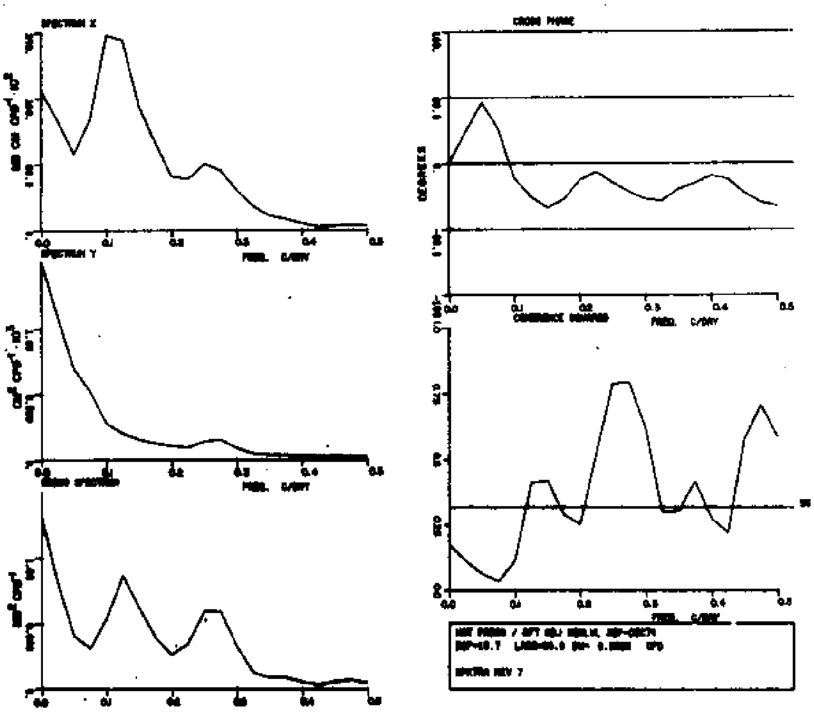

Figure 140 Spectra of pressure at Cape Hatteras, N. C. vs. adjusted sea level at Beaufort, N.C., Sept.-Dec. 1974

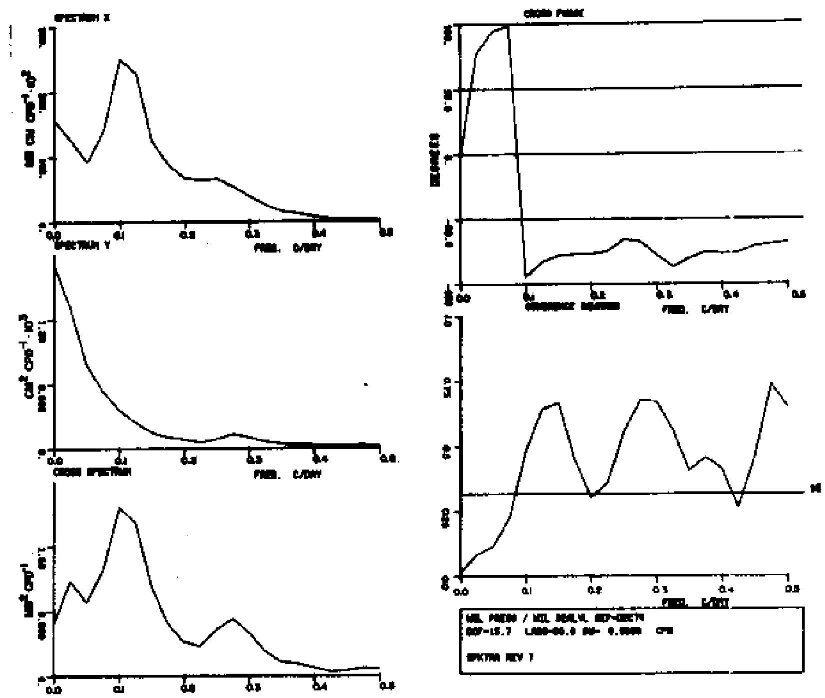

Figure 141 Spectra of pressure at Wilmington, N. C. vs. sea level at Wilmington, N. C., Sept.-Dec. 1974

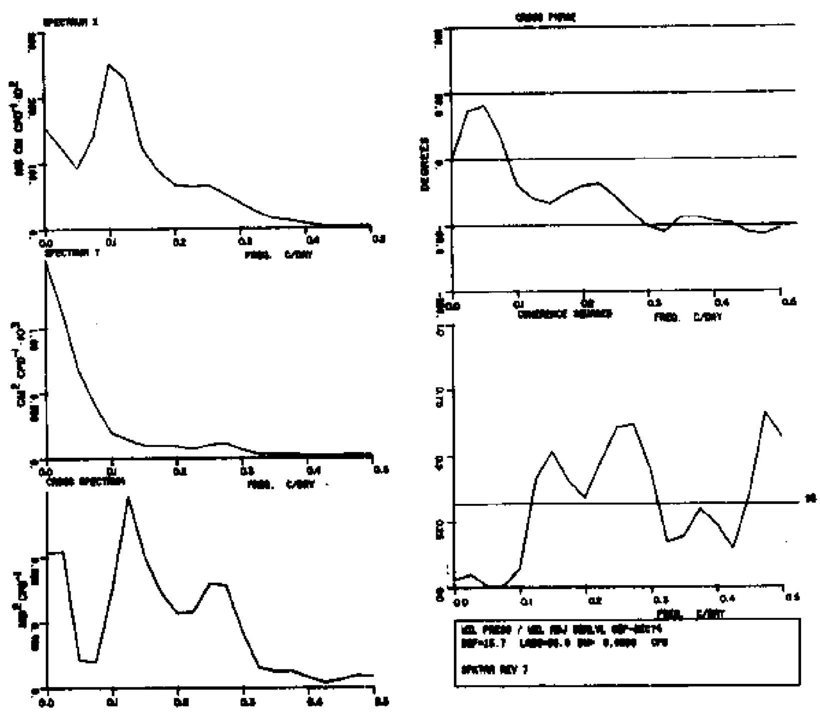

Figure 142 Spectra of pressure at Wilmington, N. C. vs. adjusted sea level at Wilmington, N. C., Sept.-Dec. 1974

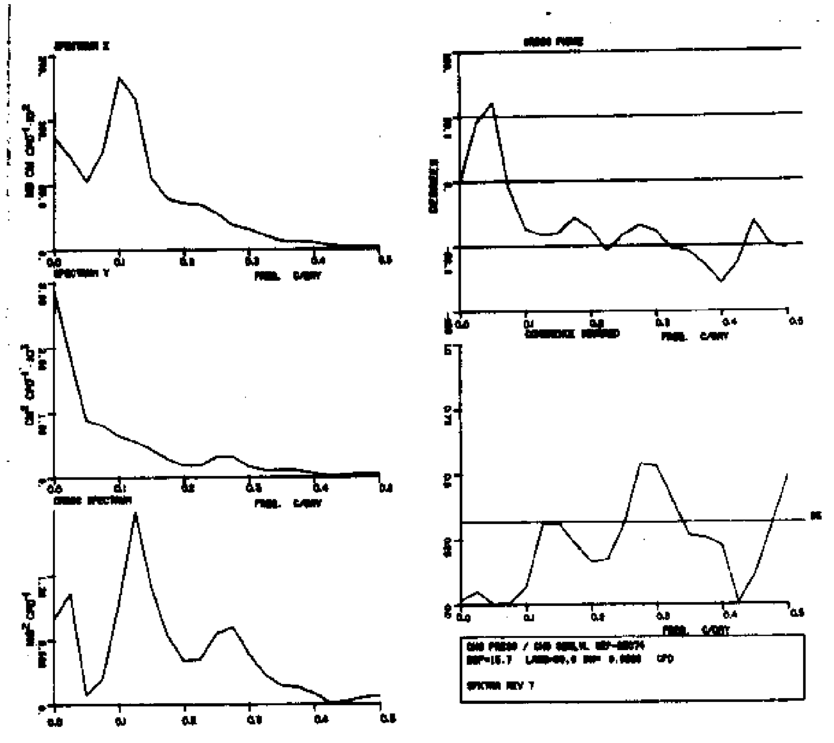

Figure 143 Spectra of pressure at Charleston, S. C. vs. sea level at Charleston, S. C., Sept.-Dec. 1974

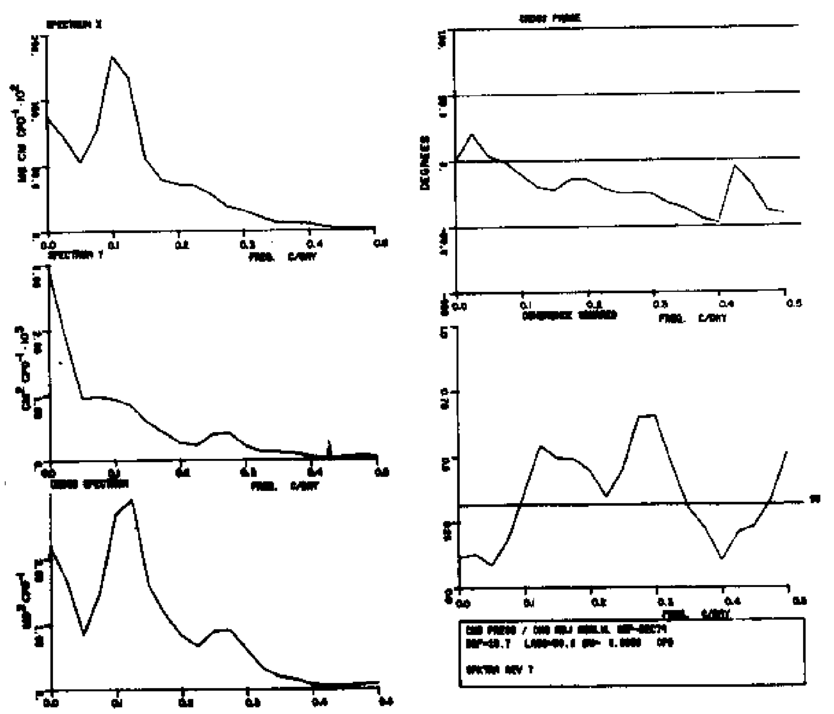

Figure 144 Spectra of pressure at Charleston, S. C. vs. adjusted sea level at Charleston, S. C., Sept. - Dec. 1974

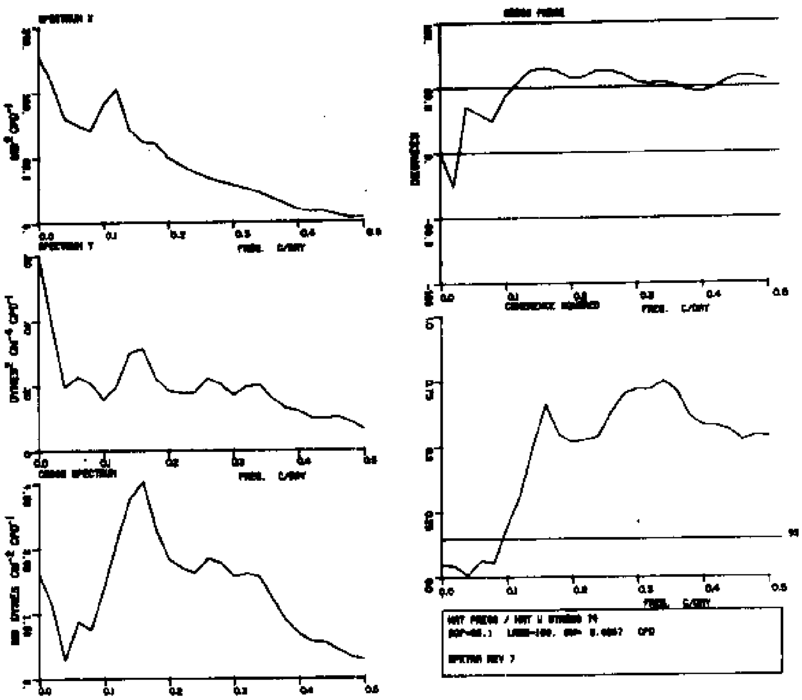

Figure 145 Spectra of pressure at Cape Hatteras, N. C. vs. wind stress u component at Cape Hatteras, N. C., 1974

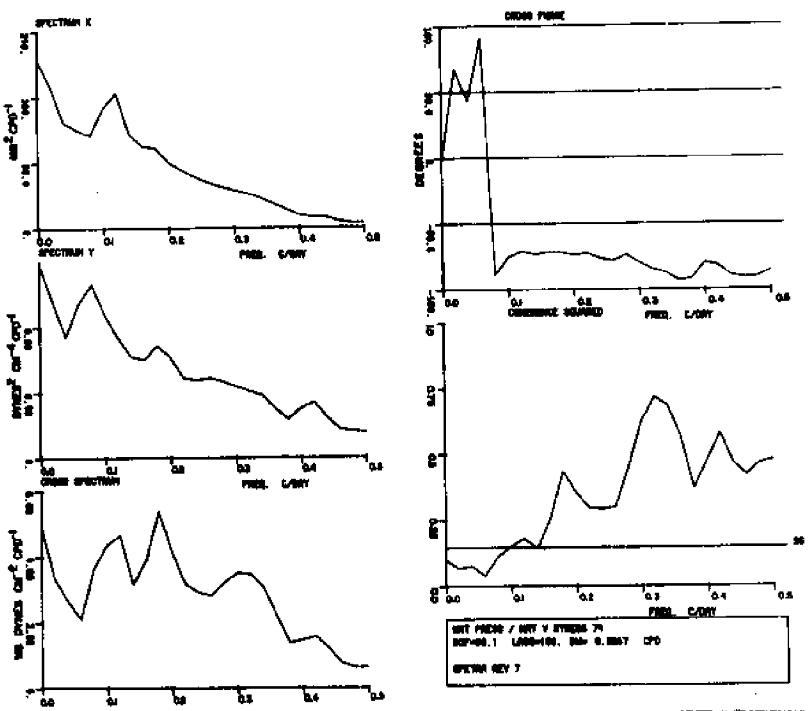

Figure 146 Spectra of pressure at Cape Hatteras, N. C. vs. wind stress v component at Cape Hatteras, N. C., 1974

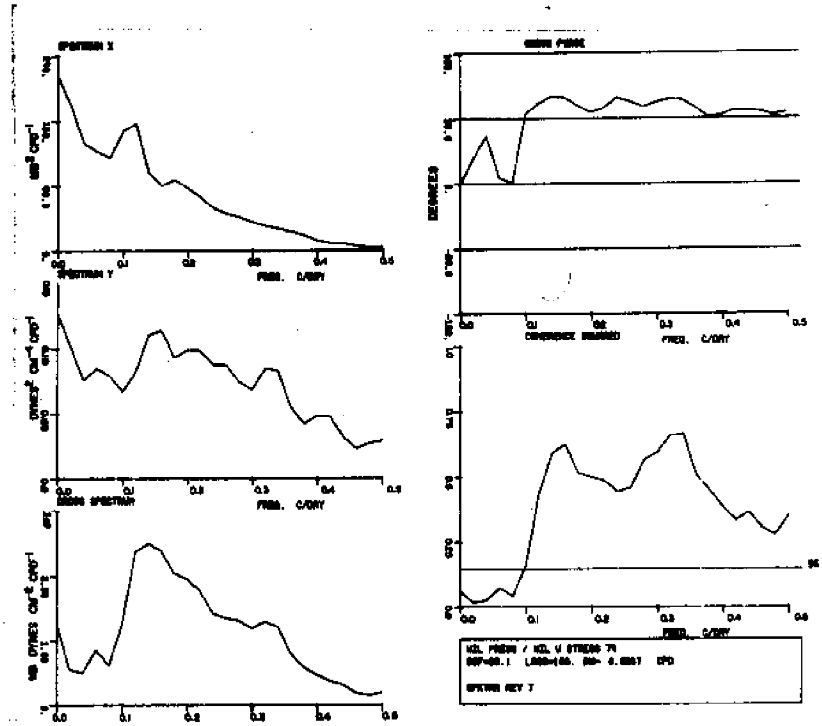

Figure 147 Spectra of pressure at Wilmington, N. C. vs. wind stress u component at Wilmington, N. C., 1974

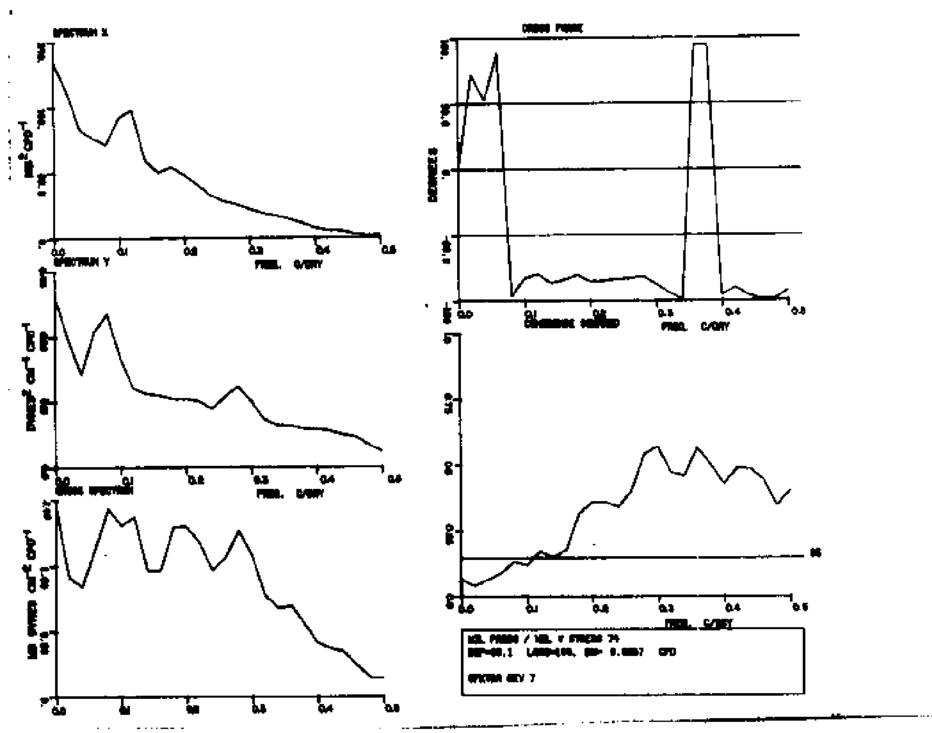

Figure 148 Spectra of pressure at Wilmington, N. C. vs wind stress v component at Wilmington, N. C., 1974

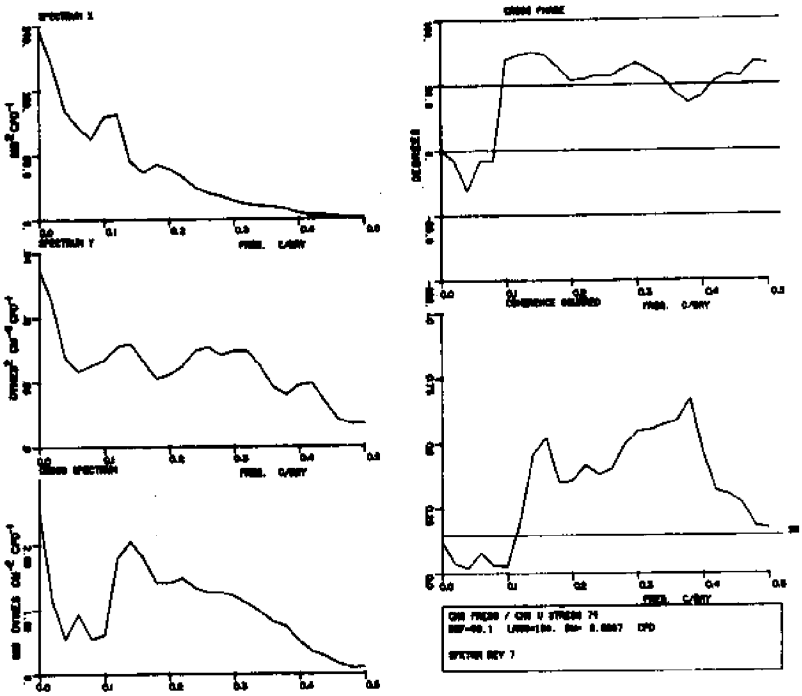

Figure 149 Spectra of pressure at Charleston, S. C. vs. wind stress u component at Charleston, S. C., 1974

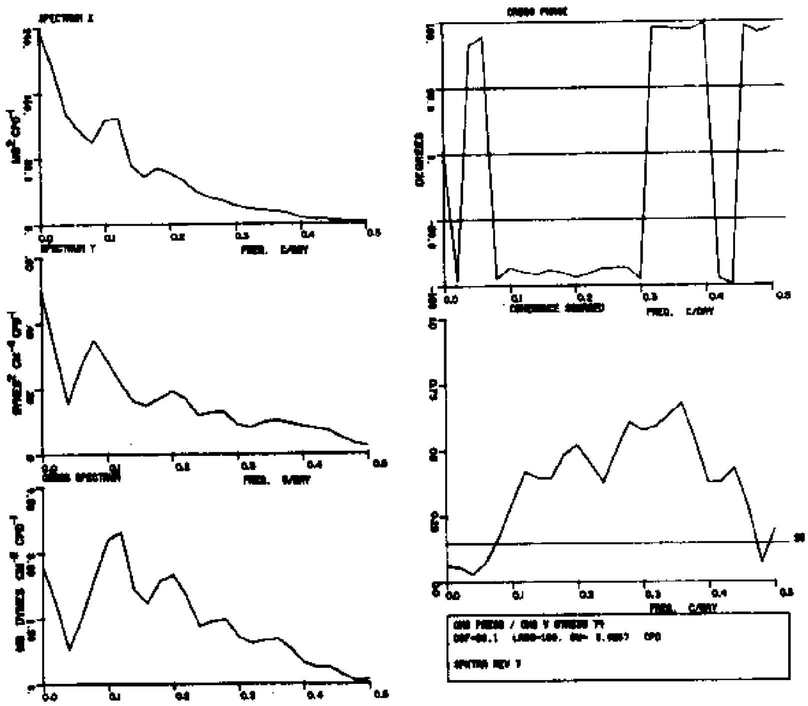

Figure 150 Spectra of pressure at Charleston, S. C. vs. wind stress v component at Charleston, S. C., 1974

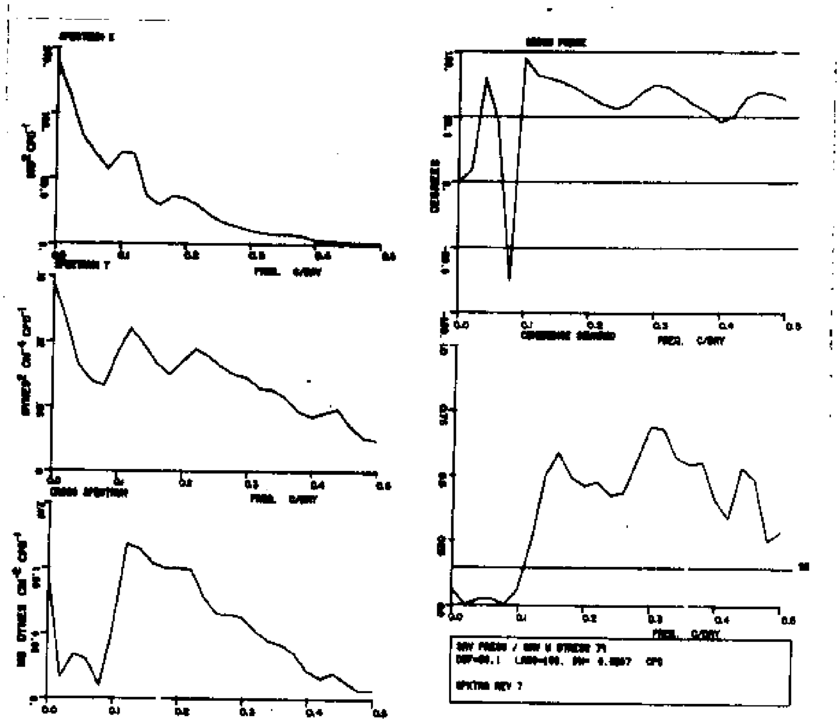

Figure 151 Spectra of pressure at Savannah, Ga. vs. wind stress u component at Savannah, Ga., 1974

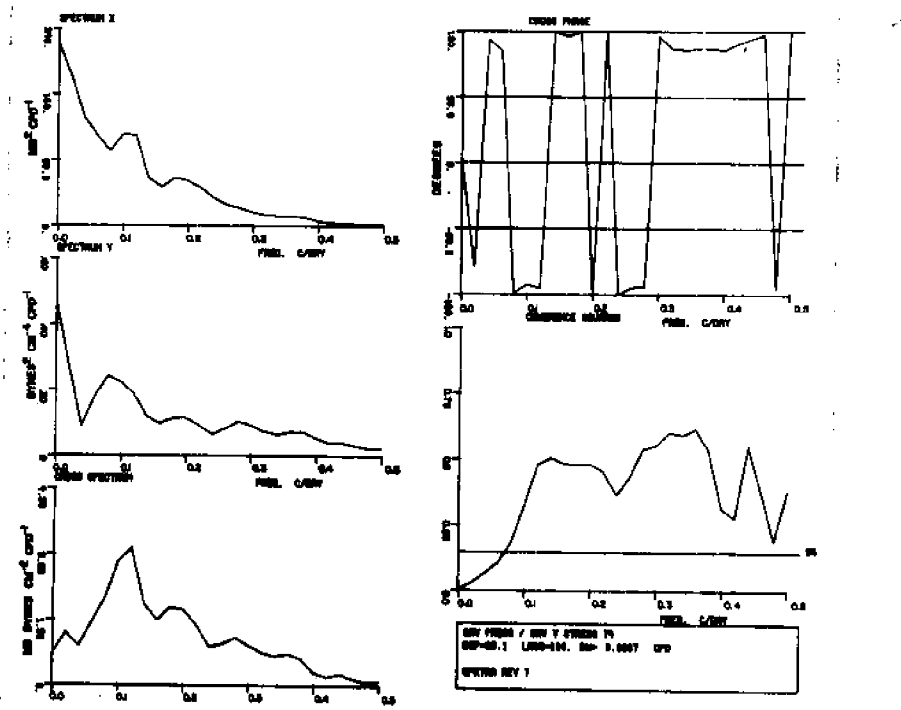

Figure 152 Spectra of pressure at Savannah, Ga. vs. wind stress v component at Savannah, Ga., 1974

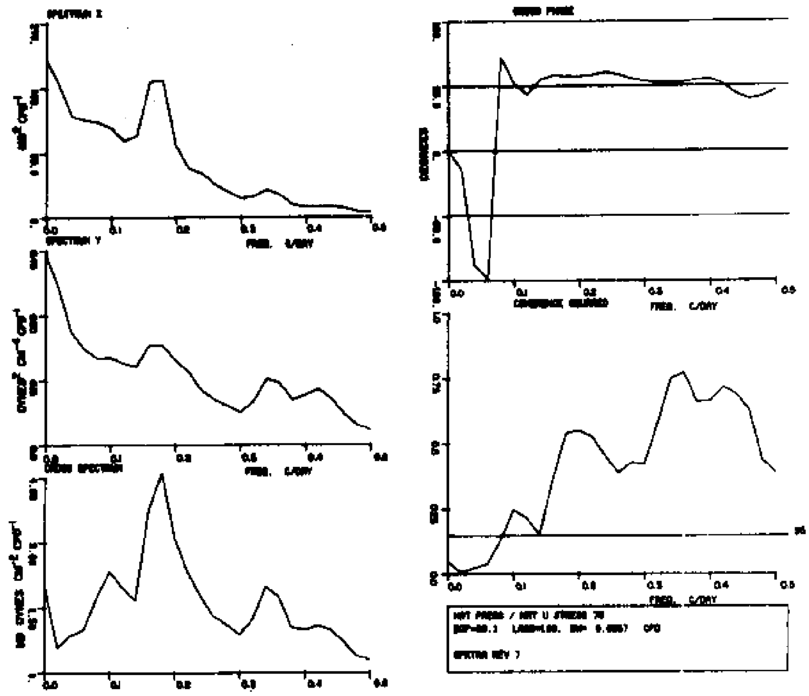

Figure 153 Spectra of pressure at Cape Hatteras, N. C. vs. wind stress u component at Cape Hatteras, N. C., 1975

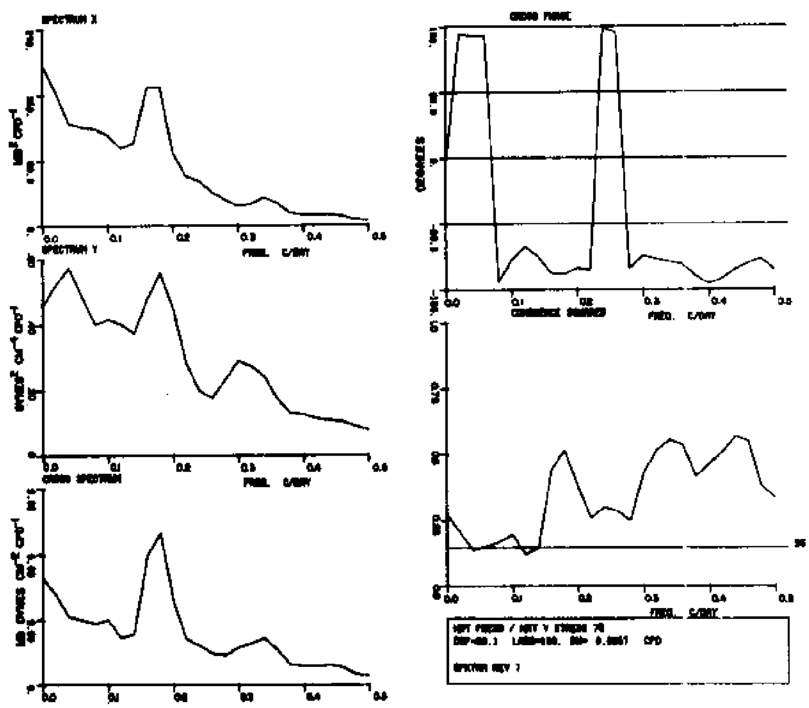

Figure 154 Spectra of pressure at Cape Hatteras, N. C. vs. wind stress v component at Cape Hatteras, N. C., 1975

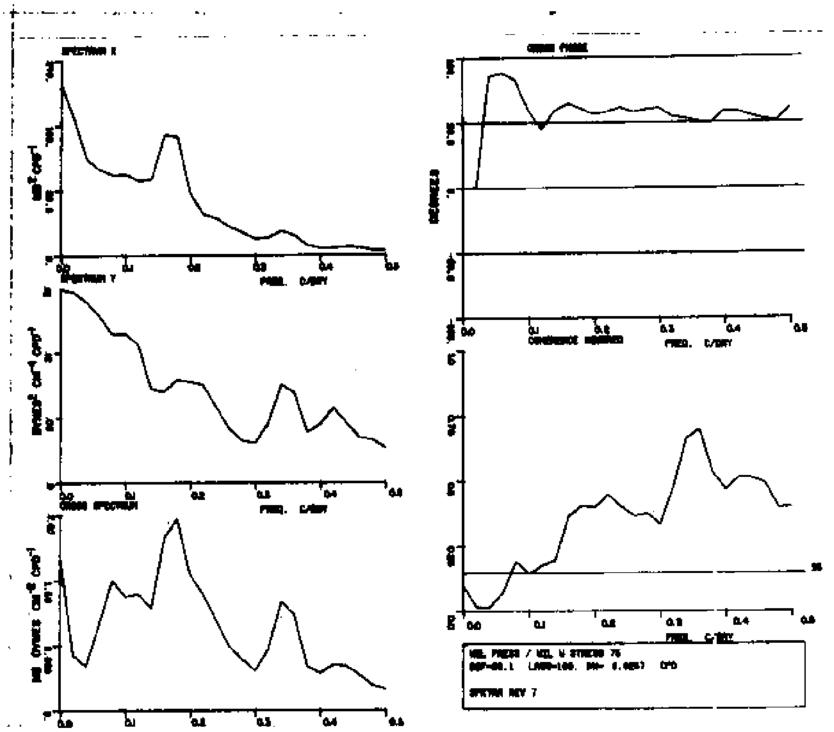

Figure 155 Spectra of pressure at Wilmington, N. C. vs. wind stress u component at Wilmington, N. C., 1975

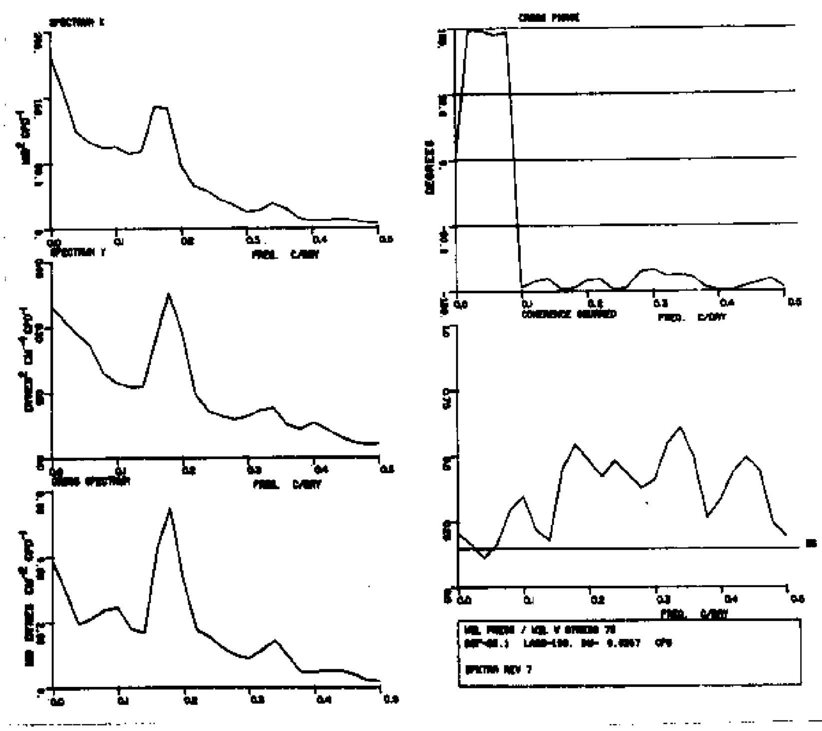

Figure 156 Spectra of pressure at Wilmington, N. C. vs. wind stress v component at Wilmington, N. C., 1975

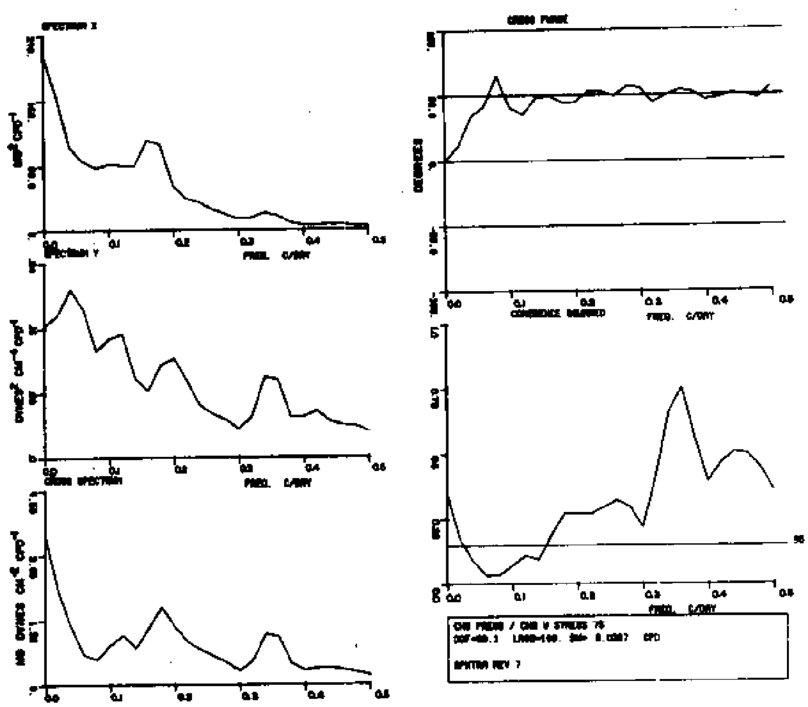

Figure 157 Spectra of pressure at Charleston, S. C. vs. wind stress u component at Charleston, S. C., 1975

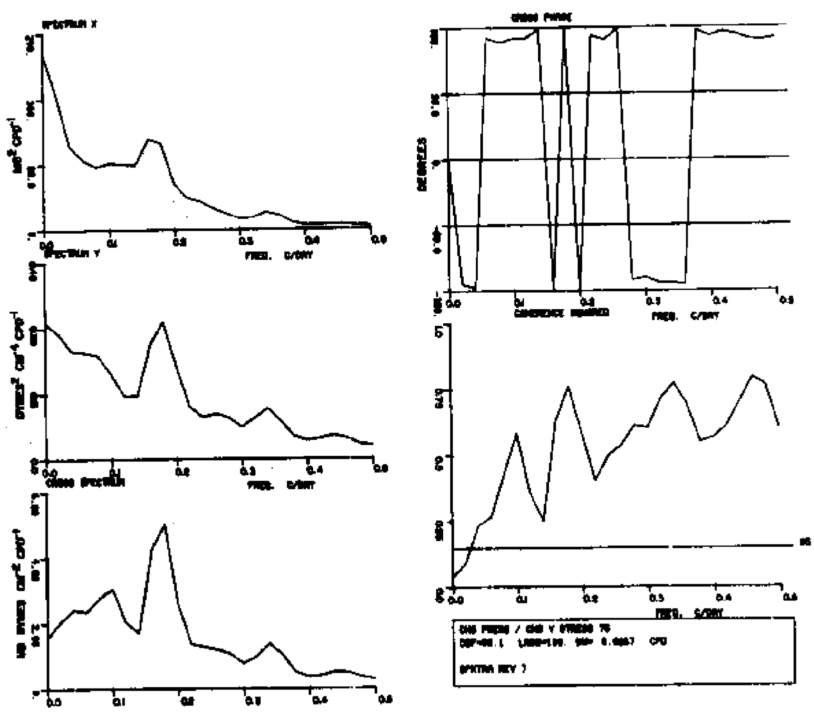

Figure 158 Spectra of pressure at Charleston, S. C. vs. wind stress v component at Charleston, S. C., 1975

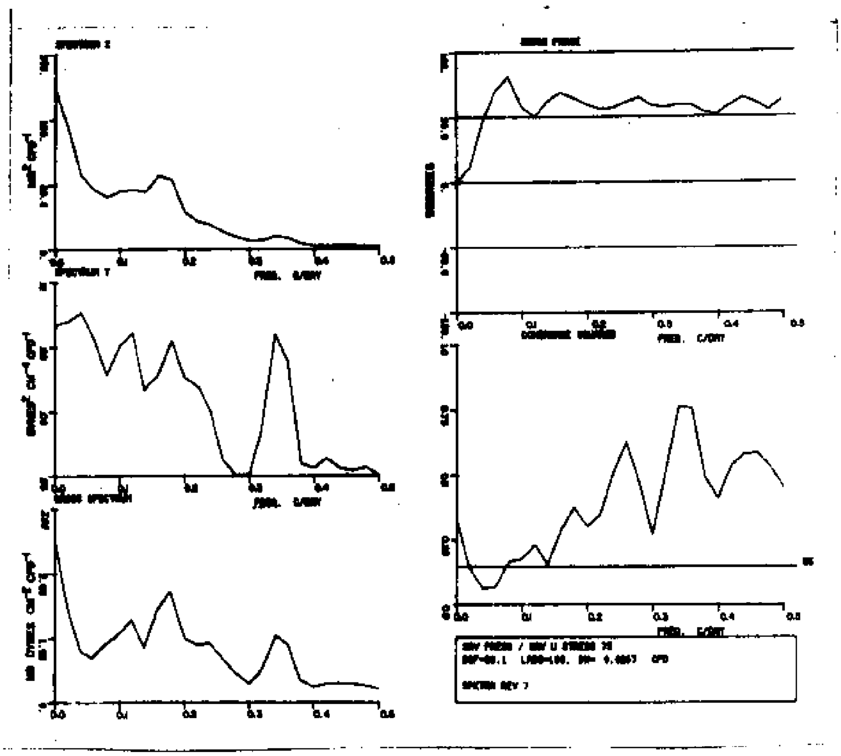

Figure 159 Spectra of pressure at Savannah, Ga. vs. wind stress u component at Savannah, Ga., 1975

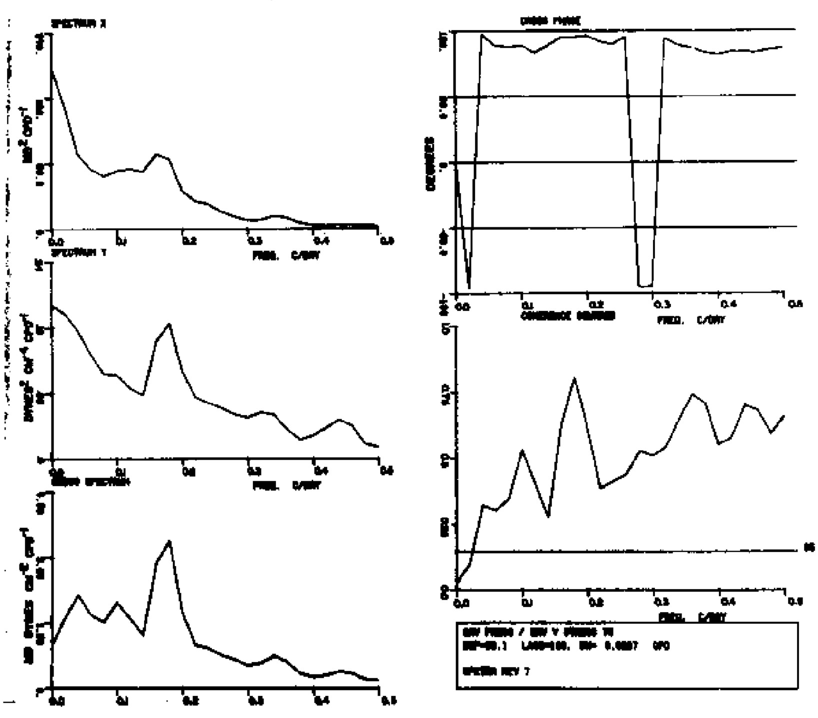

Figure 160 Spectra of pressure at Savannah, Ga. vs. wind stress v component at Savannah, Ga., 1975

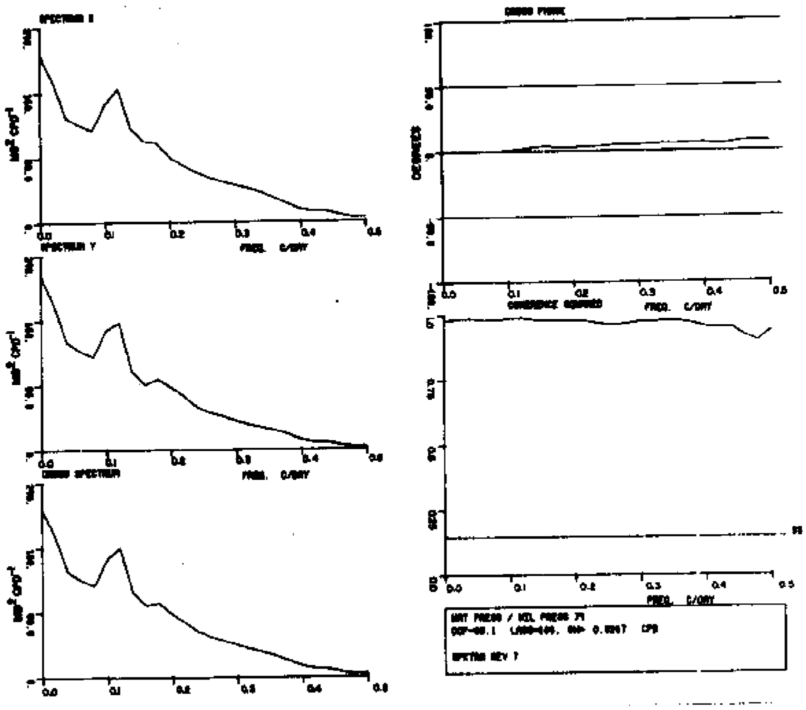

Figure 161 Spectra of pressure at Cape Hatteras, N. C. vs. pressure at Wilmington, N. C., 1974

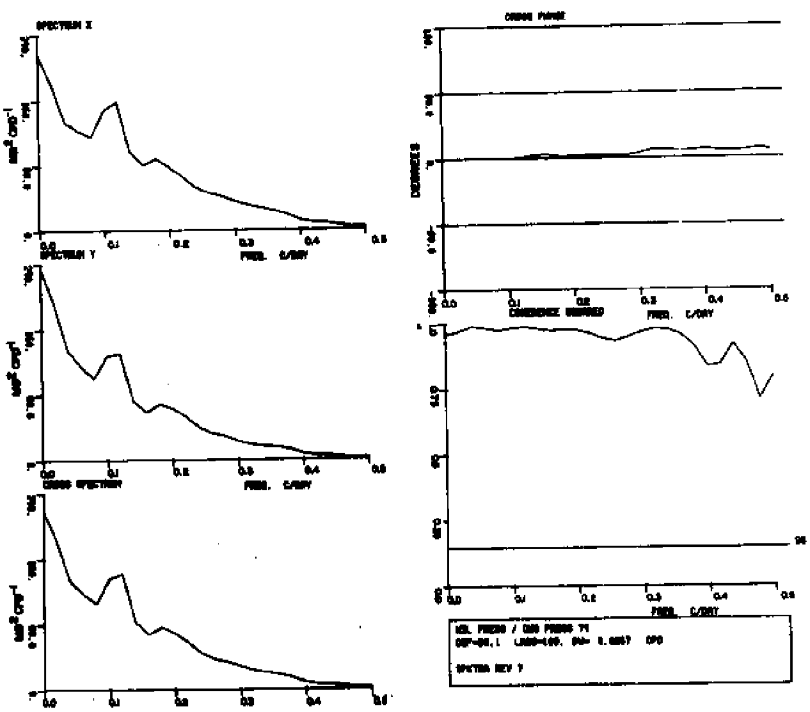

Figure 162 Spectra of pressure at Wilmington, N. C. vs. pressure at Charleston, S. C., 1974

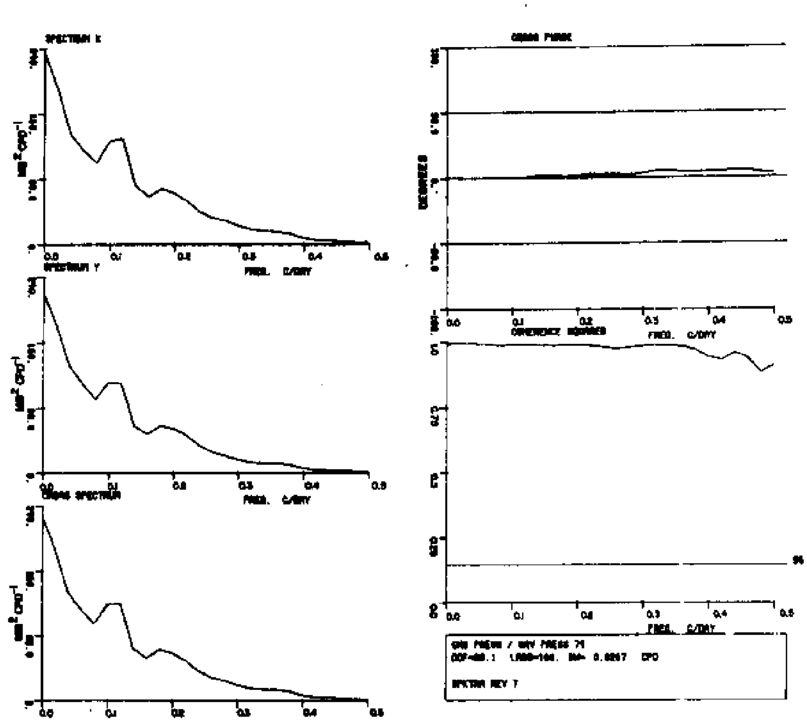

Figure 163 Spectra of pressure at Charleston, S. C. vs. pressure at Savannah, Ga., 1974

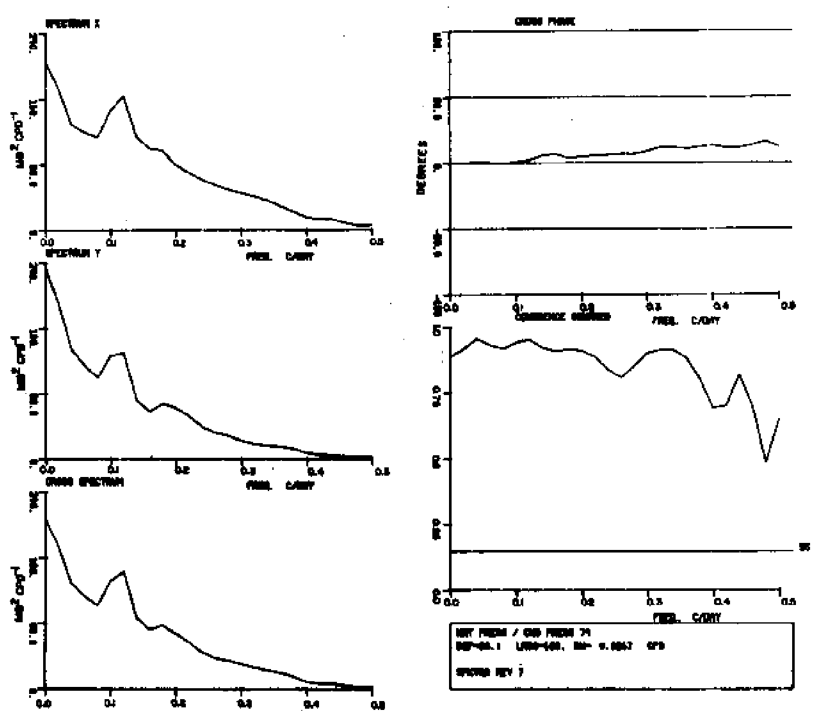

Figure 164 Spectra of pressure at Cape Hatteras, N. C. vs. pressure at Charleston, S. C., 1974

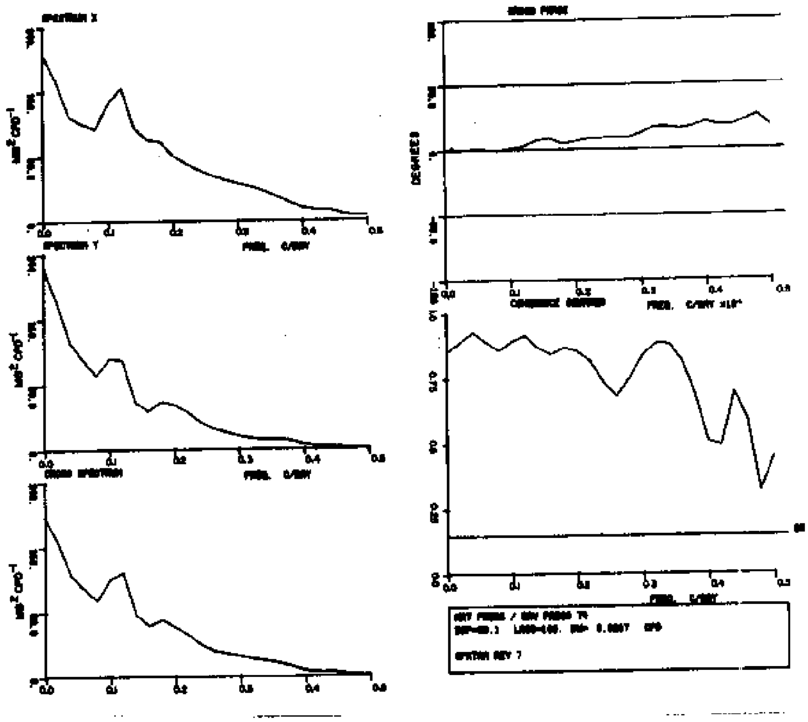

Figure 165 Spectra of pressure at Cape Hatteras, N. C. vs pressure at Savannah, Ga., 1974

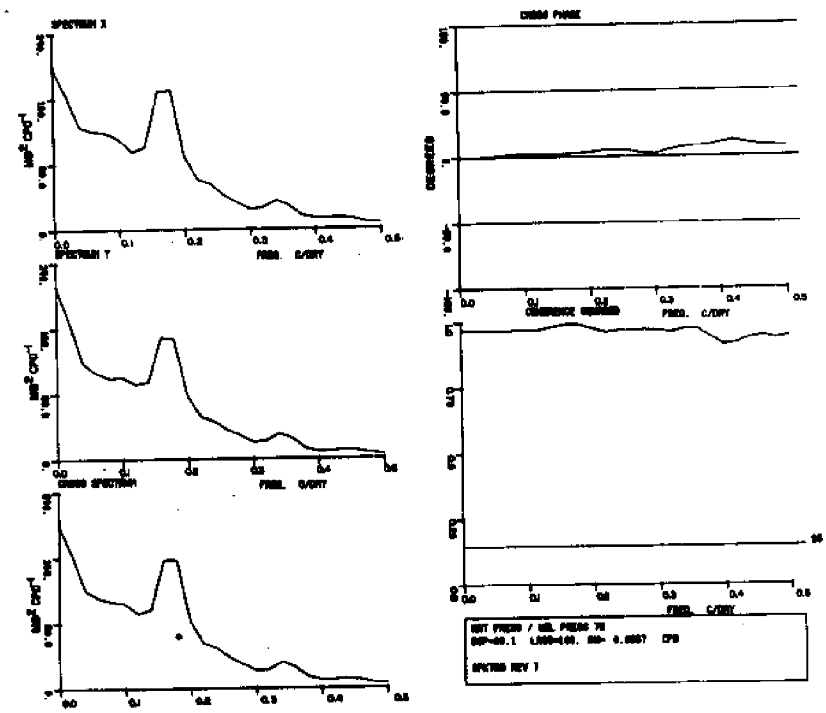

Figure 166 Spectra of pressure at Cape Hatteras, N. C. vs. pressure at Wilmington, N. C., 1975

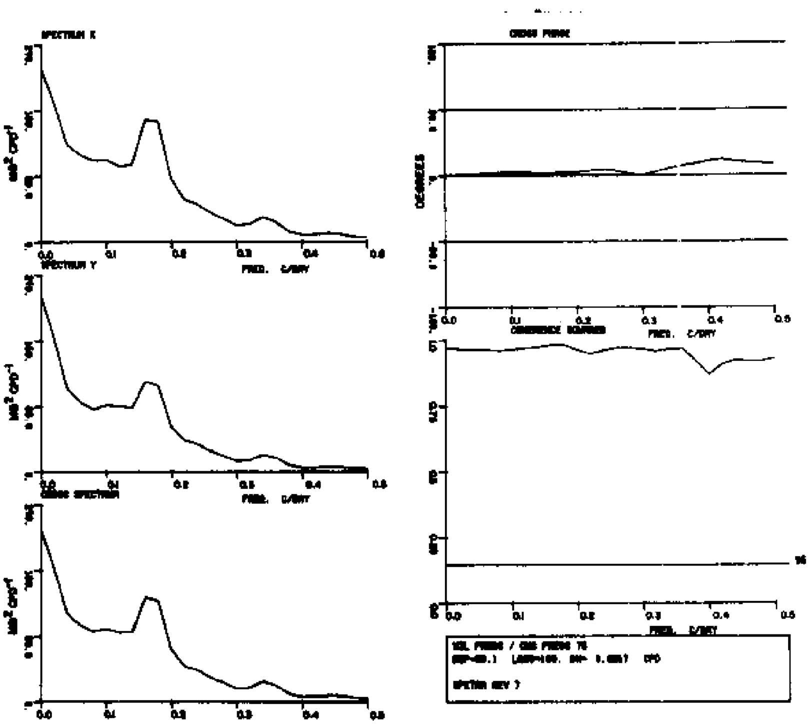

Figure 167 Spectra of pressure at Wilmington, N. C. vs. pressure at Charleston, S. C., 1975

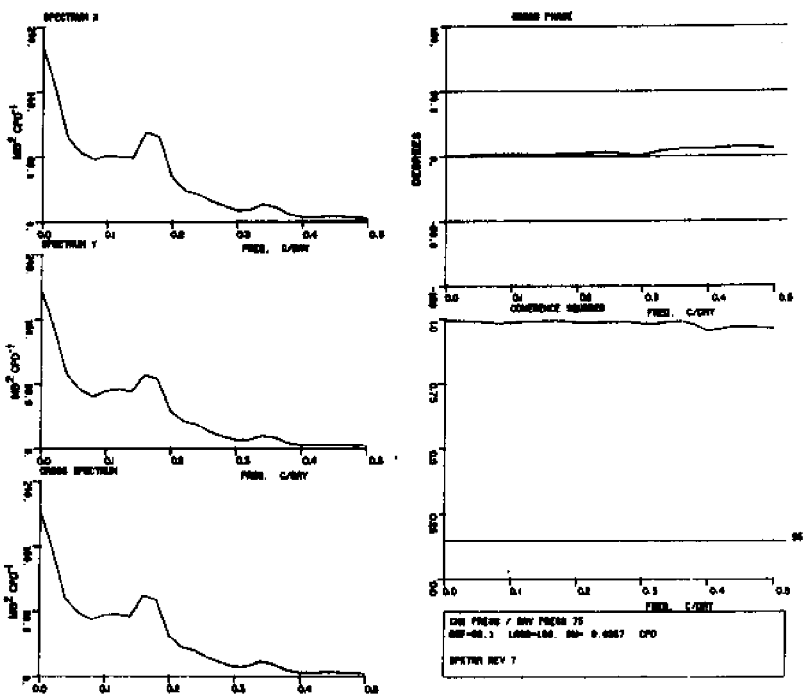

Figure 168 Spectra of pressure at Charleston, S. C. vs. pressure at Savannah, Ga., 175

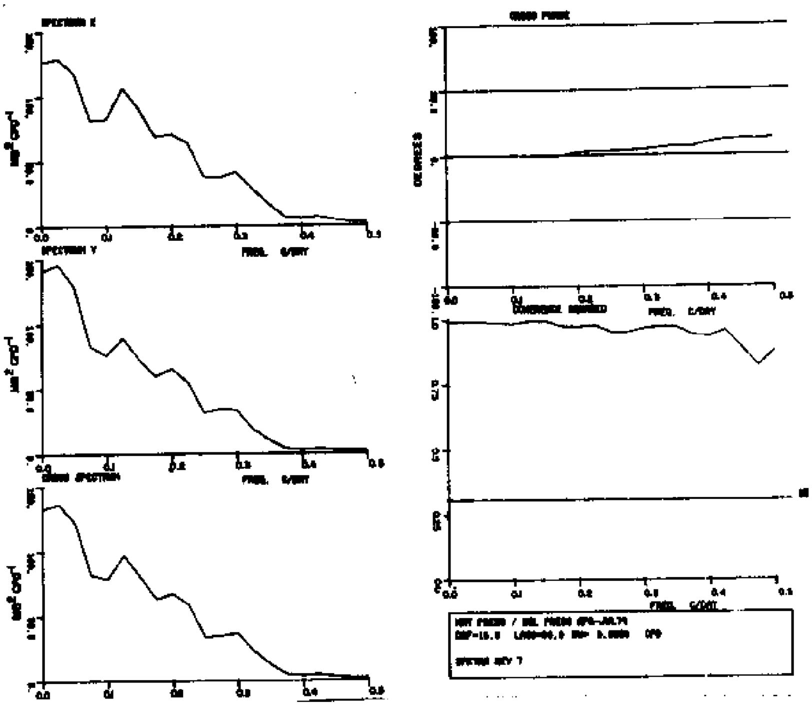

Figure 169 Spectra of pressure at Cape Hatteras, N. C. vs. pressure at Wilmington, N. C., April-July 1974

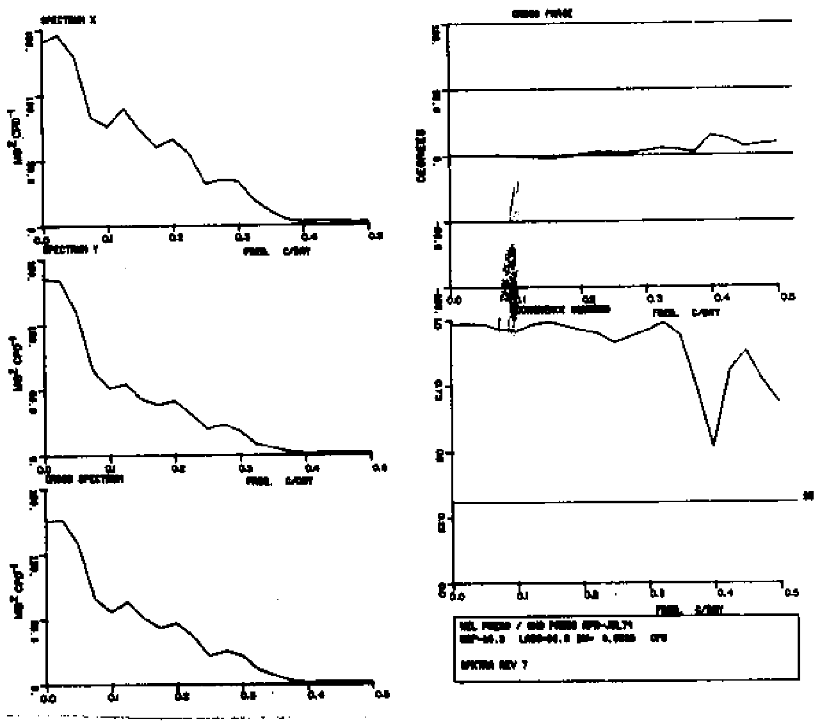

Figure 170 Spectra of pressure at Wilmington, N. C. vs. pressure at Charleston, S. C., April-July 1974

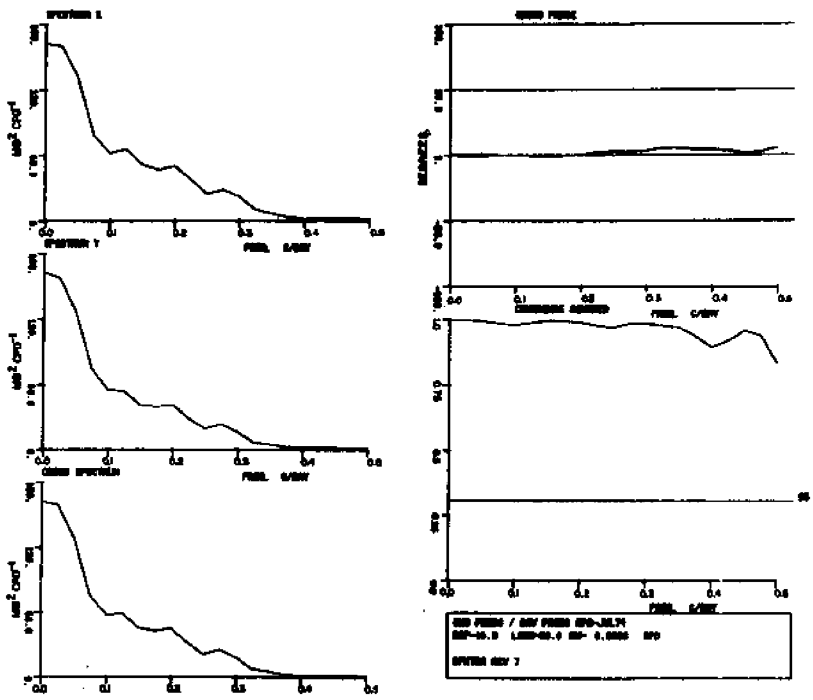

Figure 171 Spectra of pressure at Charleston, S. C. vs. pressure at Savannah, Ga., April-July 1974

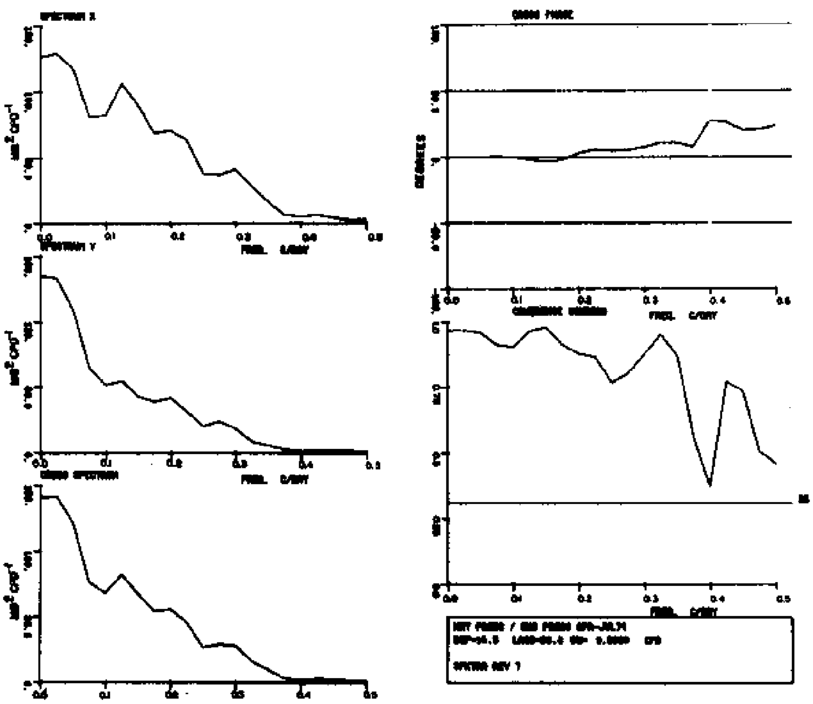

Figure 172 Spectra of pressure at Cape Hatteras, N. C. vs. pressure at Charleston, S. C., April-July 1974

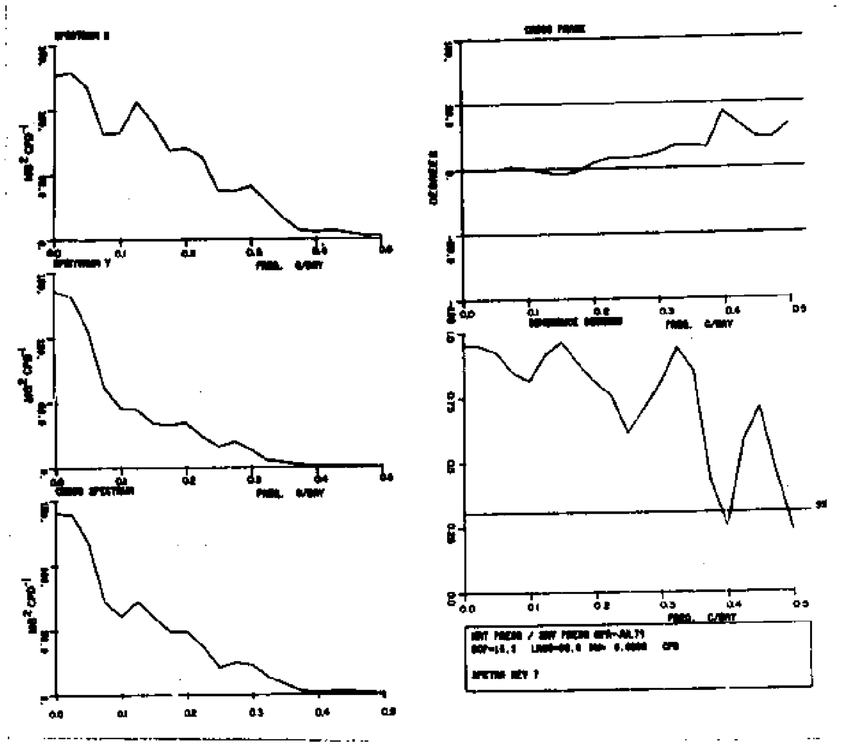

Figure 173 Spectra of pressure at Cape Hatteras, N. C. vs. pressure at Savannah, Ga., April-July 1974

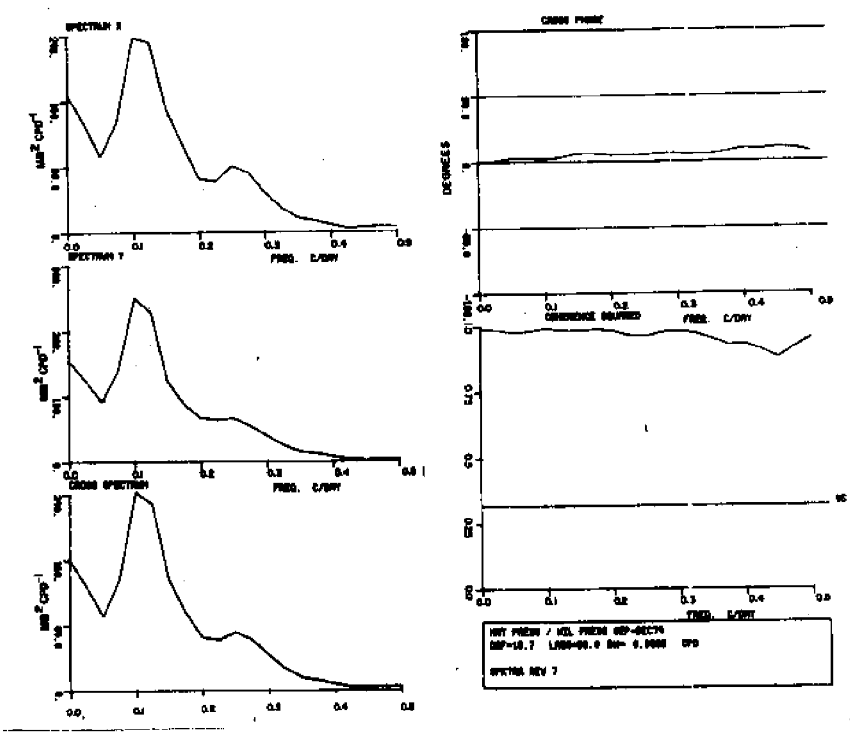

Figure 174 Spectra of pressure at Cape Hatteras, N. C. vs. pressure at Wilmington, N. C., Sept.-Dec. 1974

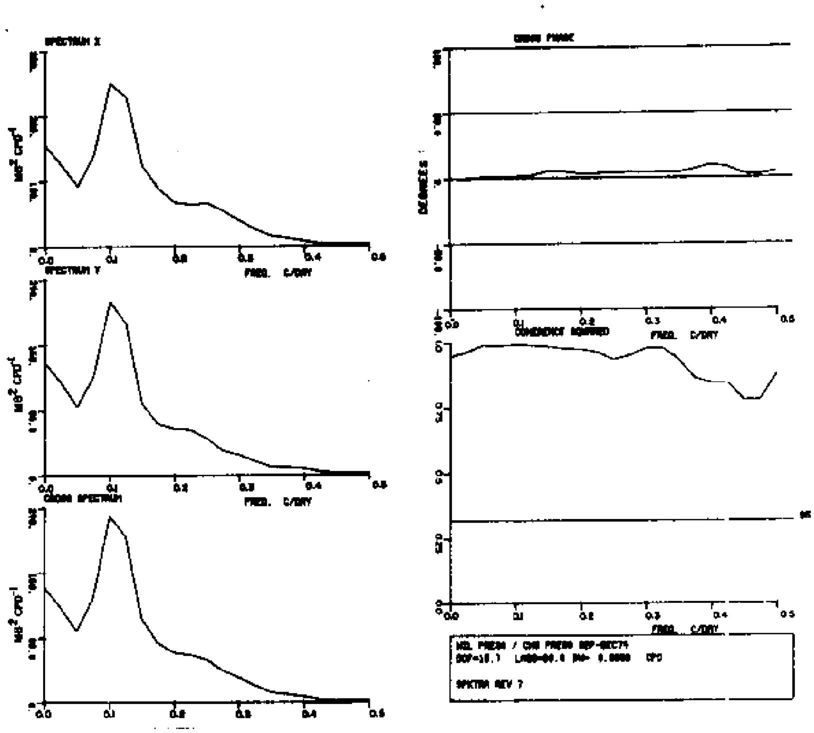

Figure 175 Spectra of pressure at Wilmington, N. C. vs. pressure at Charleston, S. C., Sept.-Dec. 1974

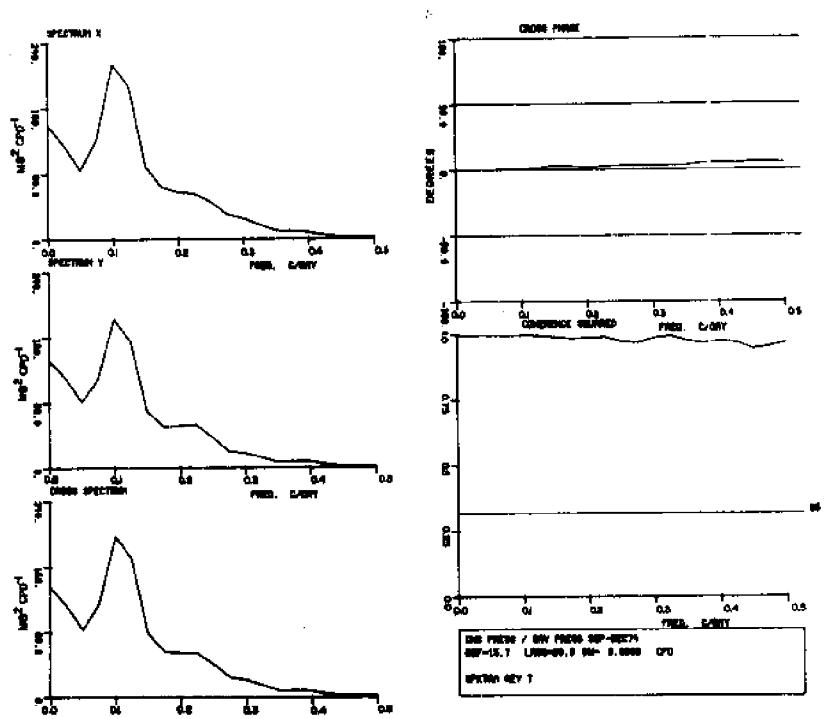

Figure 176 Spectra of pressure at Charleston, S. C. vs. pressure at Savannah, Ga., Sept.-Dec. 1974

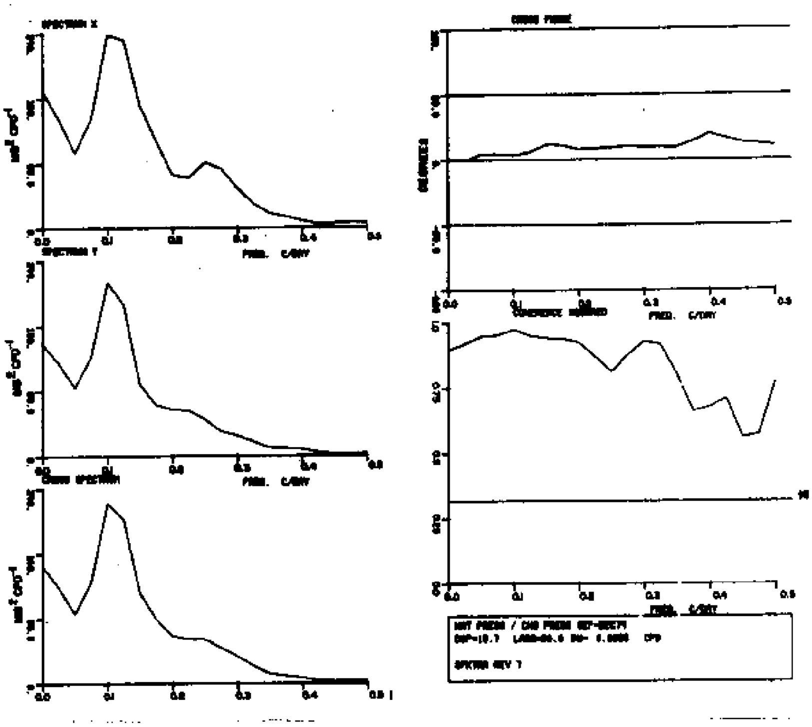

Figure 177 Spectra of pressure at Cape Hatteras, N. C. vs. pressure at Charleston, S. C., Sept.-Dec. 1974

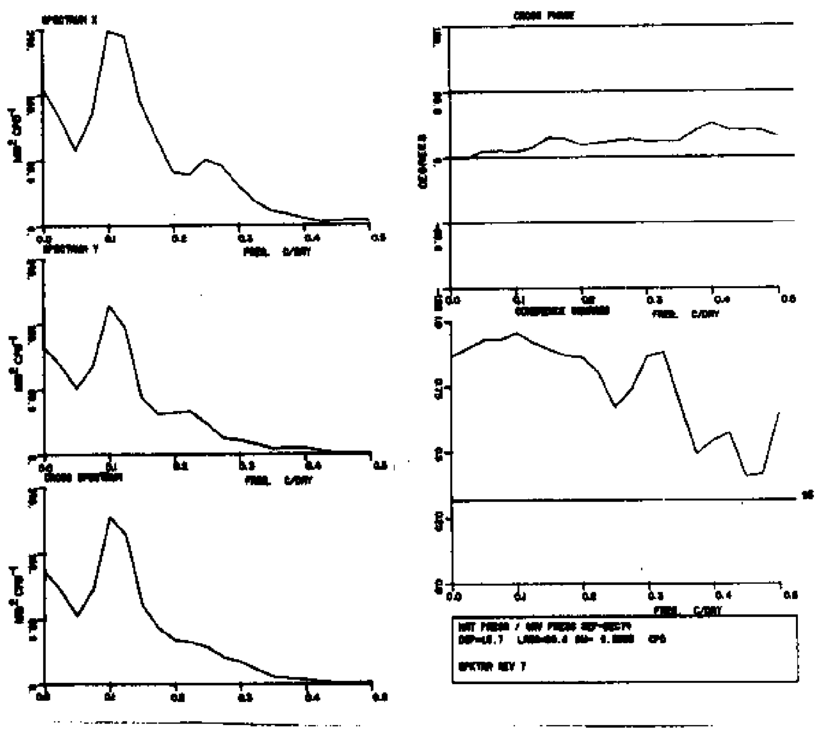

Figure 178 Spectra of pressure at Cape Hatteras, N. C. vs. pressure at Savannah, Ga., Sept.-Dec. 1974

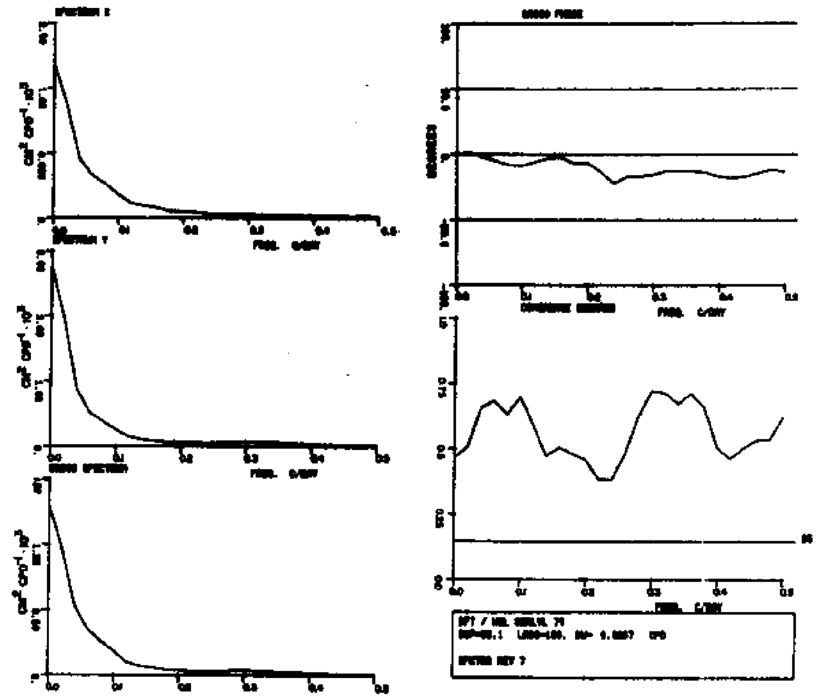

Figure 179 Spectra of sea level at Beaufort, N. C. vs. sea level at Wilmington, N. C., 1974

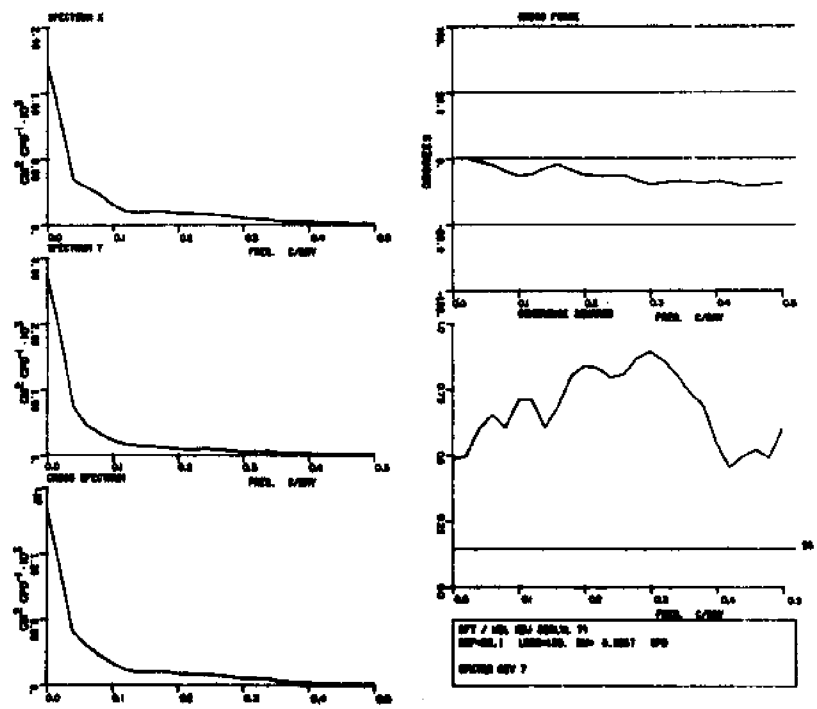

Figure 180 Spectra of adjusted sea level at Beaufort, N. C. vs. adjusted sea level at Wilmington, N. C., 1974

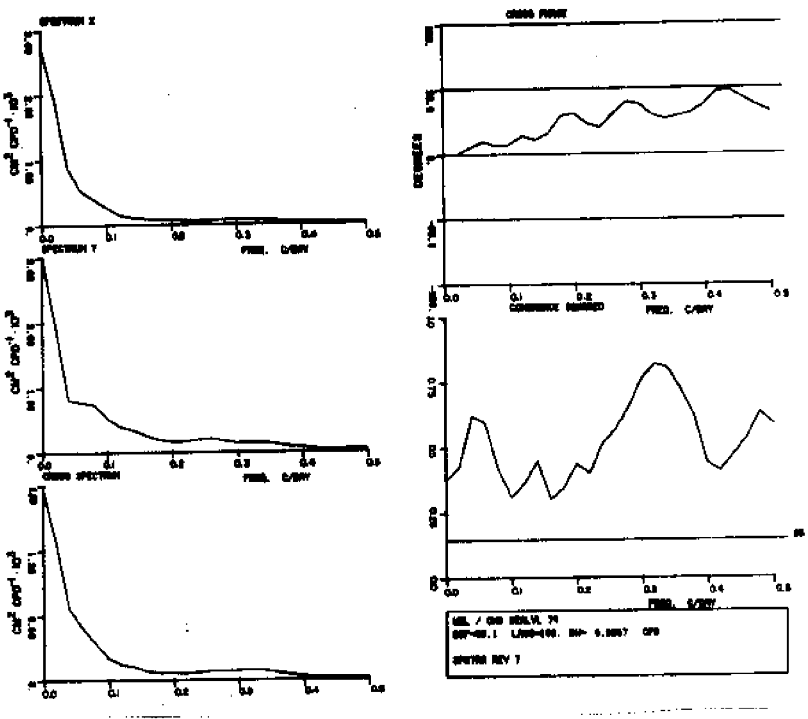

Figure 181 Spectra of sea level at Wilmington, N.C. vs. sea level at Charleston, S. C., 1974

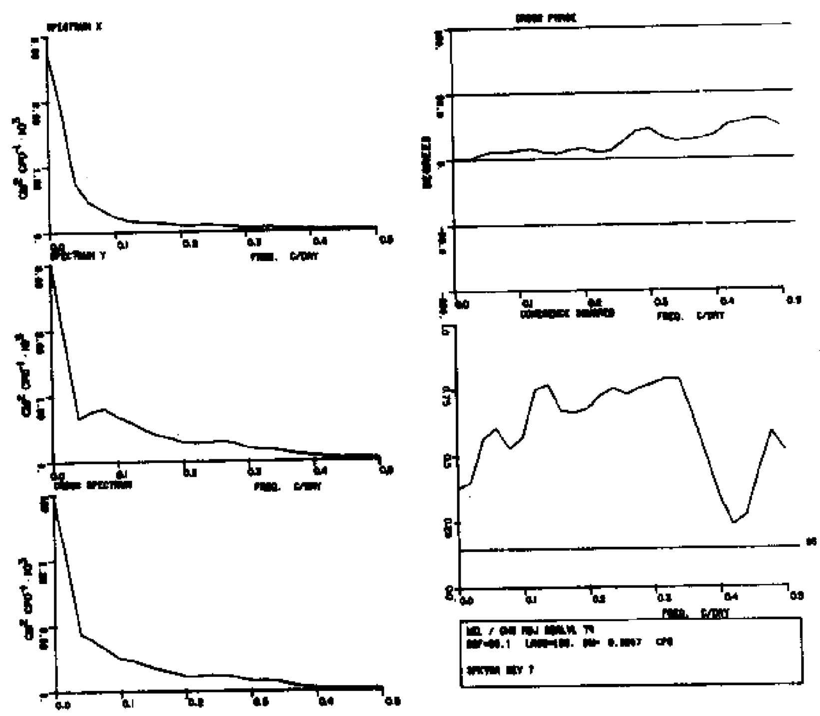

Figure 182 Spectra of adjusted sea level at Wilmington, N. C. vs. adjusted sea level at Charleston, S. C., 1974

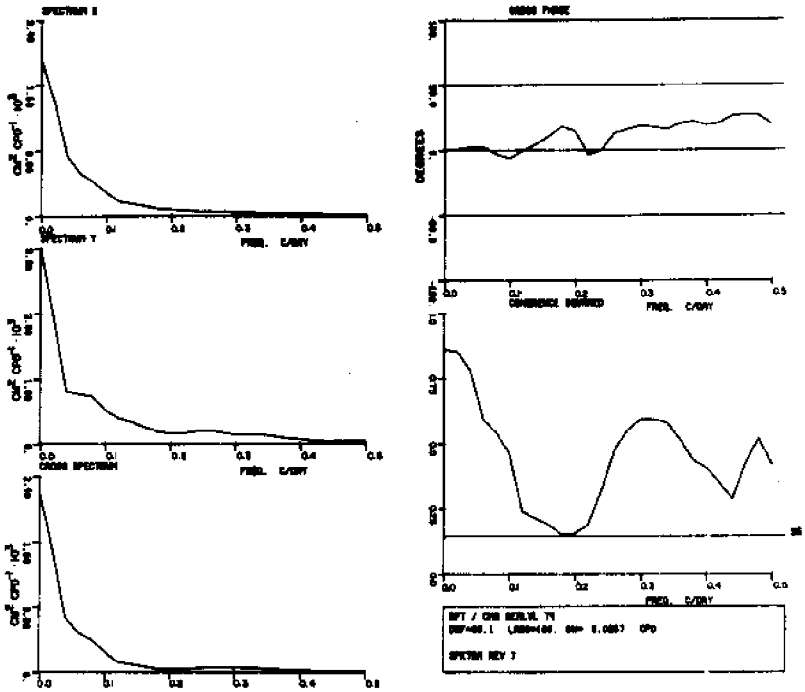

Figure 183 Spectra of sea level at Beaufort, N. C. vs. sea level at Charleston, S. C., 1974

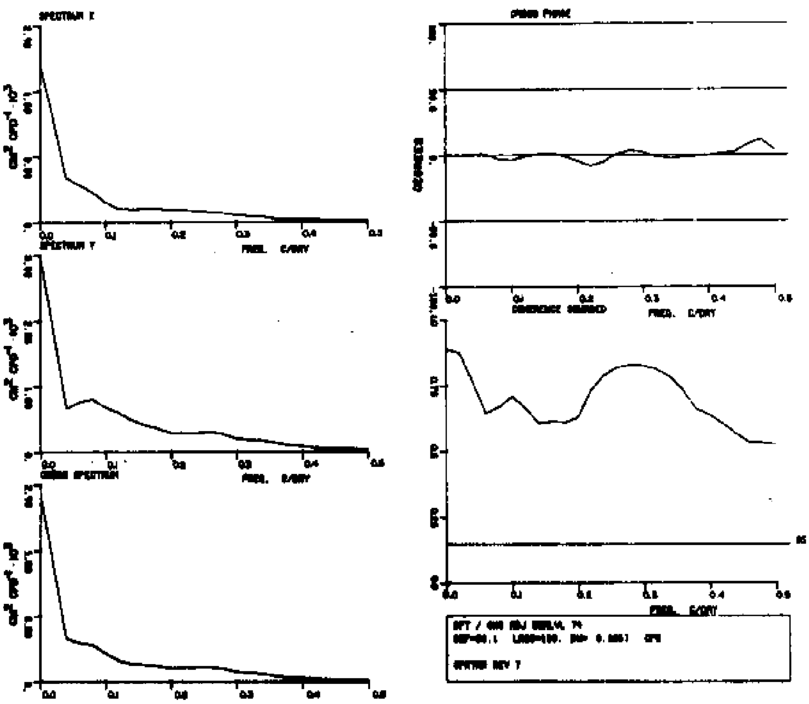

Figure 184 Spectra of adjusted sea level at Beaufort, N. C. vs. adjusted sea level at Charleston, S. C., 1974

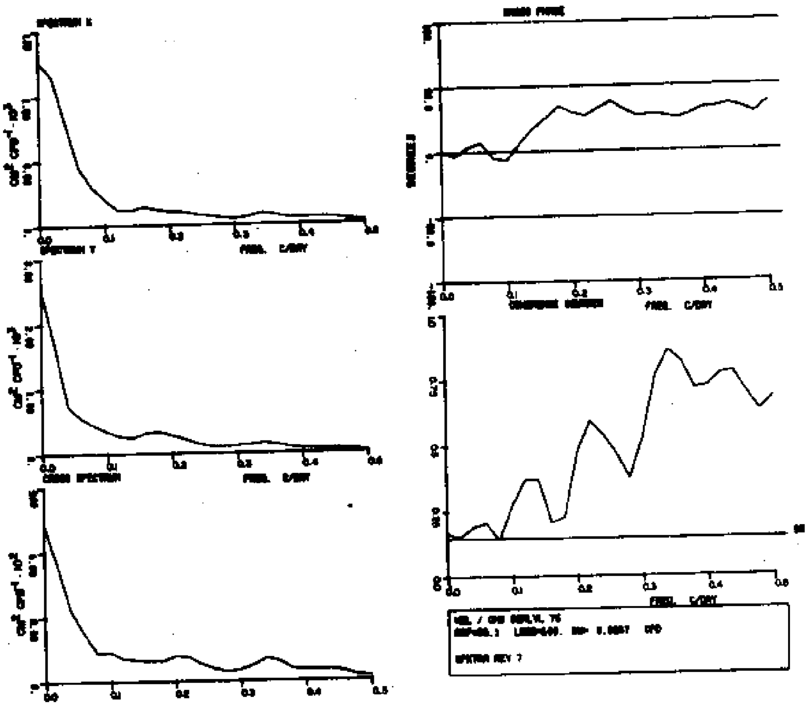

Figure 185 Spectra of sea level at Wilmington, N. C. vs. sea level at Charleston, S. C., 1975

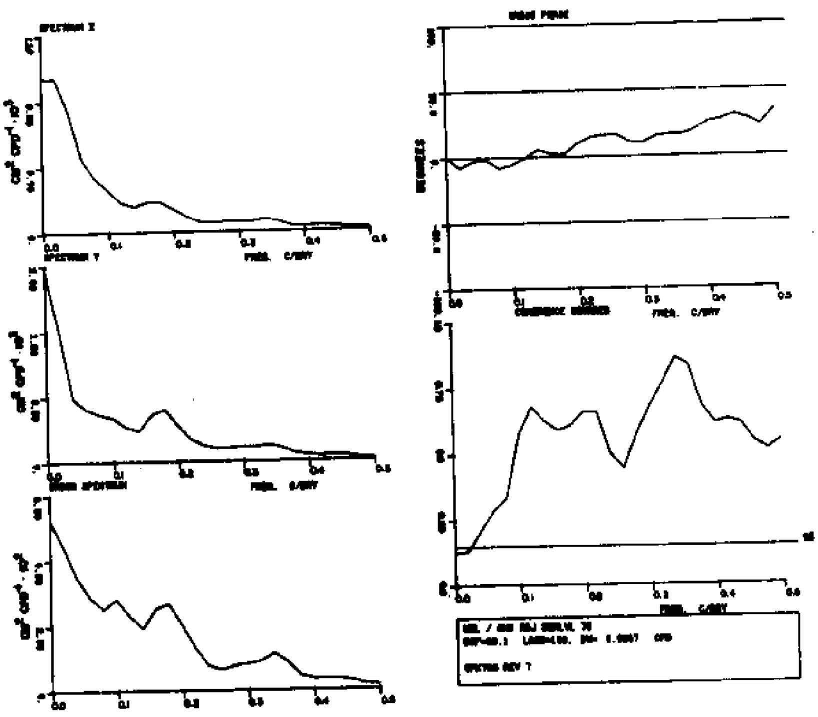

Figure 186 Spectra of adjusted sea level at Wilmington, N. C. vs. adjusted sea level at Charleston, S. C., 1975

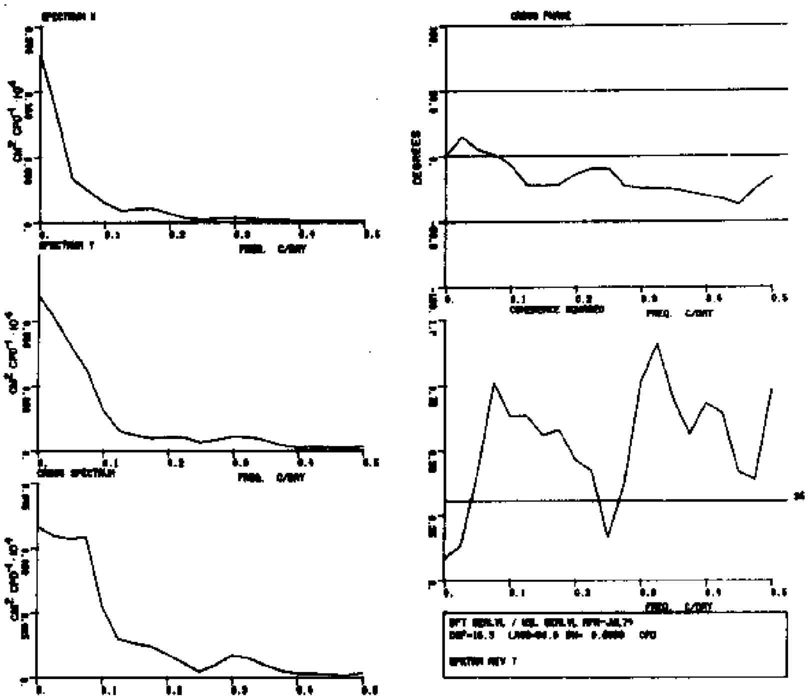

Figure 187 Spectra of sea level at Beaufort, N. C. vs. sea level at Wilmington, N. C., April-July 1974

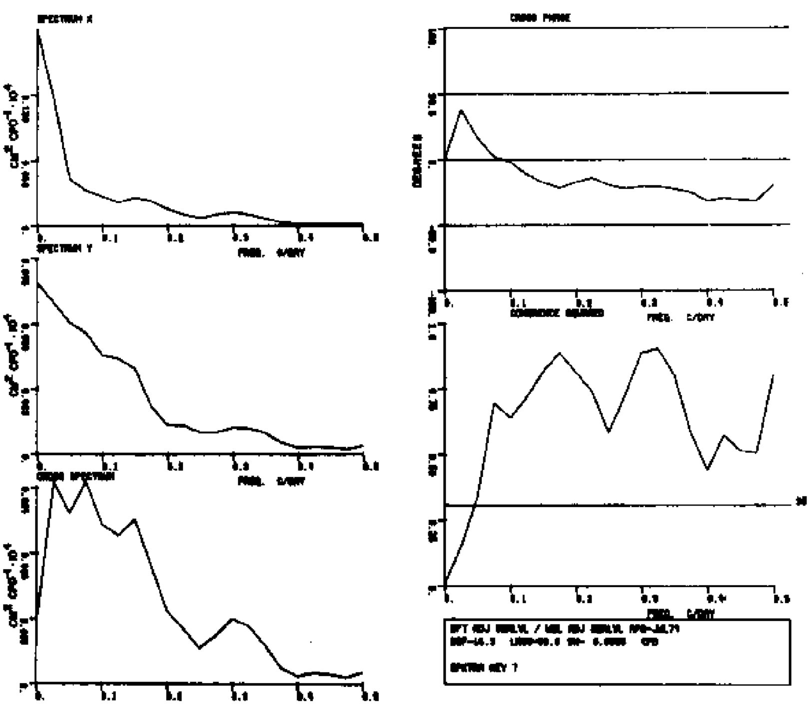

Figure 188 Spectra of adjusted sea level at Beaufort, N. C. vs. adjusted sea level at Wilmington, N. C., April-July 1974

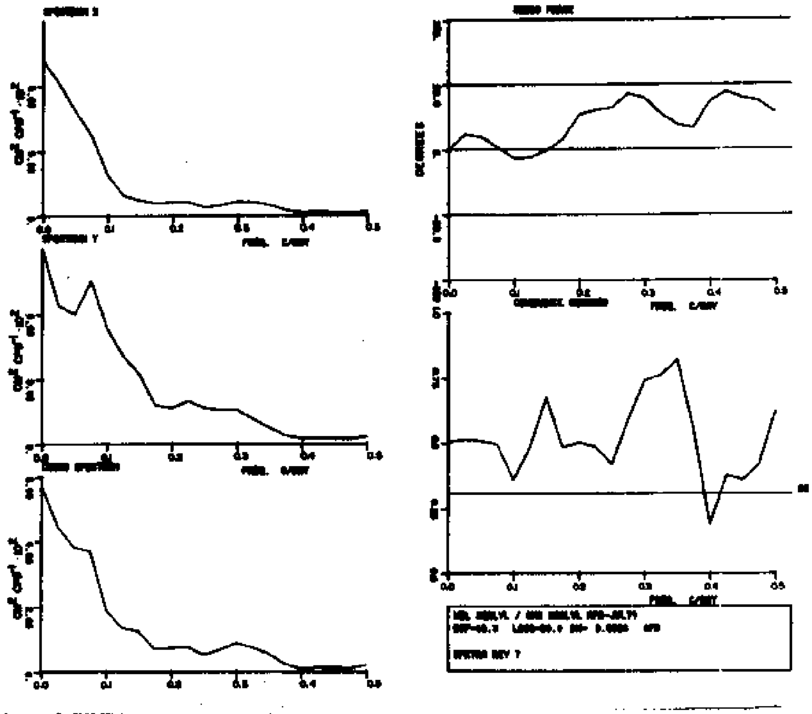

Figure 189 Spectra of sea level at Wilmington, N. C. vs. sea level at Charleston, S. C., April-July 1974

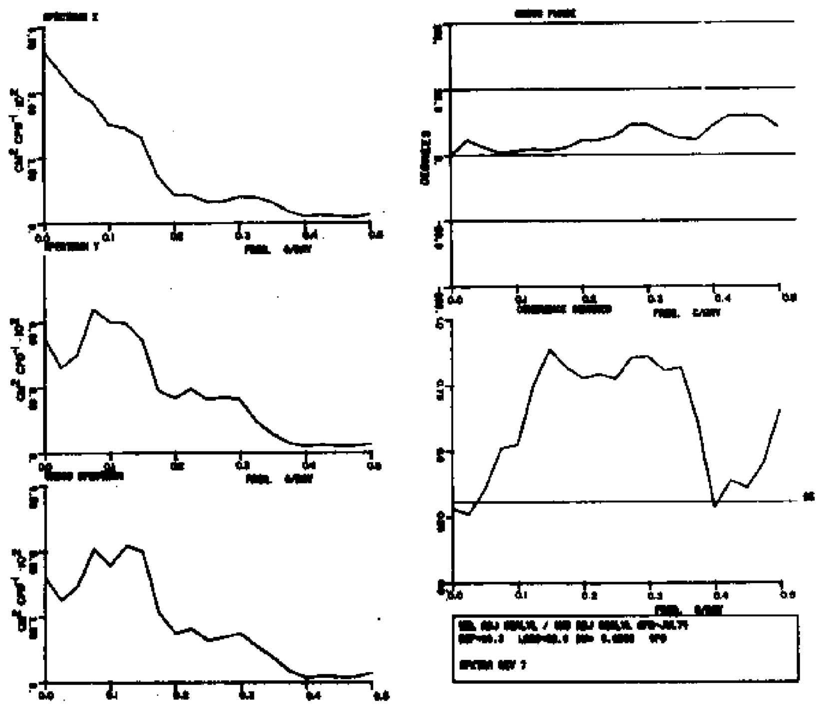

Figure 190 Spectra of adjusted sea level at Wilmington, N. C. vs. adjusted sea level at Charleston, S. C., April-July 1974

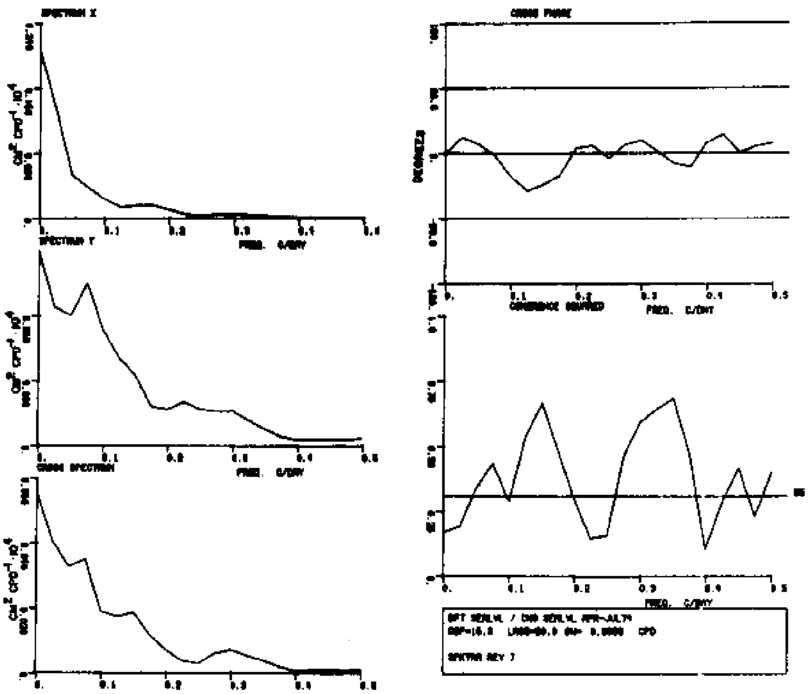

Figure 191 Spectra of sea level at Beaufort, N. C. vs. sea level at Charleston, S. C., April-July 1974

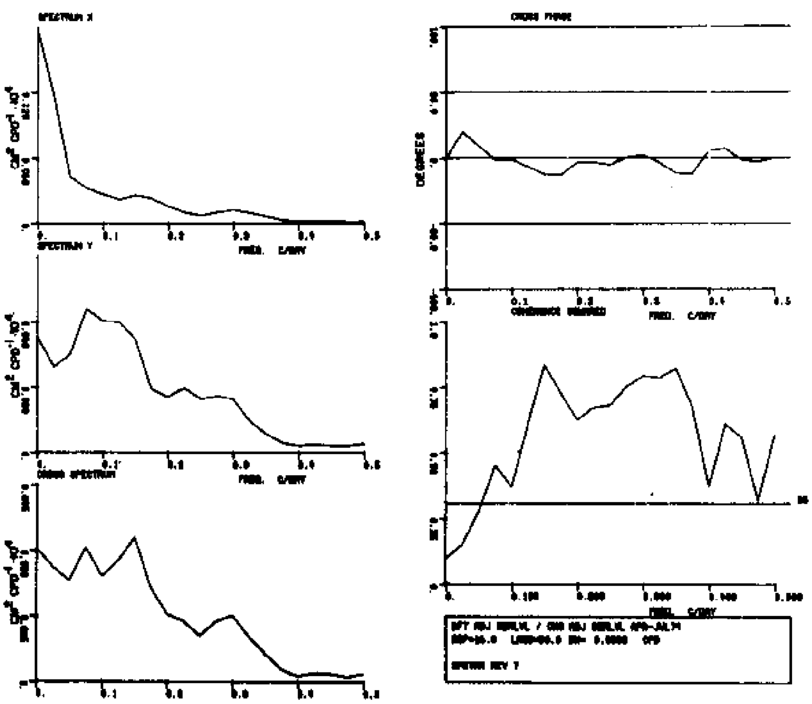

Figure 192 Spectra of adjusted sea level at Beaufort, N. C. vs. adjusted sea level at Charleston, S. C., April-July 1974

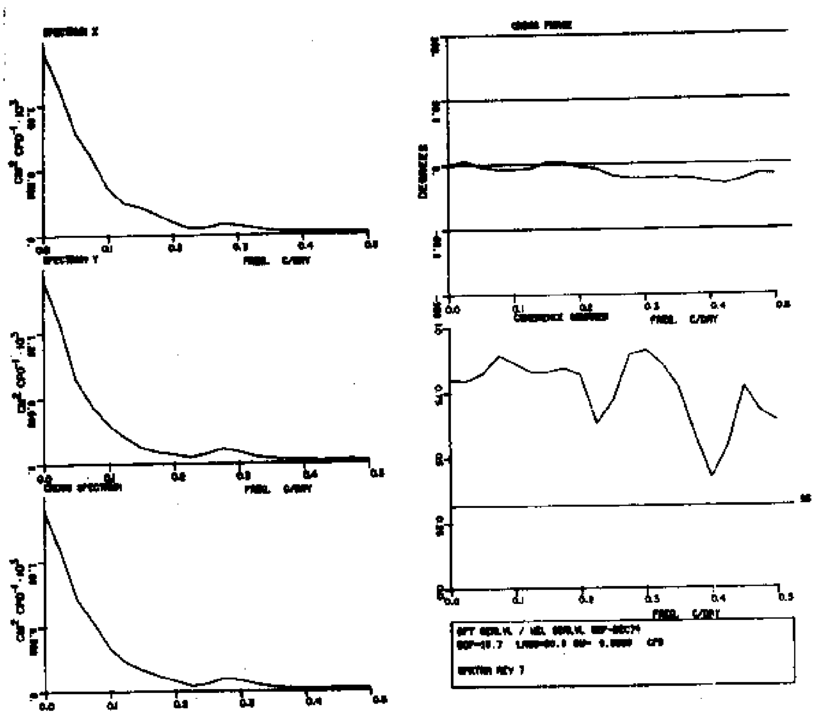

Figure 193   Spectra of sea level at Beaufort, N. C. vs. sea level at Wilmington, N. C., Sept.-Dec. 1974

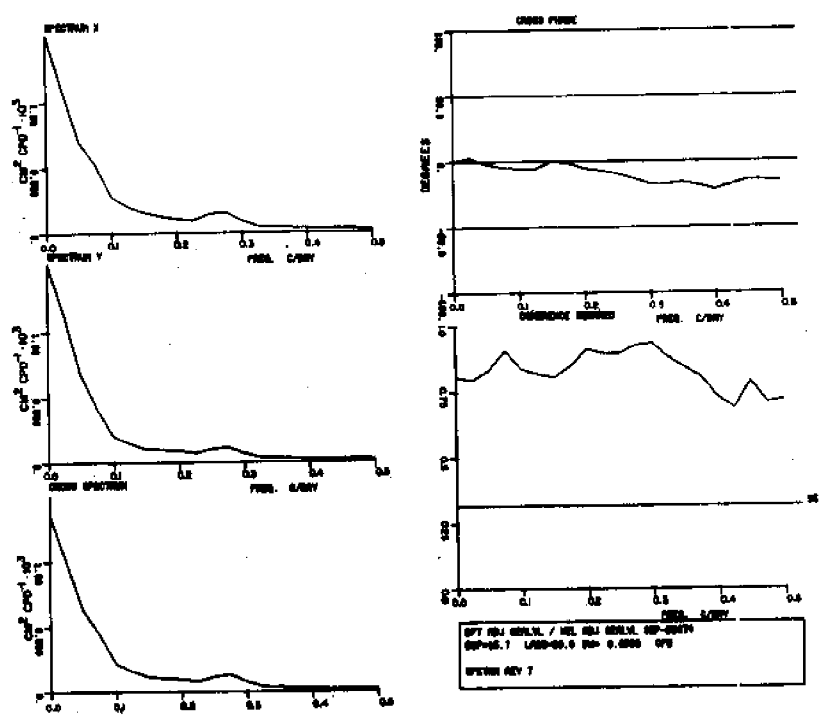

Figure 194   Spectra of adjusted sea level at Beaufort, N. C. vs. adjusted sea level at Wilmington, N. C., Sept.-Dec. 1974

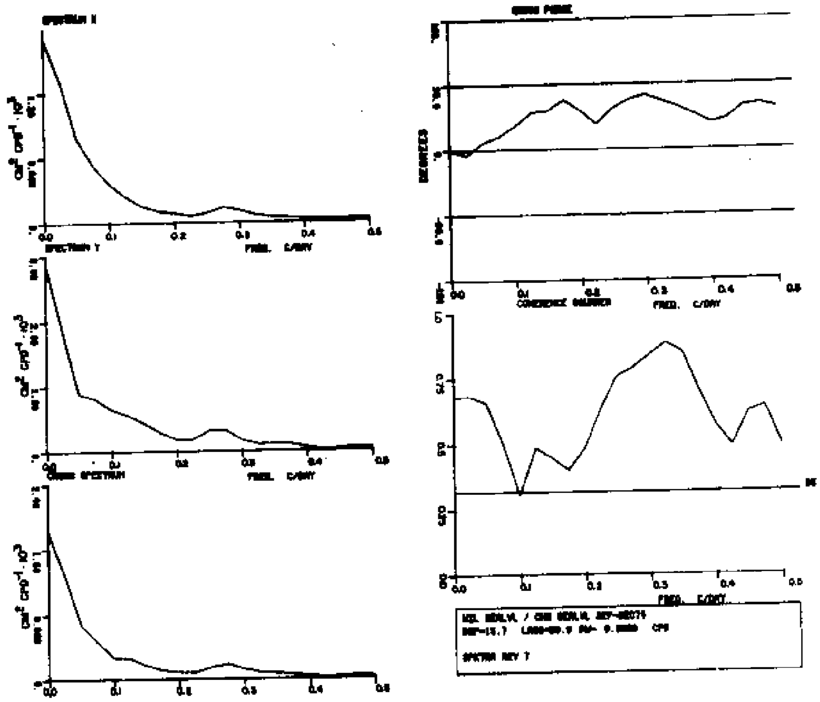

Figure 195   Spectra of sea level at Wilmington, N. C. vs. sea level at Charleston, S. C. Sept.-Dec. 1974

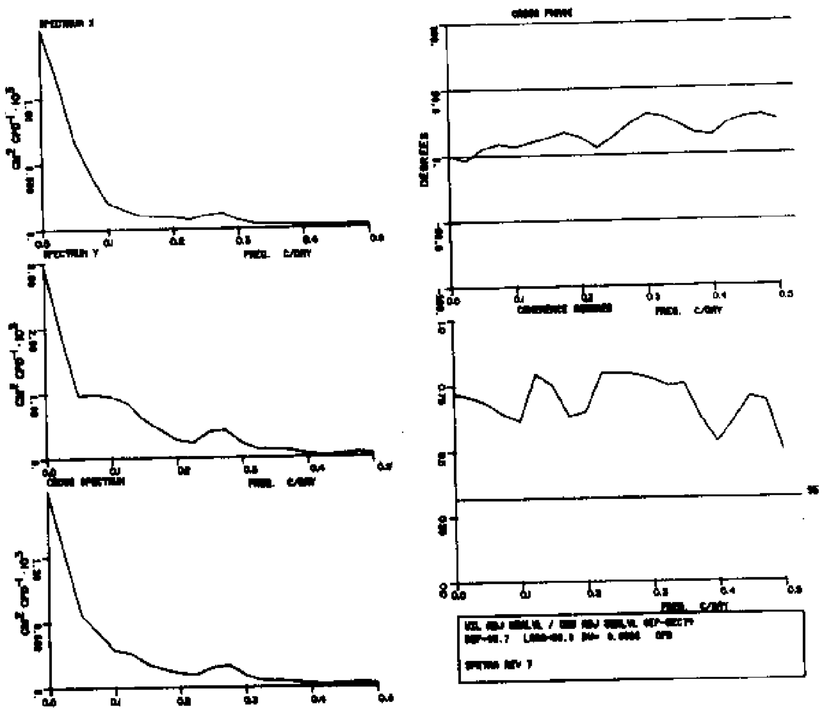

Figure 196   Spectra of adjusted sea level at Wilmington, N. C. vs. adjusted sea level at Charleston, S. C., Sept.-Dec. 1974

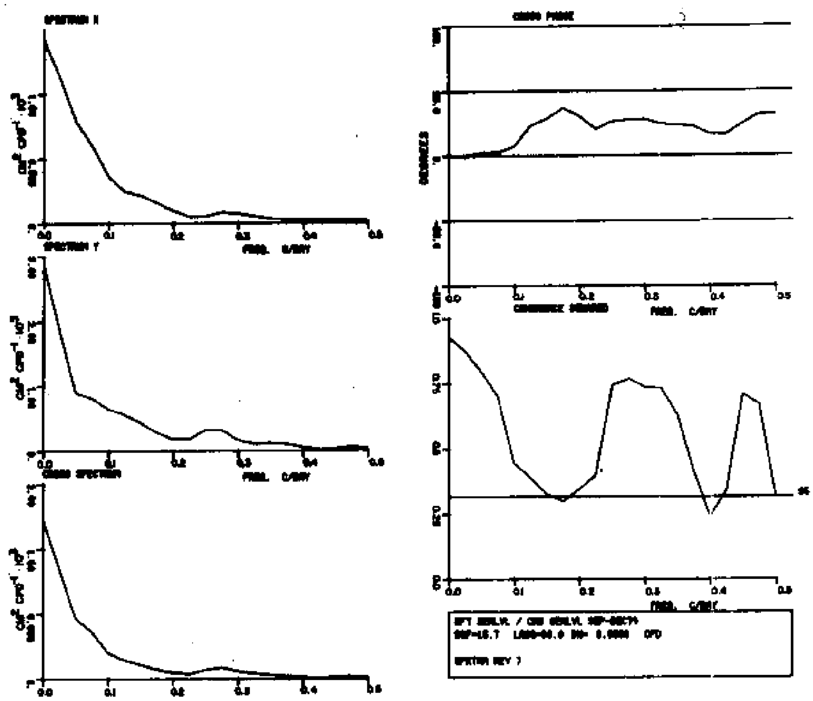

Figure 197 Spectra of sea level at Beaufort, N. C. vs. sea level at Charleston, S. C., Sept.-Dec. 1974

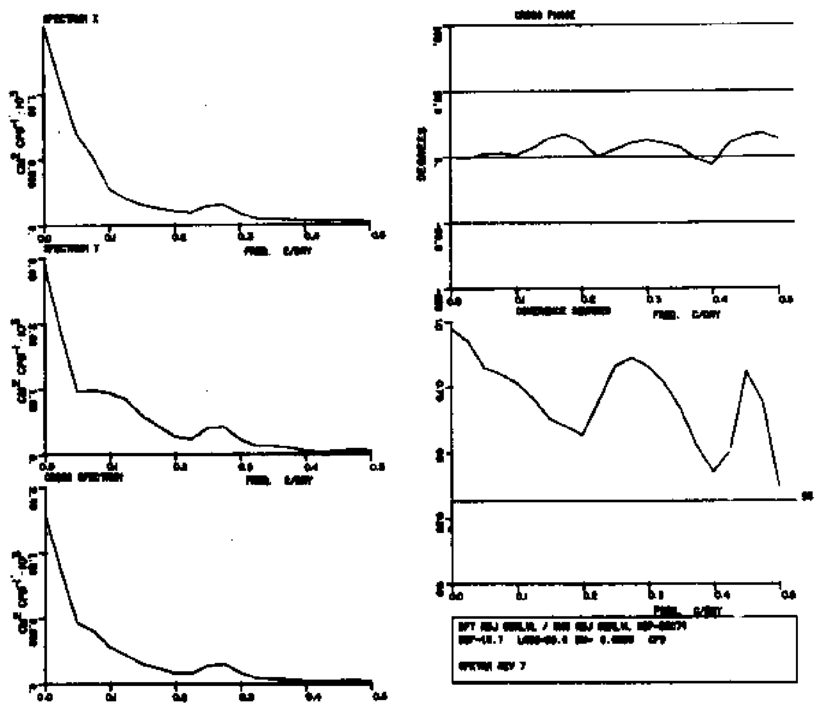

Figure 198 Spectra of adjusted sea level at Beaufort, N. C. vs. adjusted sea level at Charleston, S. C., Sept.-Dec. 1974

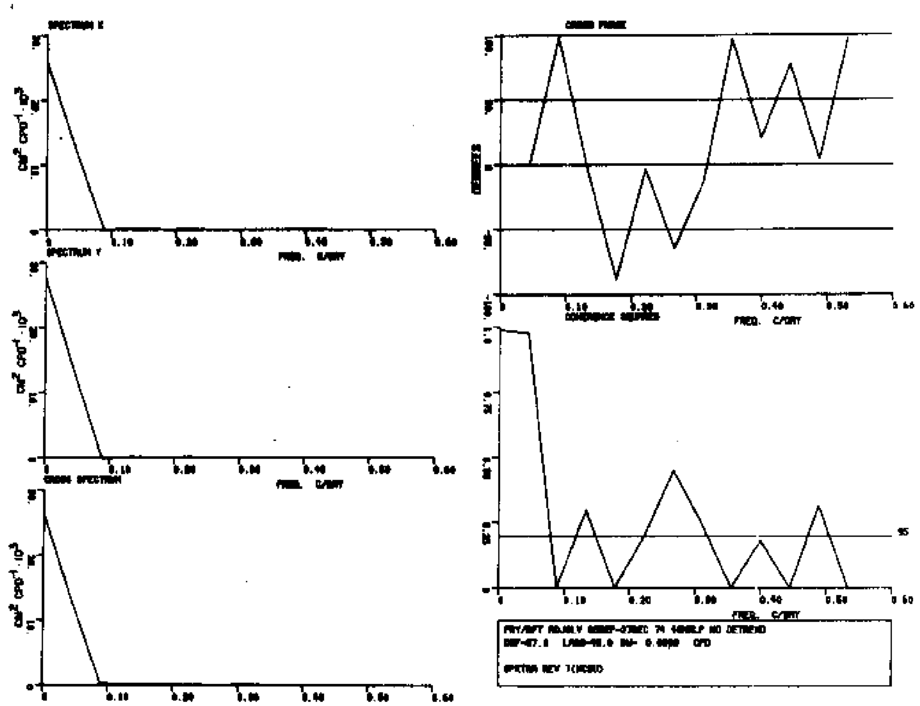

Figure 199 Spectra of adjusted sea level at Frying Pan Shoals, N. C. vs. adjusted sea level at Beaufort, N. C., 5 Sept.-27 Dec. 1974 (no detrend)

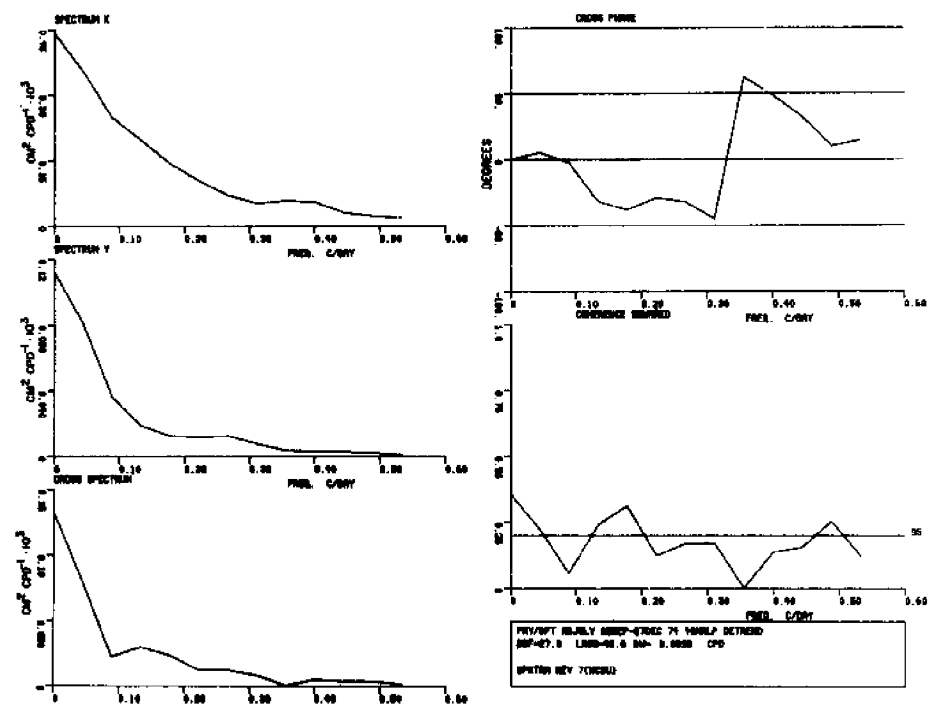

Figure 200 Spectra of adjusted sea level at Frying Pan Shoals, N. C. vs. adjusted sea level at Beaufort, N. C., 5 Sept.-27 Dec. 1974 (detrended)

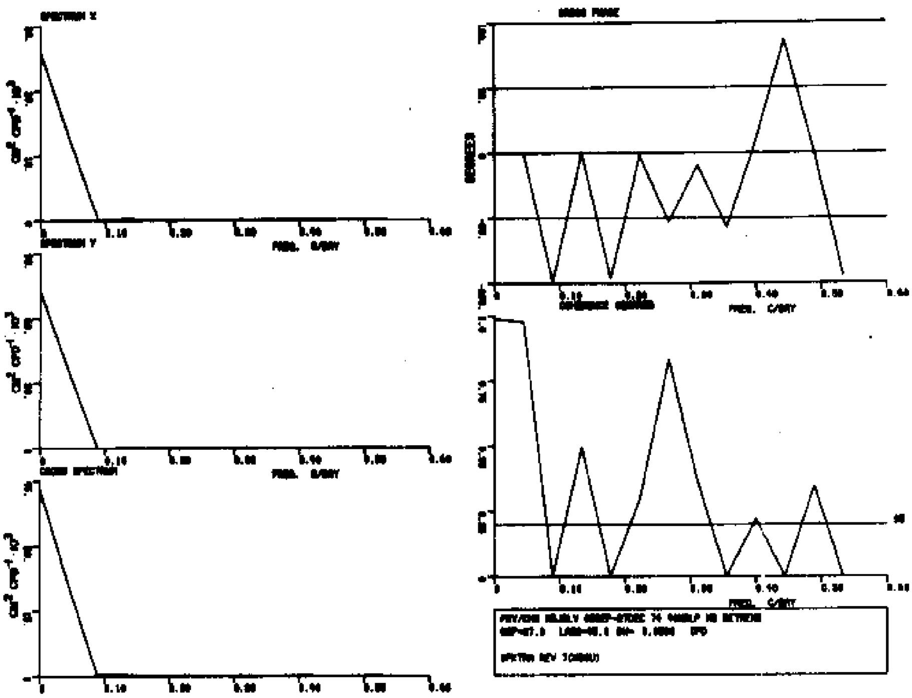

Figure 201 Spectra of adjusted sea level at Frying Pan Shoals, N. C. vs. adjusted sea level at Charleston, S. C., 5 Sept.-27 Dec. 1974 (no detrend)

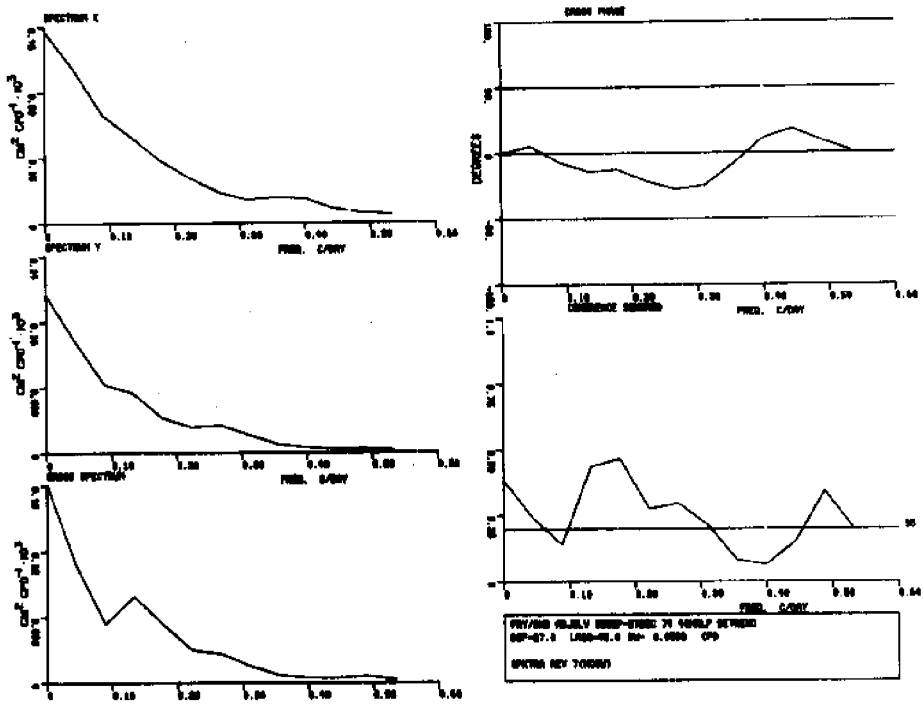

Figure 202 Spectra of adjusted sea level at Frying Pan Shoals, N. C. vs. adjusted sea level at Charleston, S. C., 5 Sept.-27 Dec. 1974 (detrended)

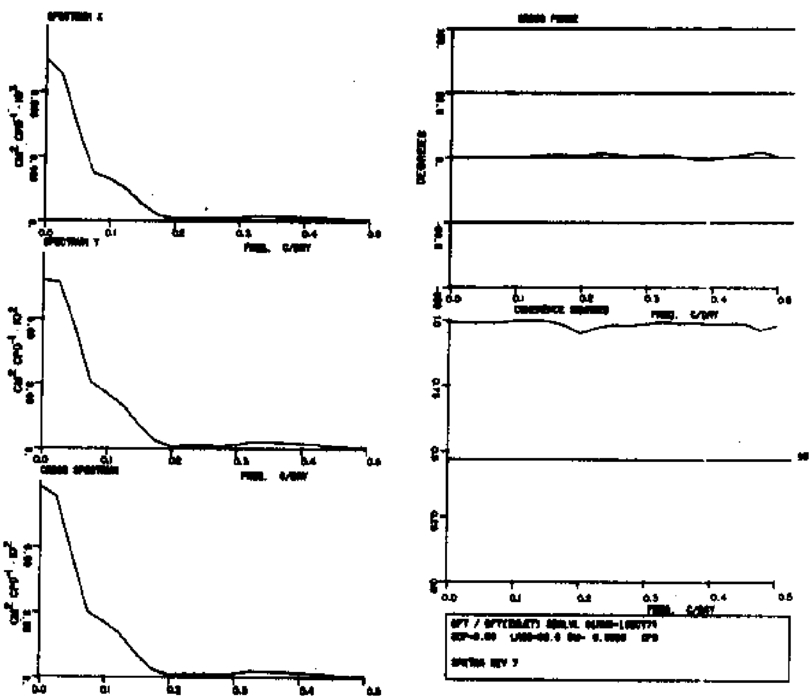

Figure 203 Spectra of sea level at Beaufort, N. C. vs. sea level at Beaufort Inlet, N. C., 1 Aug.-10 Oct., 1974

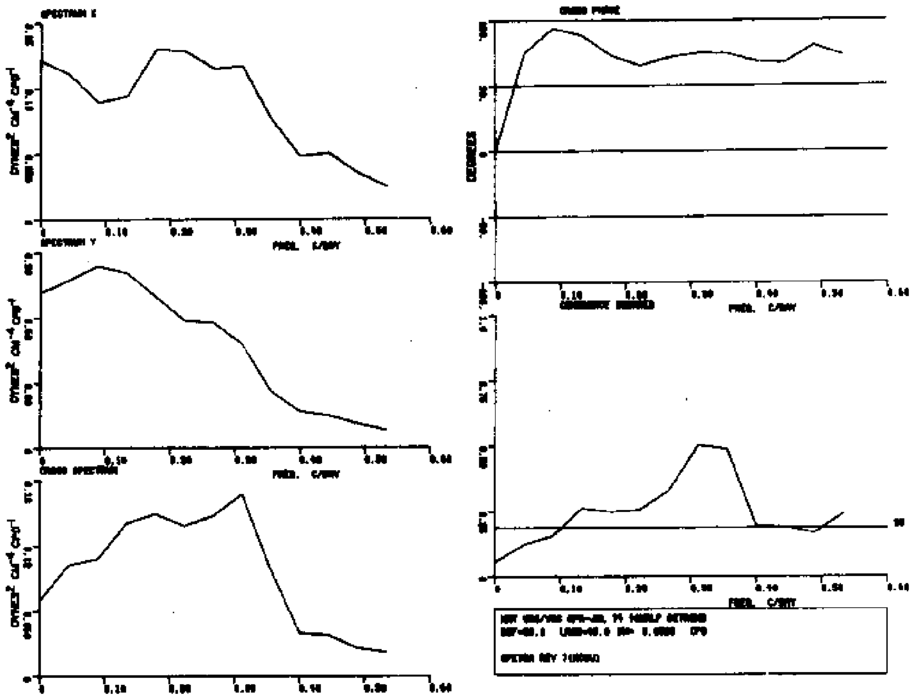

Figure 204 Spectra of wind stress components (u vs. v) at Cape Hatteras, N. C., April–July 1974

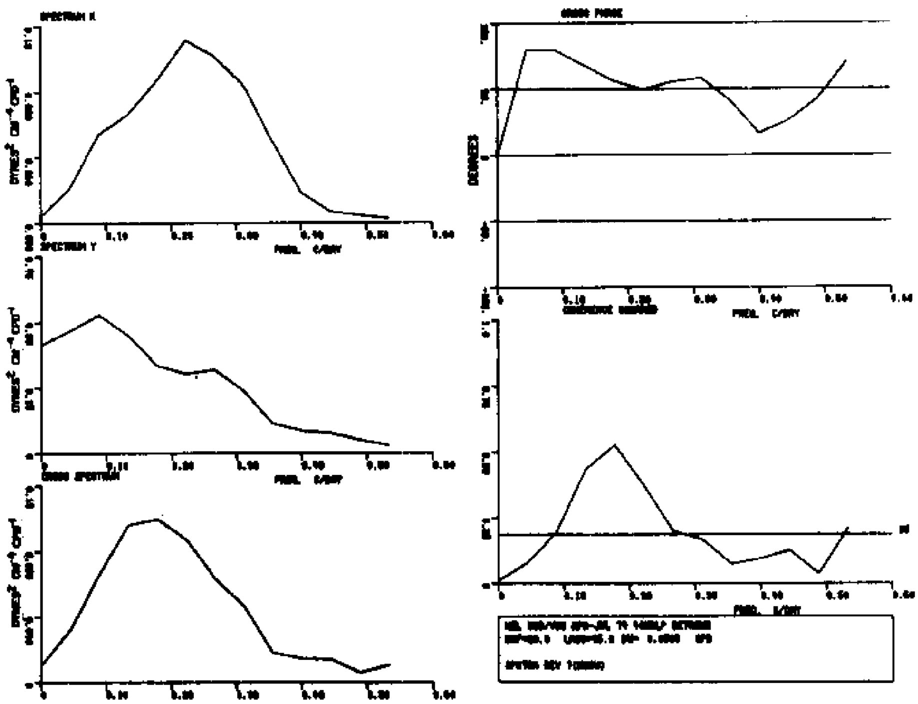

Figure 205 Spectra of wind stress components (u vs. v) at Wilmington, N. C., April–July 1974

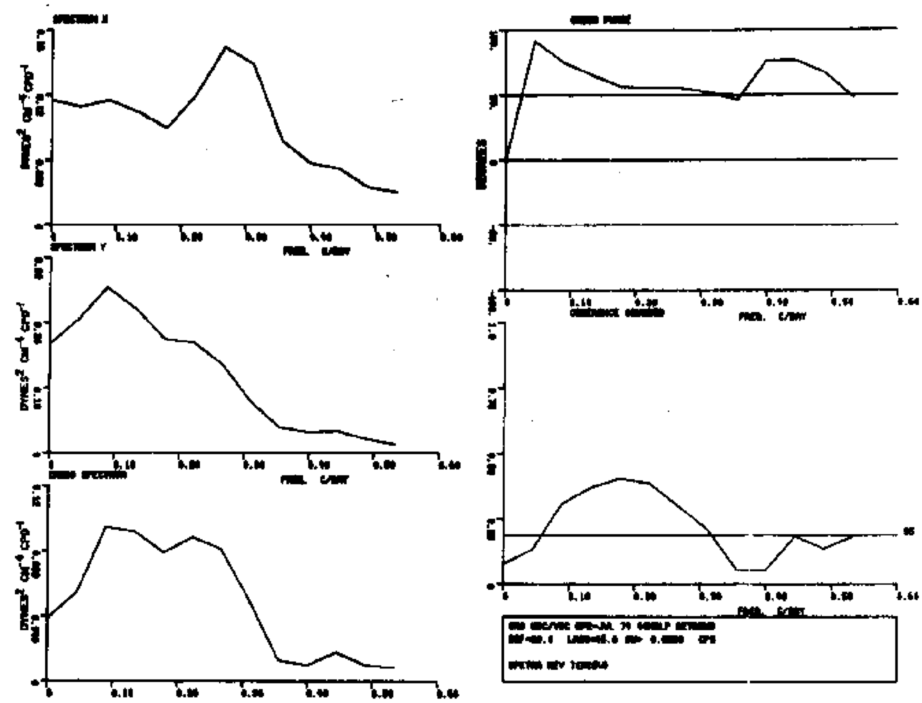

Figure 206 Spectra of wind stress components (u vs. v) at Charleston, S. C., April–July 1974

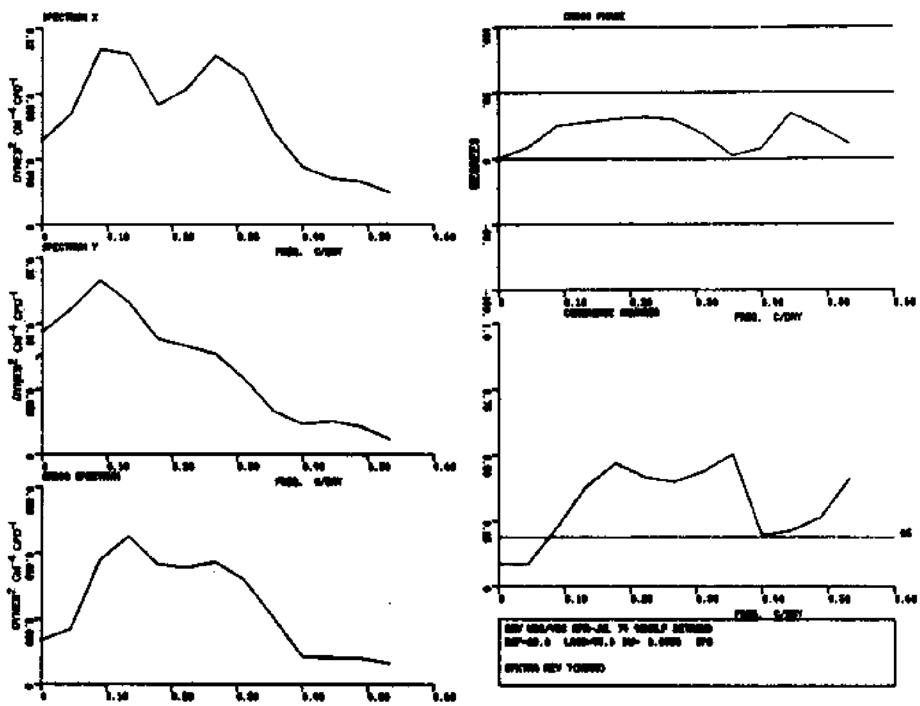

Figure 207 Spectra of wind stress components (u vs. v) at Savannah, Ga., April–July 1974

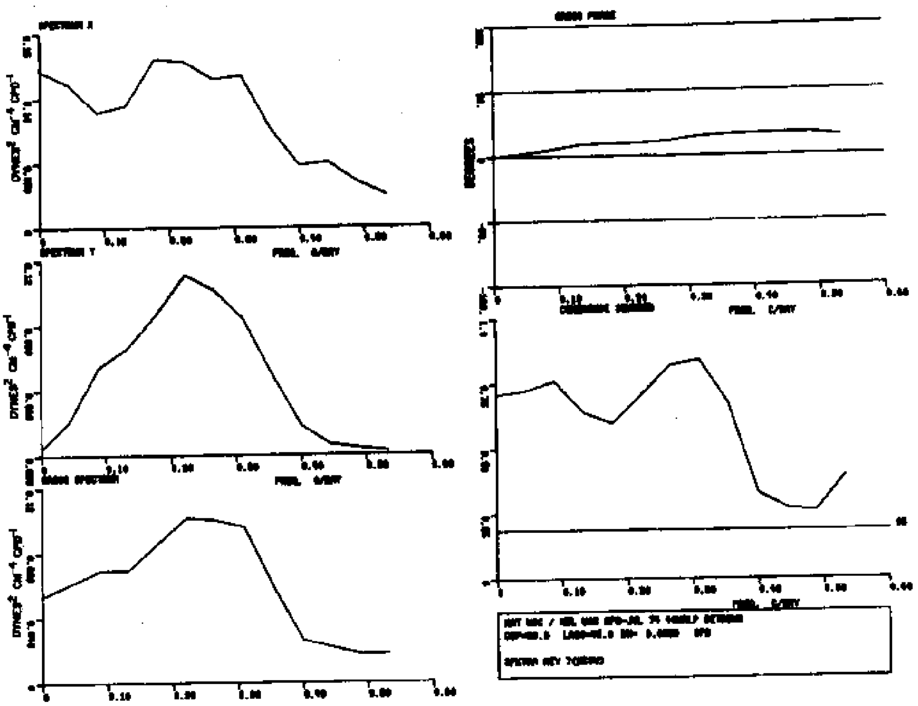

Figure 208 Spectra of wind stress u component at Cape Hatteras, N. C. vs. the wind stress u component at Wilmington, N. C., April-July 1974

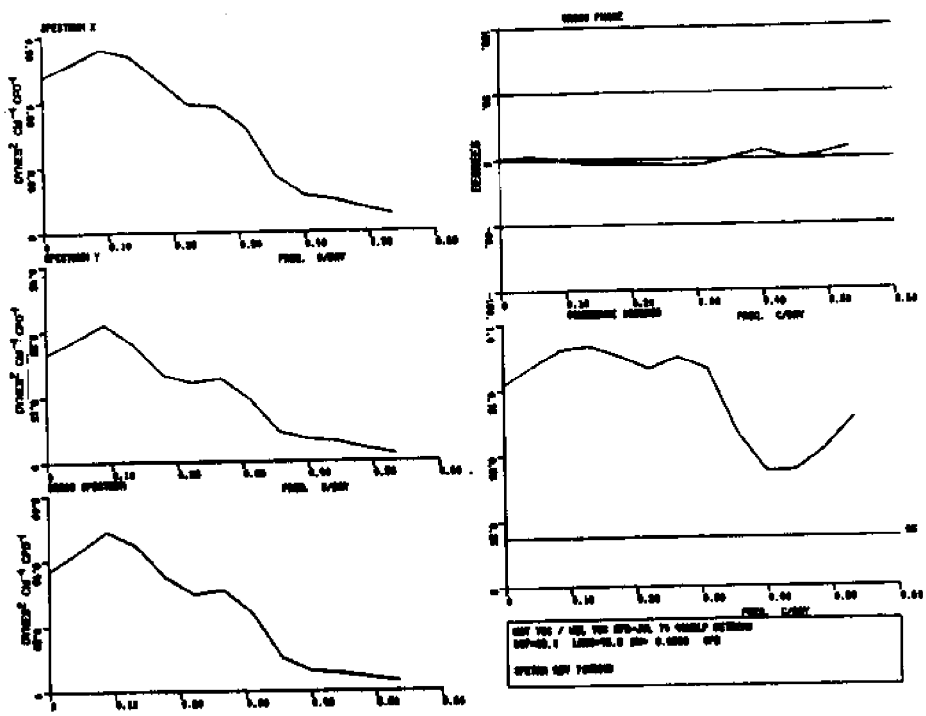

Figure 209 Spectra of wind stress v component at Cape Hatteras, N. C. vs. the wind stress v component at Wilmington, N. C., April-July 1974

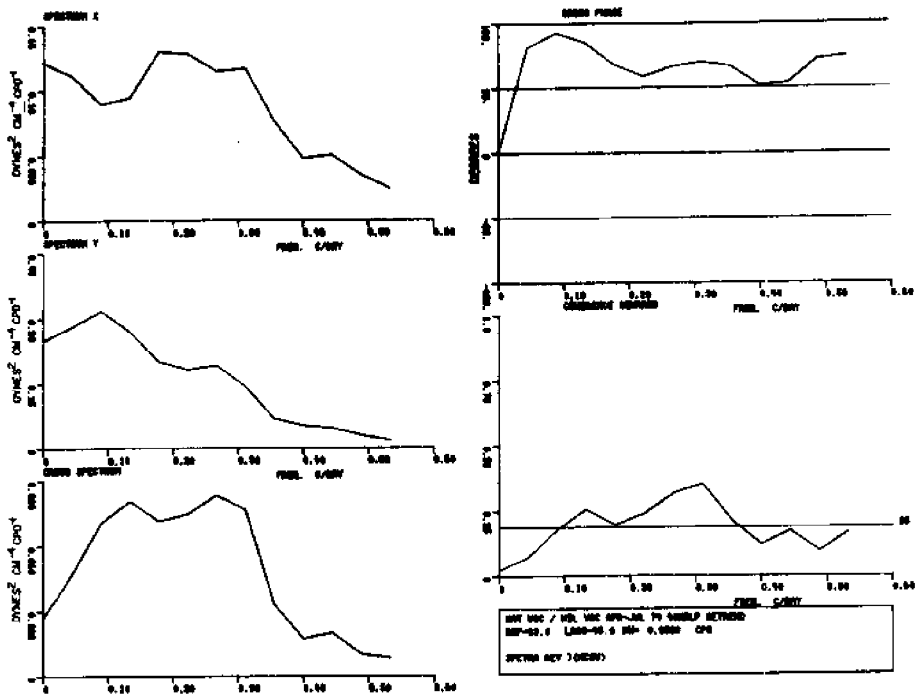

Figure 210 Spectra of wind stress u component at Cape Hatteras, N. C. vs. the wind stress v component at Wilmington, N. C., April–July 1974

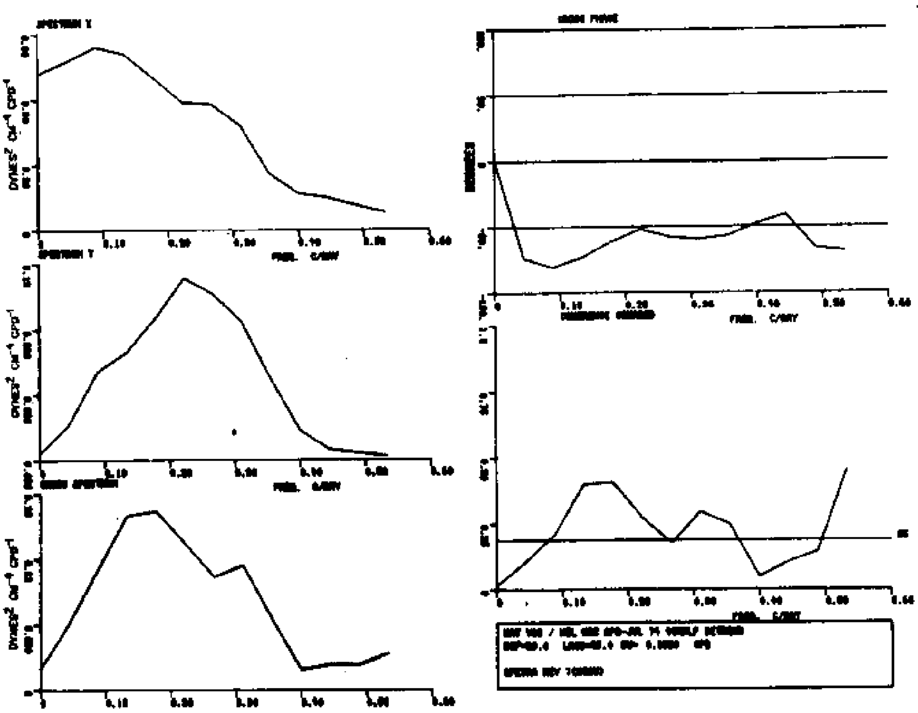

Figure 211 Spectra of wind stress v component at Cape Hatteras, N. C. vs. the wind stress u component at Wilmington, N. C., April–July 1974

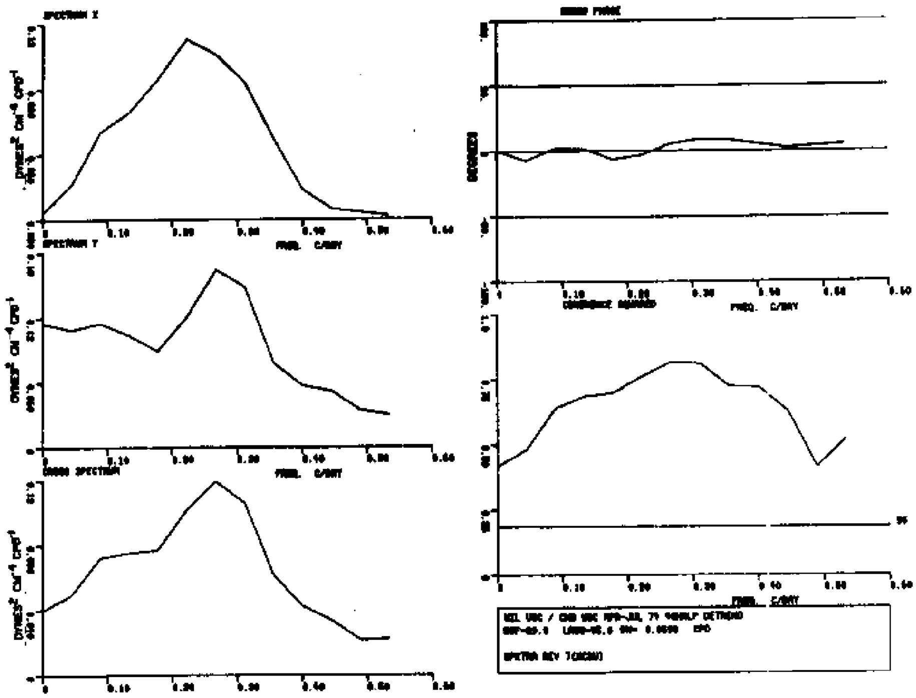

Figure 212 Spectra of wind stress u component at Wilmington, N. C. vs. the wind stress u component at Charleston, S. C., April-July 1974

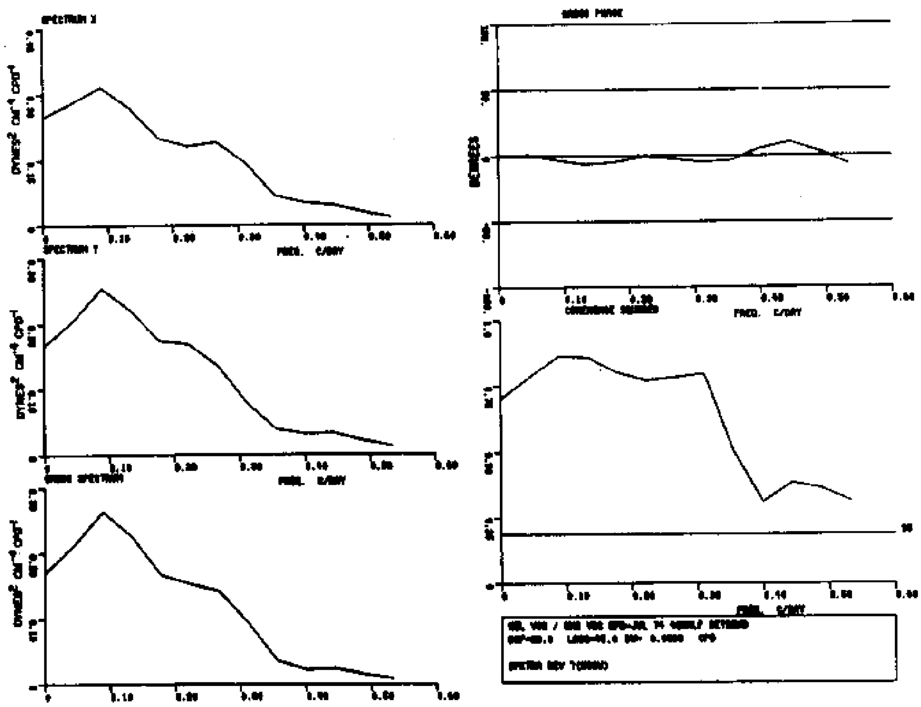

Figure 213 Spectra of wind stress v component at Wilmington, N. C. vs. the wind stress v component at Charleston, S. C., April-July 1974

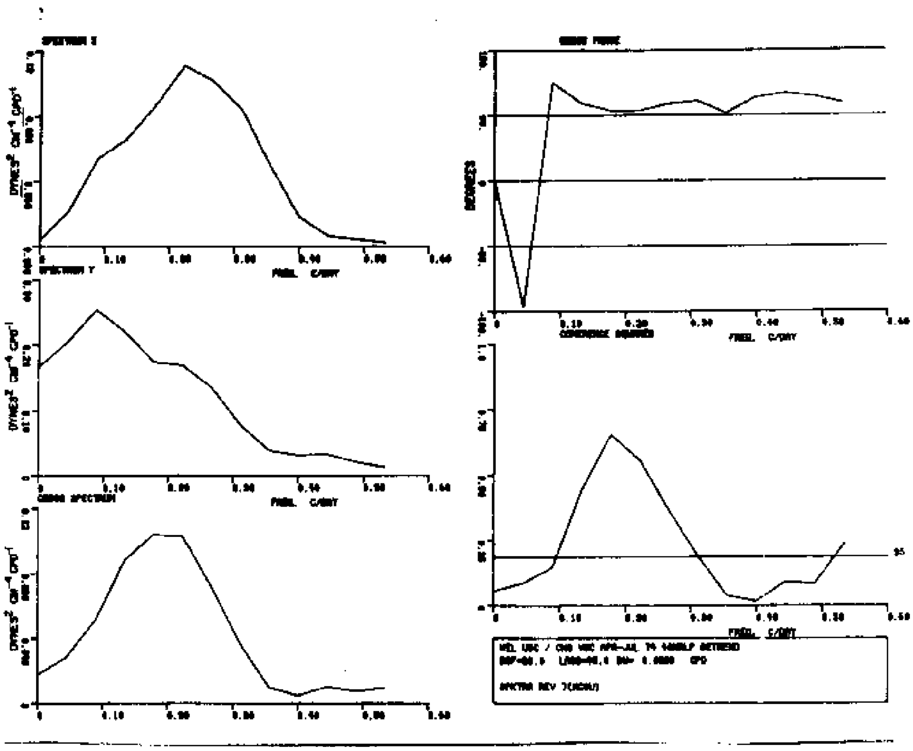

Figure 214 Spectra of wind stress u component at Wilmington, N. C. vs. the wind stress v component at Charleston, S. C., April-July 1974

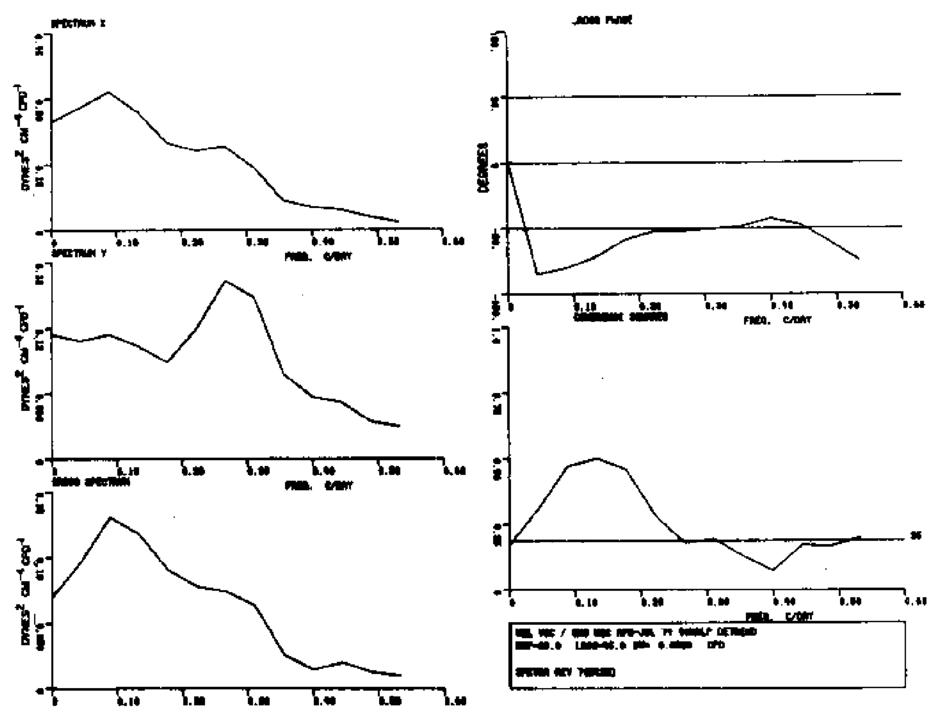

Figure 215 Spectra of wind stress v component at Wilmington, N. C. vs. the wind stress u component at Charleston, S. C., April-July 1974

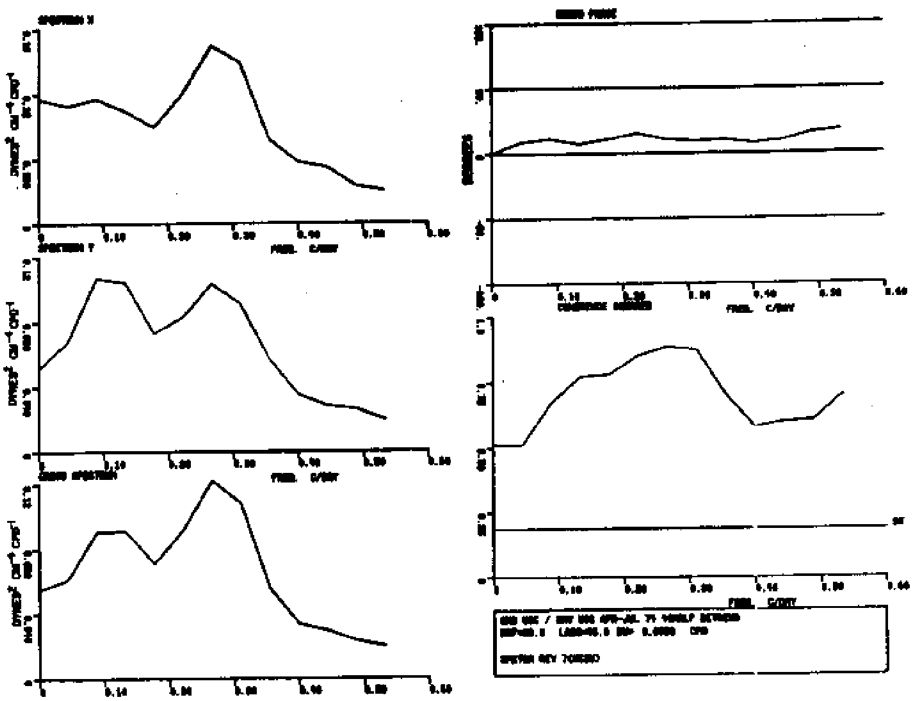

Figure 216 Spectra of wind stress u component at Charleston, S. C. vs. the wind stress u component at Savannah, Ga., April-July 1974

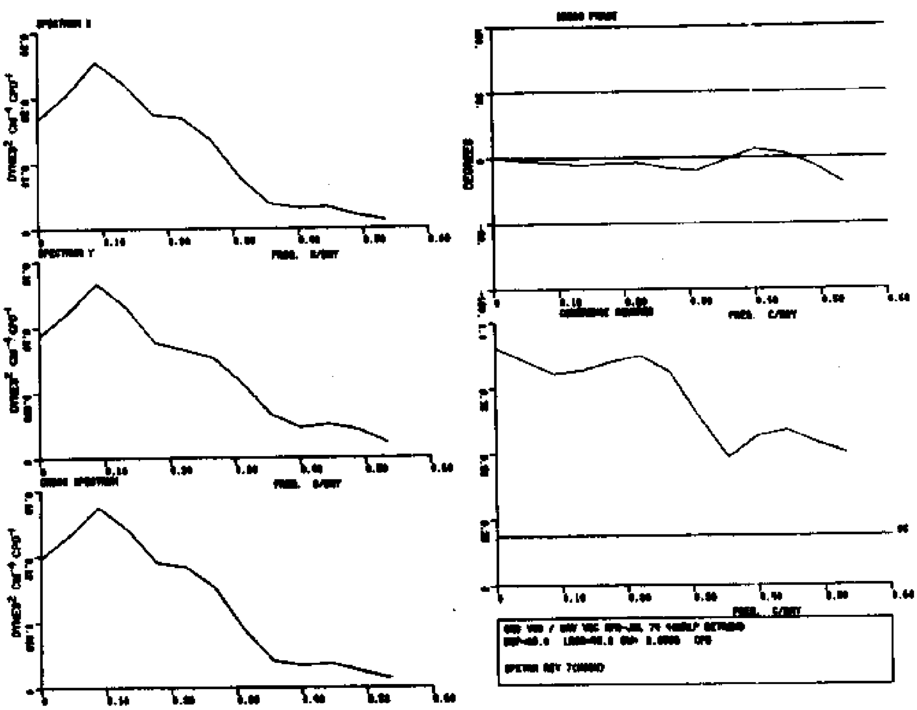

Figure 217 Spectra of wind stress v component at Charleston, S.C. vs. the wind stress v component at Savannah, Ga., April-July 1974

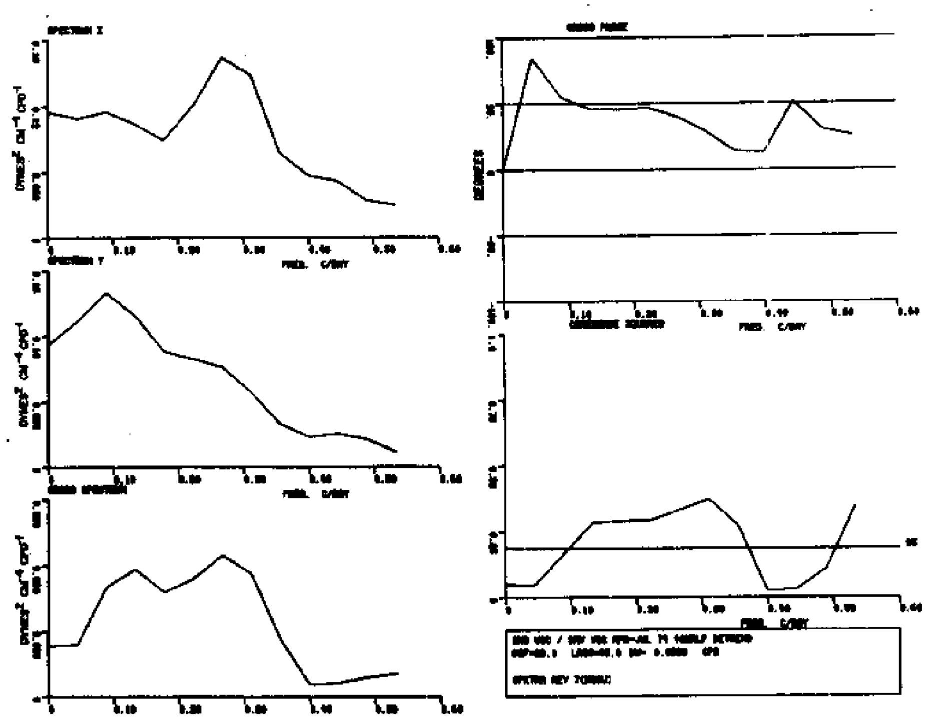

Figure 218 Spectra of wind stress u component at Charleston, S. C. vs. the wind stress v component at Savannah, Ga., April-July 1974

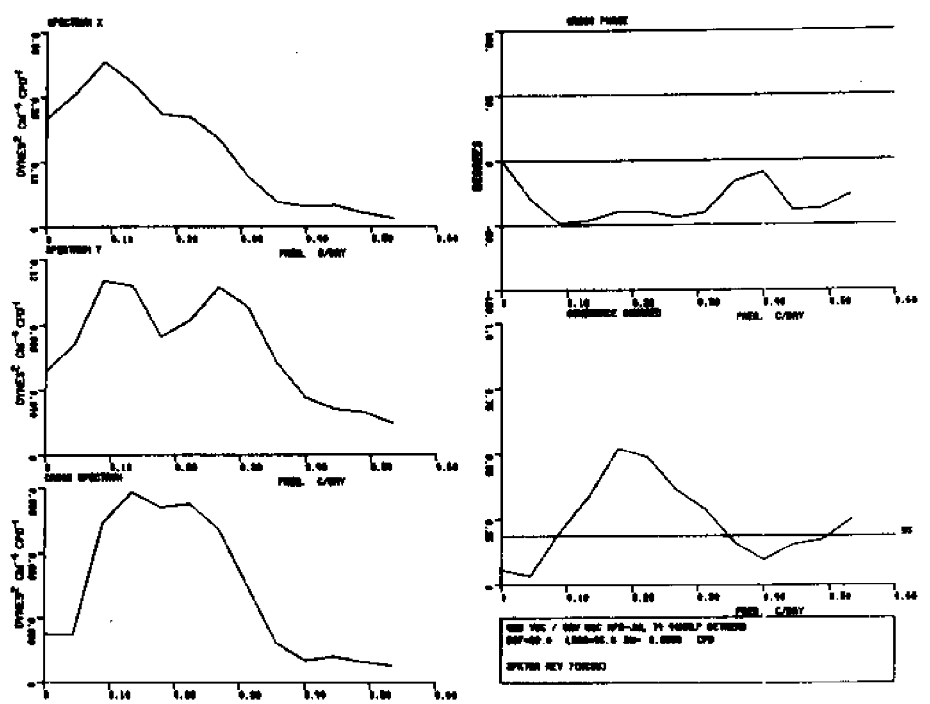

Figure 219 Spectra of wind stress v component at Charleston, S. C. vs. the wind stress u component at Savannah, Ga., April-July 1974

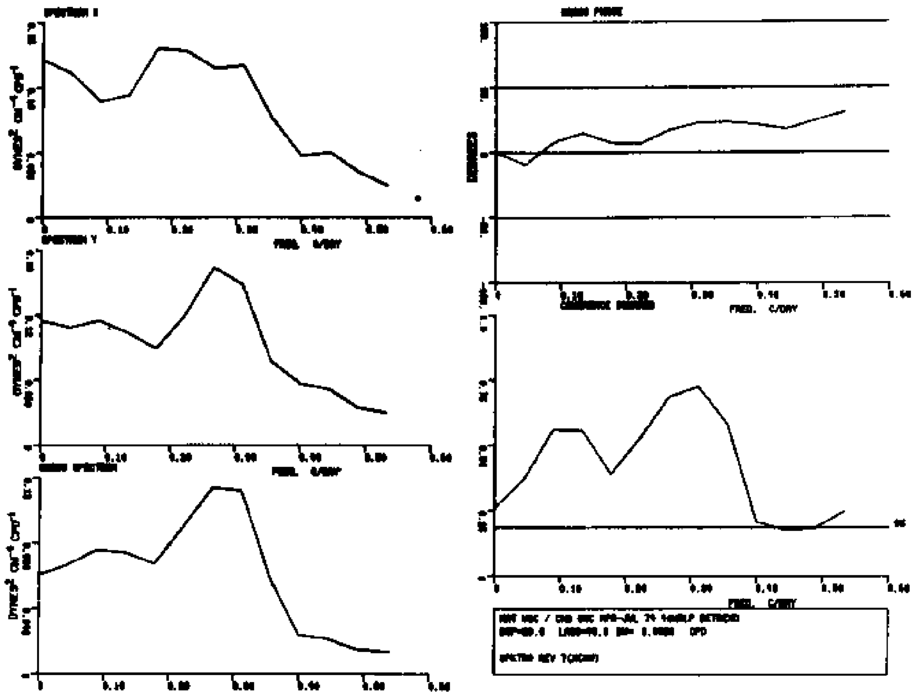

Figure 220 Spectra of wind stress u component at Cape Hatteras, N. C. vs. the wind stress u component at Charleston, S. C., April-July 1974

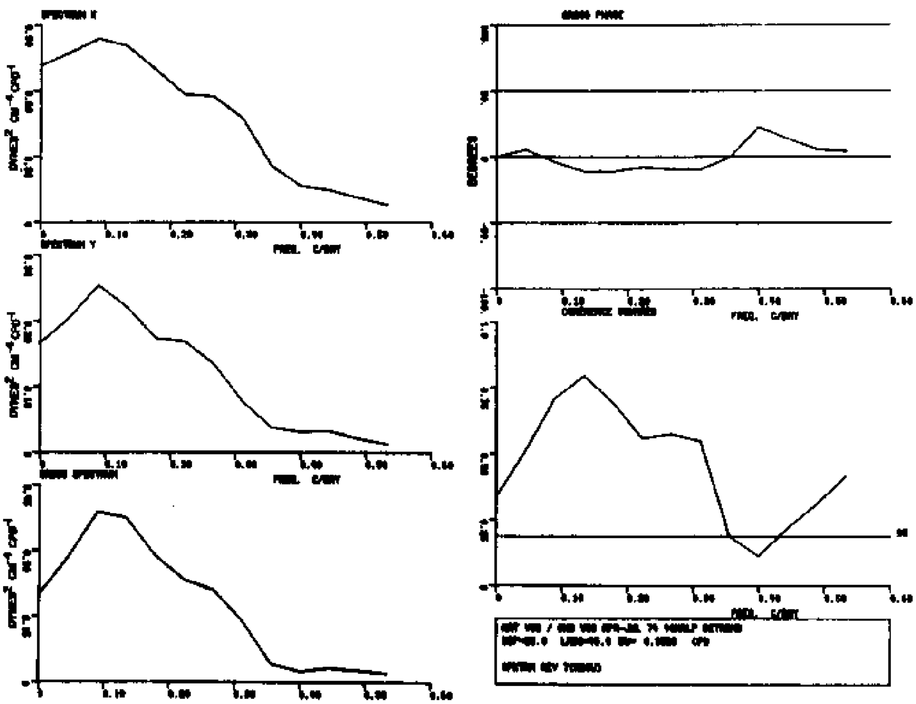

Figure 221 Spectra of wind stress v component at Cape Hatteras, N. C. vs. the wind stress v component at Charleston, S. C., April-July 1974

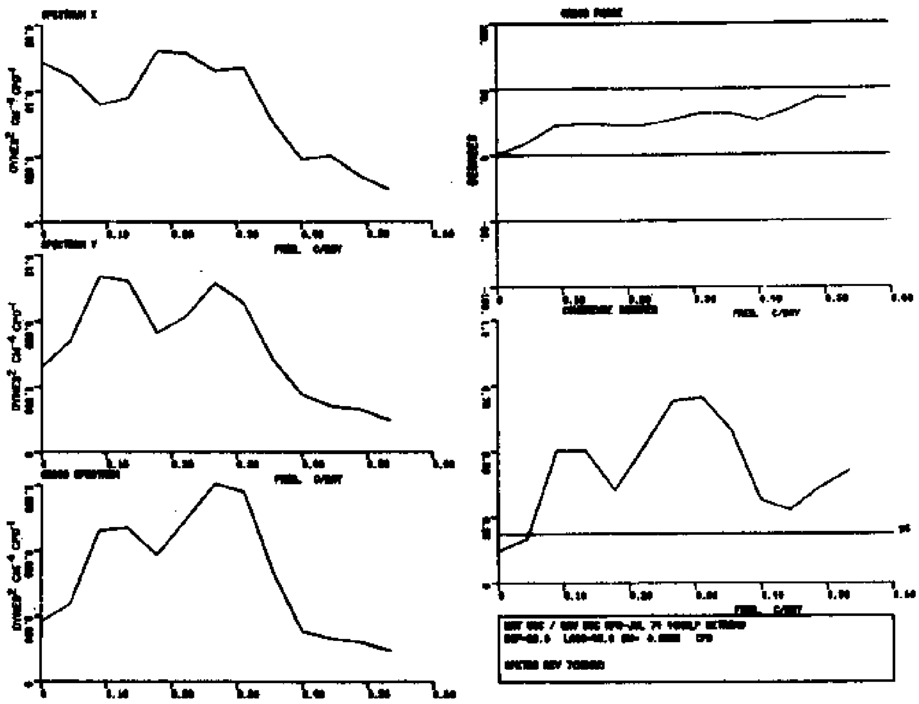

Figure 222 Spectra of wind stress u component at Cape Hatteras, N. C. vs. the wind stress u component at Savannah, Ga., April-July 1974

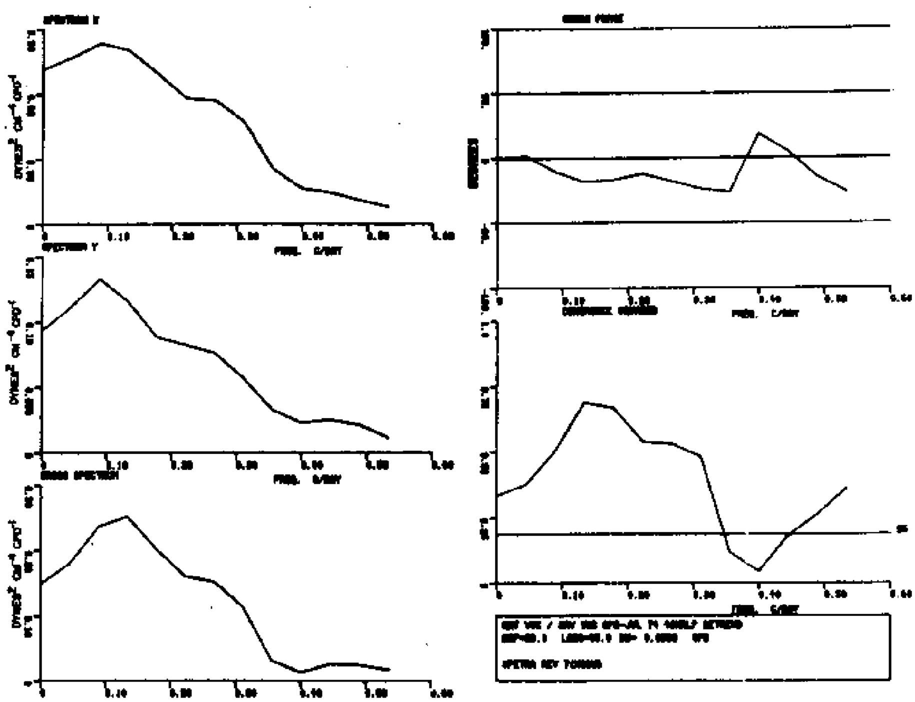

Figure 223 Spectra of wind stress v component at Cape Hatteras, N. C. vs. the wind stress v component at Savannah, Ga, April-July 1974

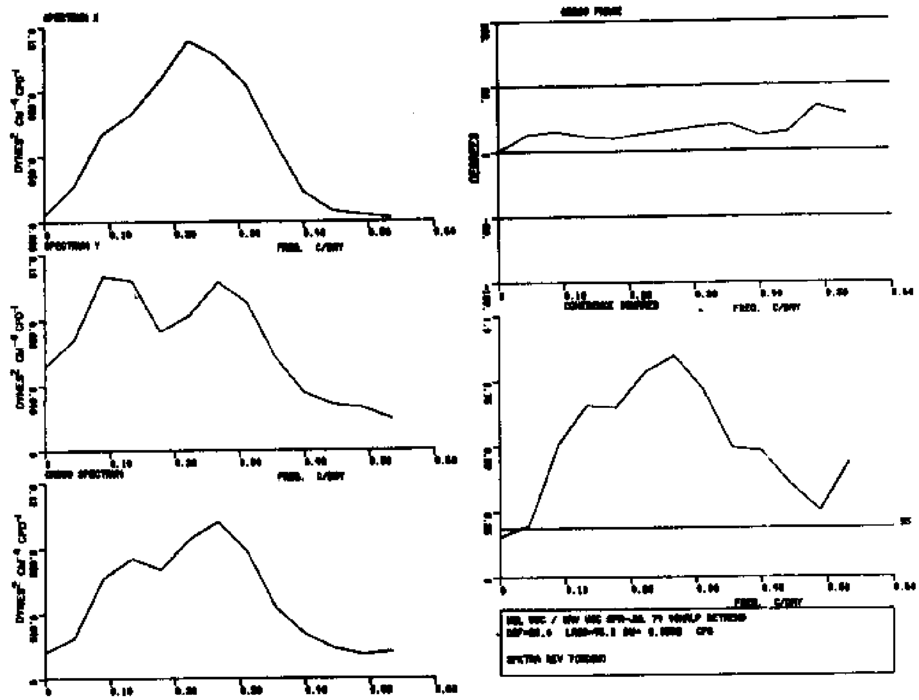

Figure 224 Spectra of wind stress u component at Wilmington, N. C. vs. the wind stress u component at Savannah, Ga., April-July 1974

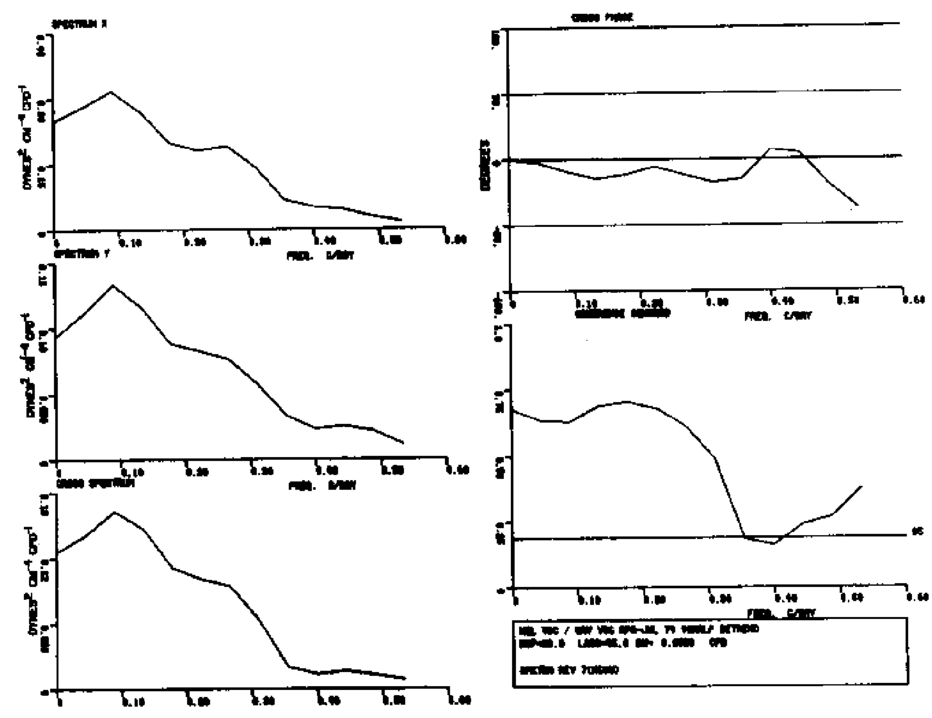

Figure 225 Spectra of wind stress v component at Wilmington, N. C. vs. the wind stress v component at Savannah, Ga., April-July 1974

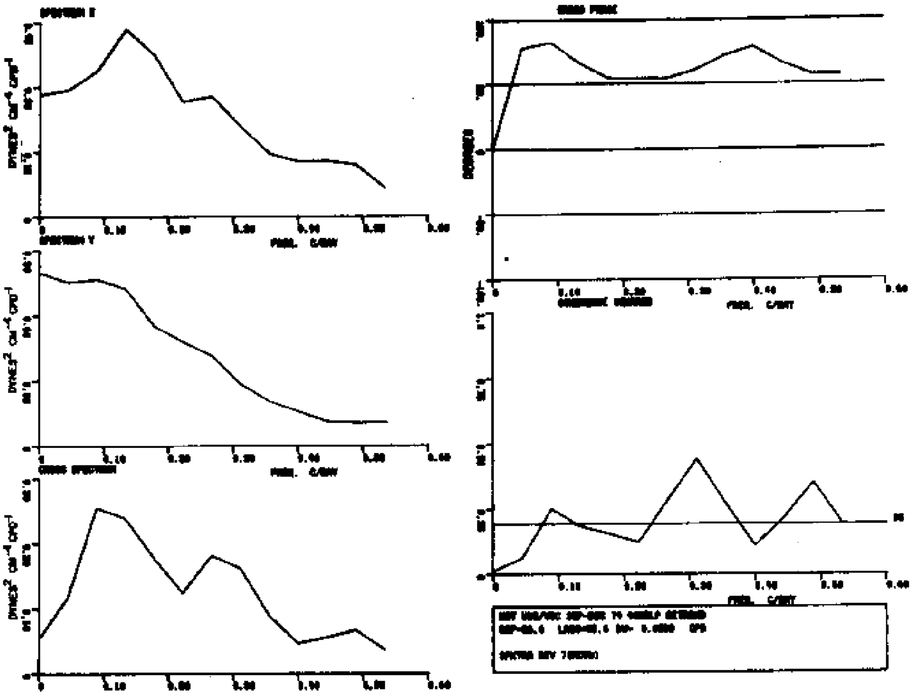

Figure 226 Spectra of wind stress components (u vs. v) at Cape Hatteras, N. C., Sept.-Dec. 1974

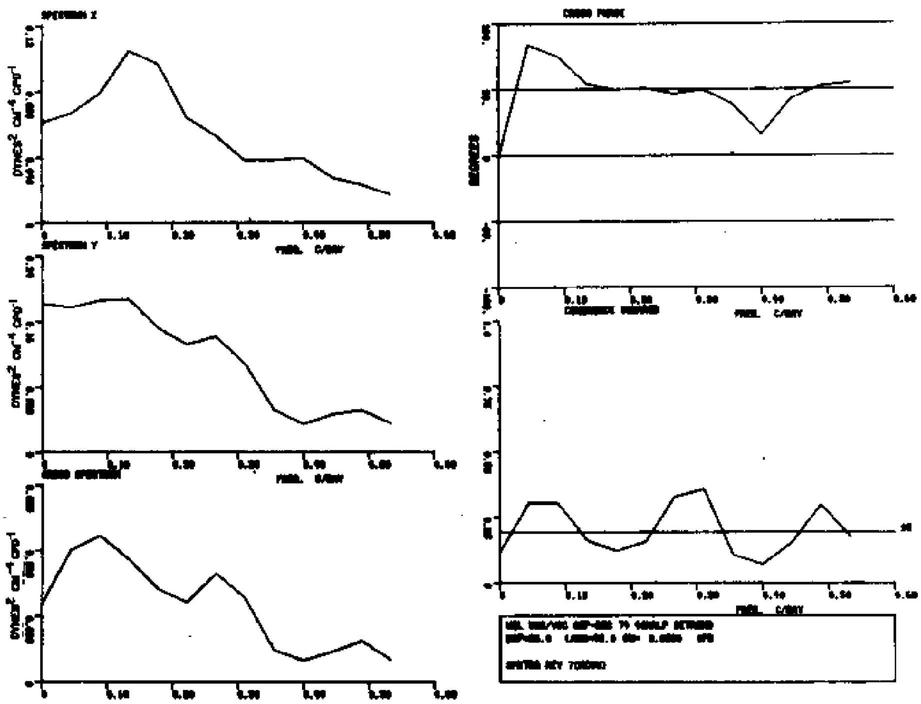

Figure 227 Spectra of wind stress components (u vs. v) at Wilmington, N. C., Sept. - Dec. 1974

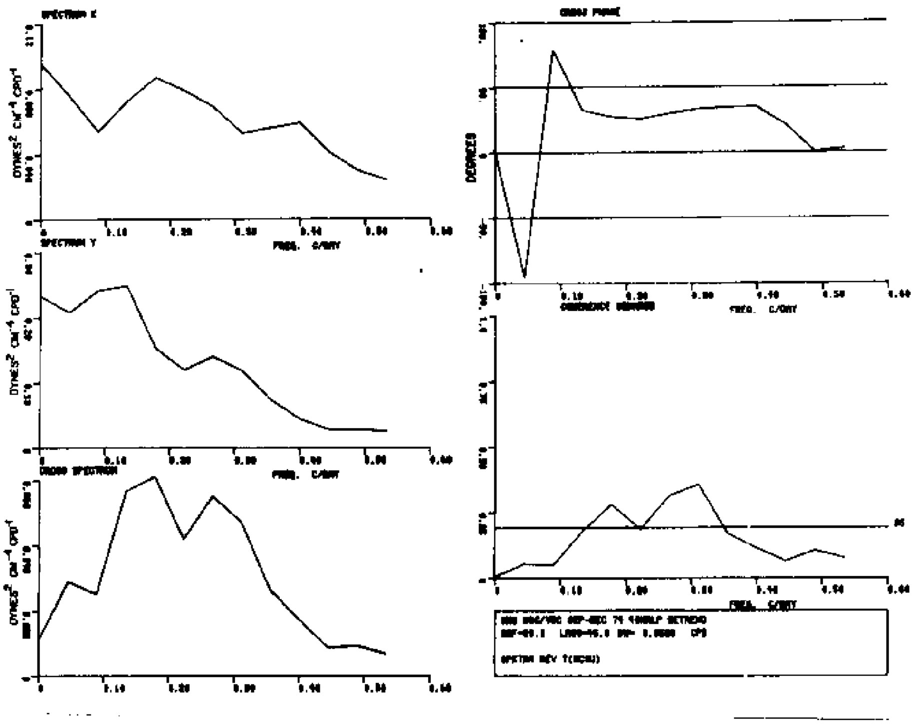

Figure 228 Spectra of wind stress components (u vs. v) at Charleston, S. C., Sept.-Dec. 1974

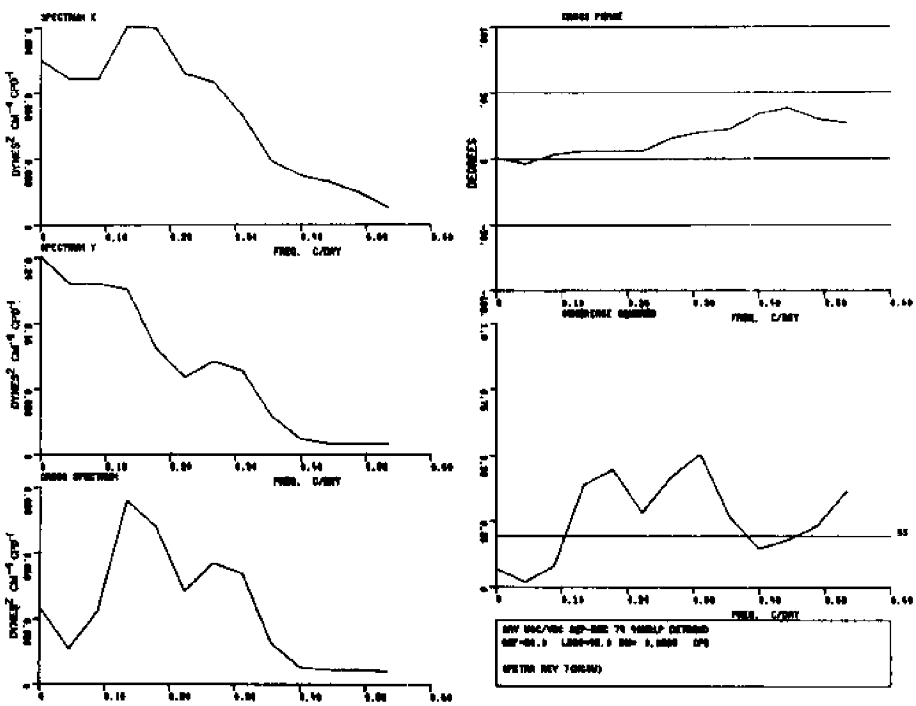

Figure 229 Spectra of wind stress components (u vs. v) at Savannah, Ga., Sept.-Dec. 1974

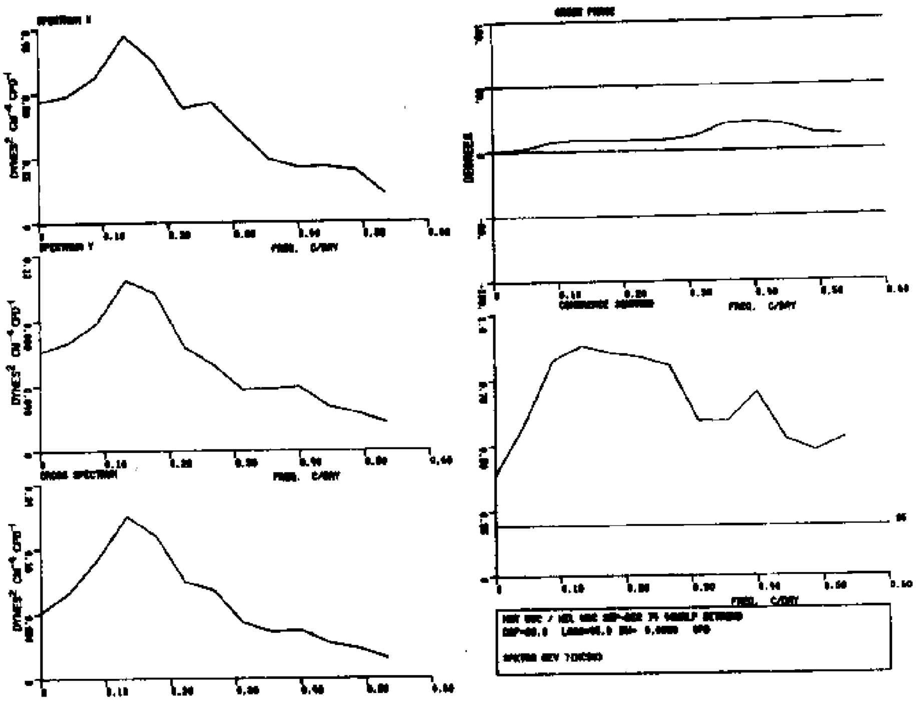

Figure 230 Spectra of wind stress u component at Cape Hatteras, N. C. vs. the wind stress u component at Wilmington, N. C., Sept.-Dec. 1974

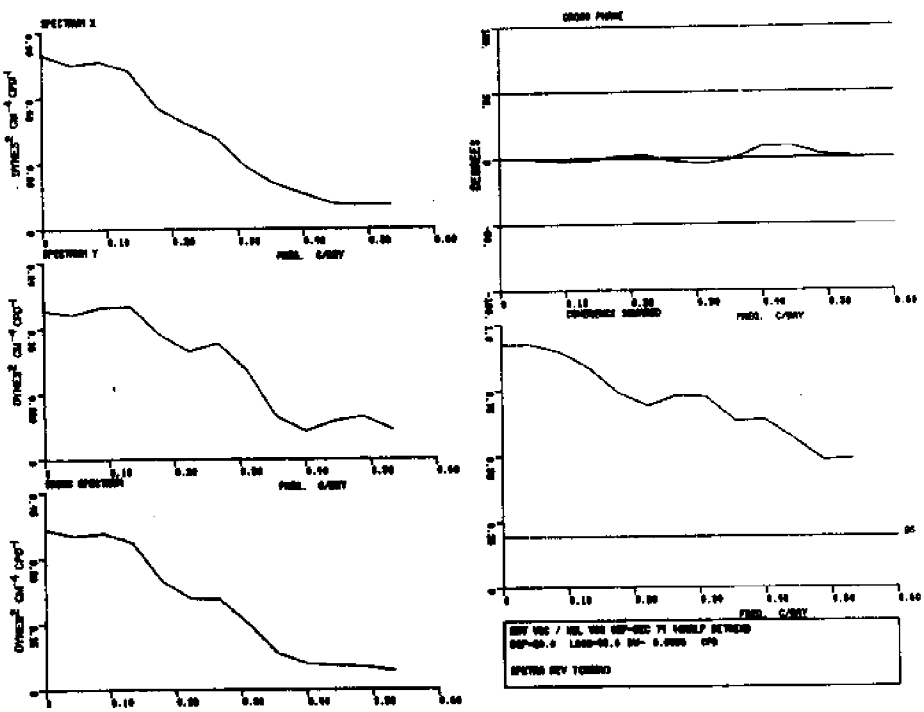

Figure 231 Spectra of wind stress v component at Cape Hatteras, N. C. vs. the wind stress v component at Wilmington, N. C., Sept.-Dec. 1974

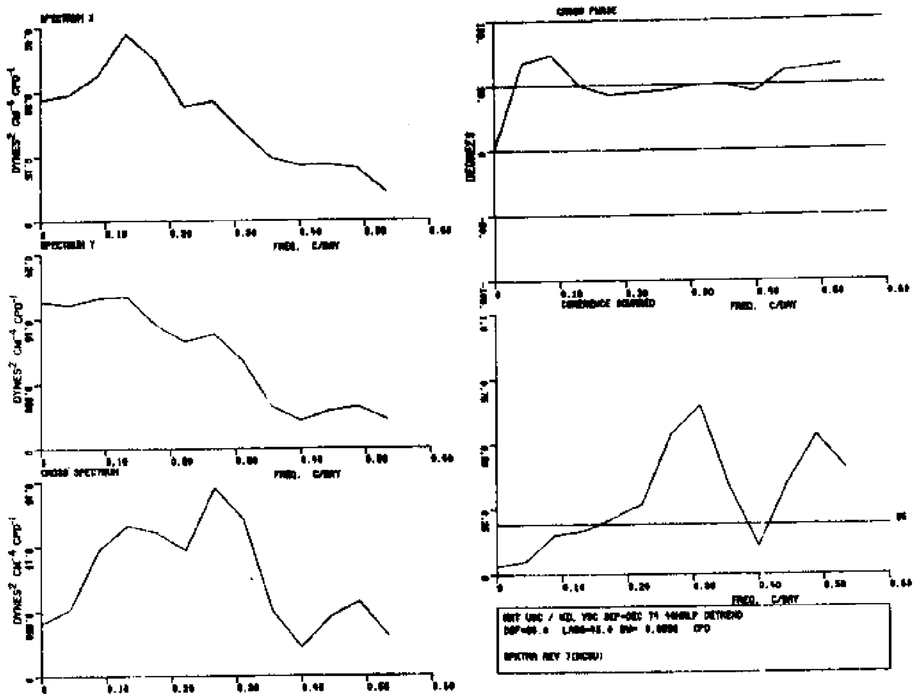

Figure 232 Spectra of wind stress u component at Cape Hatteras, N. C. vs. the wind stress v component at Wilmington, N. C., Sept.-Dec., 1974

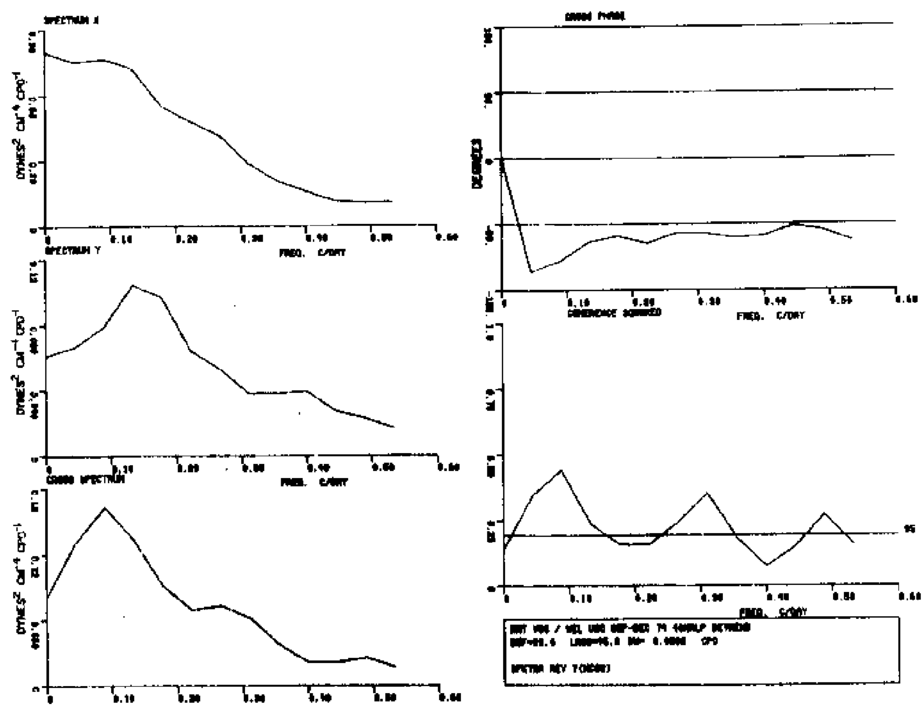

Figure 233 Spectra of wind stress v component at Cape Hatteras, N. C. vs. the wind stress u component at Wilmington, N. C., Sept.-Dec. 1974

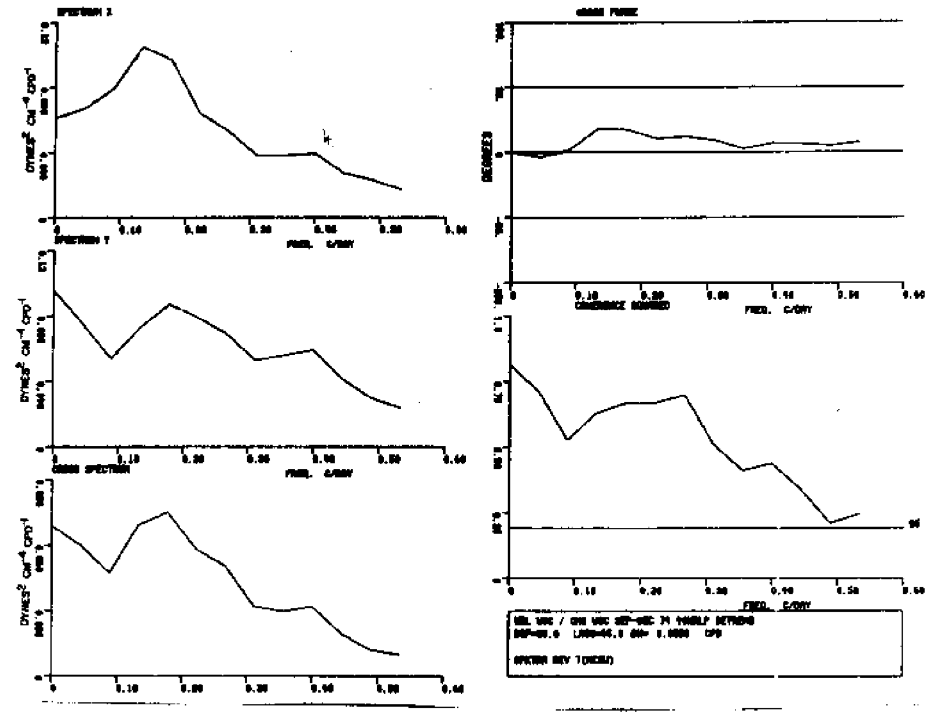

Figure 234 Spectra of wind stress u component at Wilmington N. C. vs. the wind stress u component at Charleston, S. C., Sept.-Dec. 1974

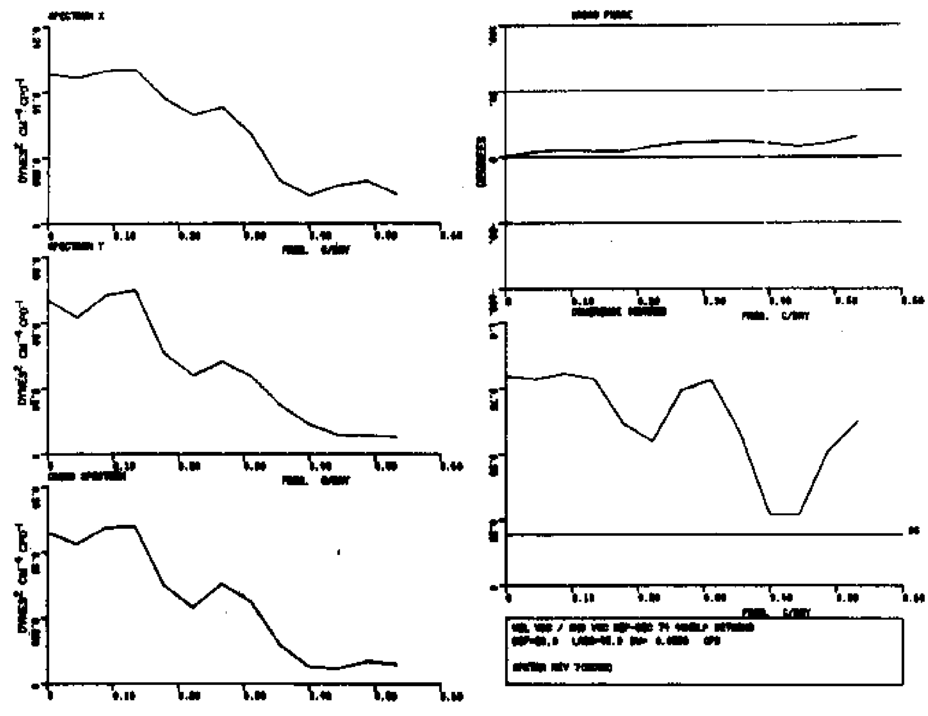

Figure 235 Spectra of wind stress v component at Wilmington, N. C. vs. the wind stress v component at Charleston, S. C., Sept.-Dec. 1974

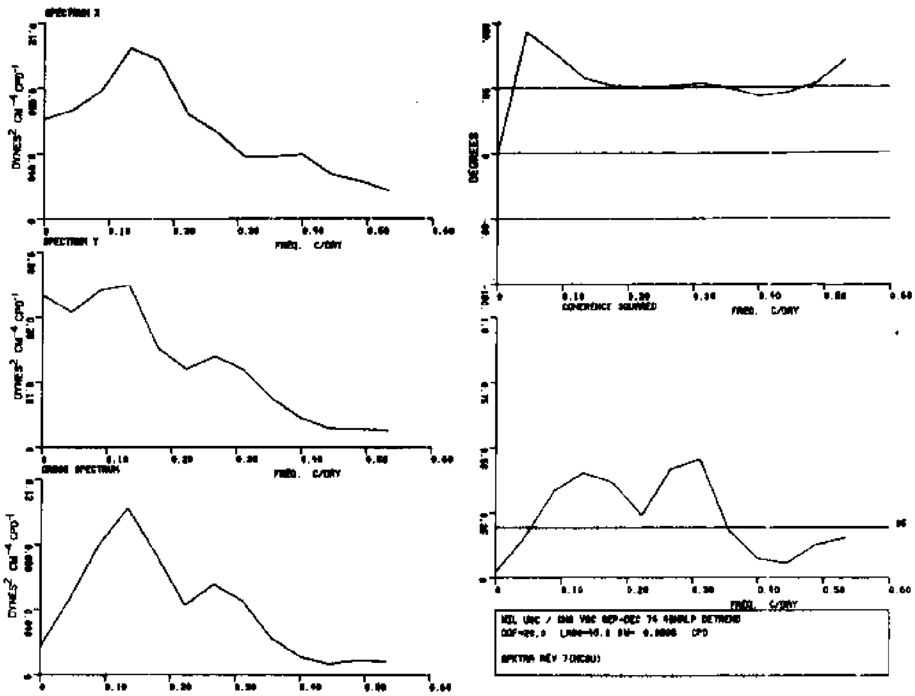

Figure 236 Spectra of wind stress u component at Wilmington, N. C. vs. the wind stress v component at Charleston, S. C., Sept.-Dec. 1974

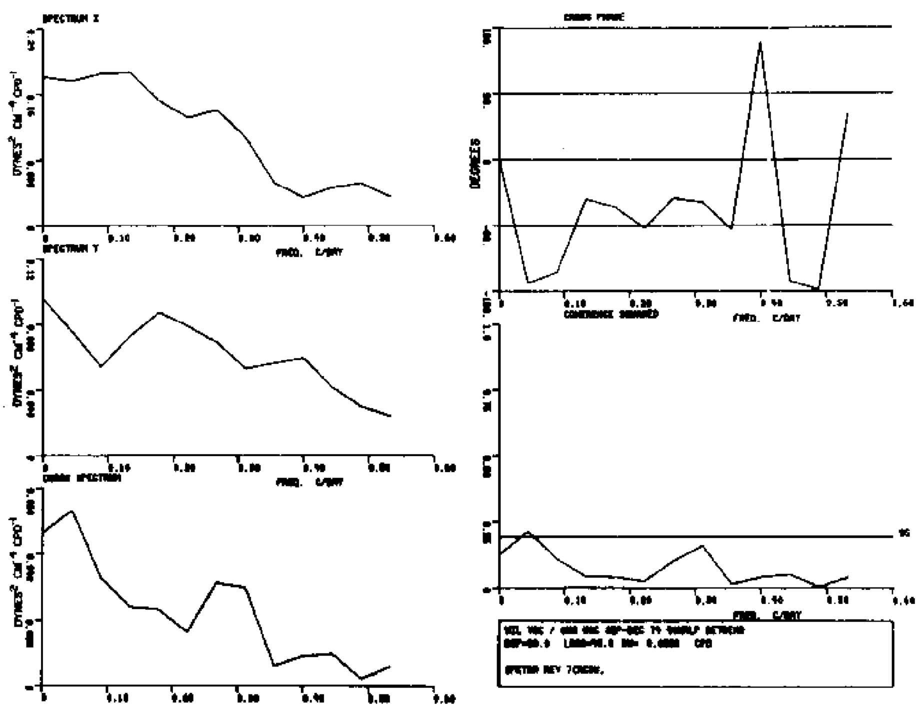

Figure 237 Spectra of wind stress v component at Wilmington, N. C. vs. the wind stress u component at Charleston, S. C., Sept.-Dec. 1974

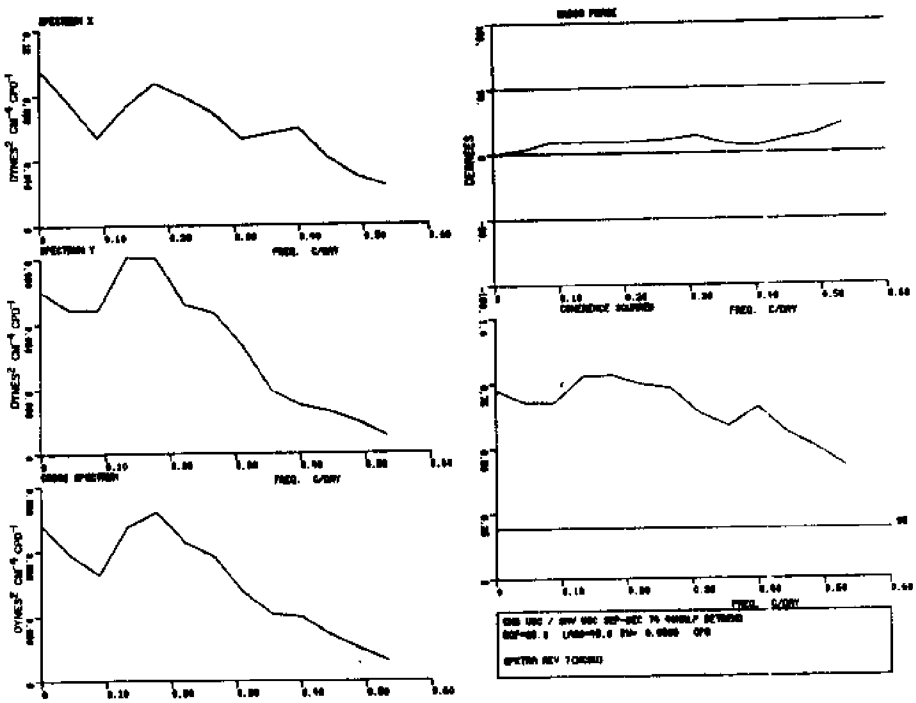

Figure 238 Spectra of wind stress u component at Charleston S. C. vs. the wind stress u component at Savannah, Ga., Sept.-Dec. 1974

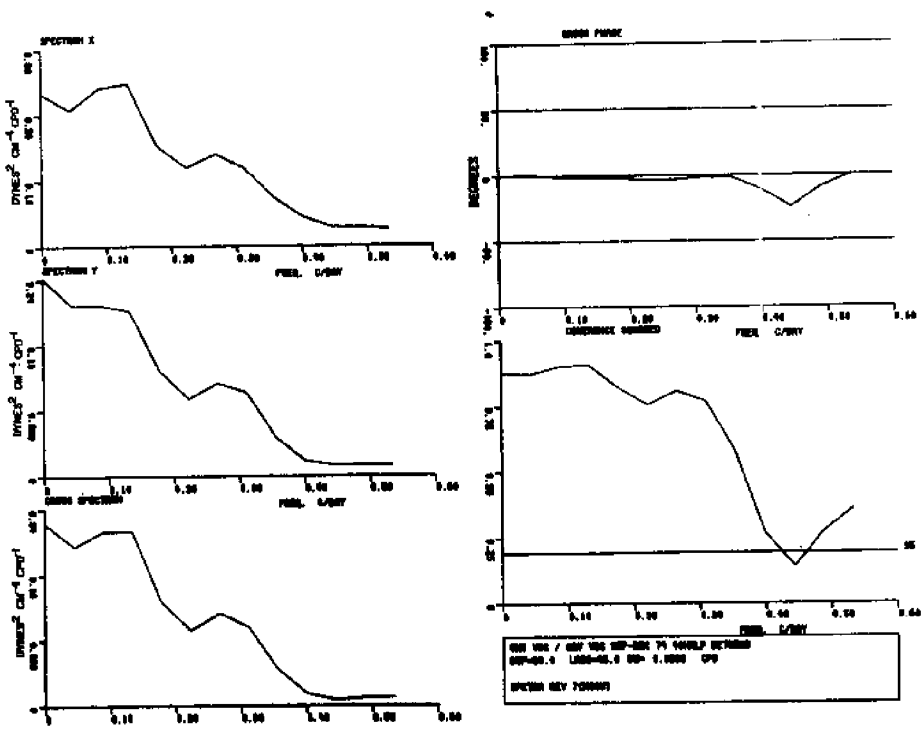

Figure 239 Spectra of wind stress v component at Charleston, S. C. vs. the wind stress v component at Savannah, Ga., Sept.-Dec. 1974

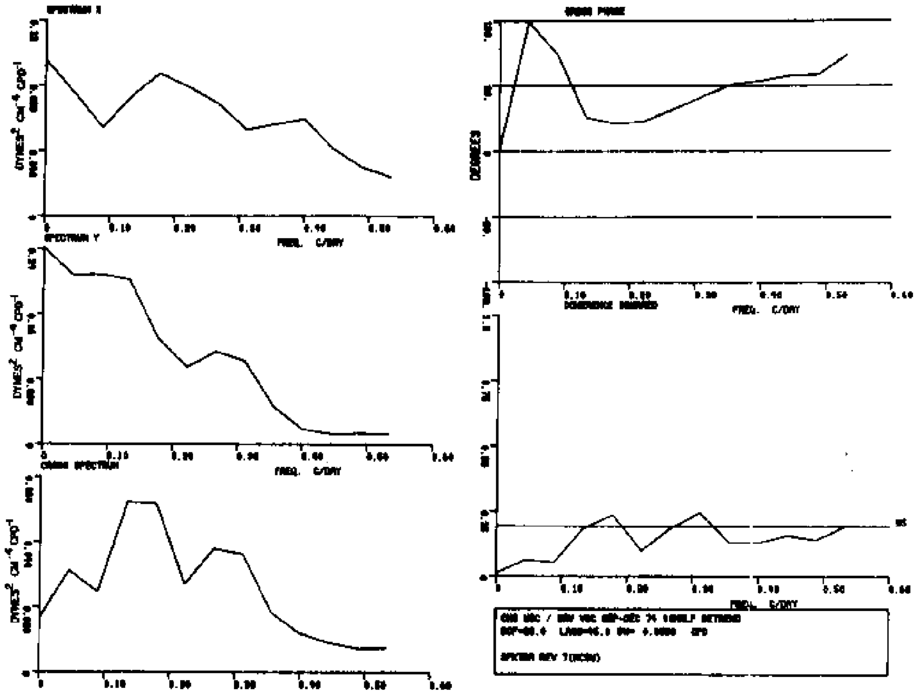

Figure 240 Spectra of wind stress u component at Charleston, S. C. vs. the wind stress v component at Savannah, Ga., Sept.-Dec. 1974

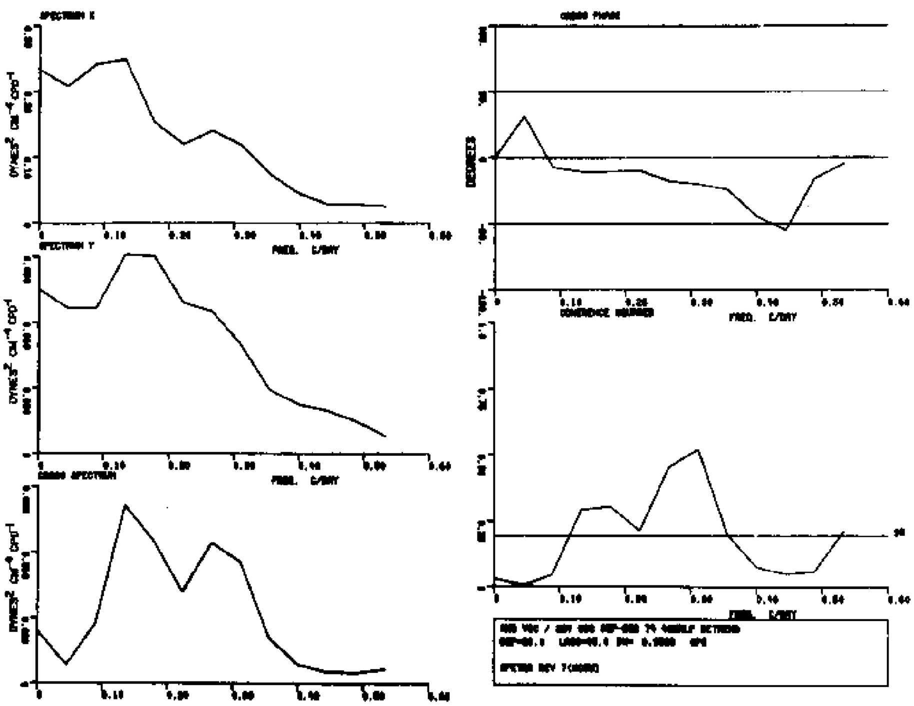

Figure 241 Spectra of wind stress v component at Charleston, S. C. vs. the wind stress u component at Savannah, Ga., Sept.-Dec. 1974

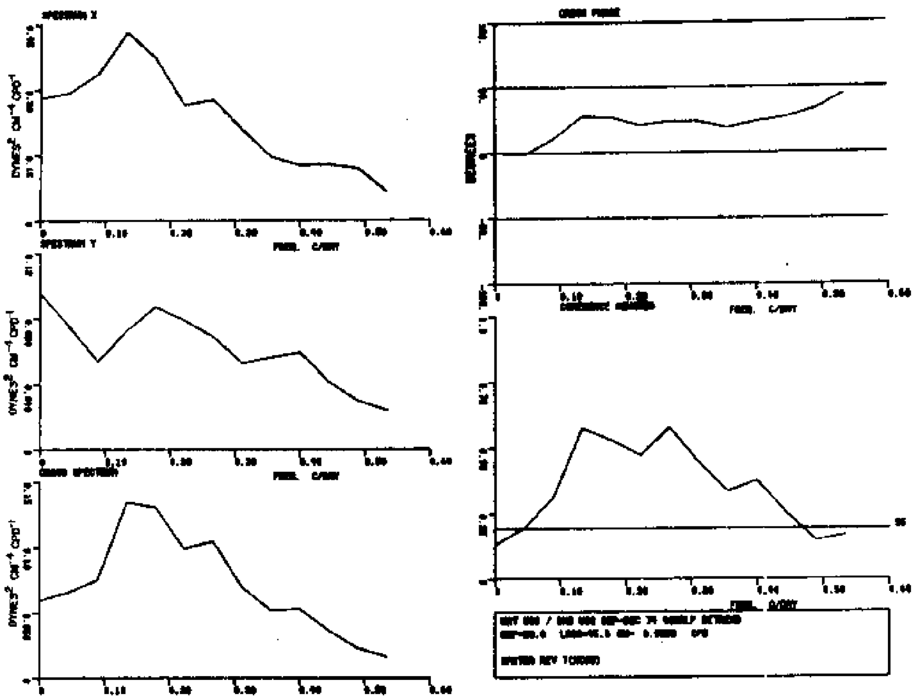

Figure 242 Spectra of wind stress u component at Cape Hatteras, N. C. vs. the wind stress u component at Charleston, S. C., Sept.-Dec. 1974

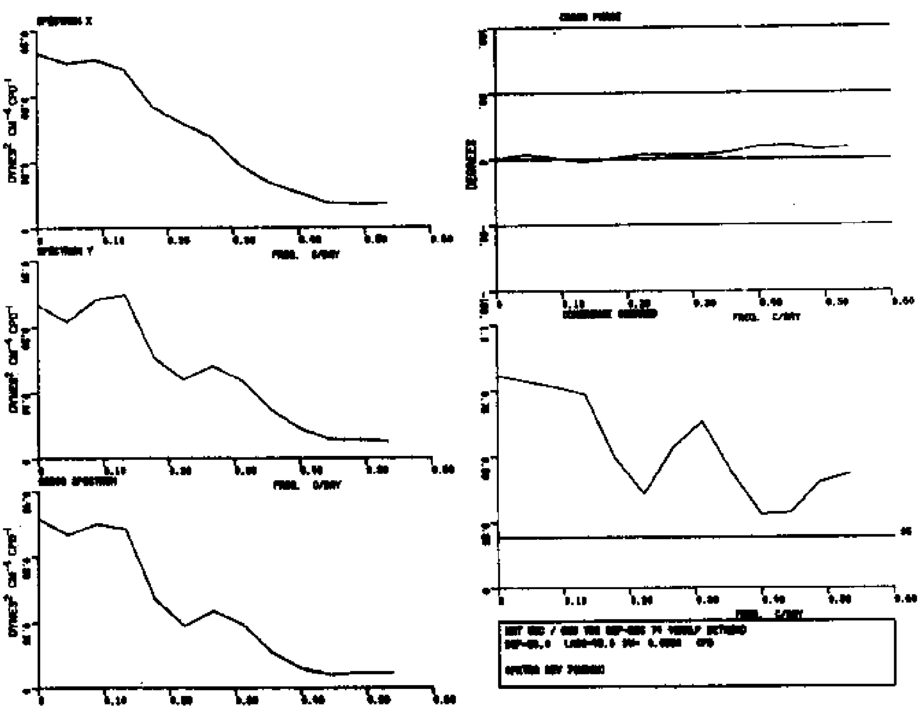

Figure 243 Spectra of wind stress v component at Cape Hatteras, N. C. vs. the wind stress v component at Charleston, S. C., Sept.-Dec. 1974

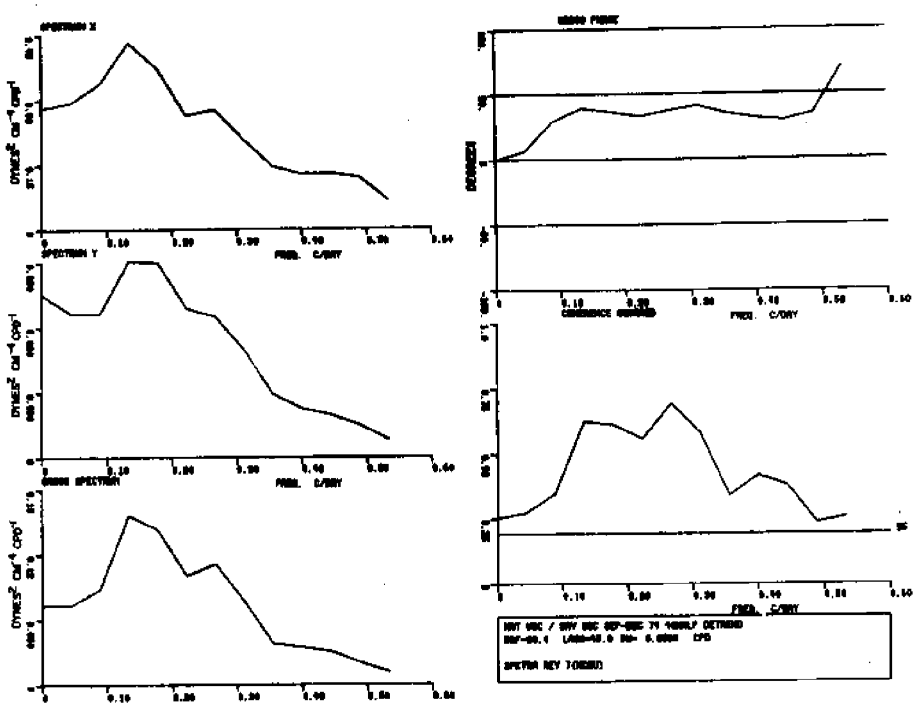

Figure 244 Spectra of wind stress u component at Cape Hatteras, N. C. vs. the wind stress u component at Savannah, Ga., Sept.-Dec. 1974

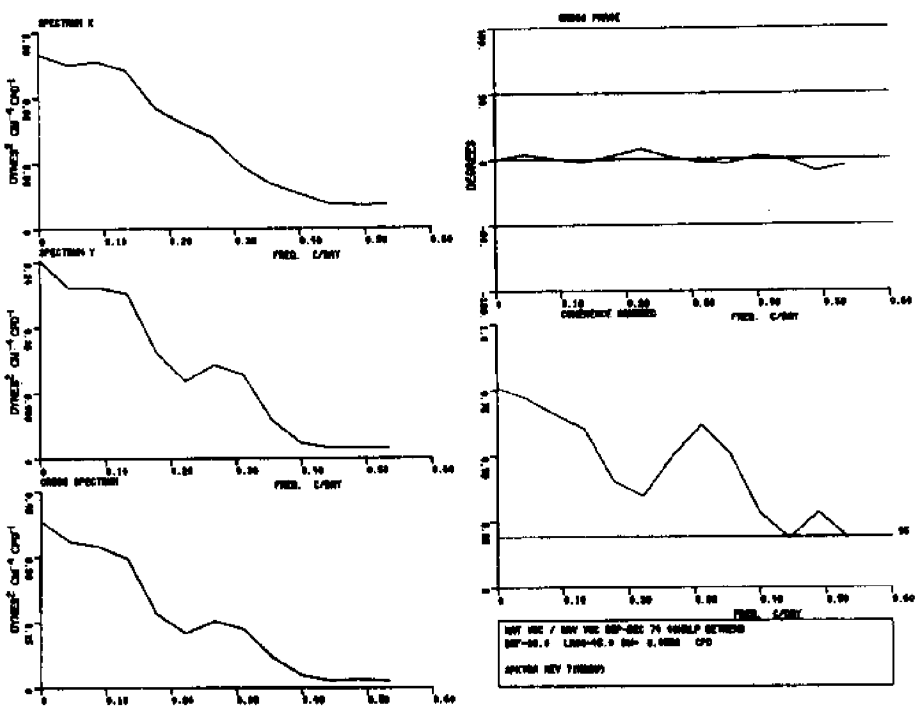

Figure 245 Spectra of wind stress v component at Cape Hatteras, N. C. vs. the wind stress v component at Savannah, Ga., Sept.-Dec. 1974

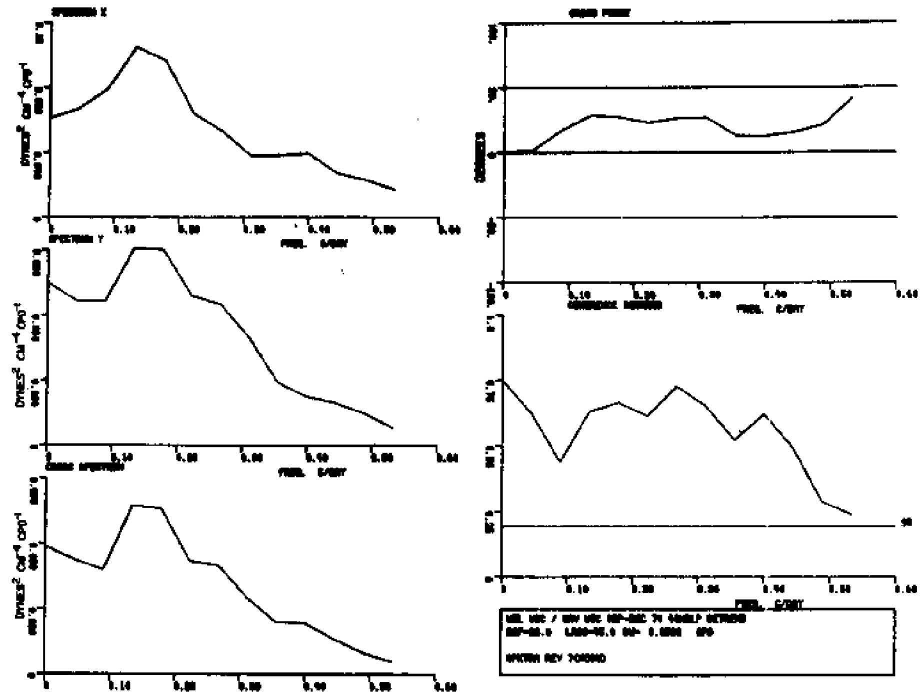

Figure 246 Spectra of wind stress u component at Wilmington, N. C. vs. the wind stress u component at Savannah, Ga., Sept.-Dec. 1974

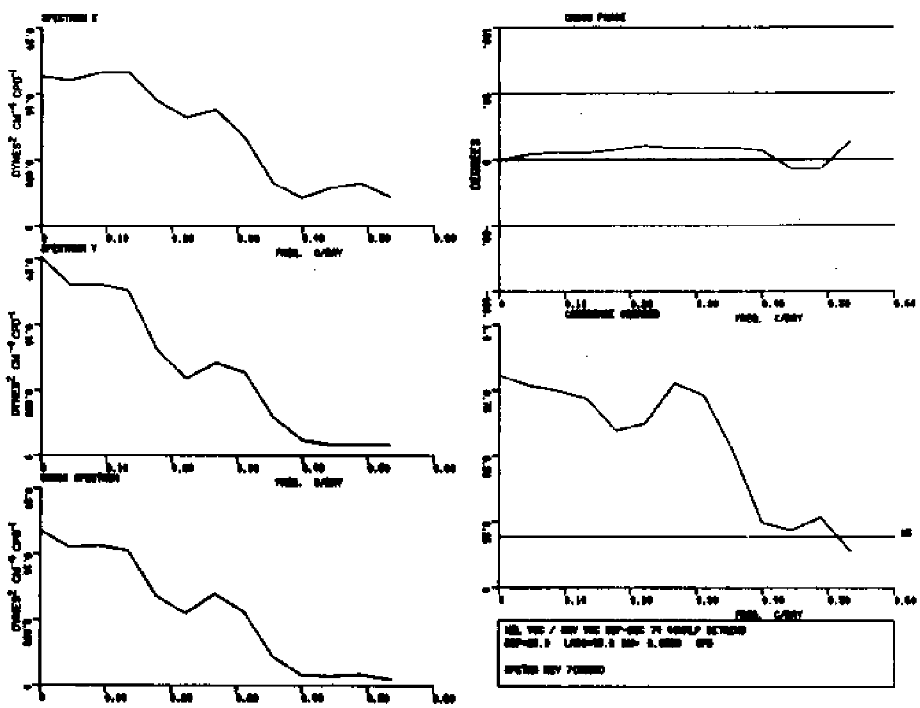

Figure 247 Spectra of wind stress v component at Wilmington, N. C. vs. the wind stress v component at Savannah, Ga., Sept.-Dec. 1974

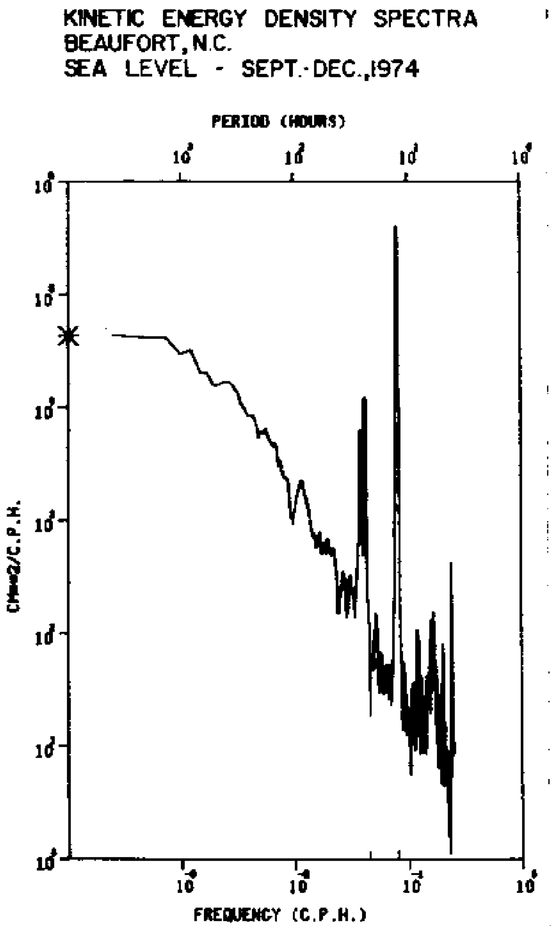

Figure 248

Kinetic energy density spectra for Beaufort, N. C. sea level, Sept.-Dec. 1974

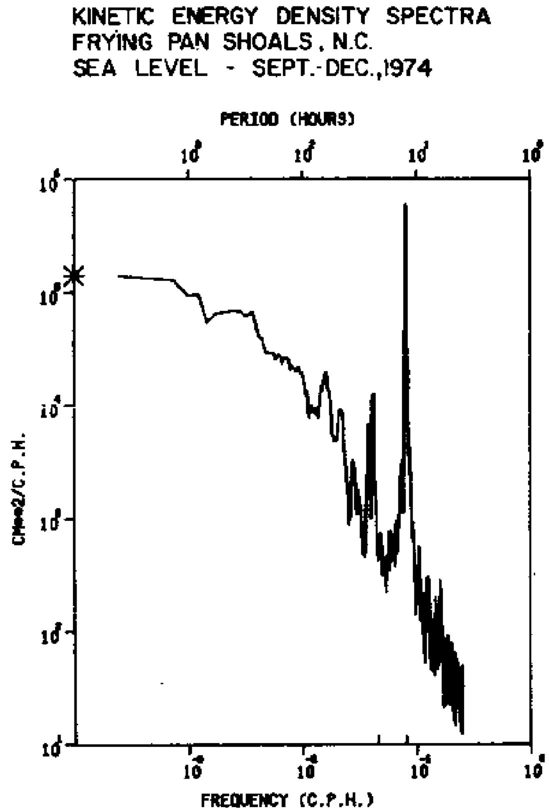

Figure 249

Kinetic energy density spectra for Frying Pan Shoals, N. C. sea level, Sept.-Dec. 1974

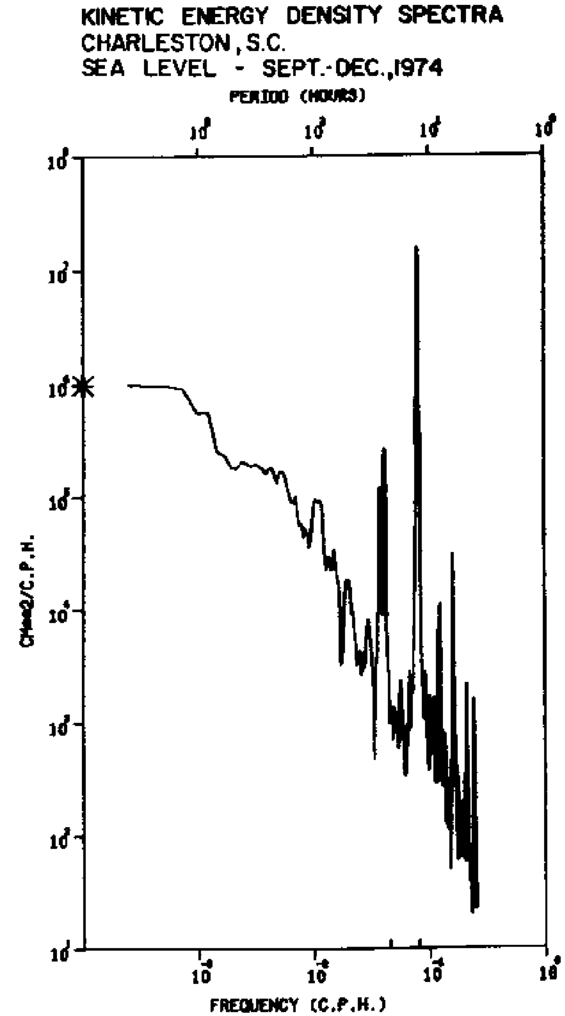

Figure 250

Kinetic energy density spectra for Charleston, S. C. sea level, Sept.-Dec. 1974

References

Bosart, L. 1973. Detailed analysis of precipitation patterns associated with meso scale features accompanying United States east coast cyclogenesis. Mon. Wea. Rev. 101 (1), 1-12.

Bosart, L., C. Vando and J. Helsdon 1972. Coastal frontogenesis. J. of Appl. Meteor. 11 (8), 1236-1258.

Bosart, L. and J. Cussen 1973. Gravity wave phenomena accompanying east coast cyclogenesis. Mon. Wea. Rev. 101 (5), 446-454.

Brooks, D.A. Sea level Fluctuations off the Carolina Coasts and their relation to atmospheric forcing. Center for Marine and Coastal Studies, North Carolina State University, Technical Report 77-6.

Brooks, D.A. and C.N.K. Mooers 1977. Tidal and longer period motions in the Florida Current. Summer 1970. Deep Sea Res. 24, 399-425.

Bumpus, D.F. 1973. A description at the circulation on the continental shelf of the east coast of the United States. Progress in Oceanography, Vol. 6., New York, Pergamon, 111-156.

Cragg, J. and W. Sturges 1974. Wind induced currents and sea surface slopes in the eastern Gulf of Mexico. Florida State University Technical Report. June.

Cutchin, P.L. and R.L. Smith 1973. Continental shelf waves: low frequency variations in sea level and currents over the Oregon continental shelf. J. Phys. Oceanogr. 3 (1), 73-82.

Duing, W., 1975. Synoptic studies of transients in the Florida Current. J. Mar. Res. 33, 53-73.

Duing, W., C.N.K. Mooers and T.N. Lee 1977. Low Frequency variability in the Florida Current and relations to atmospheric forcing from 1972 to 1974. J. Geophys. Res. (in press).

Ekman, V.W. 1905. On the influence of the earth's rotation on ocean current. Arkiv fur Matematik, Astronomi ock Fysik 2, 1-52.

Garvine, R.W. 1971. A simple model of coastal upwelling dynamics. J. Phys. Oceanogr. 1, 169-179

Green, C.K. 1944. Summer Upwelling-northeast coast of Florida. Science, 100 (2607), 546-547.

Hamon, B.V. 1962. The spectrums of mean sea level at Sydney, Coff's Harbor and Lord Howe Island. J. Geophys. Res. 67, 5147-5155. 1963 (correction) J. Geophys. Res., 68 4635.

Hamon, B.V. 1966. Continental shelf waves and the effects of atmospheric pressure and wind stress on sea level. J. Geophys. Res. 71, 2883-2893.

Hidaka, K. 1953. Wind-driven sea level change over a continental shelf. Tech. Rept. No. 9, Texas A and M Research Foundation, October.

Huyer, A., B.M. Hickey, J.D. Smith, R.L. Smith, and R.P. Pillsbury 1975. Alongshore coherence at low frequencies in currents observed over the Continental shelf off Oregon and Washington. J. Geophys. Res. 80 (24), 3496-3505.

Kundu, P.K., J.S. Allen, R.L. Smith 1975. Modal decomposition of the velocity field near the Oregon Coast. J. Phys. Oceanogr. 5, 683-704.

Lee, T.N., and D.A. Mayer 1977. Low frequency current variability and spin-off eddies along the shelf off southeast Florida. J. Mar. Res., 35 (1), 193-220.

Miller, A.R. 1957. The effect of steady winds on sea level at Atlantic City. Meteoral. Monogr. 2, 29-31.

Miller, A.R. 1958. The effects of winds on outer levels on the New England Coast. Limnol. and Oceanogr. 3, 1-14.

Mooers, C.N.K. and R.L. Smith 1968. Continental Shelf Waves off Oregon. J. Geophys. Res. 73, 549-557.

Mysak, L.A., and B.V. Hamon 1969. Low frequency sea level behavior and continental shelf waves. J. Geophys. Res., 74, 1397-1405.

Niiler, P.P. and L.A. Mysak 1971. Barotropic waves along the eastern continental shelf. Geophys. Fluid Dyn. 2, 273-288.

NOAA 1970. Environmental conditions within specific geographical regions: offshore east and west coasts of the United States and in the Gulf of Mexico. Final Report, NODC, Environmental Data Service, NOAA, Washington, D.C.

Oort, A.H., and A. Taylor 1969. On the kinetic energy spectrum near the ground. Mon. Wea. Rev. 97, 623-636.

Orlanski, I. 1969. The influence of bottom topography on the stability of jets in a baroclinic flud. J. Atm. Sci. 26, 1216-1232.

Orlanski, I. and M.D. Cox 1973. Baroclinic instability in ocean currents. Geophys. Fluid Dyn. 4, 297-332.

Panshin, D.A. 1967. Sea level, winds and upwelling along the Oregon Coast. MS thesis, Oregon State University, Corvallis.

Parr, A.E. 1933. A geographic-ecological analysis of the seasonal change in temperature correlations in shallow water along the Atlantic coast of the U.S. Bull. Bingham Oceanogr. Coll. 4 (3), 1-90.

Petterson, S. 1969. Introduction to Meteorology 3rd edition. McGraw-Hill, New York, 333 pp.

Pietrafesa, L.J. 1970. Trapped and leaky shelf wave modes. unpublished M.S.

Pietrafesa, L.J. 1973. Steady, baroclinic circulation on a continental shelf, Ph.D. Dissertation. University of Washington, June.

Pietrafesa, L.J., D.A. Brooks, L.P. Atkinson, R. D'Amato, and J. Bane 1977. Preliminary data report, physical/dynamical observations made in Onslow Bay; summer, fall and winter 1975. Center for Marine and Coastal Studies, North Carolina State University, Tech. Report, 77-05

Pietrafesa, L.J., D.A. Brooks, R. D'Amato, L.P. Atkinson 1978. Onslow Bay physical/dynamical experiments; summer - fall, 1975. University of North Carolina, Sea Grant College Program Publication, UNC - SG - 77 - 07.

Pillsbury, J.E. 1891. The Gulf Stream. Rept. Supt., U.S. Coast and Geod Surv. for year ending June, 1890 p. 459-620.

Pond, S. 1975. The exchanges of momentum, heat and moisture at the ocean-atmosphere interface. Numerical Models of Ocean Circulation, National Academy of Science, Washington, D.C. p 26-38.

Roden, G.I., 1960. On the nonseasonal variations in sea level along the west coast of North America. J. Geophys. Res. 65, 2809-2826.

Ruzeeki, E.P. 1974. A souo-economic environmental baseline summary for the south atlantic region between Cape Hatteras, North Carolina and Cape Canaveral, Florida: Vol. II - Climatology. Virginia Institute of Marine Science Technical Report, September.

Saunders, P.M. 1977. Wind stress on the ocean over the eastern continental shelf of North America. J. Phys. Oceanogr. 7, 555-566.

Schmitz, W.J. and W.S. Richardson 1968. On the transport of the Florida Current. Deep Sea Res., 15, 679-693

Smith, R.L. 1974. A description of current, wind and sea level variations during coastal upwelling off the Oregon coast, July-August 1972. J. Geophys. Res. 79 (3), 435-443.

Taylor, C.B. and H.B. Stewart, Jr. 1959. Summer Upwelling along the east coast of Flordia. J. Geophys. Res. 64 (1), 33-40.

U.S. Navy 1970. Summary of Synoptic meteorological observations (SSMO) for North American coastal Marine areas. Naval Weather Service Environmental Detachment, Fed. Bldg., Asheville, N.C.

Ward, R. 1925. The Climates of the United States. Ginn, Boston, 338 pp.

Webster, F. 1961. The effects of meanders on the kinetic energy balance of the Gulf Stream. Tellus, 13, 392-401.

Welander, P. 1957. Wind action on a shallow sea: Some generalization on Ekman's theory. Tellus, 9, 45-52.

Wunsch, C., D.V. Hansen, and D.D. Fetler, 1969. Fluctuations of the Florida Current inferred for sea level records. Deep Sea Res. 16 (supplement), 447-470.